THE PROCEEDINGS OF
THE PHYSICAL SOCIETY

VOL. 51, PART 3 1 *May* 1939 No. 285

PHYSICS AND THE PHYSICISTS OF THE EIGHTEEN-SEVENTIES

BY SIR AMBROSE FLEMING, F.R.S.
Honorary Fellow of the Institute of Physics

Address delivered 13 *January* 1939

INTRODUCTORY REMARKS BY PROF. ALLAN FERGUSON, PRESIDENT OF THE SOCIETY

WE meet this afternoon to celebrate an event which is, I think, unique in the history of learned societies. The Physical Society was founded in 1874, mainly through the efforts of the late Prof. Guthrie. Its first scientific meeting was held on the 21st of March in that year, and the first paper at this meeting, on the "New contact theory of the galvanic cell", was read by Mr J. A. Fleming. Now, sixty-five years later, Sir Ambrose Fleming, in his ninetieth year, stands once again at the rostrum of the Society of which he is so distinguished a Fellow, to tell us something of that past in which he has played so great a part. Sir Ambrose has touched the scientific life of our age at many points. To his skill in design, electrical science owes many beautiful measuring instruments; for his many books and papers, which have contributed so largely to the advancement and dissemination of knowledge, the science owes him a heavy debt; his invention of the thermionic valve has made it possible for listeners in far corners of the earth to hear the very words of the inventor as he speaks; and, more than all else, he lives in the veneration and affection of those many generations of engineers whom he has taught.

Of the 99 founder members of the Society, Sir Ambrose Fleming is the sole survivor, for our venerated Past President, Sir Oliver Lodge, joined the ranks at a little later date.

I now call on our Founder Fellow and Duddell Medallist to add yet one more to the long list of the papers which he has read before the Society.

SIR AMBROSE FLEMING'S ADDRESS

AT the especial request of our President, Prof. Allan Ferguson, I have undertaken to give a short account of "The physics and physicists of the eighteen-seventies". Perhaps some may ask why that particular decade has been selected, and the answer is that in 1874 the Physical Society of London was founded by a well-known physicist, Prof. Frederick Guthrie. There must therefore have been at that time some events drawing special attention to physical research. Although the idea of forming a fresh learned Society concerned with physics specially was welcome to many, not all of the most eminent physicists of that day thought it a necessary addition to our resources. For instance no less an authority than James Clerk Maxwell considered that the *Proceedings* or *Transactions* of the Royal Society were the proper avenues of publication for the results of any meritorious research or discovery in physics and that if a Society was to publish papers which were not of sufficient importance to find a place in the records of our premier learned Society its progress towards dissolution would be very rapid.

But what was not clearly evident at the time was that though a paper or a research might fall short of the standard required for the Royal Society reception it might yet stimulate general discussion or thought which would yield valuable results in time. This proved to be the case and the records of the Physical Society for the past sixty-four years have amply justified the foresight of Guthrie in founding this Society. The first meeting of the Physical Society was held on 21 March 1874 in Guthrie's lecture room in the Science Schools, South Kensington, and by his great kindness I had the privilege of reading the first given paper to the Members, the subject being "The new contact theory of the galvanic cell".

Let us then take a glance backward at the state of physics in the years 1870–80, and the men who were foremost in advancing it. We may divide them into two broad classes. There were first a few who were highly competent mathematicians and conformed to the model of Newton in being able not only to wield the powerful weapon of mathematical analysis but also were competent experimentalists. In Great Britain at that time this class was chiefly represented by Sir George Stokes, Lucasian Professor of Mathematics in the University of Cambridge, by Sir William Thomson who had held the Chair of Natural Philosophy in the University of Glasgow since the time when he was twenty-two years of age and by his enormous knowledge, brilliant experimental researches, and practical inventions held a foremost place in universal opinion as a physicist.

Then next by James Clerk Maxwell, who even as an undergraduate had made notable contributions to mathematics and physics. He had translated Faraday's physical conceptions into mathematical language, explored the phenomena of colour, laid firm the foundations of the kinetic theory of gases and made important measurements of the viscosity of air. He had held professorships of Natural Philosophy at Aberdeen and King's College, London. In 1865 he had resigned this latter appointment and retired to his Scotch estate at Glenlair to engage in writing his great treatise on Electricity and Magnetism. Peter Guthrie Tait was then Professor of Physics in the University of Edinburgh. As a mathematician he had inherited the mantle of Sir W. R. Hamilton, the inventor of quaternions, but Tait also made many very important contributions to experimental physics. Then in the same rank of great mathematical physicists we had in Germany, von Helmholtz and Kirchhoff; in France, Cornu; and in the United States, Willard Gibbs.

On the other hand there were many eminent physicists who, like Faraday, had not much mathematical knowledge but attained their results purely by experimental work. Amongst these in the eighteen-seventies, John Tyndall was one of the most popular. He had very great abilities as an exponent of science. J. P. Joule had made the most valuable contributions to physical measurements by his proof of the so-called Joule's law in electricity and in his determinations of the mechanical equivalent of Heat. A reprint of Joule's scientific papers was issued by the Physical Society in 1884.

Very prominent in this group was Sir William Crookes. He had, like many of the experimental physicists, begun as a chemist. Crookes discovered by spectrum analysis the element thallium and had isolated the metal and determined its atomic weight. Crookes had then turned to research on electrical discharge in high vacua. He had improved methods of vacuum technique and had rediscovered many important facts concerning electric discharge in high vacua noticed by Hittorff, Puluj and others. Finally he devised the light mill or radiometer.

Another of this group was Dr J. H. Gladstone, the first President of the Physical Society, and he also was first of all a chemist and latterly an experimental physicist. His work on refractive indices was of special importance. Neither must we omit to mention in this group the name of Frederick Guthrie who made several very important additions to physical knowledge. Other experimental physicists of that date were R. B. Clifton at Oxford, W. Grylls Adams and G. Carey Foster in London, Balfour Stewart in Manchester. Prior to about 1866 there were in Great Britain hardly any laboratories properly equipped for research or teaching in physics.

The necessity for quantitative work especially in electricity had been emphasized by the technical advances in telegraphy. In 1856 a far-seeing man, Cyrus Field, had conceived the idea of a transatlantic submarine cable to unite Great Britain and the United States and had formed a company in 1856 to undertake it. But the question at once presented itself whether signals could be sent through such a long cable quickly enough to enable a sufficient income to be earned to pay interest on the capital and also the working expenses. Faraday had been consulted and pointed out that such a submarine cable was a large condenser or Leyden jar but he thought signals might be sent through it sufficiently quickly to make it pay.

Here we see the immense power of mathematical analysis guided by correct physical ideas. In 1855 William Thomson, then a young professor, sent a paper on the theory of the electric telegraph to the Royal Society. Assuming the cable to have a certain resistance and also electrostatic capacity per mile, he proved that when a steady electromotive force was applied at one end the outcoming current at the other rose up gradually according to a certain curve of arrival. The time taken to reach a certain current strength was directly proportional to the square of the length of the cable and directly as the product of the resistance and capacity per mile of the cable. This showed that the right method for signalling was to have as sensitive a detector as possible at the receiving end and to use the lowest possible applied electromotive force at the sending end. The first Atlantic cable was made in 1857, but an attempt to lay it failed. The cable broke repeatedly and was finally lost.

In 1858 a second attempt was made. Thomson had meanwhile invented and made his sensitive mirror galvanometer for cable signalling. The officials in charge of the cable could not understand Thomson's mathematical conclusions and would not accept his advice, but attempted to work ordinary telegraphic instruments by applying large electromotive forces at the sending end by induction coils and batteries. The result was that in about a month's time they broke down the insulation by piercing the gutta percha and killed the cable. Before its death however Thomson had been able to show the merits of his mirror galvanometer. The result was to indicate the necessity for possessing absolute methods of electrical measurement, and, urged by Thomson, the British Association had appointed in 1862 a Committee to consider this subject. An absolute system of units was selected based on the centimetre gramme, and second as units of length, mass and time and practical electrical units of resistance, capacity inductance, etc., created to represent certain multiples or fractions of the absolute electrical units based on the centimetre, gramme and second. This Committee continued to report every year up to 1870 but was re-appointed in 1881 to continue its work.

The comprehension and adoption of this absolute system of c.g.s. units was facilitated greatly by the publication in 1875 by the Physical Society of a treatise on it by Prof. J. D. Everett called "Illustrations of the c.g.s. system of units". An enlarged edition was published in 1879 under the title "Units and physical constants". Since that date it has passed into general use. The British Association Committee published a Report in 1863 containing descriptions of the methods of determining the absolute values of certain practical standards of electrical resistance and capacity. This was written by Prof. J. Clerk Maxwell and Prof. Fleeming Jenkin and described the experiments made at King's College, London, with this object. In 1865 a third Atlantic cable was laid and lost. But in 1866 success finally crowned the efforts of the promotors and a fourth cable was made and laid and the 1865 cable raised and repaired. Thus two complete Atlantic cables effected communication between England and the United States, which were worked with Thomson's instruments.

In 1870 Thomson invented his remarkable syphon recorder to receive and print cable messages and this has remained to this day the standard instrument for all cable reception. On one occasion Mr Latimer Clark showed the sensitivity of Thomson's mirror galvanometer in a very interesting way. He had the ends of the 1865 and 1866 Atlantic cables joined in Newfoundland, and at Valencia in Ireland he had the ends of a submarine cable 4000 miles long at hand. He made a single voltaic cell of a lady's silver thimble, having in it a small amount of dilute sulphuric-acid. Dipping into this a small rod of zinc he used this cell to make signals detected by Thomson's mirror galvanometer through the united length of the two cables. Thus the year 1870 saw the practical achievement of submarine telegraphy accomplished and the invention of the instruments needed for working. From that time the making and laying of submarine cables became a particularly British industry.

But the same year (1870) witnessed another event of great importance with regard to physical research, viz. the founding of the Cavendish Laboratory at

Cambridge. Although some attempts had been made to foster physical research there the University was without means to provide for it.

In October 1780 the Seventh Duke of Devonshire, then Chancellor of the University of Cambridge, sent a letter to the Vice-Chancellor offering to defray the cost of erecting and equipping a physical laboratory in the University. This munificent offer was gratefully accepted. In March 1871 Maxwell was elected as the first Cavendish Professor of Physics. The building of the laboratory was completed early in 1874. A year before, in 1873, Maxwell had published his great *Treatise on Electricity and Magnetism* and physicists everywhere were trying to master the new ideas he had introduced into the subject. He had embodied in it his earlier work of expressing in mathematical language Faraday's ideas of lines of electric and magnetic force and of the dielectric as the true seat of the energy involved. He had also included in the second volume a reproduction and exposition of his great paper sent to the Royal Society in 1864 on "A dynamical theory of the electromagnetic field". In this paper he had shown that electric and magnetic effects are propagated through space with a velocity equal to that of light in the medium and had foretold the existence of the electromagnetic waves now utilized to give us radio-telegraphy and telephony. After Maxwell's death in 1879 I remember that an eminent mathematician, Sir W. D. Niven, said to me that he regarded this paper with its wonderful originality and power to be one of the greatest productions of the human mind.

In his Introductory Lecture given by Maxwell in October 1871, on his installation as Cavendish Professor, he had expressed his ideas of the aim and functions of the Laboratory. He did not contemplate that its main use should be that of training undergraduate students in the repetition of experiments described in text books, but he considered rather that its principal object should be quantitative measurements and the production of new knowledge by research by post-graduate or other students. Very magnificently has this ideal been held in view by Maxwell's successors in the Chair. For more than sixty years under the guidance of Lord Rayleigh, Sir J. J. Thomson and Lord Rutherford, a continual stream of vastly important additions to our knowledge of the physical universe has issued from the Cavendish Laboratory and men trained there have gone out to all parts of the world to continue that work and increase the fame of the Cavendish Laboratory, Cambridge, as a fountain head of new scientific knowledge of unspeakable importance.

Another event in the year 1870 which had an influence on physical research was the taking over by the State of the telegraph system of Great Britain. Up to that time land telegraphy had been conducted by several public companies each with its special area of operations. This of course greatly limited the use of the electric telegraph.

The Government of that day passed Acts of Parliament in 1868 and 1869 entitling them to buy out, take over, and place under the General Post Office all telegraphic work in Great Britain. At the same time that work was greatly extended and the country overlaid with a network of telegraphic wires enabling communications to be made between all places where there was a post office. This called for the production of practical standards of the electrical units such as the ohm, the volt, the ampere, and the farad, and accurate methods of electrical measurement. The British Association Committee had constructed a number of coils of wire of various alloys, the resistance of each of which was asserted by them to be at certain marked temperatures equal to 10^9 absolute units of resistance on the electromagnetic system. These had been deposited in the Cavendish Laboratory. It had been suspected however that their true resistance was less by about 1·3 per cent than 10^9 cm./sec.

When I went up to Cambridge in October 1877 to work in the Cavendish Laboratory, Maxwell suggested to me to undertake the work of comparing these coils and ascertaining from them their resistances at certain temperatures and hence the most probable value of the B.A. unit.

For this purpose I devised a special form of Wheatstone's bridge which was described to the Physical Society in 1880. I prepared, as the result of about two years' work, a chart showing the variation of resistance with temperature of each of the coils. The true absolute value of these were determined later on (after Maxwell's early lamented death in November 1879) by Lord Rayleigh, who was Cavendish Professor until 1884. This B.A. unit proved to have an electrical resistance of $0{\cdot}9867 \times 10^9$ cm./sec. or less than a true ohm of 10^9 cm./sec. The workers in the Cavendish Laboratory during Maxwell's life included Arthur Schuster, R. T. Glazebrook, Donald MacAlister, J. E. H. Gordon, G. Chrystal, W. M. Hicks, W. Garnett and J. A. Fleming.

When I began to attend at the Cavendish Laboratory, Maxwell gave one or two courses of lectures each session. I was astonished to find that the attendance at these did not exceed two or three students in place of the one or two hundred who in a German or Scottish University would have eagerly listened to one of the greatest of British physicists. For one course on electricity in 1879 the only attendants were Mr Middleton (an American gentleman) and myself. Yet Maxwell gave to us much original matter he had in preparation for an elementary treatise he was writing. In one of the last lectures he delivered in his life, Maxwell gave us an elegant method of solving problems on networks of conductors. Mr Middleton turned to me at the end and said "Sir! this man (Maxwell) is great! He does not come here and tell us what he has read in books, but gives it to us hot from his brain!"

Part of Maxwell's work during the last years of his life comprised the editing for publication the unpublished electrical researches of the Hon. Henry Cavendish (1731–1810). Cavendish was an experimentalist of great ingenuity and with the most rudimentary apparatus carried out important researches. Maxwell repeated with similar apparatus all Cavendish's results. Amongst other things Cavendish anticipated Faraday's discovery of specific inductive capacity and made researches to find out if the law of electrical attractions or repulsions varies in any sensible degree from the inverse square of the distance. Maxwell carefully repeated this with improved apparatus and found that the index deviated from 2 by not more than 1/21,600 either way. Cavendish made measurements of the comparative electrical resistance of various materials by taking the shock of a Leyden jar through a certain length of each material and adjusting the lengths until the shocks were estimated to be about equally painful. Most of the workers in the laboratory were called upon at various times to act as shock-meters in Maxwell's repetition of Cavendish's experiments.

Maxwell's lecture experiments were always marked by great ingenuity and he could give copious new information on even the most familiar scientific facts or discoveries. In conversation he was often difficult to understand by reason of a certain paradoxical and humorous mode of speech. At a celebration of the centenary of Maxwell's birth at Cambridge in June 1931 I ventured to say at a memorial meeting: "To have enjoyed even a brief personal acquaintance with Maxwell and the privilege of his oral instruction was in itself a liberal education; nay more, it was an inspiration, because everything he said or did carried the unmistakeable mark of a genius which compelled not only the highest admiration but the greatest reverence for the man himself as well."

No mention of Maxwell's work would be complete without a brief reference to his other writings written in the eighteen-seventies. He published a treatise, the *Theory of Heat*, which had all the characteristics of lucidity and novelty which marked his authorship. In it he gave the elements of the science of thermodynamics and the contributions to it made by Carnot, Clausius, Willard Gibbs, Rankine and W. Thomson. His other small book, *Matter and Motion*, was a delightfully interesting small treatise on dynamics. It was re-edited with some additions after Maxwell's death by Sir Joseph Larmor. In addition to this he wrote many articles for the 9th edition of the *Encyclopaedia Britannica* and in 1873 gave a memorable lecture on "Molecules" to the British Association at Bradford, parts of which have been often quoted.

We must then return to consider the work of Sir W. Thomson (later Lord Kelvin) during the decade 1870–80 under consideration. He was at this time engaged in improving the mariner's compass. As a yachtsman and the owner of the Lalla Rookh he took an extreme interest in all things connected with navigation, and he left his improvement on everything. In 1874 he was asked to write an article on the magnetic compass for *Good Words* and at once took note of the defects of the type then used. Little by little he brought it to a state of perfection in which it was adopted all over the world. He gives a full account of it in the third volume of his popular *Lectures and Addresses*. At the same time he vastly improved the method of deep sea sounding by using steel pianoforte wire instead of hemp rope. The depth was measured by the degree to which the air in a glass tube, open at the bottom but closed at the top, was compressed when the sea floor was reached. In 1876 he made known his enormously ingenious machines for recording, analysing, and predicting the tides at any port, and in a lecture at Glasgow in 1875 he gave a most instructive account of methods of determining the position of a ship at sea by means of Sumner circles. His knowledge of everything connected with navigation, tides and waves was vast and accurate, and he touched nothing he did not elucidate and improve. It is impossible therefore to mention here more than a fraction of his scientific work.

In personal character Lord Kelvin (as Sir W. Thomson became in 1892) was infinitely attractive and admirable. His kindness and courtesy to younger men and modesty with regard to his own great achievement were his chief characteristics. Although I had seen and heard him at several British Association Meetings in 1871 at Edinburgh as President and in 1876 at Glasgow, I did not become personally known to him until 1882. He was then engaged in inventing his ampere balances and other electrical instruments. As Electrician to the Edison Electric Light Company of London I was able to afford him, at 57 Holborn Viaduct, some facilities for using large electric currents, and that led to personal intercourse. I had the privilege of visiting him at his home in Glasgow and on his yacht. I have still in my possession some autograph letters he wrote to me about his work and inventions.

The decade we are considering was remarkable also for the completed invention of two important electrical appliances, viz. the speaking telephone and the incandescent electric lamp, the achievement of which had long been an object of physical research.

Without reference to early attempts, we all know that Alexander Graham Bell was the first to produce a simple speaking telephone which was publicly exhibited in 1876 at the Philadelphia Exhibition. Sir W. Thomson saw and used it there, and on return to England he described it enthusiastically to an audience at the Glasgow meeting of the British Association. Bell was actually engaged in trying to effect multiple telegraphy when he stumbled across the principle of his magneto-telephone.

The Bell telephone was a good receiver but poor transmitter. T. A. Edison had meanwhile invented his carbon-button transmitter, in which the motions of a sound-actuated diaphragm compressed a button of lamp black and varied its resistance and therefore the current in the circuit.

D. E. Hughes, the inventor of a printing telegraph, then came into the field in 1878 with his discovery of the effects of light pressure on a loose contact between two pieces of graphite carbon. This in time gave us the modern microphone transmitter. Bell had suggested meanwhile the idea of a telephone exchange, and the Edison and Bell interests in England had to unite to provide the most effective transmitter and receiver.

In 1879 Hughes made an appliance, which Lodge subsequently called a "coherer", by using an imperfect contact between two pieces of graphite carbon or of carbon and metal. He joined this in series with a Bell magneto telephone and a voltaic cell. He found that this apparatus gave sounds in the telephone when placed even at some distance from an induction coil giving sparks. He showed these experiments to the President of the Royal Society and others. But he was unfortunately told by them that there was nothing new in it but simply ordinary Faradaic electromagnetic induction. On the contrary, Hughes had in fact made an arrangement for detecting Maxwell electromagnetic waves being sent out from the induction coil. If he had not been discouraged he might have gone further and anticipated the researches of Branly, Lodge, and Marconi, and given us radio-telegraphy fifteen years earlier than we did actually obtain it.

The problem of incandescent electric lighting had occupied attention for thirty years or more in the endeavour to provide a small unit of light for domestic illumination. J. W. Swan solved the problem early in 1880 of producing a carbon filament by carbonizing a cotton thread which had been parchmentized with sulphuric acid, and mounting a loop of this carbon filament in a glass bulb exhausted of its air. Edison about the same time carbonized slender filaments of bamboo in horse-shoe shape and also produced an effective carbon-filament lamp.

The early lamps gave a light of about 16 candles at a power expenditure of about 64 w. From that date electric illumination by incandescent lamps became practicable.

In conclusion it may be useful to attempt to sum up briefly the achievements in physics during the decade 1870–80. Broadly speaking it was an age of practical invention in which well ascertained scientific principles were applied in various ways to create new industries or useful arts. In telegraphy there were many very important additions. Wheatstone automatic, quadruplex, and high-speed printing telegraphs came into use. The speaking telephone and telephone exchanges added to the convenience of life. Electric incandescent lamps and the invention of the dynamo had made possible public electric supply stations, and domestic electric illumination. In 1873 the reversibility of the dynamo was discovered, viz. that it could act as a motor when current was put into it, and some degree of progress had been made in the use of electric motors and possible electric transmission of power. Not by any means the least important of the practical inventions of the eighteen-seventies was that of the gelatine dry plate in photography devised by R. L. Maddox in 1871, which greatly extended the uses of photography.

In relation to physical theories, the period we are considering was essentially mechanistic and deterministic in ideas. The conception of a universal aether having elasticity and density was widely held, and numerous mechanical aether theories were proposed. Atoms in vibration were supposed to agitate the aether and produce waves in it, but no one had explained how the vibrating atoms got a grip on the aether, seeing that the aether offers no resistance to the motion of the earth and planets through it.

Theories of atomic structure were in a very vague and nebulous state. Thomson's theory of atoms as vortex rings in the aether had not explained anything of importance. The science of thermodynamics had, however, been well developed, and much progress made by the writings of Clausius, Rankine, W. Thomson, and Willard Gibbs. The foundation stone of the science for thermodynamics was laid by the publication in 1824 of the remarkable essay by Sadi Carnot on the "Motive power of heat", in which he gave the Carnot cycle. This essay was, however, then known to very few. W. Thomson made acquaintance with it when as a young graduate he went for a year to Paris to work with the great experimentalist Regnault. Thomson published in 1849 a paper in which he made known and expounded Carnot's work. Carnot's essay in French was republished in 1878, having been thus lost sight of for many years, but Thomson's paper in 1849 had by that time brought it to the notice of physicists of that day. On the basis of the Carnot cycle Thomson subsequently suggested his absolute scale of temperature independent of any working substance. He also enunciated his law of dissipation of energy. The facts that heat is the kinetic energy of atoms, and that mass kinetic energy could be converted into heat at a certain rate, were fully appreciated. But it was not so generally realized that the whole of any quantity of heat energy cannot be converted into mass kinetic energy. There was a widely diffused belief in that day that the physical theories corresponded closely to reality and that such words as "size", "time", "mass" and "energy" denoted actualities independent of any observer. The physical theories of 1870–80 were looked upon as well-established explanations of facts. Not every physicist, however, shared this view. Maxwell once said in my hearing "Because we can imagine a mechanism which can achieve some result we find in Nature it does not in the least follow that it is done in that way."

Not ten years later, however, the first of the events occurred, namely the Michelson and Morley experiment, which were to undermine and destroy this confidence and to show that our interpretation of physical phenomena involves the observer as well as the thing observed.

There was a strong tendency in the eighteen-seventies and even later to adopt physical theories which were mechanistic or involved ideas capable of visualization. At present we are content to obtain mathematical expressions which are consistent with facts. Hence, regarding Maxwell's theory of electromagnetic propagation, we accept the view taken by Hertz that Maxwell's theory is expressed in Maxwell's equations, without demanding the statement of it in terms of visualized mechanism.

When we come to look back then on the work of physicists during the eighteen-seventies, what we find is that their inventions, discoveries of fact, and ascertained principles remain with us to-day as of permanent value, forming part of our useful knowledge. But their theories and speculations as to underlying causes in Nature have nearly all passed away. Perhaps it will also be the same with our present-day work. If some sixty years hence a Fellow of the Physical Society gives a talk on the "Physics of the nineteen-thirties", he will have to record the great additions then made to knowledge of physical facts. But he may also have to say that our explanations and theories concerning them have all vanished, or at least been replaced by others also destined in turn to pass away.

MARCH 21, 1874

I. ON THE NEW CONTACT THEORY OF THE GALVANIC CELL

By J. A. Fleming, B.Sc., F.C.S.

This paper is reprinted here in view of its historic interest. The original will be found on pages 1 to 12 of volume 1 of the Proceedings

The contest that has for so long been waged between the supporters of the two theories of the galvanic cell, the *contact* and the *chemical*, can hardly be said to have been brought even now to a decisive issue. For although the contact theory, as originally proposed by Volta, received a fatal blow when the law of conservation of energy became clearly understood, yet in its place a *new contact theory* has arisen, supported by novel and important experimental evidence, which has again been placed by recent writers on electrical science in formidable opposition to its old rival.

The old contact theory of Volta had its origin in an entire ignorance of the science of energy. It simply referred the current produced through the circuit of a pile to the effect of the metallic contacts, and it ignored the thermal and chemical changes which are also necessarily present; but it had to be finally abandoned when once it became clearly understood that the appearance of a current involved the disappearance of some other energy, actual or potential, as an invariable accompaniment. The new contact theory may be said to have had its source in the discovery of Sir W. Thomson, that there is undoubtedly a difference of potential produced when dissimilar metals are placed in contact—a fact not only abundantly proved by Thomson by direct experimental evidence, but, as he has pointed out, confirmed in a remarkable way by the phenomena of the Peltier effect, which, when interpreted by the dynamical theory of heat, furnish the most reliable measures of its amount. These facts, together with others presently to be referred to, have been made to furnish the key to a fresh explanation of the dynamics of the galvanic cell, which I have ventured to call the *new* contact theory, as opposed to the old or voltaic one.

It is not possible, however, to define in a few words the precise details of the new theory; they can only be arrived at by collecting together the statements as we find them laid down by their authors. The object of the present paper is to draw the attention of those interested in this question to the objections that may be raised against this new contact theory—objections based on facts, some old and some which perhaps may prove new, but all of which alike seem to throw fresh difficulties in the way of this theory, although capable of simple explanation by the old chemical hypothesis. It will be necessary then to review briefly the precise statements of this new contact theory, in order to show exactly what are the points against which objection may be taken. This will be best accomplished by collecting the statements of its principal supporters and arranging together their explanations of the phenomena which arise

(1) when dissimilar metals at the same temperature are placed in contact,

(2) when one insulated metal is placed in a liquid capable of acting chemically upon it,

(3) when two different metals are placed insulated and unconnected in one such liquid,

(4) when the two metals are joined across by a metallic arc or when two or more cells are joined up in series.

1. That the contact of metals is always attended with the production of a difference of potential between them was for a long time denied by ardent supporters of the chemical theory. De la Rive endeavoured to show that the effects observed might be attributed to oxidation; but his experiments are not conclusive; and to Sir W. Thomson belongs the credit of having established the fact by experiment, irrespective of his theoretical deductions from the facts of thermoelectricity. He thus describes his decisive experiment: "A metal bar insulated so as to be movable about an axis perpendicular to the plane of a metal ring, made up half of copper and half of zinc, the two halves being soldered together, turns *from* the zinc *towards* the copper when positively electrified, and *from* the copper *towards* the zinc when negatively electrified."* The difference of potential he finds to be about 0·6 or 0·7 of that of a Daniell's cell when the metals are perfectly clean; but by oxidation of the copper it may be made equal to or even greater than that of a Daniell's cell. He has also shown that if zinc and copper cylinders be connected by a wire, the electrometer detects a difference between the potentials of the air in the interior, and, lastly, that if copper filings be allowed to fall from a copper funnel in contact with a vertical zinc cylinder, they convey a negative charge to a receiver placed below. Sir W. Thomson concludes that there is sufficient evidence to show that zinc and copper attract one another chemically at any distance if connected by a fine wire, and that, as Prof. Tait remarks, "when *any* two bodies of different kinds are brought into contact, there is a certain amount of exhaustion of the potential energy of chemical affinity between them, and that the equivalent of this is, partly at least, developed in the new potential form of a separation of the so-called electric fluids, one of the bodies receiving a positive, the other a negative charge, the quantity depending on the nature and form of the bodies".†

This is equivalent to saying that at the surface of contact there is perpetually a force tending to separate the two electricities in a direction perpendicular to that surface, while at all points ever so little within it there is no such force.

Prof. Maxwell reiterates essentially the same facts. He gives Thomson's proof that the electromotive contact-force at a junction of two metals is represented by

---

* Reprint of papers on *Electrostatics and Magnetism*, p. 316, § 400.

† *Thermodynamics*, p. 62, § 107.

PJ, where P = the coefficient of the Peltier effect, or the head absorbed at the junction due to the passage of a unit of current for a unit of time; and J is Joule's equivalent. He remarks that the electromotive force, as determined by this method experimentally, does not account for the whole electromotive force of a simple couple. This latter is in general far greater than that given by the Peltier effect for the same pair of metals. "Hence the greater part of Volta's force must be sought for, not at the junctions of the two metals, but at one or both of the surfaces which separate the metals from the air or other medium which forms the third element of the circuit."*

Prof. Jenkin, referring to these experiments of Thomson, adds that "In cases where no known chemical action occurs, as where zinc and copper touch each other, and yet difference of potential is produced, since this involves a redistribution of electricity, a small but definite consumption of energy must then occur; the source of this power cannot yet be said to be known."†

2. It seems to be universally admitted that when an insulated metal is placed in a liquid capable of acting chemically upon it, a difference of potential is produced between the metal and the liquid, a sudden rise in potential taking place in passing from the metal-surface to the liquid in contact with it, or that the metal becomes negatively and the liquid positively electrified, metals differing in the degree of electrification they can produce with any one electrolyte.

3. But if we ask what are the conditions when two different metals are so immersed, we find the most contradictory statements given. Sir W. Thomson expresses his opinion thus in 1862: "For nearly two years I have felt quite sure that the proper explanation of voltaic action in the common voltaic arrangement is very near Volta's. I now think it quite certain that two metals dipped in one electrolytic liquid will (when polarization is done away with) reduce *two* dry pieces of the same metals when connected each to each by metallic arcs to the same potential",‡ which seems equivalent to saying that there is no difference of potential produced other than that due to dissimilar contact. Thus also Prof. Tait: "By interposing between two metals which have been electrified by contact a compound liquid or electrolyte, these metals are at once reduced to the same potential—a result which could not have been obtained by connecting them by any metallic conductor. By the passage of the electricity a portion of the electrolyte is decomposed, and the potential energy thus developed is equal to that possessed by the electricity while separated in the metals."§

Prof. Jenkin advocates essentially the same views: "When two dissimilar metals are plunged side by side into a liquid such as water or dilute sulphuric acid, they do not exhibit *any* sign of electrification; the three materials remain at one potential, or nearly so. If while the two dissimilar metals are in the liquid they are joined by metallic contact to terminal pieces of one and the same metal, these terminal pieces will be brought to the same difference of potentials as that which would be produced by direct contact between the dissimilar metals."* This amounts simply to saying that, as long as no wires are attached to the plates of a single cell, there is no difference of potential; but that when wires are joined on, the observed difference of potential is due to the contact of the *wire* with that metal plate to which it is dissimilar.

---

* Treatise on *Electricity and Magnetism*, 1, 302.

† *Electricity and Magnetism*, p. 55.

‡ *Electrostatics*, p. 317, § 400.

§ *Thermodynamics*, p. 66, § 116.

Again: "When a single metal is placed in contact with an electrolyte, a definite difference of potentials is produced between them; zinc in water becomes negative, copper in water becomes negative, but less so than zinc. If, however, the two metals are plunged *together* into water, the copper, zinc, and water forming a galvanic cell, all remain at one potential, and no charge of electricity is observed on any part of the system." "If a piece of copper be now joined to the zinc, it (the copper) will become negative, and the other copper plate positive, the difference of potentials being that due to the direct contact between the zinc and piece of copper *only*, the water having the effect of simply conducting the charge from the zinc to the copper plate and maintaining them at one potential."†

The foundation for these statements is found apparently in an experiment due to Sir W. Thomson. He finds that if half-disks of zinc and copper be arranged under a movable metallic needle maintained at a high positive potential, if they are connected by a wire or by contact, the needle moves in such a way as to show that the copper is negative and the zinc positive; while if they are separated by a slight interval and connected by a drop of water, *no* difference of potential is observed. Prof. Jenkin also lays great stress on the fact that, whereas copper in contact with zinc becomes negative, in a single cell with wires attached it is the wire attached to the zinc that shows a negative potential. This he holds to be conclusive that the junction of the wire with the zinc plate is the real seat of the electrical separation; although he admits that there may be a slight difference due to the liquid, and that different liquids may augment or decrease this difference.

In another place he says: "If the voltaic theory of the cell were absolutely correct, the electromotive force of the cell would depend wholly on the plates in the electrolyte, and not at all on the solution employed to connect them."‡ But it has been found that the potential series of the metals is slightly changed by the solution employed to join the plates: in order to account for this fact it is necessary to treat the voltaic theory as incomplete. He adds, however, that the potential series of the metals for water, dilute acids, and ammonic chloride do not differ so much as to invalidate the theory, although the series for alkaline sulphides is quite different and anomalous.§

---

* *Electricity and Magnetism*, p. 22.

† *Electricity and Magnetism*, p. 44.

‡ *Electricity and Magnetism*, p. 215.

§ It may be remarked in passing, that this identity of the potential series for different acids may perhaps arise from a different cause, and not be altogether such a proof of the contact theory as Prof. Jenkin concludes it is. Andrews has shown that, when *one* metal combines chemically with *different* acids, the amount of heat liberated is the same, or nearly so. Hence, if the metals be arranged in the order of their heat-producing power when combined with the same acid, that order will remain the same for most other acids. But the order is quite different when the metals are combined with sulphur or oxygen. It is true that this order is not the electrochemical one; but various causes may interfere to disturb it. At any rate it is sufficient to show that this fact of the partial identity of the potential series for different acids cannot by any means be claimed as conclusive of the contact theory. Moreover, although the *order* may be the same for the different liquids, we do not know that the *coefficients* are the same for each metal in every dilute acid.

4. When the two plates in one electrolyte are joined by a wire, or when simple cells are joined up in series and the circuit closed by a wire, we find it stated that there is a constant separation of the electricities at the point of contact of different metals and a constant recombination, attended with decomposition, through the electrolyte. "Perhaps it is strictly accurate to say that the difference of potential is produced by the contact, and that the current which is maintained by it is produced by chemical action."* And, lastly, that in a series of cells the electromotive force is due to the sum of the differences of potential produced by all the contacts.

The above quotations may be taken as affording the plainest notion of the new contact theory; and it will be seen that its fundamental propositions are briefly these:

I. That two plates of different metals in one liquid are at the same potential when insulated and separated; i.e. there is *no* difference of potential due to chemical affinity.

II. In a cell series the gradual rise in potential, or the electromotive force, is due only to the dissimilar metallic contacts.

III. The chemical action in the battery is the result rather than the cause of the difference of potential, and is looked upon as an accompanying action rather than as the actual creator of the current, it having little or no share in the production of the difference of potential between the terminals.

These are, I venture to think, points not to be admitted as proved without further inquiry, and against which, as I shall hope to show, some grave if not insuperable objections may be urged, founded on other experimental evidence.

The first question to be settled is, then, whether in a series of cells the *whole* of the difference of potential between the terminals is due to the contacts, as above stated, or whether *any* portion is due to the tendency towards chemical combination existing between the metals and the electrolytes; and, as a consequence, whether in a single cell the plates are at the same potential or at different potentials, owing to the difference of chemical action upon them. Now I think this point will be sufficiently proved if we can establish by experiment, (i) that a battery of cells can be constructed without any dissimilar metallic contacts and with terminal plates of the same metal, and which shall yet exhibit difference of potential and continuous current; for if this is possible, it must follow that chemical affinity *alone* is capable of *creating* electromotive force as well as of maintaining a current, and that, in an ordinary cell-series, *some* part at least of the electromotive force is due to this cause, whilst the remainder is the result of the metallic contacts that may exist. Or (ii) if we can establish directly that the two plates in one cell are not at the same potential, as stated by more than one authority.

With regard to the first point, it will be remembered that an old experiment of Faraday's proved that a current can be maintained and decomposition effected by a single cell where there is no dissimilar contact. It is not easy to see how this experiment can be explained by any form of contact theory; indeed it appears unanswerable. But in order to leave no point unsettled by experiment, it seemed desirable to try and arrange a series of cells in which all dissimilar contact was absent, so that the difference of potential due to chemical action might be separated from that due to the contacts and rendered visible by the electroscope.

---

* *Electricity and Magnetism*, pp. 53–5.

It is obvious that we can make no attempt to do this unless we can in some way or other obtain a battery with terminals of the same metals; for otherwise the very junctions with the electroscope introduce what we want to eliminate, viz. dissimilar metallic contact. But the following is a method by which this can be accomplished. If plates of lead and copper be placed in nitric acid the lead is positive to the copper, since it is most acted upon; but if lead and copper be placed in solutions of alkaline persulphides, then the copper is most readily acted upon and is positive to the lead; that is, the positions are reversed.

Now, if we place in a cell *A* dilute nitric acid and a copper and a lead plate, we cannot join up another cell of the same sort in series without introducing contact.

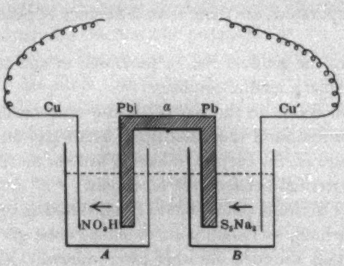

Figure 1.

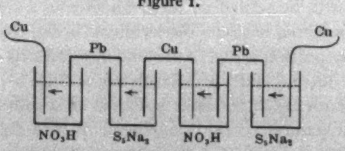

Figure 2.

But if, instead of using a cell containing acid, we place next *A* a cell, *B*, containing sodic pentasulphide, and bend over the lead plate of *A* to dip into the liquid in *B*, and place in *B* also a copper plate, we shall then have two cells joined up in series without dissimilar contact and with similar metals for terminals; and yet the action of the liquids on the metals is such that in *A* the lead is positive to the copper Cu, and in *B* the copper Cu′ is positive to the lead. Hence there is a regular rise in potential in passing through the two cells; and on joining CuCu′ by a copper wire a current flows through both cells in the same direction, and the general effect is to urge round a current in the direction shown by the arrows. It is obvious that we need not limit ourselves to two cells. By forming a pile of alternate cells filled with acid and alkaline persulphide, connected by bent copper and lead plates alternately (figure 2), we shall be able to accumulate difference of potential to any extent; and if the number of acid and alkaline cells be equal, we shall always end with a plate similar to that with which we began. Such a battery will exhibit a difference of potential between its two terminals when the circuit is opened, and will give a current when it is closed. In it we have nothing but chemical action to rely upon both for creating electromotive force and for maintaining the current. We have no dissimilar contacts; and as the terminal plates are similar, we can effect the junctions with the electroscope without introducing an unbalanced dissimilar contact. I have constructed such a battery of sixty cells; and by the kindness of Prof. Guthrie, to whom my thanks are due, I have been permitted to compare its potential with that of a Daniell's cell, by means of a quadrant electrometer belonging to his laboratory. By this means it is at once seen that the difference of potential increases proportionally to the number of cells, the electromotive force of four cells being about equal to that of one Daniell. Joined up with a galvanometer it indicates a current, which, however, rapidly falls off in strength, owing to the formation of an insoluble cupric sulphide upon the copper plates. Joined up in opposition to a single Daniell's cell, with a galvanometer included in the circuit, I find that it requires from four to five cells to balance the force of the Daniell at first immersion; but after leaving it to work on short circuit for 2½ hr. its electromotive force had fallen off 50 per cent; it then required about eight cells to bring the needle to zero. This gives for the electromotive force of two cells at first about 0·5 of a volt; or the whole sixty cells are equal nearly to fifteen Daniell's cells. It readily effects the decomposition of many electrolytes, and exhibits therefore every property of an ordinary cell-series. Above all, it will therefore be noticed that since there is a regular rise in potential in passing from cell to cell, and as all parts of each plate must be at the same potential, that rise can only take place at the surfaces where the active metals are in contact with the electrolyte (that is, at the seat of the chemical action), and that therefore two metals in one electrolyte *cannot* be at exactly the same potential. But I find that more direct evidence still of this fact is to be found in an experiment of Faraday's, which seems to have escaped the notice of the contact theorists.

In his *Experimental Researches* he gives the following fact: "I took a voltaic apparatus, consisting of a single pair of large plates, namely a cylinder of amalgamated zinc and a double cylinder of copper. These were put into a jar containing dilute sulphuric acid, and could at pleasure be placed in metallic communication by a copper wire connecting the two plates. Being thus arranged, there was no chemical action whilst the plates were not connected; on *making* the contact a spark was obtained. In this case it is evident that the first spark must have occurred before metallic contact was made, for it passed through an interval of air; and also that it must have tended to pass before the electrolytic action began, for the latter could not take place until the current passed, and the current could not pass before the spark appeared." "Hence," he says, "I think there is sufficient proof that the zinc and water were in a state of powerful *tension* previous to the actual contact."* It is difficult to reconcile this with the experiment of the half-disks and drop of water made by Sir W. Thomson. But, at any rate, a consideration of the whole of the facts would seem to point out that the only safe conclusion is, that in any series of cells of any sort the electromotive force is a complex effect, being due to the algebraical sum of all the differences of potential due to dissimilar contacts *plus* the algebraical sum of the differences of potential due to the chemical affinities of the metals and electrolytes *minus* any opposing force due to polarization etc.; and that so far from being the exclusive cause, the contacts can only be said strictly to have a share in producing the difference of potentials between the extremities of a battery.* And, lastly, we may with advantage compare the statements of the contact theory with certain other well-ascertained facts. Such statements, for instance, as these: "If we close the circuit by connecting the metals by a wire, we then have constant separation of electricities at the point of contact of different metals, and constant recombination attended with decomposition through the electrolyte."† "The electricities separated at the metallic junctions recombine through the water", "whilst the current flows the water is decomposed"‡—which seem based on the assumption that the principal seat of the electrical actions is *not* to be looked for at the seat of the chemical actions. But, now, how does this fit in with those cases of electrochemical inversions noticed by De la Rive, where the direction of the current in a cell is *reversed* by simply diluting the electrolyte. Thus zinc is negative to tin in strong nitric acid, and mercury negative to lead; but in weak nitric acid the positions are reversed. Hence, if couples be formed of these metals in strong nitric acid, and the acid be gradually diluted, the current first ceases and then is reversed in direction.

---

* *Experimental Researches in Electricity*, Series viii, ¶ 956.

Here, without altering the metallic junctions, we can at pleasure alter the direction of the current, and therefore also the direction of the fall in potential, since the current must flow from high to low potential. This seems conclusive that the chemical electromotive force must be even greater than the contact electromotive force. This reversal of the current, by changing the seat of the chemical activity, may be shown in another way, depending on the application of a very old principle. If plates of copper and clean iron be connected by copper wires with a galvanometer, and the iron rendered passive by immersion for a moment in strong nitric acid, then if these plates are plunged into dilute nitric acid the galvanometer indicates a strong current going through the cell from the copper to the iron. If they be removed for an instant and the iron plate touched, on again immersing the current is found to be reversed. Or we may again change the conditions, and notice that it is not sufficient to have merely two different metals and an electrolyte to form a cell. If plates of pure gold and platinum be placed in nitric acid, the most delicate galvanometer detects no current, and the same for many other pairs of metals and electrolytes.

Here we have contact of different metals producing its difference of potential; yet no current flows round "decomposing the electrolyte", as, according to the contact theory, it should do; but the instant we give play to chemical combination the ordinary results ensue. If the extremities of the copper wires from a galvanometer be attached to iron plates, and these plunged into separate cups of dilute nitric acid, on making connexion between the two cups by a bent iron plate dipping into each no current is detected. On making one limb of the connecting plate passive and re-immersing, a strong current is visible; and we find that we have the direction of the current completely under command by making any of the four plates more or less acted on than the other three.

---

* Amounting in a Daniell's cell perhaps to 60 or 70 per cent of the whole electromotive force.
† Tait, *Thermodynamics*, § 116.
‡ Jenkin, *Electricity and Magnetism*, p. 54.

If these experiments are to have any importance attached to them, it can scarcely be doubted that they land us in conclusions similar to the others, namely: that we must look for the principal source of the electrical disturbance at that place where the greatest chemical activity is being brought into play; and that whereas contact of metals is in itself productive of definite electrical separation, there is in the battery another cause assisting in the production of difference of electrical potential between the terminals, viz. the potential chemical combination between the metals and electrolytes existing when the circuit is open—the energy of the current produced when the circuit is closed being, of course, the equivalent of this potential energy which disappears.

A NEW METHOD OF CREATING ELECTRIFICATION

By SIR AMBROSE FLEMING, D.Sc., F.R.S.
Honorary Fellow of the Institute of Physics

Received 6 *March* 1939. *Read* 28 *April* 1939

It is somewhat hazardous to call any electrical experiments "new" in view of the enormous amount of research in that subject past and current. Nevertheless, the experiments about to be now shown have not, as far as I can find, been put on record precisely as here described and hence I think their novelty can be tentatively assumed.

The fundamental fact to be noticed is that when certain insulating materials, the best of which appears to be pure silica (SiO_2), in a certain state of fineness of powder are allowed to fall down a tube and strike a metal plate perforated with small holes or a metal wire gauze of zinc, copper, nickel or iron, the metal plate becomes electrified positively and the insulating powder negatively. There are however certain conditions to be satisfied. The powder, which may be of silica, sulphur, silver, or river sand or of certain other materials, must have grains of nearly equal size and must be dried so as to be free from all moisture. Also the size of those grains must be such that when they fall on the perforated metal sheet or gauze they fall through the apertures and do not accumulate on the metal. There are wide limits permissible in the ratio of area of hole or mesh-aperture to size of grain.

Thus I find that with silica granules about 0·01 in. in diameter and a perforated zinc plate with holes about $\frac{1}{16}$ in. in diameter and interstices of the same width, the effect is well shown. But it is also exhibited nearly as well if copper wire gauze is used, the apertures being about $\frac{1}{25}$ in. in width so that there are 600 holes to the square inch in place of 70 for the zinc plate. The electrification is not so great when nickel or iron wire gauze of the same mesh is used. It can also be shown when dried and sifted silver or river sand is used as the powder, and less perfectly with crushed sulphur. To obtain the best effect the powder must strike the perforated plate with a certain velocity, as it is this blow which creates the electrification. The powder must not heap up or stay on the plate but fall instantly through the holes.

The following arrangement works well. In a metal tray or dish three blocks of paraffin wax are placed, and on them a circular metal dish which can be connected by a wire with a gold-leaf electroscope. On this dish is placed an ebonite tube about 6 in. high and 4 in. in diameter. On the top of this is placed a sheet of perforated zinc or copper wire gauze which also can be connected at pleasure with the electroscope. The powder, say pure silica, as above described is placed in a tin funnel which has a metal tap at the end of its nozzle, and beyond that there is a length of metal tube a quarter or half an inch in diameter and a foot or several feet in length. The end of this tube is held about 2 or 3 in. from the metal plate and the tap is slowly opened. The powder then strikes the plate and the attached electroscope indicates a strong positive electrification. If the insulated tray catching the powder which falls through the apertures in the plate is connected to the electroscope it will be found to be negatively electrified.

The material of the tube down which the powder falls has no effect on the result. The tube may be of brass, iron, glass or ebonite. It is all the same. This shows that the effect is not due to friction of the powder falling down the tube, but to the impact of the particles on the plate. The metal of which the plate is made and the material of which the powder consists affect the potential to which they are electrified as regards amount but not as regards sign. The plate becomes positive and the transmitted powder negative. In figure 1 are shown the arrangements above described for exhibiting this impact electrification. With this arrangement the powder has to be gathered up from the tray and put back into the funnel to try another experiment.

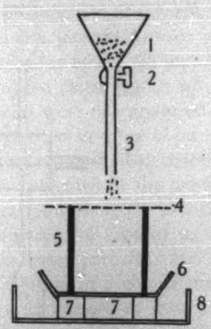

Figure 1.

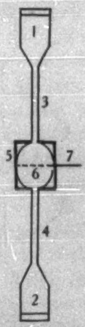

Figure 2.

Figure 1. 1, metal funnel for containing the powdered material; 2, control tap; 3, fall tube; 4, perforated metal plate or metal gauze; 5, ebonite cylinder; 6, insulated disk; 7, paraffin blocks; 8, tray for catching powder.

Figure 2. 1, 2, metal hoppers for containing powdered silica or other material; 3, 4, metal fall tubes; 5, ebonite cylinder; 6, partition of perforated zinc or metal gauze; 7, wire connexion from partition to an electric condenser.

But I have devised a plan in which a certain small quantity of the powder is used again and again without waste or loss. It is as follows. Two glass bottles or tin canisters, figure 2, have brass tubes fixed in their necks. These brass tubes are fixed into the opposite ends of a short and wide ebonite tube. In this latter a disk of perforated zinc is placed as a diaphragm across its centre. The arrangement is then like an hour-glass or egg-boiler. If one canister is filled with powdered silica or any other such material and the appliance placed so that this canister is at the top, the silica falls down through the zinc diaphragm and collects in the bottom canister. The apparatus can then be turned over like an hour-glass and the silica powder again falls on the perforated zinc diaphragm. At each such passage positive electricity accumulates on the zinc plate and by an external wire connected to the diaphragm the charge can be given up to an electric condenser consisting of two metal plates with a thin layer of ebonite between them. If then these plates are separated, their capacity will be reduced and the potential correspondingly raised. We can thus obtain electricity at very high potentials or many thousands of volts.

By a small modification of this last arrangement we can make an electrical machine which will continuously provide electricity at very high potentials as follows. A cylinder of ebonite has hollow ebonite axes fixed in its flat ends, figures 3 and 4. These are supported in wood bearings so that the cylinder can rotate about the hollow axes. Metal tubes are fixed in this drum like spokes of a wheel, and each tube carries at its outer end a metal canister or hopper in which powdered silica can be contained. As this drum and its spokes revolve, the powder will fall down out of the canisters at the high position and be collected again in those in the lowest position.

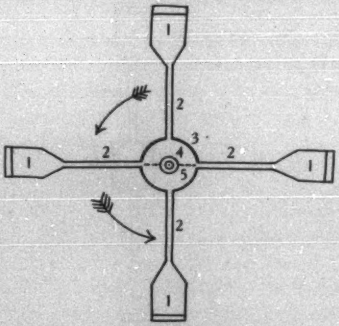

Figure 3.

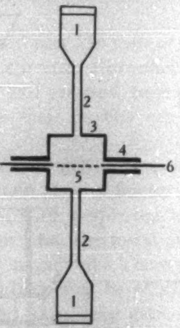

Figure 4.

Figure 3. A new electrical machine. 1, metal hoppers for delivering or receiving the powdered silica or other powder; 2, metal fall tubes; 3, ebonite cylinder; 4, hollow ebonite axes on which the cylinder revolves; 5, a fixed diaphragm of perforated zinc.

Figure 4. Sideway view of the machine in figure 3. 1, metal hoppers; 2, metal fall tubes; 3, ebonite cylinder; 4, hollow ebonite axes; 5, fixed diaphragm of perforated zinc; 6, metal wire connexion from diaphragm to the electric storage condenser.

Across the inside of the ebonite drum is fixed a rectangular partition of perforated zinc. This is carried on fixed metal axes which pass loosely through the hollow ebonite axes of the drum, and therefore the partition does not rotate with the drum. As the drum is rotated the silica powder is continually being dropped on the upper side of the zinc partition and passing through it is collected again by the radial tubes in hour-glass fashion. The charges of positive electricity given to the zinc partition are led away by the metal axes to an electric condenser. By separating the plates of this condenser at intervals we can then obtain electric charge at very high potentials.

This novel type of electrical machine does not depend on friction or induction but on the electrification created when the silica powder falls through a perforated zinc plate.

In seeking for possible anticipations of the results here recorded, my attention was drawn to some experiments of Faraday mentioned in vol. 2 of the *Eighteenth Series* of his *Experimental Researches in Electricity*, published in 1843.

A workman in the employ of Sir W. Armstrong had noticed that steam escaping from a steam boiler sometimes gave an electric shock to a hand held in it. Faraday took up the investigation of this effect in his usual exhaustive manner. He used a steam boiler with internal furnace insulated on blocks of resin. He used jets of various forms at the end of the pipe by which the steam escaped and also different forms of insulated plates against which the steam was blown. He soon found that electrical effects were not produced if the steam was dry, but only if the steam carried in it particles or drops of pure water. The presence of any salt or acid in the water droplets destroyed all electrical manifestations. Also he proved that temperature was not concerned in the production. The function of the steam as such is confined to carrying along the particles of water.

It then occurred to Faraday to try if a jet of compressed air could act as the vehicle of the water particles. His anticipation proved correct. If air was compressed by a pump in a copper vessel and made completely dry, then when it escaped by a jet against an insulated plate no electrical effect was created. If, however, the air was made damp with pure water, then the electrical phenomena took place. Lastly he had the idea of substituting for the water particles some powder of an insulating substance such as sulphur, shellac or silica and he found that when a jet of dry air carrying particles of these insulators was allowed to impinge on a cone made of wood, metal, or other substances, the particles which bounced off were electrified.

I repeated some of these experiments but could not obtain by the air-blast method results nearly as good as those obtained by my method of allowing streams of particles of insulators to fall down a tube and strike a sheet of perforated metal or metal gauze. Faraday however had noticed the great superiority and constancy of results when silica powder was used. He also noted, as I did, some anomalous results.

Thus a rod of silica rubbed with silk, wood or even metal in the mass becomes positively electrified. But when the silica dust is allowed to fall on metal gauze or impinge on a wood cone the silica flies off negatively electrified. This seems to indicate that there is something not yet explained and that the electrification involves more than mere friction.

Returning then to the experiments I have exhibited, viz. the impact of falling particles of insulators on perforated metal sheets or metal gauze, it will be noted that very good results are obtained when zinc is used as the metal sheet and silica as the powder. I was at first inclined to attribute this partly at least to the fact that zinc is highly electropositive and that its atom readily gives up 1 or 2 electrons from its outer ring. But when I later on found that copper wire gauze gives almost as good results with silica, the above suggestion seemed inadmissible. Again no explanation has yet been given why silica is so easily electrified positively in the mass and yet in the powder takes a negative charge by impact against either zinc or copper, which metals lie so far apart in the electrochemical series. There seems therefore to be much room left for further investigation.

While I submit then that Faraday's experiments above described do not anticipate mine so as to deprive them of novelty, it is clear that much additional research is required to obtain an understanding of the electric phenomena involved. It is with the object of suggesting such research that I have brought them to the notice of the members of the Physical Society.

NOTE ADDED 13 APRIL 1939

I find that it is not necessary to use any tube to guide the falling powder. If the silica powder or other material is poured out of a jug and allowed to fall on the perforated metal sheet in a stream, the electrical effects are produced as stated. It has been suggested to me that since quartz or silica is piezoelectric this might be the cause of the electrification. But this is negatived by the fact that Rochelle salt, which is strongly piezoelectric, gives no electrification by my methods, whilst sulphur, which is not piezoelectric, gives good electrification as has been stated above. Hence the facts described cannot, I think, be in any way due to piezo-electrification.

FURTHER MEASUREMENTS OF THE THERMAL AND ELECTRICAL CONDUCTIVITY OF IRON AT HIGH TEMPERATURES

By R. W. POWELL, B.Sc., Ph.D., Physics Department,
The National Physical Laboratory

Received 21 *November* 1938. *Read* 10 *February* 1939

ABSTRACT. The author's previously published results for the thermal conductivity of Armco iron up to a temperature of 800° C. have been confirmed by two independent methods. The first was a comparative method involving longitudinal heat-flow, and the second an absolute method in which the heat flowed radially from the centre to the circumference of a thick-walled cylinder. By means of the latter method the thermal conductivity has since been determined up to a temperature of just over 1000° C. The thermal conductivity of this sample of iron is found to decrease steadily as the temperature is raised through the magnetic transformation region, and to reach a minimum value of 0·065 cal./cm.-sec.-° C. in the vicinity of the α-γ transformation point.

Determinations of the electrical resistivity of the same iron have been extended to a temperature of 1430° C., and the Lorenz function has been evaluated over the range covered by the experiments on thermal conductivity. From 200 to 800° C. this function has unusually high values of $(0{\cdot}72 \pm 0{\cdot}02) \times 10^{-8}$ but above the magnetic transformation point a steady decrease occurs, a value of $0{\cdot}60 \times 10^{-8}$ being reached at 1000° C. The Lorenz function of γ iron is thus seen to be in reasonable agreement with the value of $0{\cdot}58_8 \times 10^{-8}$ indicated by Sommerfeld's theory.

§ 1. INTRODUCTION

In 1934 the present author published⁽¹⁾ the results of an absolute determination of the thermal conductivity of a nickel-plated rod of Armco iron, up to a temperature of 800° C. It was possible to allow for the effect of the nickel-plating and to derive values for the thermal conductivity of the iron over this temperature range. At about the same time Shelton⁽²⁾ published some results for an iron of somewhat similar composition over the temperature range 100 to 500° C. which agreed closely with the aforementioned determination.

Since that time the results of two other determinations of the thermal conductivity of Armco iron to high temperatures have been published, one by Maurer⁽³⁾ and the other by Hattori⁽⁴⁾. For the purpose of comparison these four series of experimental data for certain temperatures are set out in table 1. The chemical compositions of the four specimens are given in table 2.

Up to a temperature of 600° C. the four sets of data are in no case found to differ by as much as 5 per cent, and over the range from 200 to 500° C. the results obtained by Powell, Shelton and Maurer only differ by about 1 per cent, whilst those

Table 1. Comparison of four sets of data for the thermal conductivity of iron

Temperature (° c.)	Thermal conductivity (cal./cm.-sec.-° c.) as determined by			
	Powell	Shelton	Maurer	Hattori
30	0·173	—	0·173	0·168
100	0·163	0·159	0·161	0·159
200	0·147	0·145	0·146	0·143
300	0·132	0·131	0·131	0·127
400	0·116	0·117	0·117	0·112
500	0·103$_5$	0·104	0·104	0·099
600	0·093	—	0·095	0·092
700	0·082	—	0·090	0·090
800	0·071	—	0·086	—
900	—	—	0·083	—
1000	—	—	0·083	—
1100	—	—	0·085	—
1200	—	—	0·087	—

Table 2. Chemical compositions of the four specimens for which results are given in table 1

Observer	Description of iron	Percentage composition of iron						
		C	Si	Mn	P	S	Cu	Fe (by difference)
Powell	Armco iron	0·023	0·007	0·025	0·007	0·020	—	99·918
Shelton	Basic open hearth iron	0·02	—	0·03	0·042	0·005	—	99·903
Maurer	Armco iron	0·01	Trace	0·02	0·011	0·040	0·05	99·869
Hattori	Armco iron	0·015	0·010	0·032	0·003	0·030	0·013	99·897

by Hattori are from 3 to 4 per cent lower. Agreement of this nature is very satisfactory, for the measurement of thermal conductivity is one which is known to be readily susceptible to experimental errors. In fact, in the opinion of the writer, a small source of error which would lead to too low a result appears to have been overlooked in Hattori's experiments. His specimen was in the form of a rod 14 mm. in diameter and 100 mm. long. A longitudinal-heat-flow method was employed, the temperature-gradient being measured by thermocouples inserted in holes 2 mm. in diameter, 8 mm. in depth and 4 cm. apart. In the centre plane of each hole the cross-sectional area of the iron has thus been reduced by just over 10 per cent. This will cause the lines of heat flow to become more crowded at these points, and an assumption that the flow is rectilinear will lead to too low a value for the conductivity.

In order to obtain some idea of the error involved, potential leads were attached to a metal rod of the above size at a distance of 4 cm. apart, and measurements were made of the electrical resistance of this section of the rod. Holes 2·25 mm. in diameter were then drilled in the rod to a depth of 8 mm. at points immediately opposite the potential leads, after which the measurement of electrical resistance was repeated. The presence of the holes increased the resistance by about 2·5 per cent.

In view of this result it is considered that Hattori's values for the thermal conductivity of Armco iron should be increased by some 2 per cent. When this is done all the results agree to within about 2 per cent up to 600° c.

Beyond 600° c., however, the results obtained by both Maurer and Hattori decrease less rapidly with increase in temperature than do those obtained by the writer, and at 800° c. the difference is seen to amount to about 20 per cent. It is of course possible that a real difference, which can be attributed to some difference in chemical composition or in heat treatment, exists between the conductivities of these specimens. In view, however, of the general tendency for the thermal conductivities of iron and steels of widely different compositions to converge towards a common value as the temperature is increased, such an explanation appears unlikely.

As the iron tested by the writer has been used as a comparative standard for the determination of the thermal conductivities of other materials(5, 6), and as further measurements of this kind are in progress, the removal of any doubts regarding the thermal conductivity of the iron in question is a matter of vital importance.

Some time ago the comparative method was used in an attempt to extend the work on iron to much higher temperatures(7). Results were obtained over the range 800 to 1100° c. but were thought to be rather uncertain at the highest temperatures in view of contamination of the thermocouples pegged into the iron. In the course of these experiments, however, additional values, which agreed with those previously published for the conductivity of Armco iron, were obtained at temperatures just below 800° c. After the appearance of Maurer's results these tests were repeated for another specimen of the same iron, and the original results have again been confirmed. Quite recently, still more conclusive confirmation of the original results has been obtained by means of a totally different method in which the absolute thermal conductivity is derived from measurements involving a radial flow of heat. This method has made reliable determinations of the thermal conductivity possible up to just over 1000° c.

These additional measurements and results are described in the present paper.

§ 2. ADDITIONAL MEASUREMENTS MADE BY THE COMPARATIVE LONGITUDINAL-HEAT-FLOW METHOD

Two rods each about 1·4 cm. in diameter and 7 cm. in length were machined from the original 3-in. rods of Armco iron. These rods were then drilled and tapped to a depth of about 0·25 in. at one end, and joined together by being screwed over a short piece of rod. The composite rod was then turned down to a diameter of about 1·28 cm., and mounted up in a manner similar to that shown in figure 1 of a previous paper(6), within an enclosure which could be evacuated. In the present instance the upper rod of iron replaces the rod of graphite shown in this figure as the specimen under test. Three platinum and platinum-rhodium thermocouples were again pegged along the working section of each rod. The energy flowing in the lower rod was obtained from the difference between the temperatures indicated by a pair of thermocouples in this rod, together with a knowledge of the dimensions of the rod and its thermal conductivity at the mean temperature. When the guard tube was adjusted to prevent lateral interchange of heat, this amount of energy could be assumed to flow in the upper rod and used for the derivation of its conductivity. The continuous curve given in figure 1 of the present paper represents the results originally derived for the thermal conductivity of Armco iron over the temperature range 0 to 800° C., and is the curve from which the assumed values for the thermal conductivity of the lower rod have been taken. The experimental points represented by open circles were furnished by the foregoing method for the 1·28-cm. rods. Each point has been obtained in terms of an assumed value for the thermal conductivity at a somewhat lower temperature. Thus the points plotted at 612 and 620° C. were obtained in terms of assumed values at about 440° C., whilst those plotted at 678, 728 and 773° C. were derived from assumed values at about 540° C.

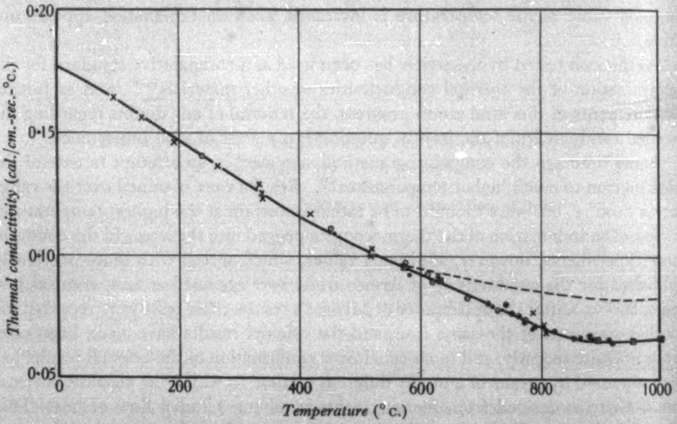

Figure 1. Variation of thermal conductivity of Armco iron with temperature. ——, Powell's original absolute determination (1934); ----, Maurer's determination (1936). Determinations by comparative method: ⊙, with $\frac{1}{2}$-in. rods; ●, with 1-in. rods. Determinations by absolute method: ×, first assembly; ⊗, second assembly; ,⊠ third assembly.

The broken line indicates the course of Maurer's curve after its deviation from that obtained by the present author, and it will be noted that at 540° C. the value assumed for the thermal conductivity is common to the two sets of data. The derived values however in the range 600 to 800° C. are seen to lie within 2 per cent of the original curve and to show no tendency to follow that obtained by Maurer.

The results of the later measurements made by the same method but with rods 2·54 cm. in diameter and 18 cm. in length are represented in figure 1 by solid circles. These points are again seen to lie very close to the original curve.

§ 3. MEASUREMENTS MADE BY THE ABSOLUTE RADIAL-HEAT-FLOW METHOD

The experimental arrangement used for the radial-heat-flow method is shown in figure 2.

The specimen, which was also machined from the original 3-in. rods of Armco iron, consisted of a number of superimposed disks, each 6·3 cm. in outer diameter and having an axial hole 1·1 cm. in diameter. The two centre disks were each 2·54 cm. thick and above and below these were 10 disks each 1 cm. in thickness. In the two centre and upper eleven 1-cm. disks, holes just under 2 mm. in diameter were drilled (with a no. 49 Morse drill) parallel to the axis at four points on a diameter and about 2 mm. in from the curved surfaces. The bottom disk was of rather greater diameter and carried three vertical steel rods which fitted corresponding slots cut in all the other disks and enabled them to be so aligned that a thermocouple, insulated by fine twin-bore silica tubing, could be moved up and down within any of the four sets of holes cut in the upper disks. It was possible to use one

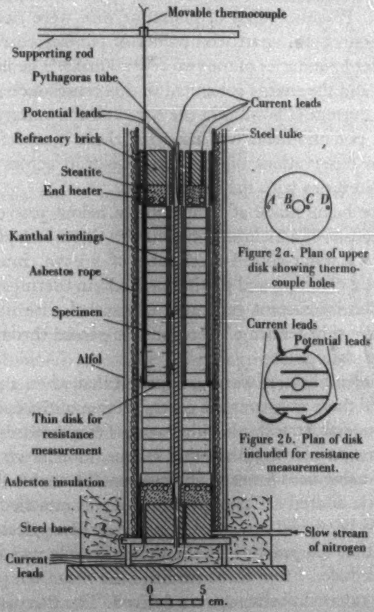
Movable thermocouple
Supporting rod
Pythagoras tube
Potential leads
Refractory brick
Steatite
End heater
Kanthal windings
Asbestos rope
Specimen
Alfol
Thin disk for resistance measurement
Asbestos insulation
Steel base
Current leads
Current leads
Steel tube
Slow stream of nitrogen
0
5
cm.
A
B
C
D
Current leads
Potential leads

Figure 2*a*. Plan of upper disk showing thermocouple holes

Figure 2*b*. Plan of disk included for resistance measurement.

Figure 2. General arrangement of apparatus for measurement of thermal conductivity by radial heat-flow method.

thermocouple for all temperature-measurements, and with it to explore the temperature-distribution in each of four positions within the specimen. The subdivision of the specimen into disks in this way was necessary to enable thermocouple holes of sufficient depth to be drilled. This procedure however has a further practical advantage in that the poor contact between each pair of disks helps to diminish the flow of heat towards either end of the specimen. To reduce this longitudinal heat-flow further, small heating-coils consisting of kanthal wire set in grooves cut in steatite blocks were placed above and below the specimen. The axial heater consisted of kanthal wire uniformly wound on a pythagoras tube about 7 mm. in diameter. Potential leads of platinum wire were tied on to the kanthal heater at points about 5 cm. apart, the points of contact corresponding approximately with the outer boundaries of the two central disks. The heater was connected to a 110-v. battery, and the energy generated in this centre section was derived from observations of the current C flowing in the wire and the voltage-drop V across the potential leads. A potentiometer was used for these measurements, the current being derived from observations of the potential-drop across a standardized resistance connected in series with the main heater.

When tests were being made at temperatures below 300° c. the temperatures were measured by means of a nichrome and eureka thermocouple and the specimen was surrounded by a water-cooled steel tube of 7·1 cm. internal diameter. At higher temperatures a platinum and platinum-rhodium thermocouple was used, the steel tube was heated by current generated in kanthal wire uniformly wound on mica insulation, and a slow stream of nitrogen was passed through the apparatus to prevent excessive oxidation.

During a test the end heaters were so adjusted that when a state of steady temperature was reached there was, over the centre section of the specimen, no appreciable gradient in temperature towards either end. Temperature-readings were then taken at five equidistant points within this section in each of the four holes, the same thermocouple being used for each observation. To enable the thermocouple to be readily held in the desired series of positions it was attached to a rod fixed to a carriage which could be moved up or down a graduated vertical column. The silica insulation ensured that the junction of the thermocouple was held approximately at the centre of each hole. From these readings the mean temperatures T_1 and T_2 for the internal and external positions were derived. The thermal conductivity K of the specimen was then calculated by means of the equation

$$K=\frac{VC\log_{10}(r_2/r_1)}{2{\cdot}73\,lJ\,(T_1-T_2)},$$

where l is the distance between the potential points on the centre heater, and r_1, r_2 are the mean distances of the two internal and two external thermocouple holes from the axis of the specimen. Division by J, the mechanical equivalent of heat, converts the thermal conductivity to the units previously employed, namely gram calories per square centimetre per second for a thickness of 1 cm. and a difference in temperature of 1° c. A typical set of results is given in table 3.

Table 3. Typical set of readings obtained with the radial-heat-flow method. Potential length l, 5·05 cm.; mean value of r_1, 0·77 cm. (holes B and C); mean value of r_2, 2·96 cm. (holes A and D); current in central heater, 3·512 amp.; voltage-drop across potential leads, 17·885; energy generated in central section, 62·8 w.

Position (cm. above lower potential point)	Thermocouple readings (μv.)						
	A	B	$(B-A)$	C	D	$(C-D)$	E*
0·5	6994	7091	97	7098	6999	99	9992
1·5	6996	7092	96	7100	7003	97	10043
2·5	6995	7088	93	7102	7005	97	9958
3·5	6991	7083	92	7097	7004	93	9674
4·5	6986	7077	91	7095	7002	93	9623
Mean	6992·4	7086·2	93·8	7098·4	7002·6	95·8	9858
Temperature (° c.)	767·2	775·8	8·6	776·9	768·1	8·8	1023·1

* In axial hole of pythagoras tube on which heater is wound.

The mean temperature was 772·0° c. and the mean value of $(T_1 - T_2)$ was 8·7° c.; hence

$$K_{772^\circ\text{c.}} = 0{\cdot}073.$$

The temperature-differences usually employed ranged from 8 to 12° c. At about 340° c., however, temperature-differences of 3 and 6·8° c. were used, the latter difference being obtained when the tube surrounding the specimen was water-cooled. At lower temperatures the temperature-differences were smaller, and it was on this account that thermocouples giving larger e.m.fs. were used for the measurement. In spite of the rather small temperature-differences involved, the departure of the points from the curve does not exceed about 3 per cent, and the accuracy of the result was confirmed by tests made at the same temperature but with a considerable change in the experimental conditions. The results shown in figure 1 were obtained with three separate assemblies, in each of which the axial heater was changed, as well as by varying the temperature-difference in the manner indicated above.

With the first assembly the previous results up to 800° c. were once more entirely confirmed. With the second assembly a series of points was obtained over the temperature range 700 to 920° c. at intervals of about 20° c. The purpose of this procedure was to ascertain the behaviour of the thermal conductivity of iron over a range of temperature which included both the magnetic and α-γ transformation points. The former of these is located at about 770° c. and the latter at about 910° c. In the third assembly a temperature of 1004° c., which extended the observations well into the γ-iron region, was reached. In these tests a temperature-difference of the order of 8° c. was used and this was considered to be sufficiently small to allow the presence of any appreciable discontinuity in the curve relating conductivity with temperature to be detected. As will be seen from the points plotted in figure 1, there does not appear to be any such discontinuity at the magnetic transformation point.

Beyond 800° C. the thermal conductivity continues to decrease as the temperature is increased, but the rate of decrease diminishes and a minimum value is reached in the neighbourhood of 910° C. The thermal conductivity of γ iron is thus seen to have a small positive temperature coefficient. This is in agreement with Maurer's conclusion, although his curve indicates absolute values some 25 per cent greater than those obtained in the present investigation. The possession of a positive temperature coefficient is also in agreement with the general behaviour of steels of the austenitic type, in which the iron is in the γ form.

§ 4. COMPARISON OF LONGITUDINAL-HEAT-FLOW AND RADIAL-HEAT-FLOW METHODS

With the object of extending our knowledge of the thermal conductivity of iron to higher temperatures a number of experiments have now been carried out by both the longitudinal-heat-flow and the radial-heat-flow methods, and it would seem desirable to make some comparison of their relative merits.

The chief source of error in the longitudinal-heat-flow method arises from lateral gain or loss of heat. This heat-interchange is normally made as small as possible by adjustment of the temperature of the guard tube, but these adjustments can occupy a considerable time before a satisfactorily matched and steady state is reached. The relative magnitude of any correction which has to be applied to allow for imperfectly matched conditions decreases as the quantity of heat flowing along the rod is increased. In the original experiments with rods of iron 3 in. in diameter the heat-flow in the rods at 800° C. was such as to establish a temperature-difference of some 60° C. between the two points, 19·4 cm. apart, on which the determination of thermal conductivity was based. The correction amounted to 1 per cent when the mean temperature of the guard tube differed from that of the rods by about 2° C. In the subsequent experiments in which this method was used, smaller rods were employed and thermocouples were attached to the rods at much smaller distances apart, but the temperature-differences from which the thermal conductivities were derived were still of the order of 50° C.

The radial-flow method has the advantage that much smaller temperature-differences can be employed. This renders the method particularly well suited for the study of metals whose thermal conductivity may vary non-linearly with temperature. The adjustment of the end heaters to prevent longitudinal heat-flow proves to be much simpler than is that of the guard tube in the longitudinal-heat-flow method, and, provided such losses are made negligibly small, the radial-flow method also has the advantage that no corrections need be applied. This appreciably shortens the time required for the evaluation of the result. The experiment itself has also been found to yield results considerably more quickly. A steady temperature at 800° C. can be reached about 8 hr. after starting from cold, whilst a change of 50° C. at that temperature requires about 3 hr. before the conditions are sufficiently steady for a set of readings to be taken.

The main trouble which arose when attempts were made to use the longitudinal-heat-flow method for tests above 800° C. was due to contamination of the thermocouples. In the original tests with 3-in. rods one interchangeable thermocouple had been used for all temperature-measurements, but this was no longer possible when the smaller rods were heated in an evacuated enclosure. The thermocouples were then pegged into the iron, and although temperatures above 1000° C. were reached it was frequently found in these experiments that the values obtained on cooling to lower temperatures were several per cent higher than before. This did not appear to be due to a change in the conductivity of the iron, for the electrical resistivity showed little alteration, and it was thought to result from the greater contamination and consequent lowering of the readings of the thermocouples attached at the hotter end of the rod. The radial-flow method is not subject to this trouble, since it enables all temperatures to be observed with one thermocouple, which can be renewed from time to time.

In the present experiments an opening has been left at the top of the apparatus to allow of the movement of this thermocouple. A certain amount of oxide has formed on the curved surfaces of the specimen, but this does not effect the path within the specimen over which the observations of temperature are made. It was considered necessary to pass a slow stream of nitrogen through the apparatus to prevent the thermocouple holes from becoming choked with oxide. A small amount of oxide was, however, formed around the holes in the upper disk, and it was the partial closing of one of these which terminated the third run when endeavours were being made to obtain a value at 1040° C. In further experiments these upper holes will be made somewhat larger, and it may then be possible to dispense with the stream of nitrogen.

§ 5. ADDITIONAL MEASUREMENTS OF THE ELECTRICAL RESISTIVITY

In all determinations of the thermal conductivity of electrical conductors, it is of interest to observe the behaviour of the so-called Lorenz constant, which is the product of the thermal conductivity and the electrical resistivity divided by the absolute temperature. In the earlier work on Armco iron this function was found to increase from a value of 0.62×10^{-8} at 0° C. to the unusually high value of 0.74×10^{-8} at 400° C. and, after remaining more or less constant over the range 400 to 700° C., to decrease to 0.70×10^{-8} at 800° C. Now that the thermal conductivity has been satisfactorily determined at higher temperatures it is of interest to study the further behaviour of this function.

A curve showing the variation of electrical resistivity with temperature is plotted in figure 3. This figure contains results from three separate experiments. Values up to about 1000° C. were obtained in the course of one of the attempts to measure the thermal conductivity by means of the longitudinal-heat-flow method, the thermocouples pegged into one of the iron rods 1·3 cm. in diameter being used as potential leads. These values were necessarily obtained with the two ends of the working section at different temperatures, and an independent experiment has also been carried out in the absence of such a gradient. A rod 3 in. in length and 0·238 cm. in diameter was machined from one of the original iron rods, and mounted up in the centre of a silica tube wound with nichrome wire and lagged with asbestos rope. The current was led into the specimen by means of iron wires, and thinner iron wires tied to the rod at points about 3 cm. apart served as potential leads. A platinum and platinum-rhodium thermocouple was located at the centre of the specimen. The specimen and its surrounding furnace were placed in an evacuated enclosure and heated to successively higher temperatures, at each of which resistance-measurements were made. The surprisingly high temperature of 1434° C. was reached before the nichrome-wound furnace burnt out. The circuit had presumably been retained by means of molten metal held within a shell of oxide.

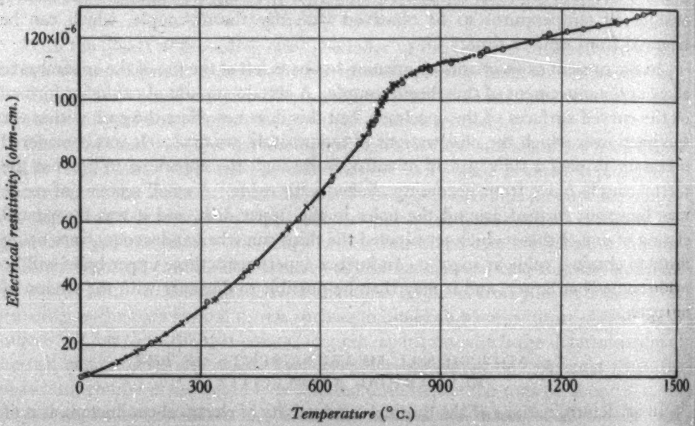

Figure 3. Variation of electrical resistivity of Armco iron with temperature. ⊙, rod 0·238 cm. in diameter uniformly heated in vacuum; ●, rod 1·3 cm. in diameter with longitudinal temperature-gradient; ×, disk 0·1 cm. thick, with radial temperature-gradient.

When the radial heat-flow method was first used for the determination of thermal conductivity, a disk only 0·1 cm. thick was included, as shown in figure 2, for the purpose of ascertaining whether measurements of electrical resistivity could be simultaneously carried out. This disk was insulated from the main specimen by disks of mica, and in order to increase its resistance it was slotted as shown in figure 2*b*. Current and potential leads of nichrome tape were welded to the disk in the positions shown in this figure and the resistance of the disk was determined by the usual method, which involved a reversal of the direction of the current to eliminate thermal e.m.fs. As the effective dimensions of the specimen were not known, the observed resistances were converted to specific resistances by means of a conversion factor derived from the specific resistance of the metal at normal temperatures.

The three sets of data are seen to agree to within some 1 or 2 per cent, which confirms the practicability of this last-mentioned method as a means of combining a measurement of specific resistance with one of thermal conductivity.

The curve drawn through the points in figure 3 is of the same form as that previously obtained for both iron and nickel in the region of their magnetic transformation points. There also appears to be a very slight decrease in the rate of change of resistivity with temperature in the neighbourhood of the α-γ transformation.

§6. THE LORENZ FUNCTION OF IRON AT HIGH TEMPERATURES

In figure 4 values of the Lorenz function of Armco iron are plotted over the temperature range 0 to 1000° c. These values have been derived from data read off from the curves drawn in figures 1 and 3. It is seen that the aforementioned decrease in the region of 800° c. commences after the iron has ceased to be ferromagnetic, and continues into the γ-iron region. No marked discontinuity accompanies the α-γ transformation, but it is a matter of considerable interest that the Lorenz function of iron in the γ form shows a strong tendency to agree with the theoretical value of $0{\cdot}586 \times 10^{-8}$ predicted by Sommerfeld on the assumption that both thermal and electrical conduction are the result of electronic agencies.

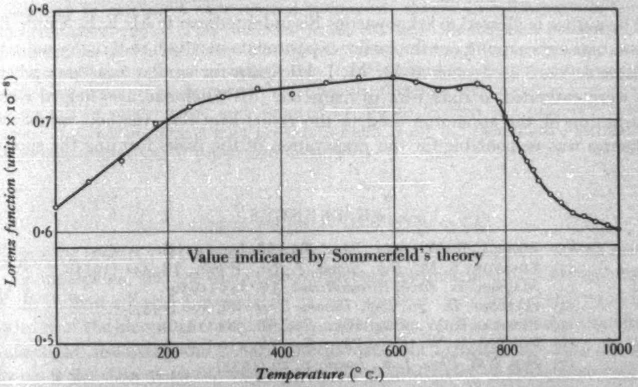

Figure 4. Variation of Lorenz function of Armco iron with temperature.

§7. SUMMARY OF RESULTS

Previously published results for the thermal conductivity of Armco iron up to a temperature of 800° c. have been confirmed in the first instance by means of a comparative method involving longitudinal heat-flow, and subsequently by an absolute determination by a radial-heat-flow method. Further use of this latter method has enabled the thermal conductivity to be satisfactorily determined to a temperature of just over 1000° C. The thermal conductivity of this sample of iron is found to decrease steadily as the temperature is raised through the magnetic transformation region, and to reach a minimum value of 0·065 cal./cm.-sec.-° C. in the vicinity of the α-γ transformation point.

Determinations of the electrical resistivity of the same iron are included up to a temperature of 1430° C.; they enable the Lorenz function to be calculated over the range covered by the experiments on thermal conductivity. From 200 to 800° C. this function has unusually high values of from $0{\cdot}70 \times 10^{-8}$ to $0{\cdot}74 \times 10^{-8}$, but above the magnetic transformation point a steady decrease occurs, and at 1000° C. the value is only $0{\cdot}60 \times 10^{-8}$. The Lorenz function of γ iron is thus seen to be in reasonable agreement with the value of $0{\cdot}586 \times 10^{-8}$ indicated by Sommerfeld's theory.

§ 8. ACKNOWLEDGEMENTS

The author is pleased to acknowledge his indebtedness to Mr E. E. Smith, B.Sc., for assistance in carrying out the earlier experiments in which rods 0·283 and 1·3 cm. in diameter were used; and to Mr M. J. Hickman for similar assistance when the tests were extended to rods 1 in. in diameter. Mr Hickman also helped with the construction of the apparatus used in the radial-heat-flow method, whilst Mr J. Balmanno was responsible for the preparation of the disks forming the specimen.

REFERENCES

(1) Powell, R. W. *Proc. Phys. Soc.* **46**, 659 (1934).
(2) Shelton, S. M. *Bur. Stand. J. Res., Wash.*, **12**, 441 (1934).
(3) Maurer, E. *Arch. Eisenhüttenw.* **10**, 145 (1936).
(4) Hattori, D. *Sci. Rep. Tôhoku Univ.* **26**, 190 (1937).
(5) Powell, R. W. *Proc. Phys. Soc.* **48**, 381 (1936).
(6) Powell, R. W. *Proc. Phys. Soc.* **49**, 419 (1937).
(7) *Rep. Nat. Phys. Lab., Lond.*, p. 26 (1933).

THE ELECTRICAL RESISTANCE OF NICKEL AMALGAMS

By L. F. BATES, D.Sc., Professor of Physics,
University College, Nottingham

AND

J. H. PRENTICE, B.Sc.

Received 9 *November* 1938. *Read in title* 10 *February* 1939

ABSTRACT. The electrical resistances of a series of nickel amalgams with concentrations between 0·013 and 0·246 g. of nickel per 100 g. of mercury were measured over the temperature range 20 to 300° c. A very marked permanent change in resistance was found to commence at about 225° c. This coincided with a change in the magnetic properties, for at low temperatures the amalgams are diamagnetic with no trace of ferromagnetism, whereas when once 225° c. has been exceeded, they exhibit pronounced and permanent ferromagnetic properties. It is suggested that, since the ferromagnetic metal in iron or cobalt amalgams can be concentrated and removed by the application of a magnetic field, the behaviour of nickel amalgams may provide a method for the quantitative estimation of cobalt in mixed solutions of cobalt and nickel salts.

§ 1. INTRODUCTION

Many researches have been made upon the electrical properties of mercury amalgams, and the earlier work has been summarized by Koenigsberger(1), Williams(2) and Edwards(3). It appears that there are several gaps in our knowledge of the electrical conductivity of amalgams, and, in particular, no study of the effects of dissolving the ferromagnetic metals in mercury has been made. In many cases the data as to the variation of the conductivity of amalgams with temperature are very meagre, and little attempt has been made to correlate the electrical properties of amalgams with other physical properties possessed by them. Recently, Bates and Day(4) examined the variation of the resistance of manganese amalgams with rise in temperature and obtained interesting results which they attempted to correlate with the magnetic properties found by Bates and Tai(5). As particular attention has lately been paid in this laboratory to the magnetic properties of ferromagnetic metals dissolved in mercury, it was considered desirable to examine their electrical properties at the same time, and accordingly the experiments on nickel amalgams described in this paper were made.

§ 2. EXPERIMENTAL PROCEDURE

Nickel amalgams are rapidly oxidized in the presence of air when the concentration of nickel is low, whereas more concentrated nickel amalgams do not appear to be attacked readily. The mercury used in this work was prepared by the Hulett(6) method as modified by Bates and Baker⁽⁷⁾, and the nickel amalgams were obtained by the electrolysis of solutions of known concentrations of nickel sulphate with the mercury as cathode until they were completely denuded of nickel, as was shown by the disappearance of the coloured ions. The freshly prepared amalgams were washed in distilled water and transferred as rapidly as possible to a conductivity apparatus similar to that employed by Bates and Day⁽⁴⁾, with the exception that the platinum contacts were now made thicker, as this appeared to give steadier working conditions with these amalgams. Immediately after the introduction of an amalgam, the apparatus was evacuated and heated for a long time at 150° C. to ensure the removal of traces of water and of occluded gases; as will be shown later, it was inadvisable to heat the amalgam until it boiled. By careful manipulation of the apparatus the amalgam was thoroughly mixed and a homogeneous thread was formed within the capillary tube. The apparatus was then connected through tubes containing alkaline pyrogallol and drying agents to a nitrogen cylinder, and a pressure of about 80 cm. of mercury was maintained upon the amalgam, a simple barometer tube being arranged as safety valve.

The resistance of the amalgam thread was measured by a double-potentiometer method; the falls of potential across a standard 100,000-Ω. resistance and across an adjustable standard resistance were respectively balanced against those across a standard 10-Ω. resistance and across the amalgam thread connected in a second circuit. A shallow trough of mercury formed in a block of paraffin provided a particularly fine resistance-adjustment in the latter circuit, and thermoelectric effects were eliminated in the usual way. The temperature variation of resistance of a pure mercury thread also was measured in the same apparatus, and to facilitate the comparison of the resistances of the amalgam and pure mercury threads the following procedure was adopted. The divergences of the experimental values for the resistance of the pure mercury thread from an arbitrary value R_T given by the formula

$$R_T = R_O\,(1 + 0{\cdot}0009\,T)$$

were plotted on a graph against the corresponding values of the temperature T. From the graph the divergence at any temperature could readily be deduced, and the true resistance of the mercury thread could be obtained by adding this divergence to the value of R_T, found by substituting the appropriate value of T in the above formula. The quantity R_O was so chosen that all values of the divergences were small and could be plotted accurately. The value of ΔR, the difference between the resistance of the amalgam thread and that of the mercury thread at the same temperature, was thus quickly obtained from the observed resistance R of the amalgam and the resistance of the pure mercury thread found in the above manner.

§ 3. RESULTS

Final measurements were made with a series of amalgams whose concentrations ranged from 0·013 to 0·246 per cent of nickel by weight. It was not possible to use amalgams of higher concentration because of lack of homogeneity and the difficulty of placing them in the capillary tube. The main results of the measurements are shown in figure 1 in which the values of $\Delta R/R_T$ for the several amalgams are plotted against the temperature. In every case the resistivity of the amalgams is less than that of pure mercury, and, except for the weakest amalgam, the curves show the same general form. There is a slight, steady fall in the numerical value of $\Delta R/R_T$ as the amalgam is heated above room-temperature, and a sudden and marked change takes place at about 220 or 230° c. Beyond this temperature the amalgam suffered a permanent change: the initial resistance-measurements could not be repeated when it was cooled, and the decrease in ΔR persisted. Apart from observations made after an amalgam had been heated above 200° c., no traces of temperature hysteresis were found. In the case of the weakest amalgam it is considered that the experimental values were unreliable, as the values of ΔR are of the same order as the maximum value of the experimental error, which was mainly determined by the accuracy with which the temperature of the thread could be maintained and recorded by means of mercury thermometers. Moreover, as has already been mentioned, weak amalgams are much less stable than strong ones and much more difficult to handle.

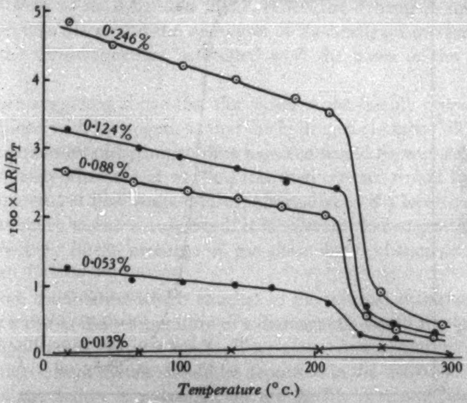

Figure 1. Variation of $\Delta R/R_T$ with temperature for nickel amalgams of stated percentages by weight.

The behaviour of $\Delta R/R_T$ in the region of sudden change is shown in more detail in figure 2, where the depression in the curve in the neighbourhood of 200° c. is considered to be a real phenomenon and not due to experimental error. It is difficult, of course, to obtain satisfactory measurements of $\Delta R/R_T$ in the steeply descending portion of the curve, because the phenomenon is irreversible, and once a particular temperature has been exceeded it is unprofitable to allow the amalgam to return to that temperature in the hope that representative resistance-measurements will be obtained. Above 300° c. the marked changes in resistance have ceased, but the amalgam is still slightly more conducting than pure mercury.

The magnetic properties of these amalgams have been measured by Mr C. J. W. Baker and one of us, by a special technique which will be described in a subsequent paper. We have found that at room-temperature the freshly prepared amalgams are diamagnetic and show no traces of ferromagnetism. This is in marked contrast to the behaviour of freshly prepared cobalt or iron amalgams which are always ferromagnetic, and in which the ferromagnetic metal may be moved and forced to occupy a tiny droplet by the action of a magnetic field. The droplet can be detached from the remainder of the amalgam and contains nearly the whole of the ferromagnetic metal. Similar behaviour is exhibited by a nickel amalgam only after it has been raised to a temperature above 225° C. We have thus found that within the limits of experimental error this magnetic change occurs at precisely that temperature at which the resistance changes begin. The magnetic changes appear to proceed rather more sharply than the electrical changes, presumably because the magnetic measurements have to be made in the presence of a magnetic field which aids the coagulation of the nickel particles. There is also a change in the magnetic properties, namely a decrease in the diamagnetic susceptibility, corresponding to the depression in the curve of figure 2 at 200° C., which is thought to be connected with the change in the magnetic properties of mercury in the presence of gas.

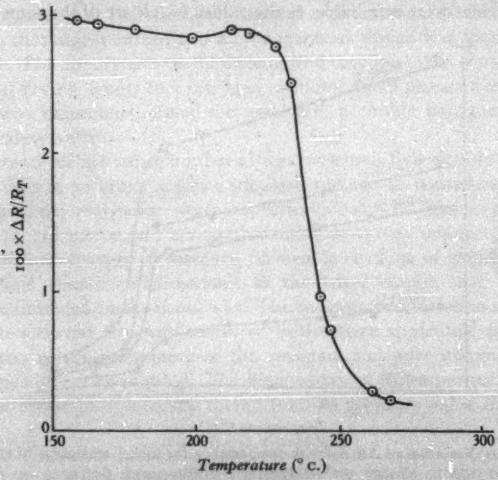

Figure 2. Variation of $\Delta R/R_T$ with temperature for a nickel amalgam containing 0·1472 per cent of nickel by weight.

Now, ferromagnetism is not an atomic phenomenon and its establishment in a nickel amalgam means that the nickel particles have coalesced to form magnetic domains. It seems clear that at lower temperatures in the freshly prepared amalgams the nickel atoms must be loosely combined with the mercury atoms or with hydrogen liberated during the electrolysis, in such a way that any holes in the 3*d* electron band of the nickel are filled. Mott and Jones(8) consider that in the case of nickel the electric current is carried by the *s* electrons which are scattered by transitions from the *s* to the *d* bands. From their work it follows that the resistivity of the metal is proportional to the cube root of the number of gaps or positive holes in the *d* bands. Consequently, anything which causes a reduction in the number of holes in the *d* bands will cause a decrease in the resistivity.

The presence of the nickel in the amalgam may be considered to distort ((8), p. 279) the first Brillouin zone of mercury and increase the number of electrons which overlap it. Consequently, the presence of nickel results in a decrease in resistance as long as its *d* band is filled. When the *d* band is opened, however, scattering can take place, and the resistance of the amalgam increases, while at the same time the ferromagnetism associated with the holes in the *d* band can be manifested.

It has been suggested above that the nickel in the freshly prepared amalgam is loosely combined with hydrogen, so that the hydrogen electrons fill the holes in the *d* bands. The quantity of hydrogen thus required would be very small, and, even if it were completely liberated at 225° C., less than 0·5 cm^3 would be set free in the magnetic apparatus at that temperature. Alternatively, if a loose coupling between nickel and mercury atoms is suggested, it is relevant that magnetic measurements with pure mercury in the presence of gas show that a change occurs in mercury below 200° C.

Apart from the interest which attaches to the unusual manufacture of a ferromagnetic by a rise in the temperature of a diamagnetic liquid amalgam, at least one interesting application suggests itself. If we electrolyse a solution containing both cobalt and nickel, both metals should be deposited in the mercury. The first can be separated by the action of a magnet on the freshly prepared amalgam, and the second by the action of a magnet on the amalgam after heating to 250° C. Whether this would lead to a quantitative method for the separation of small quantities of cobalt in the presence of nickel is not yet known. Experiments to clear up this question and to see whether the quantity of cobalt in a cobalt-nickel amalgam or the quantity of nickel in an iron-cobalt-nickel alloy can be accurately estimated, are now under consideration. The applicability of the method would be somewhat restricted by the fact that nickel amalgams containing more than 1 per cent of nickel are very pasty.

§ 4. ACKNOWLEDGEMENTS

We are indebted to the Government Grants Committee of the Royal Society for a grant with which apparatus used in these investigations was purchased.

REFERENCES

(1) Koenigsberger, J. *Handbuch der Elekt.* (Graetz), **111**, 654 (1923).
(2) Williams, E. J. *Phil. Mag.* **50**, 589 (1928).
(3) Edwards, T. I. *Phil. Mag.* **2**, 1 (1926).
(4) Bates, L. F. and Day, P. G. *Proc. Phys. Soc.* **49**, 635 (1937).
(5) Bates, L. F. and Tai, L. C. *Proc. Phys. Soc.* **49**, 230 (1937).
(6) Hulett, G. A. *Phys. Rev.* **33**, 307 (1911).
(7) Bates, L. F. and Baker, C. J. W. *Proc. Phys. Soc.* **50**, 409 (1938).
(8) Mott, N. F. and Jones, H. E. *Properties of Metals and Alloys*, p. 267 (1936).

THEORY OF THE WIDTH OF RINGS FORMED BY ELECTRON-DIFFRACTION

By G. P. THOMSON, F.R.S. and M. BLACKMAN

Received 25 *November* 1938. *Read* 24 *February* 1939

ABSTRACT. The widths of the diffraction rings formed by transmitted electrons are examined from the point of view of Bethe's theory. It is shown that these angular widths are much less than the range of angle of incidence giving strong reflection, an exception occurring in the Bragg case, where the beam enters and leaves by the same crystal face. This explains most of the discrepancy found by Trillat and Hautot between the theoretical and observed widths of diffraction rings.

§ 1. INTRODUCTION

In many experiments on electron-diffraction a fine beam of fast electrons is allowed to pass through a polycrystalline film, and the well-known diffraction rings are obtained when the beam on emerging falls on a photographic plate placed at right angles to it. The width of these rings has been known to be of the same order as that of the incident beam; i.e. the actual width due to diffraction is small.

This angular width has been the subject of a recent investigation by Trillat and Hautot(1), who used a very fine beam of electrons of energy about 40,000 ev. and took particular care to estimate the effect of the size of the beam on the width. They find the angular width to be about 1/15,000 in the case of nickel and gold films. The theoretical value to be expected on the basis of the dynamical theory due to Bethe(2) was also discussed and this, it was claimed, is of the order 1/60 or 1°. Such a discrepancy would be very serious.

It seems to us, however, that the real reason for the discrepancy lies in the fact that the conditions of the experiment are not those under which the theoretical width is derived. It is certainly true that Bethe's theory(2) will give a large reflection coefficient for a beam of 40-kv. electrons incident at an angle which may differ by as much as ±0·5° from the Bragg angle; but in a transmission experiment the width of the diffraction ring is determined by the range through which the reflected ray can vary with a fixed incident ray and any angle of incidence. We are hence dealing with the *deviation* and it is the *variation of the deviation* with angle of incidence that is the deciding factor. It will be shown below that this variation is indeed small compared with 1° in the cases which usually occur when, as in the case of fast electrons, the Bragg angle is small.

In the dynamical theory it is usual to distinguish two cases of reflection by a set of planes: (*a*) the Bragg case, in which the electrons emerge from the surface on which they fall, and (*b*) the Laue case, in which the electrons emerge from a different face of the crystal. This latter case is the one which would chiefly be expected in a transmission experiment, and here the deviation can indeed be shown to vary very little with the angle of incidence. The Bragg case is however exceptional, as will be shown in § 4.

§ 2. DYNAMICAL THEORY

The basic idea of the dynamical theory is to find the general solution of the Schrödinger equation for an electron inside a crystal, and to fit this solution to those for electrons outside the crystal. Starting with a beam of electrons incident on a face of a crystal, we should be able to determine all the beams emerging from the crystal with the help of the solutions and the boundary conditions.

In the kinematical theory the possible reflected beams are found most easily by using the reciprocal lattice. *O* and *M* are two points in the reciprocal lattice figure 1 (*a*); from *O* a vector *OP* is drawn in a direction opposite to that of the incident ray and of length $1/\lambda$, where λ is the wave-length. A sphere of radius $1/\lambda$ is drawn around *P*; if this sphere passes through the lattice point *M*, *PM* is the direction of a reflected beam.

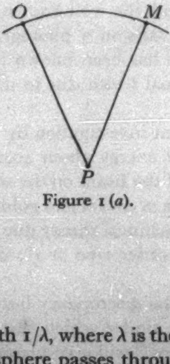

Figure 1 (*a*).

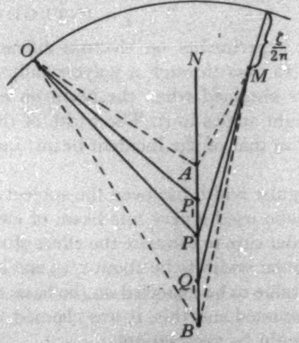

Figure 1 (*b*).

The dynamical theory starts from a solution consisting of a linear superposition of all pairs of waves of the type *PO*, *PM* even when the sphere does not go through *M*.

These have to be fitted on to the incidence wave, the boundary condition being that the component tangential to the surface should be continuous. If we take now the ray OP_1, where $|OP_1| = 1/\lambda_0$, to represent the incident ray, figure 1 (*b*), then the boundary conditions can be satisfied in the following manner. Through P_1 we draw a line P_1N parallel to the normal to the surface. Any ray drawn from *O* to a point on P_1N will have the same projection on the surface as *OP*, and hence will satisfy the boundary condition and can represent a primary ray in the crystal. As an example a possible primary ray OA has been drawn; one of the secondary rays associated with this ray is AM.

The ray OP represents the ray OP_1 modified by refraction. The difference $|PM|-|OP|=\zeta/2\pi$ in Bethe's notation⁽²⁾. It gives a measure of the deviation from the exact condition for reflection of the kinematical theory, and we should expect strong reflected rays only in those cases in which ζ is small. In the simplest example, when there is only one reflected ray, the dynamical theory shows that instead of one primary and secondary ray in the crystal there are two of each, represented by OA, AM and OB, BM in figure 1 (*b*). The distance PA, PB can be found from the detailed theory.

We are not concerned here with the details of the calculation; it suffices for our purpose to know that there is strong reflection when ζ lies in the range $\pm v/\kappa$, where v is the Fourier coefficient belonging to the reflection⁽²⁾ and $\kappa=2\pi/\lambda$.

If we are dealing with a parallel-sided slab the normals to the two surfaces are parallel, and hence the two secondary waves will have the same projection on the surface; they will therefore combine to form a single wave outside the crystal. This wave can be represented in the reciprocal lattice by a ray drawn from a point on P_1N to M. The position of this point, Q_1, is determined by the fact that the wavelength of the reflected wave is the same as that of the incident wave, i.e.

$$|Q_1M|=1/\lambda_0.$$

§ 3. THE DEVIATION IN THE LAUE CASE

We can now proceed to the calculation of the deviation. If we take the case of a parallel-sided slab (as we shall throughout) the construction is that given in § 2. We do not need to go into the discussion of the rays in the crystal at all. The incident ray in the reciprocal lattice and the normal to the surface through the end point of the ray having been drawn, the reflected ray follows immediately from a simple geometrical construction.

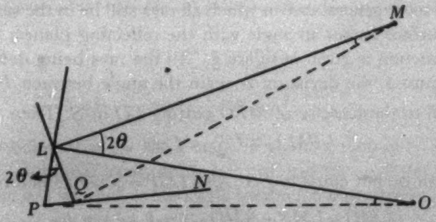

Figure 2.

In a transmission experiment we are dealing mainly with the Laue case of the dynamical theory. The deviation has its simplest form in the symmetrical Laue case, where the reflecting planes are at right angles to the surface. We may neglect the refraction too in this case, as it can be shown to be sufficiently small. The geometrical construction for it is given in figure 2. O and M are again two lattice points in the reciprocal lattice. For convenience in calculation we draw the rays LO, LM representing the incident and reflected rays when the Laue conditions hold exactly. $|OL| = |LM| = 1/\lambda_0$ and $OLM = 2\theta$, where θ is the (small) glancing angle of incidence on the reflecting planes. PO represents a ray whose glancing angle differs slightly from θ, and $|PO| = 1/\lambda_0$. Through P a line PN is drawn parallel to the normal to the surface; this will be parallel to the line bisecting MLO. A circle with M as centre and ML as radius will cut PN in Q. Then QM represents the direction of the reflected ray for reasons given in § 2, and the deviation is the angle between PO and QM. The distance $|PM| - |OP|$ is $\zeta/2\pi$ and is equal to $|PQ|$ to a sufficient degree of accuracy. It will then be seen that $|PQ| = \zeta/2\pi$. Hence

$$|LP| = |LQ| = \zeta/4\pi\theta \quad \text{and} \quad L\hat{O}P = L\hat{M}Q = \zeta/2\kappa\theta,$$

where $\kappa = 2\pi/\lambda_0$. Hence the angle between PO and QM is $M\hat{L}O + L\hat{M}Q - L\hat{O}P$ and $= 2\theta$, and the result holds approximately for all values of ζ. The deviation is independent of the angle of incidence and there is no additional width due to reflection.

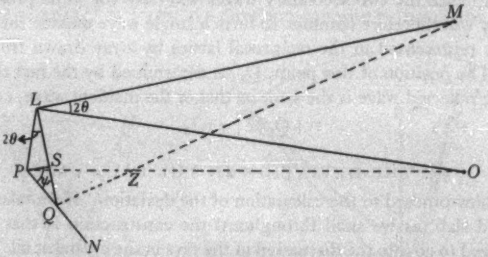

Figure 3.

In the rather more general case in which all rays still lie in the same plane and the normal to the surface makes an angle with the reflecting planes, this is no longer true. The construction is given in figure 3. All the rays being defined in the same manner as in figure 2, the deviation is again the angle between PO and QM. We draw PS parallel to the bisector of $M\hat{L}O$ cutting LQ in S. Then

$$|PM| - |OP| = \zeta/2\pi$$

as before, and can be put equal to PS. Also $L\hat{O}P = \zeta/2\kappa\theta$ as before, but

$$L\hat{M}Q = L\hat{M}S + S\hat{M}Q = \zeta/2\kappa\theta + \zeta \tan\psi/\kappa.$$

The deviation $O\hat{Z}M$ becomes $2\theta + \zeta\tan\psi/\kappa$.

We can now go on to consider the case where the normal to the surface does not lie in the same plane as the incident ray and the normal to the reflecting planes. In figure 4 we have again the same construction as in figure 3, except that PN rises out of the plane MLO which contains PO. The sphere with M as centre and LM as radius cuts PN in Q. QM is then the reflected ray.

Because of the large radius of the sphere we may represent the portion between L and Q as a plane perpendicular to the plane MLO. The line LSR is the intersection of the two planes, PS being as before parallel to the bisector of MLO. PR is then the projection of PQ, and RM is the projection of QM, on the plane MLO.

The true deviation is the angle between QM and PO which we shall call δ; the angle between RM and PO is η, and $Q\hat{M}R$ is ϵ. Then $\cos\delta = \cos\eta \, . \cos\epsilon$;

$$|PM| - |OP| = \zeta/2\pi,$$

and may be put equal to PS. The angle η has been found above in terms of ζ, and is equal to $2\theta + \zeta \tan\psi/\kappa$ if we denote the angle between PR and PS by ψ. If $R\hat{P}Q = \phi$,

$$|QR| = |PR| \tan\phi = |PS| \tan\phi/\cos\psi$$

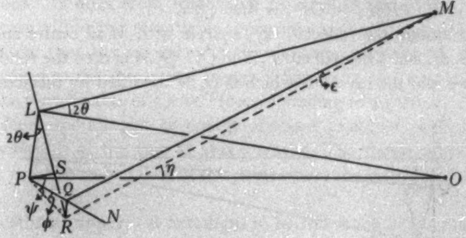

Figure 4.

unless ψ is near $\frac{1}{2}\pi$; hence

$$Q\hat{M}R = |QR|/|QM| = \zeta \tan\phi/\kappa\cos\psi.$$

Since θ is small as well as ζ/κ we can expand $\cos\delta$, $\cos\eta$ and $\cos\epsilon$ (except in very special cases $\phi \doteqdot \frac{1}{2}\pi$, $\psi \doteqdot \frac{1}{2}\pi$); the relation $\cos\delta = \cos\eta \, . \cos\epsilon$ yields

$$(\delta - \eta)(\delta + \eta) = \epsilon^2,$$

i.e.

$$\delta - \eta = \frac{\epsilon^2}{\delta + \eta} = \frac{\epsilon^2}{4\theta},$$

or

$$\delta = \eta + \frac{\epsilon^2}{4\theta} = 2\theta + \frac{\zeta}{\kappa}\tan\psi + \frac{\zeta^2}{\kappa^2}\frac{\tan^2\phi}{\cos^2\psi}\frac{1}{4\theta}.$$

It will be shown below that ζ/κ has a value of about 1/2000 in an average practical case. Hence the additional term can be left out, and the total deviation can be put equal to $2\theta + \zeta\tan\psi/\kappa$ where ψ is the angle between the projection of the normal on the plane MLO, and the line bisecting $M\hat{L}O$.

§4. THE DEVIATION IN THE BRAGG CASE

We consider now the Bragg case in which the electrons emerge from the surface on which they fall. We shall show below that this case is an unlikely one in a transmission experiment with fast electrons. Besides, the maximum of the diffraction ring formed in this way will be displaced considerably by the refraction and would therefore not form a part of the ring due to the Laue case. The Bragg case is however interesting because the deviation does actually vary considerably with angle of incidence, and we do obtain here the order of magnitude of 1° suggested by Trillat and Hautot.

In figure 5 we give the geometrical construction for determining the deviation in the simplest Bragg case, in which the surface is one of the reflecting planes. O and M are again the two lattice points in the reciprocal lattice; LO and LM are the incident and reflected rays inside the crystal when the Laue conditions hold exactly. These are drawn only for convenience in calculation. The length of LO is $1/\lambda$. P_1O represents the direction of the incident ray, PO the same ray modified by refraction; $|P_1O|=1/\lambda_0$, $|PO|=1/\lambda$. The position of P is obtained by drawing P_1N parallel to the normal to the surface; a circle with O as the centre and radius equal to OL will cut P_1N in P. $|PM|-|OP|$ is then $\zeta/2\pi$.

In order to obtain the reflected ray, a circle with M as centre and with radius equal to OP_1 is drawn. This will cut P_1N in Q_1. Q_1M is then the reflected ray. For convenience we add the ray QM, which is Q_1M modified by refraction.

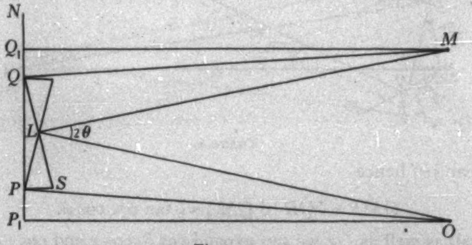

Figure 5.

The line P_1N will be perpendicular to the bisector of $M\hat{L}O$; from symmetry $L\hat{O}P=L\hat{M}Q$. By comparing figure 5 with figure 3, and from the remarks of § 3, it will be seen that $L\hat{O}P=\zeta/2\kappa\theta$, where $\kappa=2\pi/\lambda$ in this case. The angle between PO and QM is then $2\theta-\zeta/\kappa\theta$, as will be seen from figure 5. To get the true deviation we have to subtract from this the effect of refraction, i.e. twice $P\hat{O}P_1$. If V is the inner potential and E the energy of the incident electrons, it can be shown very easily that $P\hat{O}P_1=V/2E\theta$. Hence the total deviation is $2\theta-\zeta/\kappa\theta-V/E\theta$.

It will be seen that the variation of the deviation is very much larger than that found in the Laue case, as θ is very small. Furthermore the centre of the region, where $\zeta=0$, is displaced through an appreciable angle by the refraction.

In the more general case in which the normal has an arbitrary direction the deviation will have a more complicated form but will be of the same order of magnitude.

The glancing angle of incidence for electrons of the energy used in the transmission experiments is a few degrees. Since the crystals are also very small, about

200 A., the electrons will not emerge from the surface on which they fall unless it is one of the reflecting planes. In this case the projection of the surface on to the incident beam will be small compared with that of a randomly arranged surface. The intensity intercepted by the former surface is therefore relatively small, quite apart from the smallness of the probability that the required boundary plane will occur in the right position. These considerations lead one to the conclusion that the Bragg case may be neglected in comparison with the Laue case.

§ 5. DISCUSSION OF RESULTS

In a thin polycrystalline film the crystals will in general be bounded by a number of crystal planes and will not correspond directly to the thin plates assumed in the above calculations. It does seem reasonable to suppose, however, that a representative Laue case will form a reasonable approximation to the true conditions. The results of § 4 show that the variation of the deviation is given by the limits of $\zeta \tan \psi/\kappa$; according to the dynamical theory(2) the limits of ζ can be taken to be $\pm v/\kappa$. If we take for v a value of 2×10^{16} (corresponding to 7·5 v.), for $1/\lambda$ a value of 16×10^{-8} cm.$^{-1}$ (corresponding to an energy of about 40,000 ev.), and for $\tan \psi$ the value unity, the width of the ring is $2v/\kappa = 1/2500$. The theory of the Laue case shows that this width is to be taken at the point where the intensity has fallen to its half value.

The above estimate appears at first sight to be still much larger than that given by Trillat and Hautot. The uncorrected angular widths given for gold and nickel films are about 1/3000. From this the maximum error due to the width of the original beam, etc. is subtracted, yielding values of about 1/15,000. These are used to calculate the Fourier coefficients. Since the allowance for other causes of broadening has been taken at the maximum possible, the above figures give a lower limit for the width. Even so the gross width as measured by Trillat and Hautot is rather less than that calculated above, though the difference is probably not more than can be explained by the approximations of the theory.

In the authors' experience the tendency is to underestimate the width of the rings whether these are measured visually or by microphotometry. Experiments(3) made to determine the relative intensities of rings show that the base of the rings spreads more widely than would be expected from a casual examination of the microphotographs, and rough measurement of figure 1 of the paper by Trillat and Hautot suggests considerably greater breadths than he gives.

REFERENCES

(1) Trillat, J. J. and Hautot, A. *J. Phys. Radium*, **9**, 133 (1938).
(2) Bethe, H. *Ann. Phys., Lpz.*, **87**, 55 (1928).
(3) Thomson, G. P. *Proc. Roy. Soc.* A, **125**, 252 (1929).

AN X-RAY STUDY OF LATTICE-DISTORTION IN COPPER, NICKEL AND RHODIUM

By G. W. BRINDLEY, M.Sc., Ph.D., Mackinnon Student of the Royal Society

AND

P. RIDLEY, Ph.D., Physics Laboratories, University of Leeds

Received 16 *November* 1938. *Read in title* 10 *February* 1939

ABSTRACT. The nature of the lattice-distortion in filed powders of copper, nickel and rhodium, three face-centred cubic metals, is considered on the basis of experimental determinations of the widths and intensities of x-ray reflections from these metals. The effect of extinction on the reflected intensities is discussed in detail and from the magnitude of the extinction estimates are made of the mean crystal-sizes. It is shown that lattice-distortion causes a decrease of reflected intensity which becomes more marked as we go from rhodium through nickel to copper; the broadening of the reflections increases in the reverse direction, namely copper through nickel to rhodium, which is the direction of increasing hardness.

The experimental results are discussed in relation to various hypotheses as to the nature of lattice-distortion in metals. It is shown that periodic displacements of the atoms, of the type discussed by Dehlinger and Boas, explain qualitatively that an increase in the widths of the reflections is accompanied by a decrease in the intensity effect. With this type of distortion it would be necessary to suppose that in rhodium, which shows the greatest broadening of the reflections and little or no change of intensity, the lattice-distortion takes the form of atomic displacements following a cosine law. Detailed examination shows that the theory does not give a satisfactory quantitative explanation of the observed results. It is shown that with distortions of a non-periodic type, changes of reflected intensity may occur as a result of irregular displacements of the atoms and a broadening may occur as a result of a change in the mean crystal parameter throughout an entire grain. The experimental results for the decrease of intensity and the broadening of the reflections are satisfactorily explained in this way. Values of the lattice energies associated with these changes are calculated and are compared with values obtained by direct methods; from this comparison it appears that the energy of a distorted metal resides mainly in the atomic displacements rather than in macroscopic stresses extending over entire grains. No immediate explanation is forthcoming of the fact that an increase of the broadening effect is accompanied by a decrease of the intensity effect, but a tentative explanation is suggested which is compatible with the observed correlation between the changes observed with x-rays and the cohesional properties of the metals.

§ 1. INTRODUCTION

In order to obtain further information about the nature of lattice-distortion in worked metals, we have extended our recent investigation⁽⁵⁾ of the widths of x-ray reflections from filed rhodium powder to filed powders of copper and nickel, all three metals having face-centred cubic structures. Special care was taken that the measurements should be made under the same experimental conditions in order that the results might be directly comparable. In previous papers(4, 5) we have given results for the intensities of X-ray reflections from filed powders of these metals, so that we are now able to study their distortion from the standpoint of both the widths and the intensities of the reflections. In a recently published survey of the subject, Brill and Renninger(3) have pointed out that no such investigation has yet been undertaken and have laid stress on its usefulness in checking certain theoretical conclusions arising out of the work of Dehlinger(7) and of Boas(2).

It will be convenient to give first the additional experimental data for the widths of the reflections from copper and nickel. The same experimental arrangements were used as in the previous work(5) on rhodium and no further account is necessary. Since the K absorption edges of copper and nickel come within the range of wavelengths usually used in this type of work, we have restricted the present measurements to one radiation for each powder, namely, Zn $K\alpha$ radiation for copper and Cu $K\alpha$ radiation for nickel. In the case of rhodium five radiations were employed in order to obtain special information on certain points, but it was not considered necessary to carry out the measurements on copper and nickel in such detail.

§ 2. RESULTS OF LINE-WIDTH MEASUREMENTS FOR COPPER AND NICKEL

As in the case of rhodium, we have determined the widths of the reflections as defined by v. Laue(12), namely, the integrated intensity divided by the maximum intensity. The corrections to the observed widths rendered necessary by the separation of the α_1 and α_2 components are based on the work of F. W. Jones(11). The results are set out in table 1.

Table 1. Laue widths of X-ray reflections from filed copper and nickel powders

Radiation	Reflections	θ (degrees)	Laue widths (mm.)	Separation of α_1 and α_2 components (mm.)	Correction for $\alpha_1\alpha_2$ separation	Corrected Laue widths (mm.)
			(*a*) Copper			
Zn $K\alpha$	220	34·2	0·55	0·111	0·954	0·52$_5$
	311	41·2$_5$	0·53	0·144	0·918	0·48$_5$
	222	43·5	0·45	0·156	0·869	0·39
	331	60·0$_5$	0·79	0·285	0·858	0·68
	420	62·7	0·90	0·318	0·866	0·78
			(*b*) Nickel			
Cu $K\alpha$	220	38·2	0·58$_5$	0·120	0·952	0·55$_5$
	311	46·4$_5$	0·58	0·160	0·915	0·53
	222	49·2$_5$	0·54	0·177	0·882	0·47$_5$
	331	72·3$_5$	1·30	0·479	0·852	1·11
	420	77·9	1·96	0·710	0·858	1·68

§ 3. COMPARISON OF THE WIDTHS OF REFLECTIONS FROM COPPER, NICKEL AND RHODIUM

The widths of the reflections may be compared most satisfactorily by plotting them against tan θ, θ being the Bragg angle; this places the points for the higher angles of reflection practically on a straight line, whereas plotting against θ gives a curve rising steeply as θ tends to 90°. The results are shown in figure 1, the solid points indicating results for rhodium, while the open circles and crosses indicate the results for nickel and copper.

It was emphasized previously that for rhodium the widths of all reflections except the 222 lie near a single curve, the 222 reflections lying on a slightly lower and almost parallel curve. Similar results are obtained for copper and nickel; all points except the 222 lie on curves similar to that through the rhodium points, but the 222 points fall below these curves. A further point of similarity is that for all three metals the widths of the 420 reflections tend to lie above the mean curve, and of the 331 reflections below the mean curve; the points corresponding to these reflections are indicated in figure 1.

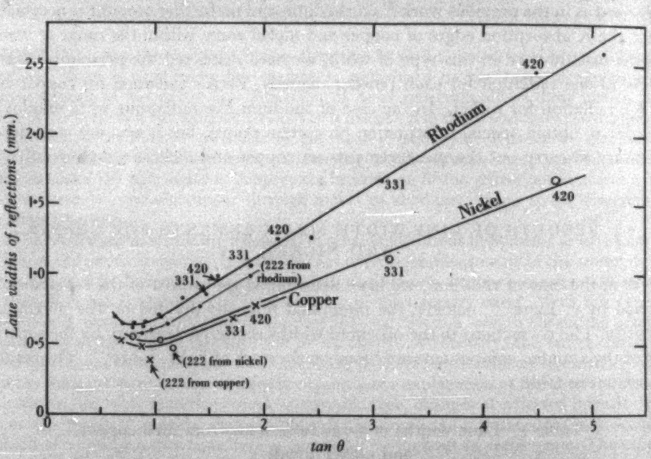

Figure 1. Laue widths of x-ray reflections from filed powders of copper, nickel and rhodium, plotted against tan θ for the following radiations. Rhodium, $K\alpha$ radiations of zinc, copper, nickel, cobalt and iron; copper, $K\alpha$ radiation of zinc; nickel, $K\alpha$ radiation of copper.

Figure 1 shows that the reflections from rhodium are markedly broader than those from copper and nickel, and that the nickel reflections are slightly broader than those from copper. The broadening of the reflections increases therefore in the order copper to nickel to rhodium. This corresponds to the order of the metals when they are grouped according to their hardness or other cohesional properties, such as melting points, and indicates a possible correlation of the broadening of the x-ray reflections with the cohesional properties. Further discussion of these results is given later, after the intensity measurements have been compared.

§4. DISCUSSION OF THE EXPERIMENTAL DATA FOR THE INTENSITIES OF REFLECTIONS FROM FILED POWDERS OF COPPER, NICKEL AND RHODIUM

The results for copper and nickel were obtained by Brindley and Spiers⁽⁴⁾, and for rhodium by the present writers⁽⁵⁾. The intensities reflected by the filed powders were compared with those reflected by chemically prepared powders of the same metal, the results being expressed in terms of the scattering factor f_T (T denoting a measurement at temperature T), rather than in terms of reflected intensity I. We have

$$\frac{f_{T\,(\text{filed powder})}}{f_{T\,(\text{chem. powder})}}=\sqrt{\frac{I_{(\text{filed powder})}}{I_{(\text{chem. powder})}}}.$$

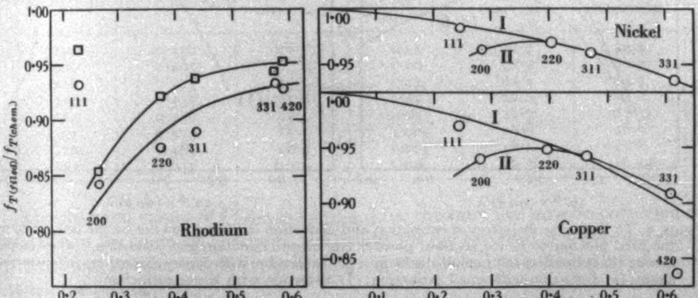

(*a*) $10^{-8}\times(\sin\theta)/\lambda$ (*b*) $10^{-8}\times(\sin\theta)/\lambda$

Figure 2. Experimental values of $[f_{T\,(\text{filed})}/f_{T\,(\text{chem.})}]$ plotted against $(\sin\theta)/\lambda$. In figure 2 (*a*), the circles and squares denote values obtained with moderately coarse and with very fine files respectively. In figure 2 (*b*), curves marked I are calculated theoretically on the assumption that the atoms are randomly displaced; curves marked II are discussed in the text.

The results for the three metals are reproduced in figure 2, where $[f_{T\,(\text{filed})}/f_{T\,(\text{chem.})}]$ is plotted against $(\sin\theta)/\lambda$. The two sets of results for rhodium were obtained by using a moderately coarse file, shown by circles, and an almost dead-smooth file, shown by squares; in both cases the powders actually used were passed through a fine sieve having 350 meshes to the inch. The rhodium results are strikingly different from those for copper and nickel, and an explanation for this fact must now be sought.

The intensities reflected by a filed powder are likely to be affected by extinction and by lattice-distortion, extinction affecting mainly the lower-order reflections and distortion mainly the higher-order reflections; the nature of the results will therefore depend on the relative magnitudes of the two effects. Figure 3 shows the kind of results to be expected. The curves taken in order show the effect of (*a*) extinction alone, (*b*) extinction with a small amount of distortion, (*c*) extinction with larger distortion, (*d*) distortion alone, (*e*) distortion with a small amount of extinction, and (*f*) distortion with larger extinction.* Comparing the experimental results in figure 2 with the curves in figure 3, we see that the rhodium results resemble curves (*a*) and (*b*), the copper and nickel results curves (*d*) and (*e*).

Before the effects of filing on the intensities reflected by the three metals can be quantitatively compared, we have to decide whether the chemically prepared powders are themselves free from distortion and/or extinction. Ideally the reflections from the latter should be unaffected by either extinction or distortion, and we could then regard the variation of $[f_{T(\text{filed})}/f_{T(\text{chem.})}]$ with $(\sin\theta)/\lambda$ as arising solely from the effect of the filing process. A check on the suitability of the chemical powders is obtained by comparing the scattering factors f_T for the chemical powders in absolute units with theoretically calculated scattering factors.

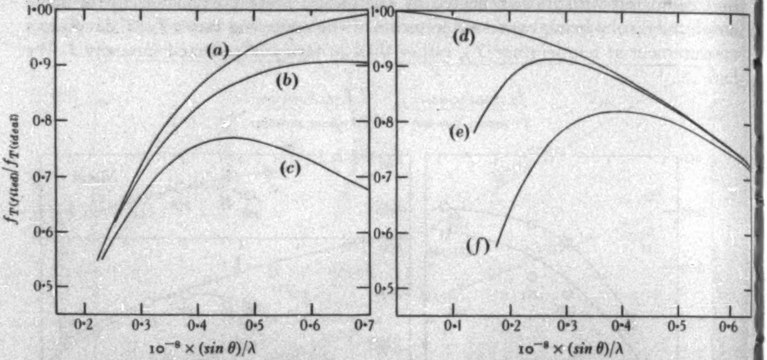

Figure 3. To illustrate the effect of extinction and distortion in a filed powder on the ratio of f_T for the filed powder to f_T for an ideal powder free from extinction and distortion. (*a*) extinction alone; (*b*) extinction with small distortion; (*c*) extinction with larger distortion; (*d*) distortion alone; (*e*) distortion with small extinction; (*f*) distortion with larger extinction.

In the case of copper and nickel⁽⁶⁾ the good agreement between the experimental and the theoretical values of f_T over the whole range of $(\sin\theta)/\lambda$ investigated indicated negligible extinction and distortion in these powders, which may therefore be regarded as approximating closely to the ideal.

In the case of chemically prepared rhodium there is reasonably good agreement for the reflections of higher order but the observed values of f_T fall considerably below the theoretical values for the reflections of lower order. This points to the existence of appreciable primary extinction in the chemical powder, a correction for which is essential before comparison of the results for filed rhodium with those for filed copper and nickel. This correction was described in the previous paper on rhodium(5); it is made by obtaining a mean crystal-size for the powder from the depression of the observed values of f_T for one reflection below the theoretical curve and the subsequent use of this mean crystal-size to correct the observed values for other reflections. In table 2 we give the observed values of f_T for chemical rhodium before and after correction for extinction in this manner, and also the theoretical values of f_T, which were calculated in our previous paper(5). The reasonably good agreement which exists between the corrected experimental values and the theoretical values over the whole range of $(\sin\theta)/\lambda$ indicates that the former may be taken as fairly reliable values for rhodium powder when free from both extinction and distortion.

---

* The exact shape of the distortion curve will depend on the nature of the distortion, but if the atomic displacements are approximately random, the decrease in intensity will follow the same law as the temperature effect; this has been assumed in drawing the curves in figure 3.

Table 2. Values of f_T for chemically prepared rhodium powder

Reflections	$10^{-8} \times (\sin\theta)/\lambda$	f_T observed	Correction for extinction	f_T corrected	f_T theoretical
111	0·228	28·5	1·15	32·7	32·2
200	0·263	$27\cdot4_5$	1·10	30·2	30·2
220	0·373	$23\cdot5_5$	$1\cdot03_5$	24·4	24·7
311	0·437	21·8	1·02	$22\cdot2_5$	22·2
222	0·456	21·3	1·02	21·7	$21\cdot5_5$
331	0·574	18·7	$1\cdot00_5$	18·8	18·2
420	0·589	18·3	$1\cdot00_5$	18·4	17·8
422	0·645	16·6	$1\cdot00_5$	16·7	$16\cdot4_5$

The observed values of $[f_{T(\text{filed})}/f_{T(\text{chem.})}]$ for rhodium can now be corrected for extinction in the chemical rhodium; the results for the two filed powders are shown by circles and squares respectively in figure 4, the dashed lines being mean curves through the points.

We now have for comparison the copper and nickel results in figure 2(*b*) and the rhodium results in figure 4. We have first to consider how far the intensities from the filed powders are affected by extinction before we can come to any conclusion as to the magnitude of the distortion effect.

The results for copper and nickel approximate to curves (*d*) or (*e*) in figure 3. In their original paper, Brindley and Spiers(4) considered that the filed copper and nickel powders had negligible extinction and that the curves marked I in figure 2(*b*) adequately fitted the experimental points. Actually these curves were calculated on the assumption that the atoms in the filed metals have effectively random displacements from their normal lattice positions. The observed values seemed to agree with this hypothesis, with the exception of the 200 reflections which appeared to give low values. In the light of the rhodium values, however, it now appears more probable that the values for the 200 reflections are not abnormally low, but rather that those for the 111 reflections are high. Reasons why the 111 reflection might give high values have been discussed in the previous paper(5). We consider, therefore, that the experimental values are better represented by curves passing through the

200 points, such as those marked II in figure 2 (*b*). These curves ressemble case (*e*) in figure 3; in other words, lattice-distortion is the major effect, but extinction is not entirely negligible. If we take the depressions of the 200 points below curves I to be due to extinction, the values found for the mean crystal-sizes are $3{\cdot}6\times10^{-5}$ cm. for filed copper, and $2{\cdot}9\times10^{-5}$ cm. for filed nickel. The corresponding effect of extinction on the reflections of the higher orders is entirely negligible, so that curves I calculated on the assumption of random atomic displacements are not appreciably changed.

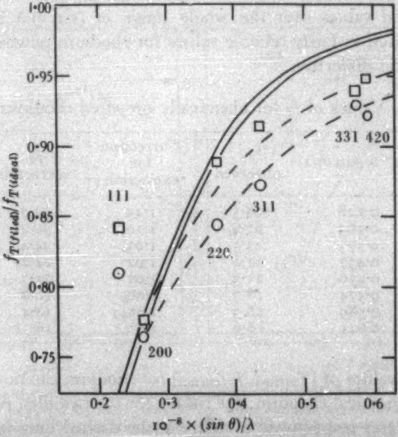

Figure 4. Ratio of f_T for filed rhodium to f_T for ideal rhodium powder free from extinction and distortion, plotted against $(\sin\theta)/\lambda$. The squares and circles correspond to the two filed powders.

In figure 4 the general run of the dashed lines through the observed points resembles curves (*b*) or (*a*) in figure 3; there is extinction with little or no distortion. To determine how far primary extinction will account for the results, the full curves in figure 4 were calculated on the assumption that the values of f_T for the 200 reflections from the filed powders are low, entirely owing to primary extinction. The mean crystal-sizes calculated in this way are respectively 6·3 and $6{\cdot}6\times10^{-5}$ cm. for the two filed powders. These calculated curves do not fit the experimental results exactly, though the agreement could be improved somewhat by making some allowance for the distribution of crystal-sizes about the mean value. The tendency of the experimental points to fall slightly below the calculated curves as $(\sin\theta)/\lambda$ increases may indicate that in addition to extinction there may be a small distortion effect, but we can be certain that even for large values of $(\sin\theta)/\lambda$, about 0·6, lattice-distortion cannot reduce the values of f_T for the filed rhodium by more than 3 or 4 per cent.

§ 5. COMPARISON OF THE EFFECTS OF LATTICE-DISTORTION IN COPPER, NICKEL AND RHODIUM ON THE INTENSITIES OF X-RAY REFLECTIONS

In the preceding section we have attempted to disentangle the combined effects of lattice-distortion and extinction on the reflected intensities. In rhodium, the relatively large extinction effect makes it difficult to come to any conclusion as to the magnitude of the distortion effect except at large values of $(\sin\theta)/\lambda$; in copper and nickel, extinction has a smaller effect and is negligible at the larger values of $(\sin\theta)/\lambda$. It is in this region, therefore, that the most satisfactory comparison can be made of the distortion effects in the three metals. Table 3 gives values of the ratio of f_T for the distorted metal to f_T for the undistorted metal when $(\sin\theta)/\lambda$ is equal to 0·5 and 0·6.

Table 3. Values of $[f_{T\,(\text{distorted metal})}/f_{T\,(\text{undistorted metal})}]$ for copper, nickel and rhodium

	$f_{T\,(\text{distorted metal})}/f_{T\,(\text{undistorted metal})}$	
	$10^{-8}\times(\sin\theta)/\lambda=0{\cdot}5$	$10^{-8}\times(\sin\theta)/\lambda=0{\cdot}6$
Copper	0·92	0·89
Nickel	0·95	0·93
Rhodium	0·96 to 1·00	0·97 to 1·00

The general run of the results is clear; the effect of distortion in reducing the reflected intensities becomes more marked as we go from rhodium through nickel to copper. This is the reverse order to that found for the increase of the widths of the reflections. *We see, therefore, that if lattice-distortion is measured in terms of the broadening of the x-ray reflections, rhodium has the largest and copper the smallest distortion, whereas if it is measured in terms of the reduction of the reflected intensity, the opposite conclusion is obtained.*

§ 6. TYPES OF LATTICE-DISTORTION AND THEIR EFFECT ON THE WIDTHS AND INTENSITIES OF X-RAY REFLECTIONS

The problem of determining the nature of the distortion in a worked metal from the widths and intensities of x-ray reflections has received considerable attention both experimentally and theoretically, but the problem is still far from solved. In a recent survey of the subject, Brill and Renninger(3) point out that no one has hitherto measured both the widths and the intensities for a group of metals, so that in this respect the present experiments provide a wider basis for examining the problem than has previously been available. It will be convenient to consider first distortions of a periodic type and then those of a non-periodic type.

(*a*) *Distortions of a periodic type* (*Dehlinger-Boas*). Dehlinger(7) first discussed the results to be expected from a lattice distorted by periodic displacements of the atoms from their normal positions, and he considered in detail displacements which follow a cosine law. Lattices deformed in this way give rise to diffraction ghosts which are of appreciable intensity only in the immediate neighbourhood of the principal reflections; the reflections are therefore broadened, but the total integrated intensity remains unchanged. Hengstenberg and Mark(10) considered a similar type of distortion but obtained contradictory results, namely a decrease of intensity with no broadening, but the origin of this discrepancy, according to Brill and Renninger(3), lies in the fact that no account was taken of the diffraction ghosts.

Boas(2) also has considered a periodic type of lattice-distortion in which equal blocks of the lattice at regular intervals are displaced in a direction normal to the reflecting planes. This is equivalent to the superposition of a large number of Fourier components and is shown to produce a decrease of the reflected intensities without appreciable broadening. The transition from the simple to the more complex type of distortion is examined by Boas(2) by means of Fourier analysis and he concludes that as the type of distortion becomes more complex, requiring more Fourier terms to describe it, so the broadening of the reflections becomes less and the change of intensity greater. This is consistent with the fact that lattice vibrations (heat motion) affect only the intensities and not the widths of X-ray reflections. Brill and Renninger lay particular emphasis on this complementary character of the broadening effect and the intensity effect.

(*b*) *Distortions of a non-periodic type*. Theoretical discussions of distortions of this type in relation to X-ray results have not as yet been forthcoming, owing, doubtless, to the difficulty of obtaining an exact mathematical formulation of the problem. When a polycrystalline metal is distorted, we may suppose that the individual grains exert stresses on each other which result in a breaking up of the grains and also in a bending and twisting of the lattice planes. The atoms will be displaced from their normal positions but in general the displacements will not follow any simple law and, throughout an entire fragment of crystal, they may be so irregular as to approximate to a random displacement. This would result in a change of the reflected intensity which could be treated mathematically in the same way as the random displacements due to heat motion.

The stresses exerted by the grains on each other may also result in the mean lattice spacing throughout a grain (i.e. a region throughout which there is coherent reflection) being slightly different from the spacing of the undistorted lattice and this would cause a shift in the positions of the reflections. If the mean lattice spacing in some grains is slightly greater and in others slightly less than in the undistorted metal, and if the two are equally probable, a symmetrical broadening of the reflections will be produced. It is not essential to this view that certain grains *as a whole* should be compressed and others expanded; in any one grain there may be groups of atoms in closer proximity than in the ideal lattice and other groups in which the atoms are farther apart, but if the net result is that the mean lattice spacing differs from that of the undistorted metal, then a shift of the X-ray reflections is to be expected.

The separate consideration of the intensity effect and of the broadening effect does not necessarily imply that a particular model cannot be found which will satisfy the requirements of both, but in the absence of a full mathematical treatment along these lines it is simpler in the first place to consider the two effects separately.

§ 7. EXPERIMENTAL RESULTS CONSIDERED IN RELATION TO DISTORTIONS OF A PERIODIC TYPE

An outstanding feature of the experimental results is that the broadening of the reflections increases and the intensity effect decreases as we go from copper through nickel to rhodium. This agrees with the conclusions arising out of the work of Dehlinger and of Boas. If the experimental results can be interpreted in terms of periodic lattice-disturbances, then in rhodium the disturbances must approximate to a cosine type, since this appears to be the only periodic type of distortion giving line broadening with little or no intensity effect, while in copper and nickel the disturbances must be of a more complex type.

This conclusion cannot be reconciled, however, with that arrived at in the previous paper on rhodium(5). There the view was taken that distortions approximating to the pure cosine type are unlikely to occur and that, since broadening will not occur with more complex types of distortion, the observed broadening probably has another origin. This, in fact, was also the conclusion finally arrived at by Boas(2), who stated, "Wir glauben, daher, dass die nach Deformation von Kristallen beobachtete Linienverbreiterung nicht von periodischen Gitterstörungen herrührt". We then proceeded to show that a satisfactory explanation of the observed widths of the rhodium reflections could be obtained in terms of a variation of the lattice parameter from one crystal grain to another.

The qualitative agreement which now appears between the experimental results for the three metals and the theoretical results for periodic distortions necessitates a reconsideration of the question. The most rigorous test which can at present be applied is to consider whether a satisfactory quantitative explanation is obtainable for the broadening of the rhodium reflections in terms of periodic distortions of the cosine type. The theory was given first by Dehlinger and subsequently, in a slightly modified form, by Boas. For a lattice in which after every period of distortion there is an undistorted region, Boas has expressed the angular width B of the reflected radiation in the following form:

$$B=\frac{\lambda}{2a\cos\theta}\,\frac{\sqrt{\pi}}{M}\left\{\frac{1-2p\,(1-p)\,[1-J_0\,(2\pi hv)]}{[(1-p)\,J_0\,(2\pi hv)+p]^2}\right\}. \qquad \text{......(1)}$$

In this expression, h is the order of the reflection from planes with spacing a, p the fraction of the lattice free from distortion, v the amplitude of the distortion, $2M$ the number of atoms in the lattice, and J_0 the Bessel function of zero order. This equation resembles Scherrer's equation for the breadth of reflections from small crystals. If we write $L=2aM$, the length of a side of a crystal, Boas's expression reduces to

$$B_{(\mathrm{Boas})}=\frac{\lambda}{L\cos\theta}\,\sqrt{\pi}\left\{\frac{1-2p\,(1-p)\,[1-J_0\,(2\pi hv)]}{[(1-p)\,J_0\,(2\pi hv)+p]^2}\right\}, \qquad \text{......(2)}$$

and the corresponding expression given by Scherrer is

$$B_{(\mathrm{Scherrer})}=\frac{\lambda}{L\cos\theta}\,2\sqrt{\frac{\log_e 2}{\pi}}. \qquad \ldots\ldots(3)$$

This similarity is not fortuitous, for reference to the paper by Boas shows that similar theoretical considerations are involved in their derivation.

Now in the previous paper on rhodium we have already considered in detail the possibility that the broadening of the reflections might be due to the production of a very small crystal-size L. The experimental results were shown to be incompatible with this view, for whereas according to Scherrer's expression (or subsequent more exact expressions given by v. Laue and by Kochendörfer) the breadth B must increase linearly with λ for any given value of θ (or some function of θ, such as $\tan\theta$, figure 1), actually we find that the widths of the reflections for different values of λ fall on a single curve. Furthermore, the order of magnitude of L calculated from the observed broadening by means of Scherrer's expression, or the more accurate expressions given later by v. Laue and by Kochendörfer, is entirely incompatible with the relatively large extinction found in the rhodium powder. From the similarity of expressions (2) and (3) it would be expected that similar arguments would equally well disprove the hypothesis that the broadening arises from periodic distortions of cosine type, and detailed examination shows that this is so. The complex character of the expression in curly brackets in equation (2) and the fact that the parameters v and p occur, make any detailed consideration of this equation more difficult than the corresponding problem discussed in the previous paper. If we rewrite equation (2) in the following form:

$$B(\cos\theta)/\lambda=(\sqrt{\pi}/L)\,F(h, v, p), \qquad \ldots\ldots(4)$$

where $F(h, v, p)$ stands for the expression in curly brackets in equation (2), then the left-hand side of equation (4) can be obtained from the experimental data and the right-hand side can be calculated for various values of L, h, v and p. These, then, are two convenient quantities for comparison.

In calculating $B(\cos\theta)/\lambda$ from the experimental data, allowance has been made for the natural widths of the reflections due to the focusing properties of the camera by subtracting from the observed widths for the filed powder the corresponding widths for the chemically prepared powder; this method, though not exact, is the one usually adopted and at present there appears to be no better alternative. If W is the linear width of the reflections, then

$$B=(W_{\text{filed powder}}-W_{\text{chem. powder}})/R,$$

where R, the camera radius, is 30·5 mm. The observed values of W are given in the previous paper⁽⁵⁾.

In figure 5 values of $B(\cos\theta)/\lambda$ obtained from the experimental data are plotted against h, the order of the reflections, calculated from the Bragg equation,

$$h=2a(\sin\theta)/\lambda;$$

the symbols used in the figure indicate the radiations employed.

In the first place we note that if the broadening is correctly given by equation (1), then $B(\cos\theta)/\lambda$ should be constant for a given value of h; actually we find a considerable spread of the observed values. It is seen, however, that for the most part there is no progressive change of $B(\cos\theta)/\lambda$ with the wave-length λ, which suggests that the spread of the points for each value of h may arise either from experimental error or from the approximate nature of the correction for the natural line-widths. It cannot, therefore, be concluded that the spread of the points necessarily disproves that the main cause of the broadening is distortion of a periodic cosine type.

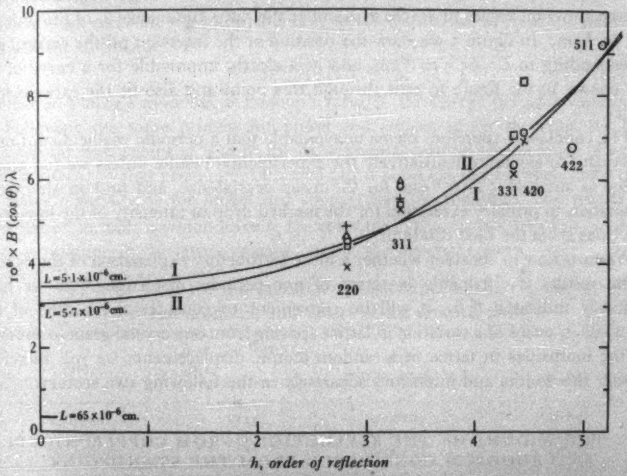

Figure 5. Experimental values of $B(\cos\theta)/\lambda$ plotted against h. The symbols indicate the radiations employed, as follows: ○, Zn $K\alpha$; ×, Cu $K\alpha$; □, Ni $K\alpha$; △, Co $K\alpha$; +, Fe $K\alpha$. The full curves are calculated from the expression $(\sqrt{\pi}/L)\,F(h, v, p)$, with the following values for the parameters. Curve I: $L=5{\cdot}10\times10^{-6}$ cm.; $v=0{\cdot}0637$, $p=\frac{3}{8}$; $v=0{\cdot}0517$, $p=\frac{1}{4}$; $v=0{\cdot}0398$, $p=0$. Curve II: $L=5{\cdot}75\times10^{-6}$ cm.; $v=0{\cdot}0955$, $p=\frac{1}{2}$. Note also the position on the vertical axis of the intercept for a curve with L equal to 65×10^{-6} cm.

The curves in figure 5 are calculated from the expression $(\sqrt{\pi}/L)\,F(h, v, p)$ for the following values of L, v and p:

Curve I: $L=5{\cdot}10\times10^{-6}$ cm.; $v=0{\cdot}0637$, $p=\frac{3}{8}$; or $v=0{\cdot}0517$, $p=\frac{1}{4}$; or $v=0{\cdot}0398$, $p=0$. These three pairs of values of v and p give almost identical curves.

Curve II: $L=5{\cdot}75\times10^{-6}$ cm.; $v=0{\cdot}0955$, $p=\frac{1}{2}$.

Values of L, v and p of these magnitudes give the best agreement between the theoretical expression and the observed values of $B(\cos\theta)/\lambda$. Within fairly wide limits, the parameters v and p can be adjusted so that over the range in which we are interested in the function $F(h, v, p)$, which is from $h=0$ to $h=5$, practically identical curves are obtained; this is illustrated by the three pairs of values of v and p which fit curve I. This means that the experimental data are inadequate to enable any conclusion to be drawn as to the magnitudes of v and p.

A further property of this function is that it tends to unity as h tends to zero. Hence, as h tends to zero, $B(\cos\theta)/\lambda$ tends to $\sqrt{\pi}/L$; the intercept of the calculated curve on the vertical axis depends therefore only on L. For the two curves shown in figure 5, L is of the order of 5×10^{-6} cm., which is much smaller than the value 65×10^{-6} cm. estimated from the extinction. If the crystal-size were really as small as 5×10^{-6} cm., then there should be negligible extinction. A careful examination shows that the parameters L, v and p cannot be chosen so as to give agreement with the experimental values of $B(\cos\theta)/\lambda$ and at the same time make L of the order of 65×10^{-6} cm. In figure 5 we show the position of the intercept on the vertical axis corresponding to $L = 65 \times 10^{-6}$ cm. and it is clearly impossible for a curve of the type shown in the figure to pass through this point and also fit the experimental results.

The conclusion therefore seems unavoidable that a periodic cosine distortion is inadequate to explain quantitatively the experimental results unless we can accept a value as small as 5×10^{-6} cm. for the mean crystal-size, and find an alternative explanation to primary extinction for the marked drop of intensity of the low-order reflections from the filed rhodium.

We turn now to consider whether a more satisfactory explanation of the experimental results is obtainable in terms of non-periodic distortions. As we have previously indicated (§ 6), it will be convenient to consider the widths of the reflections in terms of a variation in lattice spacing from one crystal grain to another, and the intensities in terms of a random atomic displacement; we will therefore consider the widths and intensities separately in the following two sections.

§ 8. THE WIDTHS OF THE REFLECTIONS FROM COPPER, NICKEL AND RHODIUM CONSIDERED FROM THE STANDPOINT OF A VARIATION IN LATTICE SPACING

Corresponding to a change δa in the lattice parameter, there will be a shift of the reflected line a distance δx given by

$$\delta x = -2R \tan\theta \, \delta a/a,$$

where R is the camera radius. If dp is the probability that $\delta a/a$ lies in a small range between z and $(z+dz)$, then, assuming a Gaussian distribution, we have

$$dp = (h/\sqrt{\pi})\, e^{-h^2z^2}\, dz.$$

If the distribution of intensity on the photographic film of a reflection from the undistorted metal at the same angle θ is represented by the function $I(x)$, then for the distorted metal a fraction of this intensity, $I(x)\,\delta p$, will be displaced a distance δx, and may be represented as $I(x')\,\delta p$. The total intensity of the line is not changed by this process so that the integrated intensity is given by

$$\int I(x)\, dx = \int \left[\Sigma I(x')\, \delta p\right] dx.$$

The maximum intensity of the line, however, is reduced. The linear Laue-width is then given by

$$W = \frac{\int I(x)\,dx}{[\Sigma I(x')\,\delta p]_{\max}}.$$

The calculation of W as a function of θ is a laborious process, because for each value of θ a different intensity distribution $I(x)$ must be used. Assuming a Gaussian distribution for $\delta a/a$, we see that there is only one adjustable parameter, h. Writing z for da/a, we easily obtain the r.-m.-s. value,

$$\sqrt{\overline{z^2}} = 1/h\sqrt{2}.$$

and hence can calculate the internal energy of the worked metal from the following formula due to Stibitz(14):

$$V = 3E\overline{z^2}/[2(1+2\sigma^2)],$$

where E is Young's modulus, σ Poisson's ratio, V the energy per unit volume.

Following the same process for nickel and copper as for rhodium, we have obtained the best values of h to fit the experimental results; the measure of agreement is similar to that previously obtained but is naturally less rigorous, since there are fewer observations for nickel and copper than for rhodium. The results are summarized in table 4 which gives h, the constant in the distribution law, $\sqrt{\overline{z^2}}$, the r.-m.-s. variation in the lattice spacing, and V the internal energy.

Table 4. Data for the variation of lattice spacings in copper, nickel and rhodium, and values of the internal energy

Metal	h in the formula $dp = (h/\sqrt{\pi})\,e^{-h^2z^2}\,dz$	$\sqrt{\overline{z^2}}$ where $z = da/a$	V cal./g.
Copper	345	0·00205	0·0169
Nickel	317·5	0·00223	0·0340
Rhodium	207	0·00431	0·0834

The values of V in table 4 are of a very different order of magnitude from the results of Taylor and Quinney(15) who measured the internal energy of several worked metals calorimetrically. For pure annealed copper subjected to rapid twisting they find that the maximum absorbed energy is 1·149 cal./g. and the corresponding figures for annealed mild steel and decarburized mild steel are respectively 1·267 and 0·660. In earlier measurements on metals worked by stretching Farren and Taylor(8) gave for the maximum absorbed energy 0·38 cal./g. for copper and 0·33 cal./g. for aluminium. In both these methods of cold-working it is evident that the amount of energy absorbed is far greater than that calculated above. This discrepancy is not due to the fact that the present results are for metals distorted by filing, since Boas(1) has made similar calculations using results for metals worked by drawing and rolling, and his estimates of V are even smaller than those given in table 4. These results suggest that the energy of a distorted metal does not reside mainly in the macroscopic stresses set up in the individual grains of the worked metal.

§ 9. THE DECREASE OF REFLECTED INTENSITY CONSIDERED IN TERMS OF RANDOM ATOMIC DISPLACEMENTS, AND THE LATTICE ENERGY ASSOCIATED WITH SUCH DISPLACEMENTS

We have seen (§§ 4 and 5, and figure 2(*b*)) that it is only for copper and nickel that there is a well-marked decrease of intensity which can be associated with lattice-distortion; for rhodium the effect of extinction predominates over any change of intensity due to lattice-distortion. In their original paper, Brindley and Spiers(4) showed that for copper and nickel the decrease of intensity could be interpreted in terms of random atomic displacements, and the more detailed considerations of the present paper which attempt to assess the magnitude of the extinction in these metals have not affected this conclusion.

Calculations of the latent energy from the r.-m.-s. atomic displacements found by Brindley and Spiers(4) were first published by Boas(1) who used these results to find an apparent temperature increase by applying the well-known Debye-Waller expression for the effect of heat motion on X-ray intensities and hence he obtained the equivalent energy content. His results were 7·4 cal./g. for copper and 6·4 cal./g. for nickel. Comparing these results with direct calorimetric measurements, he inadvertently quoted an earlier measurement by Rosenhain and Stott(13), namely, 0·23 cal./g. for copper, erroneously attributing it to Taylor and Quinney(15), whereas actually they gave the value 1·149 cal./g. for copper. Instead therefore of the X-ray value being about 30 times too large, as Boas stated, it is only about 6 times too large. The discrepancy is, of course, still appreciable, but we can now say that the lattice energy calculated from the intensity-measurements is at least comparable with the calorimetric value, whereas the energy calculated from the line-broadening experiments is of an entirely different order of magnitude. In a subsequent paper Boas(2) emphasized that if it is assumed that instead of the atoms being displaced purely at random, groups of atoms are similarly displaced, then the internal energy will be less than that calculated for a random displacement, a suggestion which may well be the true explanation of the difference between the two estimates of the internal energy. It seems reasonable to conclude that the seat of the energy in a worked metal lies in atomic displacements rather than in macroscopic stresses extending over entire grains; this, however, does not exclude the possibility that such stresses may exist and be responsible for the broadening of the X-ray reflections.

It is of interest to note that experiments by Fricke and his collaborators(9) also point to a connection between internal energy and the intensity of X-ray reflections; they find, for example, that the energy-content of zinc oxide prepared by dehydration of the hydrate depends on the temperature of dehydration; the lower the temperature, the greater the energy content. X-ray examination shows that the reflected intensities decrease with increase of internal energy; there is, however, practically no change in the widths of the reflections. The increased energy-content and decreased intensity of reflection are attributed to lattice-distortion of a type which they describe as *eingefrorene Wärmeschwingungen*, i.e. it consists of atomic displacements which are random or nearly so.

§ 10. CONCLUSIONS AND DISCUSSION OF RESULTS

Hypotheses of two kinds have been proposed to explain the changes observed in the widths and intensities of X-ray reflections from worked metals. On one hand, Dehlinger and Boas have considered distortions of a periodic type; on the other hand, the distortion may be of a non-periodic type with irregular displacements of the atoms and possibly also with a change in the mean crystal parameter throughout a grain. The final conclusion drawn by Boas was that the broadening of the reflections from worked metals could not be satisfactorily explained in terms of periodic lattice-distortions and he suggested that the effect might be due to stresses extending over entire grains. This view was shown by the present writers(5) to explain the broadening of a large number of reflections from rhodium measured with five different radiations.

The experimental results given in the present paper, however, have necessitated a reconsideration of the whole question, for we now find that as we proceed from copper through nickel to rhodium the intensity effect decreases while the broadening of the reflections increases, a result which agrees qualitatively with the conclusions arising out of the work of Dehlinger and Boas on distortions of a periodic type. Since rhodium shows little or no decrease of intensity due to distortion and a large broadening, it follows that the distortion, if periodic, must approximate to the cosine type, and this enables us to carry out a quantitative test. In the case of copper and nickel, which show both a decrease of intensity and a broadening of the reflections, we cannot say more than that if the distortions are periodic they must be of a more complex type than the simple cosine type. The discussion given in § 7 shows that we cannot obtain a satisfactory explanation of the broadening of the rhodium reflections in terms of a periodic cosine distortion. We are therefore led to consider distortions of a non-periodic type and have related the broadening of the reflections to a variation of lattice parameter from one crystal grain to another, and the decrease of reflected intensity to an irregular, effectively random, displacement of the atoms. In this way the broadening effect and the decrease of intensity can be separately explained, but we are still left with the question why the intensity effect decreases as the broadening effect increases.

The following tentative explanation is admittedly hypothetical but appears worthy of consideration. We note, in the first place, that the intensity effect decreases as we go from the softest metal, copper, to the hardest, rhodium. We may suppose that with increasing cohesional force between the atoms, the magnitude of the atomic displacements will decrease so that there will be a smaller intensity effect. If the atomic displacements tend to relieve the large-scale, macroscopic, stresses in the worked metal, then we should expect the softest metal, copper, to show the smallest line-broadening and the largest intensity effect, and vice versa.

Calculations of the lattice energy associated with (*a*) changes in the lattice spacing and (*b*) random atomic displacements have been compared with values obtained calorimetrically; (*a*) is much smaller than the directly obtained values while (*b*) is comparable with though larger than these values. From this we conclude that the seat of the internal energy is mainly in the atomic displacements; this agrees with conclusions drawn by Fricke from chemical and x-ray investigations.

§ 11. ACKNOWLEDGEMENTS

Finally we wish to thank Prof. Whiddington and Dr Stoner for their interest in these experiments, the Government Grants Committee for a grant with which part of the apparatus was obtained, and the Department of Scientific and Industrial Research for a maintenance grant to one of us (P. R.).

REFERENCES

(1) Boas, W. *Z. Kristallogr.* **96**, 214 (1937).
(2) Boas, W. *Z. Kristallogr.* **97**, 354 (1937).
(3) Brill, R. and Renninger, M. *Ergebn. techn. Röntgenk.* **6**, 141 (1938).
(4) Brindley, G. W. and Spiers, F. W. *Phil. Mag.* **20**, 882 (1935).
(5) Brindley, G. W. and Ridley, P. *Proc. Phys. Soc.* **50**, 501 (1938).
(6) Brindley, G. W. *Phil. Mag.* **21**, 778 (1936).
(7) Dehlinger, U. *Z. Kristallogr.* **65**, 615 (1927).
(8) Farren, W. S. and Taylor, G. I. *Proc. Roy. Soc.* A, **107**, 422 (1925).
(9) Fricke, R. and Ackermann, P. *Z. anorg. allg. Chem.* **214**, 177 (1933).
Fricke, R. and Meyring, K. *Z. anorg. allg. Chem.* **230**, 366 (1937).
Fricke, R., Lohrmann, O. and Wolf, W. *Z. phys. Chem.* B, **37**, 60 (1937).
Fricke, R. *Z. Elektrochem.* **44**, 291 (1938).
(10) Hengstenberg, J. and Mark, H. *Z. Phys.* **61**, 465 (1930).
Hengstenberg, J. *Ergebn. techn. Röntgenk.* **2**, 139 (1931).
(11) Jones, F. W. *Proc. Roy. Soc.* A, **166**, 16 (1938).
(12) v. Laue, M. *Z. Kristallogr.* **64**, 115 (1926).
(13) Rosenhain, W. and Stott, V. H. *Proc. Roy. Soc.* A, **140**, 9 (1933).
(14) Stibitz, G. R. *Phys. Rev.* **49**, 862 (1936).
(15) Taylor, G. I. and Quinney, H. *Proc. Roy. Soc.* A, **143**, 307 (1933).

THE EFFECT OF COOLING AND OF MAGNETIC FIELDS ON CRYSTAL RECTIFICATION

By M. A. EL SHERBINI, M.Sc., Ph.D.

AND

Y. L. YOUSEF, B.Sc.

Physics Department, Faculty of Science, The Egyptian University

Communicated by Prof. O. W. Richardson, F.R.S., 14 *September* 1938.
Read in title 13 *January* 1939

ABSTRACT. The effect of temperature on rectification has been studied in the case of six different crystals. The effect of temperature variations on crystal rectification in the interval −75 to +30° C. is especially interesting in the cases of silicium and molybdenite. In the former case there is a very marked increase in rectification at the higher temperature, and in the latter case the sign of the rectification is changed. The presence of a magnetic field appears to have no effect on rectification.

§ 1. INTRODUCTION

The effect of heat on crystal rectification was studied by Flowers$^{(1)}$, who observed that the rectifying action of galena decreases with rise of temperature and vanishes at about 270° C. Khastgir and Gupta$^{(2)}$ repeated Flowers's experiments at 30 and 100° C., and found that at the higher temperature rectification decreases for all crystals and disappears for pyrites and galena. Working on the same subject, Sen$^{(3)}$ noticed, in contradiction to the results of the former experimenters, that points having good rectifying properties may exist in galena at temperatures as high as 270° C.

In the present work, crystal rectification for direct current and for alternating current of 1000 c./sec. has been investigated, particularly in the low-temperature region from −75 to +30° C. In some cases this range has been extended up to 150° C. The experiments were made on the crystals mentioned in table 1.

Table 1

Crystal	Source
Zincite with calcite	Franklin, N. Jersey, U.S.A.
Molybdenite	Norwegen
Copper pyrites	La Gardette, Dep. Isère, France
Silicium with a little iron	—
Galena	Joplin, Missouri
Bornite with chalcocite	Butte, Montana, U.S.A.

§ 2. APPARATUS

The crystal is clamped by a copper holder, and a copper spring forms the whisker. The combination is centrally suspended in an air cryostat, figure 1, made of a triple-walled pyrex-glass enclosure surrounded by a cold bath of solid carbon dioxide and acetone. The innermost tube *H* has a diameter of 1·5 cm., and can be electrically heated by means of a coil wound non-inductively over its exterior and covering a length of 16 cm. The mean distance between two consecutive turns is 0·25 cm., and local non-uniformity in heating is prevented by covering the coil with a film of cellulose. An exploring thermocouple shows almost no temperature-gradient throughout the middle third of the radiator.

Before immersion of the concentric tubes in the cold bath, the enclosure is dried by being pumped out and refilled with dry air through the side tubes *GG*.

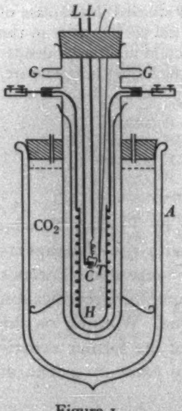

Figure 1.

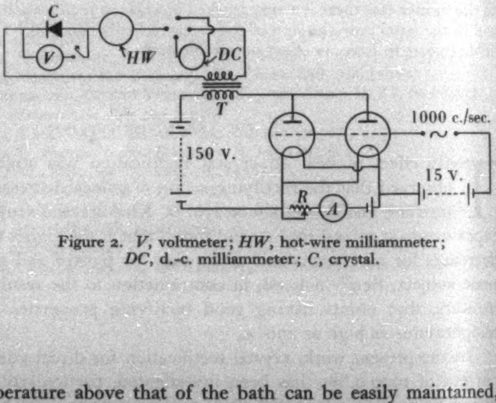

Figure 2. *V*, voltmeter; *HW*, hot-wire milliammeter; *DC*, d.-c. milliammeter; *C*, crystal.

Any particular temperature above that of the bath can be easily maintained, without disturbance of the crystal, by simply adjusting the heating current to a predetermined value obtained from a curve connecting the heating current and the corresponding equilibrium temperature. The concentric tubes assist in producing evenness, and increase the efficiency by nearly insulating thermally the heater from the bath.

The temperature of the crystal is indicated by means of a constantan-steel thermoelement *T*, connected to a high-resistance microammeter calibrated in degrees. The steady state can be reached in less than 10 min. by first passing a large heating current until the temperature approaches the required level, and then reducing the current to the value corresponding to the desired temperature.

The crystal circuit used in d.-c. rectification is of the usual potentiometric type. The a.-c. circuit is illustrated in figure 2. The voltage across the crystal is adjusted by controlling the amplification of the two power valves by means of the filament current.

§ 3. PROCEDURE

As far as possible, small currents of short duration were sent through the crystal in order to avoid electrical heating. Readings of voltage and current were taken first at the lowest temperature and then at higher temperatures. The crystal was afterwards recooled to its initial temperature, and the first set of readings was checked. In all cases it has been noticed that the currents regain very nearly their original values.

The rectification ratio in d.-c. measurements was calculated by dividing the difference between the currents I_1 and I_2 in the two directions by the larger current. In a.-c. measurements, N was taken as i/I, where i is the rectified component, measured by the d.-c. milliammeter, and I is the effective a.c. measured by the hot-wire milliammeter.

§ 4. RESULTS

Typical results are given in tables 2, 3, 4 and 5. In zincite and silicium, I_1 is the current from the whisker to the crystal, while in all other cases I_1 is the current in the reverse direction. The unit in which the currents are expressed is 0·04 mA. except for copper pyrites, bornite and galena, for which the unit is 5 mA.

Table 2. Typical results at −75 and +30° c.

Crystal	Voltage	At −75° c.			At +30° c.		
		I_1	I_2	N	I_1	I_2	N
Copper pyrites	2·4	37·7	0·2	0·995	32	0·3	0·990
	1·44	13·3	0	1	11·7	0·1	0·989
	0·48	4·2	0	1	3·5	0	1
Bornite	1·6	16·5	0·48	0·971	22	0·8	0·964
	0·96	8·1	0·16	0·981	11·5	0·3	0·974
	0·32	2·6	0·02	0·993	3·1	0·08	0·974
Galena	1·7	24·8	1	0·960	25·1	2·1	0·917
	1·02	11·4	0·2	0·982	11	0·6	0·945
	0·34	3·4	0	1	2·1	0	1
Zincite	4	38	10	0·74	42·5	8·5	0·80
	2·4	19·2	4	0·79	21·9	3·2	0·85
	0·8	4·2	1·8	0·57	4·1	1·6	0·62
Silicium	3·6	8·8	4	0·55	24	4·3	0·82
	2·16	3·4	0·6	0·83	10	0·8	0·92
	0·72	0·2	0	1	0·9	0	1
Molybdenite	2·5	0·757	0·313	0·587	2·5	7·2	−0·652
	1·5	0·235	0·118	0·497	1	3	−0·667
	0·5	0·005	0·0025	0·500	0·1	0·8	−0·875

It will be noticed from table 2 that copper pyrites, bornite and galena show, in general, a decrease in rectification as the temperature is raised, as a result of an increase in the electrical conductivity in the direction of the smaller current. With galena further tests have been carried out at 25° and 150° c. by heating the crystal in an electric furnace. It has been observed, table 3, in contradiction to Khastgir and Gupta's observations which indicate no rectification at 100° c., not only that points having very good rectifying properties may exist above 100° c., as was found by Sen, but also that N may increase with temperature, chiefly owing to a decrease in the smaller current.

Table 3. Results for galena at 25 and 150° c.

Voltage	At 25° c.			At 150° c.		
	I_1	I_2	N	I_1	I_2	N
1·4	21	3·9	0·813	21·5	0·3	0·986
1·12	14	1·8	0·871	14·2	0·1	0·993
0·84	9	0·9	0·900	9·2	0	1
0·56	4·9	0·3	0·939	5	0	1
0·28	1·4	0·1	0·929	1·3	0	1

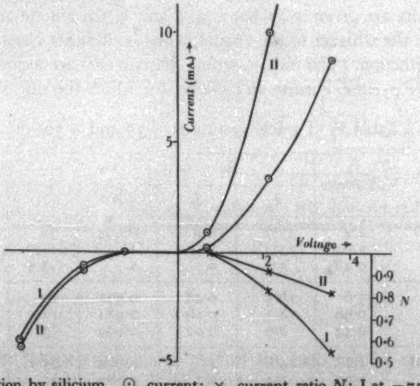

Figure 3. Rectification by silicium. ⊙, current; ×, current ratio N; I at −75° c.; II at +30° c.

Zincite shows a slight increase in N with temperature, due to an increase in I_1 and a decrease in I_2, while silicium always shows a very marked increase both in rectification and in electrical conductivity. Curves are drawn, figure 3, for silicium from the data in table 2.

Molybdenite, tables 2 and 5, is very sensitive to temperature variations, notably in the low-temperature region, for the direction of the larger current is reversed below 0° c., figures 4 and 5. This result is confirmed by a.-c. tests, table 4, figure 6. Further, the electrical conductivity in both directions rapidly increases with temperature. Between 0 and 100° c. there is no reversal, and in general N increases at a gradually diminishing rate.

Table 4. A.-c. test for molybdenite at −75 and +30° c.

Voltage	At −75° c.			At +30° c.		
	i	I	i/I	i	I	i/I
12·5	0·55	5·75	0·094	−15	85	−0·177
10	0·375	4·75	0·079	−12	66·5	−0·180
7·5	0·28	2·75	0·101	−7·3	45	−0·161
5	0·10	1·75	0·057	−4	25·5	−0·157
2·5	0·05	0·50	0·100	−1·7	8·25	−0·204

Table 5. Variation of rectification of molybdenite with temperature

Voltage	At −70° c.			At −3° c.			At +58° c.			At +100° c.		
	I_1	I_2	N	I_1	I_2	N	I_1	I_2	N	I_1	I_2	N
6·2	1·2	0·9	0·25	9·3	13·1	−0·29	25	39	−0·36	32·5	58·5	−0·44
4·96	0·9	0·7	0·22	6·7	8·3	−0·19	16	27	−0·41	22·5	42·5	−0·48
3·72	0·5	0·4	0·20	4·2	4·5	−0·07	10·2	17	−0·40	14·5	26·3	−0·45

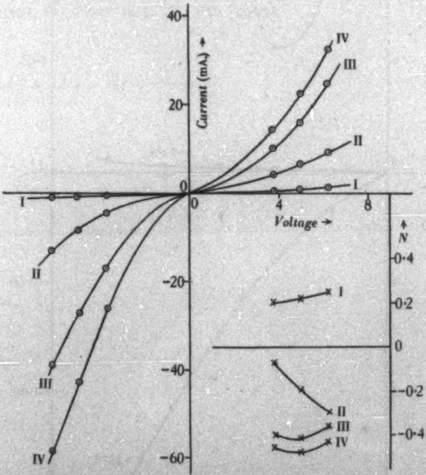

Figure 4. Change of sign of rectification by molybdenite. ⊙, current; ×, current ratio N; I at −70° c.; II at −3° c.; III at +58° c.; IV at +100° c.

The temperature coefficient of resistance of a molybdenite crystal made in the form of a resistance thermometer was determined by Pierce$^{(4)}$. The specimen showed no evidence of rectification, but it showed a very rapid decrease in resistance as the temperature is raised.

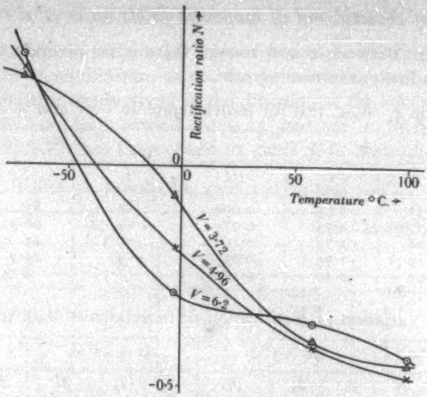

Figure 5. Rectification by molybdenite.

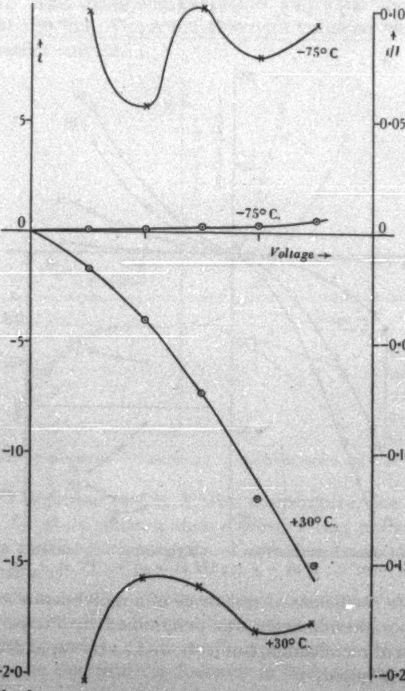

Figure 6. A.-c. test of molybdenite. ⊙, current; ×, current ratio *N*.

§ 5. EFFECT OF MAGNETIC FIELD

The small magnetic field created within the heating coil of the cryostat suggested the study of crystal rectification under the action of a magnetic field. Experiments were made on silicium in a field of 2280 gauss, produced by a Du Bois electromagnet, the lines of force being in one case parallel to the direction of the current through the crystal and in another case perpendicular to it.

The results showed that over a range from 0·8 to 4·0 v., corresponding to a range of I_1 from 0·02 to 6·00 mA., the change from $H=0$ to $H=2280$ and vice versa produced no changes in the values of N that exceeded the experimental error, which was about 1 per cent. The slight observed variations in the currents could not be attributed with certainty to the effect of the field, as they were not exactly reproducible.

REFERENCES

(1) Flowers, A. *Phys. Rev.* **29**, 455 (1909).
(2) Khastgir, S. and Gupta, A. *Phil. Mag.* **19**, 557 (March, 1935).
(3) Sen, B. *Indian J. Phys.* **10**, 91 (March, 1936)
(4) Pierce, G. *Phys. Rev.* **28**, 181 (1909).

NOTE ON THE BAR PENDULUM

By D. OWEN, B.A., D.Sc., F.Inst.P.

Received 13 *September* 1938. *Read* 10 *February* 1939

ABSTRACT. The time of oscillation of a bar pendulum is shown to be practically unaffected by the use of a carriage supporting the knife-edge and sliding along the bar; the accuracy of the usual laboratory exercise on the bar pendulum is considerably increased. With a stop-watch showing tenths of a second the value of g can be determined quickly to within a few parts in 10,000.

For teaching purposes experiments on the time of oscillation of a bar pendulum are commonly employed in the preliminary study of the compound pendulum and for determining g, the intensity of gravity. The usual form of apparatus consists of a brass bar about a metre in length and 2·54 cm. in width, drilled with a series of holes which serve as points of suspension from a fixed knife-edge. Only a rough degree of accuracy in the timing of the oscillations can be expected owing to the short length of the bearing, while the theory is confused by the presence of the holes along the bar. These defects may be eliminated by the use of a carriage which slides along the bar and can be clamped at any point, and which supports rigidly a knife-edge projecting on either side of the carriage and filed away in the interior. The knife-edges may be supported on a pair of glass plates mounted on either side of the platform of a wall-bracket, the platform between the plates being cut away to allow free passage of the pendulum and carriage. The bracket should, of course, be set by means of a plumb line so that the glass bearing surfaces are in a horizontal plane.

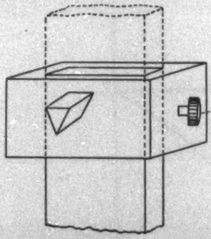

Figure 1. Bar pendulum with sliding carriage supporting knife-edge. S, clamping screw.

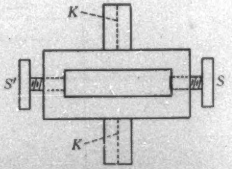

Figure 2. Sliding carriage in plan. S, clamping screw; S', balancing screw; K, knife-edge.

The pendulum is now apparently complicated by the presence of the carriage, which (1) may add to the gravitational couple, and (2) must add a term to the moment of inertia of the system. The effect of (1) may be made quite negligible by adjusting the carriage until its centre of gravity coincides with the line of the knife-edge. The effect of (2) can be reduced to well under 1 part in 10,000, whilst adequate strength and rigidity is permitted in the carriage, and may thus to this approximation be neglected. The simple formula

$$T=2\pi\sqrt{\frac{k^2+h^2}{gh}}$$

may accordingly be applied, where $k^2=(l^2+b^2)/12$, l denoting the length of the bar, b its breadth and h the distance from the knife-edge to the centre of gravity of the bar alone.

Observations for plotting T against h may now be made with a continuous variation of h on either side of the centre of gravity.

For the most accurate determination of g the value $h=k$ should be chosen, since at this position the value of T passes through a minimum. The formula thus reduces to

$$T=2\pi\sqrt{\frac{2k}{g}}, \quad \text{or} \quad g=\frac{8\pi^2k}{T^2}.$$

Calculation shows that in this particular case, if l is 1 metre, a variation in h of one millimetre affects T to the extent of only three parts in a million. A close accuracy of setting of h to equality with k is thus unimportant, and the determination depends essentially on only two measurements, namely, those of the total length of the bar and the period of oscillation. The length can be determined without special care to one or two parts in 10,000, while of course b need only be known roughly. The value of T can be measured by a good stop-watch to less than 1 part in 10,000. The bar pendulum thus affords a simple means of obtaining g to within a few parts in 10,000.

Some observations and calculations from an actual experiment may be quoted for illustration.

The length l of brass bar was 100·00 cm., its breadth b 2·54 cm., its mass M 1020 g., and the mass m of the carriage 68·5 g. Hence

$$k=\sqrt{(l^2+b^2)/12}=28{\cdot}876 \text{ cm.}$$

The value of I, the moment of inertia of the bar when at the setting $h=k$, works out at $1{\cdot}7\times10^6$ g.-cm.² I', the moment of inertia of the carriage alone about its knife-edge, is estimated to be 98 g.-cm.² Thus I'/I is $0{\cdot}57\times10^{-4}$.

The period of oscillation T' of the carriage alone about its knife-edge was observed to be 3·7 sec. (In making the carriage it is a simple matter to arrange that its centre of gravity shall be slightly below the knife-edge, and to adjust it by the removal of metal until the period of oscillation attains this order of value.) With the formula $T'=2\pi\sqrt{(I'/mgh')}$, where h' denotes the distance of the centre of gravity of the carriage below the line of the knife-edge, h' works out at 0·004 cm. and $mh'=0{\cdot}27$. Comparing mh' with Mh at the value $h=k$, we have

$$mh'/Mh=0{\cdot}27/1020\times28{\cdot}876\doteqdot10^{-5},$$

which shows that the effect of gravity control due to the carriage is quite negligible.

The use of the simple formula $T=2\pi\sqrt{\{(k^2+h^2)/gh\}}$ is thus justified, the effect of the carriage being insensible to the order of approximation aimed at.

Proceeding to the observation of T, the carriage was set approximately at $h=k=28{\cdot}87$ cm. and the pendulum was suspended. A stop-watch showing tenths of a second (supplied by the Venner Time Switch Co.) was used, allowing of estimation of times to a hundredth of a second. A telescope was focussed on the lower end of the pendulum when the latter was at rest, so that its vertical cross-wire coincided with the image of a black line inked near the extremity of the bar. The pendulum was set swinging with an amplitude of about 2 cm. and the passages across the zero were observed. For a preliminary estimate, duplicate measurements of the duration of 50 oscillations were taken. The observed times were 76·22 sec. and 76·24 sec., whence, approximately, $T=1{\cdot}5246$ watch seconds. It is found that, after a little practice, in such a pair of observations the times recorded by a stop-watch of the type specified seldom differ from the mean by more than 0·02 sec. The pendulum was now allowed to swing for about 10 min., the duration of some unknown integral number of oscillations, n, being measured with the stop-watch. The total time was 599·17 which $=nT$, whence

$$n \doteqdot 599{\cdot}17/1{\cdot}5246 \doteqdot 393{\cdot}0;$$

n is therefore taken as 393, whence $T=1{\cdot}5246$ watch seconds. The stop-watch was checked over a run of about 10 min. against a standard clock, and found to be slow by 2·5 parts in 10,000. The period T_1 corrected for watch rate is therefore 1·5249 sec.

A similar set of measurements was made with the carriage transferred to the corresponding position on the other side of the centre of the bar. On a preliminary estimate, $T=\frac{1}{2}(76{\cdot}21+76{\cdot}24)/50=1{\cdot}5245$ sec. The long period observed was 597·60 sec., whence $n\doteqdot 597{\cdot}60/1{\cdot}5245\doteqdot 391{\cdot}99$. Taking n as 392,

$$T=597{\cdot}60/392=1{\cdot}5245 \text{ watch seconds,}$$

or, when corrected for watch rate $T_2=1{\cdot}5248$ sec.

The mean value of T is $\frac{1}{2}(1{\cdot}5249+1{\cdot}5248)$, or $1{\cdot}5248_5$ sec.

Then $$g=\frac{8\pi^2 k}{T^2}=\frac{8\pi^2\times 28{\cdot}876}{1{\cdot}5248_5{}^2}=980{\cdot}6 \text{ cm./sec}^2$$

No correction has been included for the buoyancy of the air, which has the effect of virtually reducing g by about 1·5 parts in 10,000; or for the moment of inertia of the carriage, which would add a further 0·6 parts in 10,000 to the calculated value.

The pendulum, with a carriage of the design indicated, is made by Messrs Griffin & Tatlock, Kingsway, London.

A FALLING-WEIGHT TIME SWITCH: ITS STANDARDIZATION AND APPLICATION TO THE DETERMINATION OF THE TIME CONSTANT OF AN INDUCTIVE CIRCUIT

By ERIC J. IRONS, Ph.D., F.Inst.P.

AND

G. A. BENNETT, B.Sc., Queen Mary College, E. 1

Received 21 *October* 1938. *Read* 10 *March* 1939

ABSTRACT. In this apparatus the simultaneous release of two spheres, one from a fixed height and the other from a known but variable height H, causes two switches to be thrown so that the time interval between their operation is a linear function of $\sqrt{H}$. The apparatus is tested by a condenser-discharge method which affords a determination of g with an accuracy of about $\frac{1}{2}$ per cent. The use of the device is illustrated by a study of current growth in an inductive circuit for which the time constant is deduced.

§ 1. THE APPARATUS AND ITS STANDARDIZATION

This note gives an account of experiments to test the possibility of employing freely falling bodies for the successive operation of electrical circuit switches when the desired interval between their action is of the order of $\frac{1}{4}$ sec. The disposition of the apparatus may be seen by reference to figure 1 *a* which also shows the well-known condenser-discharge circuit employed for the actual measurement of the time interval between the working of the switches P and P'. The falling bodies employed were two steel Skefko ball bearings A and B, $\frac{1}{2}$ in. or 1 in. in diameter, which were released simultaneously from two electromagnets with cupped poles,* figure 1 *b*, by opening the switch S. They fell freely and were caught in pockets P, P', lined with plasticine to prevent rebounding. These pockets were at the ends of brass rods pivoted at their centres and capable of moving to an extent limited by stops K and K', in the plane of the drawing. In the preliminary experiments the pockets were fitted to condenser keys from which the springs had been removed.

The impact of A on P disconnects the battery from the circuit and allows the condenser to discharge through the resistance R until the arrival of B breaks the circuit at P'. The final potential-difference between the plates of the condenser is then estimated by making the switch S and observing the kick of the galvanometer G. It is of importance to ensure, by careful mounting of the contacts, that the arrival of A at P shall not, by mechanical vibration, momentarily break P'. A serious defect of this nature may be detected by a control experiment involving A only, in which a battery and the primary of a transformer are joined through P', and the secondary of the transformer is connected to a galvanometer which is deflected if the time interval between the equal and opposite changes in flux on break and make is sufficiently great.

---

* In our experiments the simultaneous release of the spheres was facilitated by the insertion of thin strips of paper between them and the poles: for experiments involving a large number of observations thin copper pole pieces would serve the same purpose and economize time.

If h be kept constant and H varied, then

$$H=\tfrac{1}{2}g\,(T_o-T_e)^2 \qquad \text{and} \qquad h=\tfrac{1}{2}g\,(t_o-t_e)^2,$$

where the symbols with subscripts o and e denote observed times and any constant timing errors respectively. Thus

$$T_o-t_o=\sqrt{(2/g)}\,\sqrt{H}+\{T_e-t_e-\sqrt{(2/g)}\,\sqrt{h}\}. \qquad \text{......(1)}$$

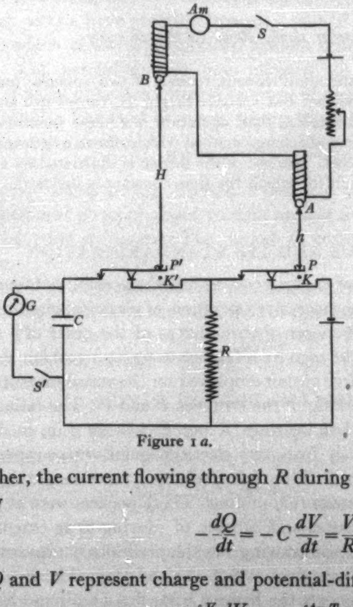

Figure 1 *a*.

Figure 1 *b*.

Further, the current flowing through R during the discharge of the condenser is given by

$$-\frac{dQ}{dt}=-C\frac{dV}{dt}=\frac{V}{R},$$

where Q and V represent charge and potential-difference respectively. Thus

$$-\int_{V_0}^{V}\frac{dV}{V}=\frac{1}{CR}\int_{t=0}^{t=T_o-t_o}dt,$$

or

$$T_o-t_o=CR\log_e(V_0/V)=2{\cdot}303CR\log_{10}(V_0/V), \qquad \text{......(2)}$$

where V_0 and V are the potential-differences between the plates of the condenser on the arrival of A at P and B at P' respectively.

Substitution in equation (1) of the value of (T_o-t_o) obtained from equation (2) gives

$$2{\cdot}303CR\log_{10}(V_0/V)=\sqrt{(2/g)}\,\sqrt{H}+\{T_e-t_e-\sqrt{(2/g)}\,\sqrt{h}\}, \qquad \text{......(3)}$$

which affords a means of demonstrating how nearly $(T_0 - t_0)$ approximates to a linear function of $\sqrt{H}$.* An alternative treatment, which affords a more interesting test and involves the accuracy of the electrical constants of the circuit, is to rewrite equation (3) in the form

$$\log_{10} V = -(1/2{\cdot}303CR)\sqrt{(2/g)}\sqrt{H} - (1/2{\cdot}303CR)\{T_e - t_e - \sqrt{(2/g)}\sqrt{h}\} + \log_{10} V_0, \qquad \text{......(4)}$$

which shows that a plot of $\log_{10} V$ against $\sqrt{H}$ will not only substantiate the required relation by its rectilinearity, but also yield a value for g from the magnitude of its gradient.

In the experimental work the practice of allowing the condenser to charge for 3 min., before releasing A and discharging C by instantaneously pressing S' directly after the impact of B with P', was adhered to as minimizing the effects of imperfections in the condenser. The condenser was shorted for 1 min. after each observation to eliminate the effects of residual charges. The relative values of V, which are all that are required, were estimated from a calibration curve which was linear over the range employed and was obtained by using the arrangement shown in figure 2. In this circuit R and R' are resistances taken from two boxes such that $(R+R')$ is constant. K_1 is a key depressed for 3 min., and K_2 a key depressed instantaneously and directly after the release of K_1: in this way the conditions of the main experiment are simulated. Check readings to ensure the constancy of V_0 are taken during the progress of the experiment by opening P' before P.

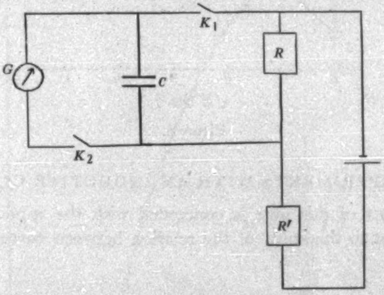

Figure 2.

Figure 3 illustrates a plot of $\log_{10} V$ against $\sqrt{H}$, obtained by using a $\frac{1}{3}$-μF. substandard condenser and a wire-wound 1-megohm resistance. It may be seen that the graph is satisfactorily linear, and the value of the gradient obtained by the method of Awbery(1) corresponds to a value of g equal to 976 cm./sec.^{2} A confirmatory experiment yielded a value of g equal to 980 cm./sec.^{2}

---

* When identical switches are employed, $(T_e - t_e)$ should be sufficiently small to make $(T_0 - t_0)$ proportional to $(\sqrt{H} - \sqrt{h})$: we desire however to keep our argument as general as possible, and accordingly we neglect this simplifying assumption.

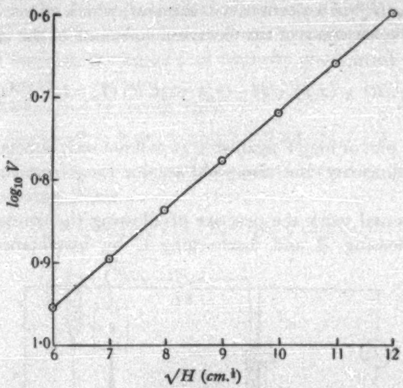

Figure 3.

§ 2. EXPERIMENTS WITH AN INDUCTIVE CIRCUIT

The second part of this note is concerned with the application of the two-sphere arrangement to the study of the relation between current and time in an inductive circuit.

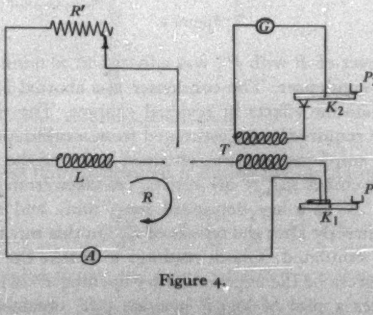

Figure 4.

Details of the circuit in question are indicated in figure 4. The key K_1 consists of a mercury-in-glass switch (for which we are indebted to Messrs The Mercury Switch Manufacturing Company) strapped to the arm of a lever. The impact of a sphere in the pocket P_1 tilts the lever and makes the circuit through L. K_2 is a key similar to those described previously. L consists of two coupled large air-cored inductances each of approximately 1 H., and T is a solenoid with two small inductance windings which serve as the primary and secondary of a transformer.

The experiment consists as before in simultaneously releasing the two spheres from different heights above P_1 and P_2 respectively, but now with the object of making the primary circuit and, after a measurable time t, breaking the secondary.

The magnitude of i, the primary current, t sec. after its initiation is then estimated by means of a subsidiary experiment in which L is replaced by a variable non-inductive resistance R' and the positions of the spheres are unaltered. R' is varied until on dropping the spheres the galvanometer kick is the same as it was previously; the reading of the ammeter A then gives the value of i in the main experiment. This is because damping due to the closing of the secondary circuit is in operation for the same time in both experiments, and the change in flux caused by the primary current growing from zero to i in the first experiment is the same as that due to the almost instantaneous establishment of the current registered by the ammeter in the second experiment, provided that in both instances the inertia of the galvanometer system is sufficient for all the charge to circulate through the coil before it moves.

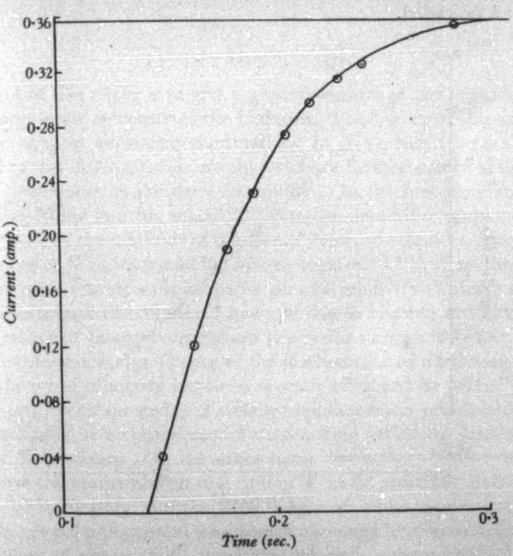

Figure 5.

Figure 5 shows a series of values of i, obtained as indicated above, plotted against corresponding values of time calculated from the expression $\sqrt{(2/g)}(\sqrt{H}-\sqrt{h})$ (see figure 1): and the production of this curve to cut the axis shows that the difference between the reaction times of the switches is of the order 0·14 sec.

To determine the time constant of the inductive circuit we write

$$t=\sqrt{(2/g)}\,\sqrt{H}+\{T_e-t_e-\sqrt{(2/g)}\,\sqrt{h}\}$$

as before, and combine it with the relation

$$i=i_\infty\{1-\exp(-Rt/L)\},$$

where i_∞ is the final steady value (0·356 amp.) of i read from A with L in circuit, to give

$$\log_{10}(1-i/i_\infty)=-(1/2{\cdot}303)\,(R/L)\,\sqrt{(2/g)}\,\sqrt{H}+\text{a constant}$$

if H and not h be varied.

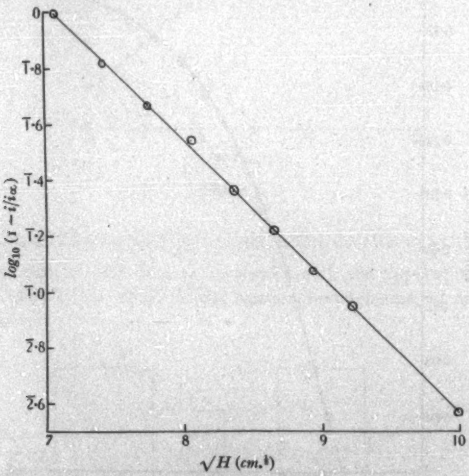

Figure 6.

A plot of $\log_{10}(1-i/i_\infty)$ against $\sqrt{H}$ is shown in figure 6: it is satisfactorily linear and thereby justifies the experimental procedure. Moreover the value of R/L, the reciprocal of the time constant, estimated from the values plotted by the method of Awbery(1) is 24·7 sec.^{-1}, and is in good agreement with the value of 24·8 sec.^{-1} calculated from tests with a Post Office box giving 57·0 Ω. and an Owen's bridge giving 2·30 H.

REFERENCE

(1) Awbery. *Proc. Phys. Soc.* **41**, 384 (1929).

RELATIVISTIC COSMOLOGY

By G. TEMPLE

Read at a discussion on the expanding universe held jointly with the Royal Astronomical Society, 27 January 1939

---

§ 1. INTRODUCTION

The object of this paper is to give a general account of the relativistic theories of the large-scale structure of the Universe. The history of this subject up to January 1933 is admirably summarized in Robertson's report(7), but the importance of recent developments amply justifies a further survey of the problem. These recent developments are three in number. In the first place there are the investigations of Milne and his school(6, 14) into the possibility of solving the cosmological problem by the methods of the *special* theory of relativity. Secondly there are the researches of Whittaker and his fellow-workers(1, 3, 5, 11, 12) on the form taken by the astronomical distance functions in general relativity. Thirdly there is the new and more extensive observational material due to Hubble and Shapley.

The importance of these investigations lies in the views which they give of the physical and astronomical significance of the mathematics of relativistic cosmology. The general theory of relativity has been severely criticized by Milne(6)* as wholly conceptual in origin and incapable of detailed application to problems of matter in motion. Accordingly he has constructed a cosmology within the framework of the special theory of relativity. On the other hand, Whittaker, Walker and McCrea have shown that the mathematical description of world structure given by general relativity can be accurately interpreted in terms of actual astronomical practice. Lastly both the special and general theories of cosmology have been subjected to the inevitable critique of observation—a critique which is unfortunately rendered indecisive by the lack of really extensive observations.

This practical problem will be treated by Dr McVittie later in this discussion (p. 529). This paper will deal only with the mathematical theories and their physical interpretation. In Robertson's report(7) the principles of general relativity were taken for granted and immediately applied to the problem of cosmology. But the whole interest of this application resides in the astronomical interpretation of the analysis, and to provide a cogent and satisfactory interpretation requires a restatement of the fundamental principles of the theory. A fresh analysis of the general theory of relativity is therefore attempted in §§ 8, 9 and 10, and it will appear that the characteristic feature of this analysis is its emphasis on the physical significance of parallel displacement. Milne's theory is also restated so as to facilitate comparison with the cosmological theory of general relativity (§§ 5, 6 and 7), and by a simplification of Walker's proof it is shown that Milne's solution of the problem is unique within the domain of special relativity.

---

* §§ 504–14.

This account of the details of modern cosmological theory would be incomplete without an introductory reference to its conceptual basis and to the general principles and prejudices which so largely determine the form of the theory. We therefore begin with an attempt to make explicit the basic presuppositions of all relativistic theories.

PART I. GENERAL PRINCIPLES AND METHODS

§ 2. THE ASSUMPTION OF THE UNIFORMITY OF PHYSICAL LAWS

The methods of cosmology are necessarily speculative. The observations made in a terrestrial laboratory of a distant nebula refer primarily to certain physical events in the laboratory itself, such as the orientation of a telescope or the darkening of a photographic plate. The customary association of these events in the immediate neighbourhood of the observer with properties of the nebula depends entirely upon hypothesis, viz. that the physical laws valid in the laboratory are also valid in a region extending to the distant nebula. Such a hypothesis is unavoidable although it is frequently made without explicit avowal. A purely empirical basis is wholly inadequate for cosmological studies. The interpretation of observations necessarily requires conceptual and speculative elements.

We therefore make the explicit assumption of the uniformity of physical laws, and especially of the laws of spatial and temporal measurement. But this assumption can be understood in two different ways. In the first place it can be understood to mean that those laws which are valid in the immediate neighbourhood of a terrestrial observer are universally valid. This global uniformity implies that space-time in the large is geometrically the same as space-time in the vicinity of our terrestrial laboratories, i.e. that it is the well-known Minkowski manifold of special relativity. In the second place physical uniformity can be understood to mean that those laws which are valid in the immediate neighbourhood of a terrestrial observer are also valid in the immediate neighbourhood of any event in space-time. This local uniformity implies, roughly speaking, that space-time is Minkowskian in the small domain near any prescribed event, but it does not place any limitation on the ways in which these small Minkowskian domains are connected together. This freedom of connexion is utilized in Einstein's general theory of relativity to exhibit gravitational force as an illusion produced by the geometry of space-time.

§ 3. THE ASSUMPTION OF HOMOGENEITY

The empirical basis of relativistic cosmology consists of observations of the orientation, the apparent brightness and the Doppler effect of the extra-galactic nebulae. Its object is to derive information about the large-scale structure of the universe, small local irregularities such as stars being neglected. To co-ordinate and unify the rather meagre observational material it is not enough to make the hypothesis of the uniformity of physical laws. It is necessary to go further and to make some hypothesis regarding the way in which the infinite potentialities of physical laws are actualized in the universe. The particular feature of the smoothed-out universe which such hypothesis must envisage is the distribution and motion of the nebulae in space and time. Of all the hypothesis which might be made it is evident that the very simplest is that, in some sense, the distribution of the nebulae is homogeneous. It is this hypothesis which is usually described as the "cosmological principle". Studies in relativistic cosmology consist essentially of precise interpretative definitions of homogeneity and of detailed mathematical deduction of the quantitative observations which these definitions imply.

Perhaps the most general and most satisfactory definition of homogeneity is that given by Milne(6),* and it is his definition which we shall adopt here. Broadly speaking this definition states that the nebular distribution is homogeneous if the smoothed-out universe of nebulae presents the same appearance from each nebula. More precisely, if *A* and *B* are observers attached to two different nebulae, the totality of the observations made by *A* on the whole universe of nebulae must be described by *A* in exactly the same way as the corresponding observations made by *B* are described by *B*. The hypothesis of the uniformity of space-time implies that there are no privileged observers for whom *physical laws* have an especial simplicity or character. The hypothesis of the homogeneity of nebular distribution implies that there are no privileged observers for whom *physical events* have an especial simplicity or character.

There is no a priori evidence for either of these principles. They are submitted for consideration only on the grounds that, as a matter of practical convenience to the mathematician and physicist, they are the simplest hypotheses which can be framed, and that their consequences are in full harmony with the general polyphony of observation.

§4. COSMOLOGY AND THE SPACE PROBLEM

Such are the basic hypotheses of relativistic cosmology. The mathematical tools required to forge them into a physical theory are tensor analysis and group theory. The mathematical apparatus required is far from novel and is, to a very large extent, an inevitable extension of that constructed by Poincaré, Helmholtz and Lie in their researches on the axiomatic basis of the metrical geometry of the space determined by rigid bodies. A brief indication of the nature of this extension will fitly close this section.

The fundamental physical fact with which the space problem begins is the persistence of the congruence of rigid rods, i.e. the fact that two rigid rods congruent in any assigned place can be separated and moved by different paths to another position, where they will again be congruent. This fact arouses the mathematical enquiry. "What are the possible groups of transformations corresponding to the motion of rigid bodies?" With certain natural subsidiary conditions this problem was completely solved by Lie. His solution however is subject to two implicit restrictions—it neglects the factor of time and it is essentially local in its validity. In other words, it tacitly assumes that the geometry of space is independent of the passage of time during the motion of rigid bodies, and it quietly ignores the fact that the final solution can be valid only in that domain in which the basic physical facts are verified, viz. the immediate neighbourhood of an observer in a terrestrial laboratory. If we endeavour to remove these restrictions we are immediately confronted with the problem of the geometry in the large of space-time, i.e. with the general cosmological problem. In the third part of this report we have given a restatement of the general theory of relativity from this point of view.

---

* Chapter 3.

PART II. COSMOLOGY IN SPECIAL RELATIVITY (MILNE'S THEORY)

The solution of the cosmological problem by the methods of the special theory of relativity, due to Milne, merits particular consideration, not only because of its extreme simplicity, but also because the solution obtained is unique in the presupposed field of discourse. To facilitate comparison between this solution of the cosmological problem and the other solutions offered by general relativity we shall give in this part a version of Milne's theory in accordance with the general principles adopted in the previous part. The investigations initiated by Milne are in fact much wider in scope than can be indicated by our version, and, in particular, they start from a completely novel discussion of the correlation of measurements made by different observers in terms of light signals only.

§ 5. THE NEBULAR CONGRUENCE

We proceed, then, to discuss the distribution of nebulae in the space-time of special relativity. If τ is the temporal co-ordinate, and ξ, η, ζ are rectangular spatial co-ordinates, the interval ds between two neighbouring events is given by

$$ds^2 = c^2 d\tau^2 - d\xi^2 - d\eta^2 - d\zeta^2,$$

c being the speed of light. (These co-ordinates are normal Riemannian co-ordinates with base-point at the origin.) The relations between the measurements made by two observers A and B at any two events A_0 and B_0 in their respective life-histories are most conveniently expressed in terms of the normal co-ordinates $(\tau_{A_0}, \xi_{A_0}, \eta_{A_0}, \zeta_{A_0})$ and $(\tau_{B_0}, \xi_{B_0}, \eta_{B_0}, \zeta_{B_0})$ with base points at A_0 and B_0 and with their temporal co-ordinates τ_A and τ_B taken in the direction of the world lines of A and B at A_0 and B_0. The required relation can then be expressed by saying that the transformation relating the two sets of co-ordinates belongs to the general Lorentz group.

The distribution of the nebulae as seen by A at the event A_0 should be given in detail by the equations of the world line of each nebula; but it is mathematically convenient to replace this atomic distribution by a hydrodynamical distribution in which the nebulae are treated as particles of a continuous fluid, which is described in gross by its density and velocity at every point and time. The world lines of the nebulae are then to be considered as a congruence of time-like curves in the space-time manifold.

We must next express the cosmological principle in terms of this nebular congruence. By the principle of homogeneity the distribution of nebulae as observed by an observer A (attached to a certain nebula) at an event A_0 must be the same as the distribution of nebulae as observed by an observer B (attached to another nebula) at some event B_0. Hence the equations of the nebular congruence must remain invariant under the transformation connecting the normal co-ordinates of A_0 and B_0 defined above.

To this principle of homogeneity Walker(14) adds the principle of symmetry, viz. that the distribution seen by each nebular observer has spherical symmetry about the observer. It may be that this further assumption is really unnecessary, but it considerably helps forward the argument, which now runs as follows.

§ 6. THE STRATIFICATION OF SPACE-TIME

The set of events such as B_0, at which a nebular observer B sees the same world-view as a prescribed observer A at a prescribed event A_0 on his world line, forms a three-dimensional manifold V_3 passing through A_0. This manifold is invariant under the transformations from one observer to another and under the rotation transformations about each observer. The aggregate of these transformations forms a continuous group G_6 with six parameters. Now, by a well-known theorem of group theory, a V_3 which admits a G_6 is a manifold of uniform curvature, i.e. a species of hypersphere.

In the immediate neighbourhood of A_0 the V_3 which passes through A_0 coincides with the instantaneous space of the observer A at A_0. Hence the world lines of the nebulae are orthogonal to the invariant manifolds V_3. These manifolds, which are hyperspheres, are therefore concentric, and the nebular world lines therefore diverge from a common event $\mathscr{E}$.

If we take normal co-ordinates with this common event $\mathscr{E}$ as base point, the equations to the world line of any nebula are

$$\xi = u\tau, \quad \eta = v\tau, \quad \zeta = w\tau,$$

u, v and w being the (constant) components of its velocity. In the world view of the observer attached to the nebula with the world line $\xi=0$, $\eta=0$, $\zeta=0$, at the epoch τ the nebulae at a distance σ, equal to $(\xi^2+\eta^2+\zeta^2)^{\frac{1}{2}}$, appear to be receding with a speed σ/τ, proportional to the distance σ. Thus Milne's theory leads very simply to Hubble's velocity, distance relation, and the coefficient of proportionality, τ^{-1}, has an immediate interpretation as the reciprocal of the age of the nebula, dated from the event $\mathscr{E}$.

In this theory space-time exhibits a natural stratification into the system of three-dimensional manifolds V_3, whose general equation is

$$(\xi^2+\eta^2+\zeta^2) - c^2\tau^2 = \text{constant.}$$

To emphasize this stratification of space-time and to facilitate a comparison of Milne's theory with the general theory of relativity we make the transformation

$$\xi = \sigma \sin\theta \cos\phi, \quad \eta = \sigma \sin\theta \sin\phi, \quad \zeta = \sigma \cos\theta,$$

introducing the spherical polar co-ordinates (σ, θ, ϕ), followed by the transformation

$$\tau = t\,(1+r^2)^{\frac{1}{2}}, \quad \sigma = ctr. \qquad \ldots\ldots(6\cdot1)$$

Then
$$ds^2 = c^2dt^2 - c^2t^2\left(\frac{dr^2}{1+r^2} + r^2d\theta^2 + r^2\sin^2\theta\, d\phi^2\right). \qquad \ldots\ldots(6\cdot2)$$

In this system of co-ordinates the world lines of the nebulae are given by

$$r = \text{constant}, \quad \theta = \text{constant} \quad \text{and} \quad \phi = \text{constant},$$

and the V's are given by

$$t = \text{constant}.$$

It is therefore a very simple matter to determine the density of the nebular distribution, which, in virtue of the cosmological principle, is a function of t only, say $n(t)$. The equation of continuity is

$$\frac{\partial}{\partial t}\{(-\Delta)^{\frac{1}{2}}\, n(t)\} = 0,$$

where Δ is the determinant of the coefficients in the expression for the metric (6·2), i.e.

$$\Delta = -(c^8t^6r^4)/(1+r^2).$$

Hence
$$n(t) = B/(c^3t^3), \qquad \ldots\ldots(6\cdot3)$$

where B is a dimensionless constant.

§ 7. OBSERVABLE RELATIONS

In order to obtain relations between directly observable quantities we shall determine the number of nebulae for which the Doppler shift factor D lies in a prescribed range dD, and the relation between the apparent brightness of a nebula and its Doppler effect$^{(5)}$.

An observer whose world line is $r=0$ receives a ray of light whose world line must be a null curve and which, by symmetry, has the equations

$$\theta = \text{constant}, \quad \phi = \text{constant}, \quad \frac{dt}{t} = -\frac{dr}{(1+r^2)^{\frac{1}{2}}},$$

whence
$$t_o/t_s = r_s + (1+r_s^2)^{\frac{1}{2}}, \qquad \ldots\ldots(7\cdot1)$$

the suffixes o and s referring respectively to the observer at the moment of reception and to the nebula at the moment of emission. The Doppler factor D is therefore given by

$$D = \frac{\text{wave-length at observer}}{\text{wave-length at nebula}} = \frac{dt_o}{dt_s} = \frac{t_o}{t_s},$$

since r_s is constant along the world line of the nebula.

Hence all the nebulae observed to have the Doppler factor D lie on the manifold given by the equations

$$\left.\begin{array}{ll} & t_s = t_o/D \\ \text{and} & r_s + (1+r_s^2)^{\frac{1}{2}} = D, \\ \text{or} & r_s = \frac{1}{2}(D - D^{-1}). \end{array}\right\} \qquad \ldots\ldots(7\cdot2)$$

The number of nebulae observed by *o* to lie in the spherical shell with radii r_s and $r_s + dr_s$ is

$$dN = \frac{4\pi r_s^2\, dr_s}{(1+r_s^2)^{\frac{1}{2}}} (ct)^3\, n(t) = 4\pi B r_s^2 \frac{|\,dt_s\,|}{t_s},$$

by equations (6·3) and (7·1). Therefore, by equation (7·2),

$$dN = \pi B (D - D^{-1})^2\, dD/D,$$

or, on writing

$$D = 1 + \delta,$$

$$\frac{dN}{d\delta} = 4\pi B \delta^2 (1 - 2\delta + \tfrac{13}{4}\delta^2 + \ldots). \qquad \text{......(7·3)}$$

To determine the apparent brightness of a nebula we first compare E_s and E_o, the energies of a photon when emitted by the nebula and when received by the observer, and also N_s and N_o, the numbers of photons emitted per unit time by the nebula and received per unit time by the observer. We have that

$$\frac{E_s}{E_o} = \frac{\text{wave-length at observer}}{\text{wave-length at star}} = \frac{dt_o}{dt_s} = \frac{t_o}{t_s},$$

and

$$\frac{N_s}{N_o} = \frac{1/dt_s}{1/dt_o} = \frac{t_o}{t_s}.$$

Now it can be shown that the cross-sectional area of this pencil of radiation from *s* varies as $(r_s t_o)^2$, so that the apparent brightness varies as $N_o E_o (r_s t_o)^{-2}$, i.e. as $N_s E_s (r_s t_o/t_s)^{-2}$. The distance *L* as judged from observations of apparent brightness is therefore given by

$$L = r_s t_o/t_s = r_s D,$$

whence

$$L = \tfrac{1}{2}(D^2 - 1) = \delta(1 + \tfrac{1}{2}\delta). \qquad \text{......(7·4)}$$

PART III. COSMOLOGY IN GENERAL RELATIVITY

§ 8. THE PROBLEM OF CONGRUENCE IN SPACE-TIME

The general theory of relativity is based on the assumption of the local uniformity of the physical laws of spatial and temporal measurement. This means that any observer *A* at any event A_0 in his world line can set up a system of local Minkowskian co-ordinates, with their origin at A_0, valid in the immediate vicinity of A_0. The observer *A* can also assign co-ordinates to any observable event *P*, however remote from A_0, in terms of observations of *P* made at A_0, but the relation of these global co-ordinates to the local co-ordinates remains a matter for investigation. In fact the first problem to be discussed is the relation between the local co-ordinates attached to different events and the global co-ordinates covering the observable universe.

The simplest methods by which two distant observers can compare and correlate their local co-ordinate systems are either the use of light signals or the transport of rigid scales and clocks. The method of correlation by means of light signals has been extensively developed by Milne and Whitrow. Here we shall consider the second method. The problem which it suggests is the natural extension of the classical space problem. This latter problem discussed the congruent transformations of a three-dimensional space into itself. The present problem discusses what may be called the "congruent transformations" of a small three-dimensional space—the local instantaneous space of an observer—free to move in four-dimensional space-time.

This general space-time problem has never been attacked, but a particular solution—which may be the only solution having physical significance—is furnished by Levi-Civita's theory of parallel displacement as interpreted by Eddington's concept of equivalence. This particular solution is effectively given by stating the components of the vector $A^\mu + dA^\mu$ at an event with (global) co-ordinates $(x^\mu + dx^\mu)$, which is equivalent or congruent to the vector A^μ at the event (x^μ). (Here and elsewhere the suffixes take the value 0, 1, 2, 3 and Einstein's summation convention is used.) The explicit formula is

$$dA^\mu = -\Gamma^\mu_{\alpha\beta} A^\alpha dx^\beta, \qquad \text{......(8·1)}$$

where $\Gamma^\mu_{\alpha\beta}$ is the Christoffel symbol of the second kind for the quadratic form

$$ds^2 = g_{\alpha\beta}\, dx^\alpha\, dx^\beta,$$

which specifies the metric in global co-ordinates.

The physical significance of the formula for parallel displacement is that it specifies the changes in the co-ordinate measure of a scale or clock which is transported from (x^μ) to $(x^\mu + dx^\mu)$ in a natural or non-violent manner. It follows that the natural motion of a particle will be obtained by taking the vector A^α to be the tangent vector dx^α/ds of the world line of the particle. The resulting equations are

$$\frac{d^2x^\mu}{ds^2} + \Gamma^\mu_{\alpha\beta}\frac{dx^\alpha}{ds}\frac{dx^\beta}{ds} = 0, \qquad \text{......(8·2)}$$

the familiar equations to geodesics.

So far nothing seems to have been gained by the preceding elaborate discussion, but a further consideration of the conditions to be satisfied by the coefficients $g_{\alpha\beta}$ shows that what has been vaguely described as the "natural motion" of a particle is in reality its motion *under gravitational forces only*. In other words those physical phenomena which are treated in classical Newtonian dynamics as motion under the inverse square law of attraction are discussed in general relativity as natural motion under no forces. It is, of course, well known that to a first approximation the two theories agree, and that to a second approximation the relativistic theory provides a satisfactory account of certain outstanding small discrepancies between observation and the Newtonian theory.

§9. THE STRESS TENSOR

It has already been emphasized in connexion with the special theory of relativity (§ 5) that the actual discrete distribution of the nebulae in space-time is to be replaced by a continuous distribution, in which the world lines of the nebulae form a congruence of curves. The same method is to be adopted in general relativity, the direction of the world line which passes through any event P being specified by a unit vector λ^μ at P. The density ρ of the continuous distribution is related to the actual discrete distribution in such a way that $\rho\, d\omega$ is, on the average, the total mass of the nebulae in a volume $d\omega$ of their instantaneous space at an event P. Considerations of continuity then show that the momentum vector $\rho\lambda^\alpha$ must satisfy the divergence equations

$$D_\alpha (\rho\lambda^\alpha) = 0,$$

where D_α, the symbol for covariant differentiation, is employed because the space-time manifold is not Minkowskian in the large.

The hydrodynamics of this continuous distribution can be expressed in two equivalent ways, viz. either by equations of the Lagrangian type which assert that the world lines are geodesics, or by equations of the Eulerian type which are satisfied by the so-called stress tensor $T^{\alpha\beta}$ or $\rho\lambda^\alpha\lambda^\beta$. The Lagrangian equations are

$$\lambda^\alpha D_\alpha \lambda^\beta = 0,$$

whence

$$D_\alpha (T_\beta^{\alpha}) = D_\alpha (\rho\lambda^\alpha\lambda_\beta) = \lambda_\beta\, D_\alpha (\rho\lambda^\alpha) + \rho\lambda^\alpha D_\alpha \lambda_\beta = 0. \qquad \ldots\ldots(9{\cdot}1)$$

The Eulerian equations therefore express the fact that the divergence of the stress tensor is zero.*

Some investigators take the stress tensor in the form

$$T^{\alpha\beta} = \rho\lambda^\alpha\lambda^\beta + p^{\alpha\beta},$$

where $p^{\alpha\beta}$ is the tensor representing the internal stresses of the continuous distribution, and they further assume that

$$p^{\alpha\beta} = 0 \quad \text{if} \quad \alpha \neq \beta, \quad \text{and} \quad p^{\alpha\alpha} = p,$$

so that the only stress is a hydrostatic pressure p. The object of this assumption is to take into account the pressure due to the radiation in the inter-nebular space, but as the effect of radiation is almost certainly negligible we shall not take it into account here.

§ 10. THE FIELD EQUATIONS

We shall obtain the conditions to be satisfied by the coefficients $g_{\alpha\beta}$ (alluded to in § 9) as the extension of Poisson's theorem ($\Delta V = -4\pi\gamma\rho$, for the gravitational potential V) appropriate to general relativity. Following Synge(10) we consider the world lines L, M of any two neighbouring particles, and two events P, Q respectively on L and M. The "absolute gravitational intensity at an event" is clearly a meaningless phrase, as we can only measure relative velocities and relative accelerations. But "the excess of the gravitational intensity at Q over the gravitational intensity at P" can be defined to be the acceleration of Q relative to P. We define corresponding events P and Q on L and M by the condition that if Q_1 corresponds to P_1 and Q_2 to P_2 then the geodesic intervals P_1Q_1 and P_2Q_2 are equal. Then if η^μ is the infinitesimal vector drawn from P on L to the corresponding event Q on M, the velocity of Q relative to P is the covariant derivative of η^μ along L, i.e.

---

* Much deeper considerations of the relation between the geodesic law (8·2) and the divergence equations (9·1) are to be found in papers by Walker(13), Robertson(8) and Synge(9).

$$D\eta^\mu = \lambda^\alpha D_\alpha \eta^\mu,$$

where λ^α is the tangent vector to L at P. Similarly the acceleration of Q relative to P is

$$f^\mu = DD\eta^\mu.$$

Now, by a classical theorem due to Levi-Civita(4),

$$DD\eta^\mu = -R^\mu{}_{\alpha\nu\beta}\,\lambda^\alpha\eta^\nu\lambda^\beta,$$

where $R^\mu{}_{\alpha\nu\beta}$ is the Riemann-Christoffel tensor. It is satisfactory to note that this expression for the relative acceleration, i.e. the gravitational force, is independent of the direction of M.

Remembering that $\eta^\mu = dx^\mu$ we see that the covariant derivatives of the gravitational intensity at P are given by

$$f^\mu/dx^\nu = -R^\mu{}_{\alpha\nu\beta}\lambda^\alpha\lambda^\beta.$$

Hence the divergence of the gravitational force at P is

$$f^\mu/dx^\mu = -R^\mu{}_{\alpha\mu\beta}\lambda^\alpha\lambda^\beta = R_{\alpha\beta}\lambda^\alpha\lambda^\beta,$$

where $R_{\alpha\beta}$ is the Ricci tensor. Synge's investigations(10) show that the divergence so defined by the contracted covariant derivative agrees with the classical definition in terms of the gravitational flux across a closed 2-way in the instantaneous space of L.

Now in classical dynamics the divergence of the gravitational force at P is proportional to the density of matter at P. In general relativity the expression for the divergence depends upon the orientation of the instantaneous space in which it is calculated, and the simplest generalization of Poisson's equation will be of the form

$$R_{\alpha\beta}\lambda^\alpha\lambda^\beta = aT_{\alpha\beta}\lambda^\alpha\lambda^\beta + b,$$

in which it is expressed as a linear function of the stress tensor $T_{\alpha\beta}$. We have inserted here a term b, independent of $T_{\alpha\beta}$, in order to allow us to consider the possibility that the effective density may not be the actual density, but the excess of the actual density over some average density of all gravitating matter. The advantage of this hypothesis is that it makes possible a uniform and static Universe—which is clearly impossible in classical dynamics except in the trivial case when there is no matter present.

It follows from our generalized Poisson's equation (which must hold for all time-like vectors λ^α) that

$$R_{\alpha\beta} = aT_{\alpha\beta} + bg_{\alpha\beta}.$$

Now we have seen (9·1) that the stress tensor $T_{\alpha\beta}$ satisfies the generalized divergence equation

$$D_\beta T_\alpha{}^\beta = 0,$$

and it is known that this is also true of the modified Ricci tensor $R_{\alpha\beta} - \frac{1}{2}g_{\alpha\beta}R$, where $R = g^{\alpha\beta}R_{\alpha\beta}$. It follows that the term b must have the form

$$b = \tfrac{1}{2}R - \lambda,$$

where λ is a constant—the so-called cosmological constant. Moreover a must be a constant, and a further comparison of the classical Poisson's equation with our generalized Poisson's equation, based on an examination of geodesics, shows that

$$a = -8\pi\gamma/c^4,$$

where γ is the Newtonian constant of gravitation and c is the speed of light.

We thus obtain Einstein's field-equations

$$R_{\alpha\beta} - \tfrac{1}{2}Rg_{\alpha\beta} + \lambda g_{\alpha\beta} = -\kappa T_{\alpha\beta}, \qquad \text{......(10·1)}$$

where $\kappa = 8\pi\gamma/c^4$.

§ 11. THE STRATIFICATION OF SPACE-TIME

The cosmological principle can be applied in the general theory of relativity exactly as in the special theory, and, when it is supplemented by the principle of symmetry, it shows that the space-time manifold contains a system of three-dimensional manifolds V_3, each of which has uniform curvature and is cut orthogonally by the world lines of the nebulae. This argument, due to Walker(14) furnishes a proof of the assumptions adopted by Robertson(7) as the foundation of relativistic cosmology. The stratification of space-time implied by this argument is exhibited by taking a system of co-ordinates such that

$$\left.\begin{aligned} ds^2 &= c^2\,dt^2 - R^2(t)\,dl^2, \\ \text{where} \qquad dl^2 &= \frac{dr^2}{1-\frac{1}{4}kr^2} + r^2\,d\theta^2 + r^2\sin^2\theta\,d\phi^2. \end{aligned}\right\} \qquad \text{......(11·1)}$$

Here $R(t)$, sometimes written as $\exp g(t)$, is an arbitrary function of t; the world lines of the nebulae are given by

$$r = \text{constant}, \quad \theta = \text{constant}, \quad \phi = \text{constant};$$

and the manifolds V_3 are given by $t = \text{constant}$, the constant k being $+1$, 0, or -1 according as the manifold is spherical, flat or hyperbolic in curvature. The isotropic and uniform character of a V_3 can be shown by making the transformation

$$r = \bar{r}/(1+\tfrac{1}{4}k\bar{r}^2), \quad (\bar{r} \geqslant 0),$$

when

$$dl^2 = (d\bar{r}^2 + \bar{r}^2\,d\theta^2 + \bar{r}^2\sin^2\theta\,d\phi^2)(1+\tfrac{1}{4}k\bar{r}^2)^{-2}.$$

It will be noticed at once that the metric of special relativity as employed in Milne's theory is obtained by taking k to be -4 and $R(t)$ to be ct.

To determine the unknown function $R(t)$ and the density ρ of the nebular distribution we now substitute the values of the Ricci tensor $R_{\alpha\beta}$ appropriate to the metric (11·1) in the field equations (10·1), the stress tensor being expressed in the form

$$T^{\alpha\beta} = \rho\lambda^\alpha\lambda^\beta,$$

where λ^α the tangent vector to the world lines of the nebulae has the components

$$\lambda^0 = c^{-1}, \quad \lambda^1 = 0, \quad \lambda^2 = 0, \quad \lambda^3 = 0.$$

After a little rearrangement we thus obtain the following two equations:

$$2RR'' + (kc^2 + R'^2) = \lambda c^2 R^2,$$

and

$$-2RR'' + 2\,(kc^2 + R'^2) = \kappa c^4 \rho\, R^2.$$

These relations were first obtained by Friedmann(2), under much more restrictive hypotheses.

The first equation shows that

$$c\,(t - t_0) = \pm \int_{R_0}^{R} \left\{\frac{3x}{D\,(x, \lambda)}\right\}^{\frac{1}{2}} dx,$$

where

$$D\,(x, \lambda) = \lambda x^3 - 3kx + \kappa E.$$

It then follows that $\rho c^2 R^3 = E$, a constant.

This result could also have been obtained from the divergence equation satisfied by the stress tensor.

§ 12. OBSERVABLE RELATIONS

Just as in the special relativistic problem observable relations can now be deduced from the form of the line element (11·1). We shall consider, as before, an observer whose world line is $r = 0$ and whose observations made at $t = t_0$ refer to a nebula at $r = r_s$, $t = t_s$. Then the Doppler shift factor is

$$D = \frac{R\,(t_0)}{R\,(t_s)} \qquad \text{......(12·1)}$$

and the number of nebulae observed to lie in the spherical shell with radii r_s and $r_s + dr_s$ is

$$dN = \frac{4\pi r_s^2\, dr_s}{(1 - \frac{1}{4}kr_s^2)^{\frac{1}{2}}}\, R^3\,(t_s)\,\rho,$$

where

$$\rho = E/c^2 R^3\,(t_s) = \alpha R^{-3}\,(t_s), \quad \text{say.}$$

Hence

$$\begin{aligned} dN &= 4\pi\alpha r_s^2\, dr_s\, (1 - \tfrac{1}{4}kr_s^2)^{-\frac{1}{2}} \\ &= 4\pi\alpha r_s^2\, c\,|dt_s|/R\,(t_s), \qquad \text{......(12·2)} \end{aligned}$$

using the equation to the null curve joining (r_s, t_s) to $(0, t_0)$. The elimination of t_s between (12·1) and (12·2) enables us to calculate the observable ratio dN/dD.

The distance as judged by apparent brightness is now

$$L = r_s\, R\,(t_0)/R\,(t_s) = r_s D, \qquad \text{......(12·3)}$$

and this can also be expressed as a function of D only when R is known as an explicit function of t.

The detailed comparison of theory and observation is given by McVittie in the succeeding paper.

§ 13. THE TOPOLOGY OF THE EXPANDING UNIVERSE

In the region of space-time occupied by the nebulae the line element is given by

$$ds^2 = c^2 dt^2 - R^2\,(t) \left\{\frac{dr^2}{1 - \frac{1}{4}kr^2} + r^2 d\theta^2 + r^2 \sin\,\theta d\phi^2\right\},$$

the world lines of the nebulae being $r = \text{constant}$, $\theta = \text{constant}$, $\phi = \text{constant}$. Since the direction of these lines is essentially time-like, dt^2 must be positive and t must be a real co-ordinate. Now $R(t)$ is implicitly given as a function of t by the integral

$$c(t-t_0) = \pm \int_{R_0}^{R} \left\{\frac{3x}{D(x, \lambda)}\right\}^{\frac{1}{2}} dx,$$

and hence the possible range of values of R must be limited so as to ensure that the integrand shall be real.

A detailed consideration of the various cases which can arise, according to the values given to the constants λ, κ and E, is given in Robertson's report. Here we wish to emphasize only this fact—that the range of values thus found for $R(t)$ refers only to that portion of space-time actually occupied by matter. The question of the existence of empty space-time outside this region still remains for further consideration.

To elucidate this situation consider the metric of Milne's expanding universe, equation (6·2),

$$ds^2 = c^2dt^2 - (ct)^2\left(\frac{dr^2}{1+r^2} + r^2d\theta^2 + r^2\sin^2\theta\, d\phi^2\right),$$

derived from the general relativity metric by writing

$$\lambda = 0, \quad k = -4, \quad \kappa = 0, \quad R(t) = ct.$$

The argument in the first paragraph of this section shows that in the portion of space-time occupied by the nebulae—let us say the nebular space-time—we must have t real. But the transformation (6·1)

$$\tau = t(1+r^2)^{\frac{1}{2}}, \quad \sigma = ctr$$

shows that $ds^2 = c^2d\tau^2 - (d\sigma^2 + \sigma^2d\theta^2 + \sigma^2\sin^2\theta\, d\phi^2)$. In these new co-ordinates $(\tau, \sigma, \theta, \phi)$ the whole of space-time is clearly given by allowing τ and σ to have the ranges

$$-\infty < \tau < +\infty, \quad 0 < \sigma < +\infty.$$

Now
$$t^2 = \tau^2 - \sigma^2/c^2,$$

so that t is real only inside the light-cone

$$\tau^2 = \sigma^2/c^2.$$

Hence the nebular space-time is surrounded by an empty region extending to infinity.

In the case of the general relativity metric we cannot make a similar transformation to exhibit at once the empty space-time with which the nebular space-time is surrounded, but we can devise another and more fundamental line of approach to this question. We consider the path of a free particle projected from an event on the boundary of the nebular space-time. If the form of this path indicates that the particle has entered nebular space-time and appeared across the boundary within a finite interval in the past, we can at once infer the existence of an empty space-time surrounding the nebular space-time.

This method can be very simply illustrated by means of Milne's metric. The curve $rt=a/c$ is easily seen to be a geodesic which meets the boundary $t=0$ at the event $(t=0,\ r=\infty)$. The value of $\int ds$ taken along this geodesic to $(t=t_0,\ r=r_0)$ is

$$\int\left(c^2dt^2-c^2t^2\frac{dr^2}{1+r^2}\right)^{\frac{1}{2}}=-\int_{\infty}^{r_0}\frac{a\,dr}{r^2\,(1+r^2)^{\frac{1}{2}}}$$

$$=\frac{a}{r_0}\,(1+r_0^2)^{\frac{1}{2}}-a.$$

Hence a particle pursuing this geodesic entered the nebular space-time at a finite interval in the past. We are therefore obliged to envisage an empty region of space-time surrounding the portion which is filled with matter. The consideration of these topological questions must, however, be reserved for subsequent investigations.

§ 14. CONCLUSION

The two main hypotheses upon which relativistic cosmology depends are the uniformity of space-time and the homogeneity of the distribution of nebulae. In the special theory of relativity these assumptions lead inevitably to Milne's cosmological theory, in which there is only one arbitrary constant at our disposal, namely, the present age of our own nebula, dated from the epoch when all the nebulae were coincident in space. In the general theory of relativity the fundamental hypotheses lead to an expression for the metric of space-time which is perfectly definite apart from three arbitrary constants, λ, κ and E. It may be that the topological consideration just adumbrated will also throw light on this problem, but for the moment we must rely on the observational evidence marshalled by McVittie for any further information about the values of these constants.

REFERENCES

(1) Etherington, I. M. H. *Phil. Mag.* (7), **15**, 761 (1933).
(2) Friedmann, A. *Z. Phys.* **10**, 377 (1922) and **21**, 326 (1924).
(3) Kermack, W. O., McCrea, W. H. and Whittaker, E. T. *Proc. Roy. Soc. Edinb.* **53**, 31 (1933).
(4) Levi-Civita, T. *Math. Ann.* **97**, 291 (1926).
(5) McCrea, W. H. *Z. Astrophys.* **9**, 290 (1935).
(6) Milne, E. A. *Relativity, Gravitation and World Structure* (Clarendon Press, 1935).
(7) Robertson, H. P. *Rev. Mod. Phys.* **5**, 62 (1933).
(8) Robertson, H. P. *Proc. Edinb. Math. Soc.* (2), **5**, 63 (1937).
(9) Synge, J. L. *Trans. Roy. Soc. Canada* (3), **28**, 127 (1934).
(10) Synge, J. L. *Proc. Edinb. Math. Soc.* (2) **5**, 93 (1937).
(11) Walker, A. G. *Quart. J. Math.* **4**, 71 (1933).
(12) Walker, A. G. *Mon. Not. R. Astr. Soc.* **94**, 159 (1933).
(13) Walker, A. G. *Proc. Edinb. Math. Soc.* (2), **4**, 238 (1935).
(14) Walker, A. G. *Proc. Lond. Math. Soc.* (2), **42**, 90 (1937).

THE DIFFRACTION OF ELECTRONS BY ANTHRACENE

By A. CHARLESBY, G. I. FINCH and H. WILMAN

Received 20 *October* 1938. *Read* 24 *February* 1939

ABSTRACT. The diffraction of electrons by anthracene crystals gives results which are in agreement with the structure as previously determined with X rays. In addition to the normal type of multispot pattern characteristic of electron diffraction by thin single crystals, however, there appears superimposed another pattern consisting of areas or islands of diffuse scattering. It is shown that this diffuse-area pattern is due to molecules which, though oriented with respect to the beam in accordance with the crystal-orientation, have nevertheless no definite phase relationship with each other. The diffuse-area pattern is thus virtually equivalent to that which would be given by a gaseous stream of oriented molecules flowing past the electron beam. Since the crystal setting cannot as a rule be directly observed as it can in X-ray analysis, it has been necessary to develop methods for determining the crystal orientation from a consideration of the normal electron-diffraction pattern features. In this way it was established that the diffuse-area pattern was furnished by molecules which, though in, or very near, their normal positions and orientations within the lattice, were acting as independent scattering groups. It is shown, by an extension of the Debye theory to molecular lattices, that the occurrence of the diffuse-area pattern in electron-scattering by molecular crystals can be satisfactorily accounted for on the supposition that the molecules vibrate thermally as practically rigid units about their mean positions within the lattice.

It is pointed out that the diffuse-area pattern can be regarded as an important adjunct to the X-ray Fourier synthesis method of determining molecular and crystal structure, in cases where the atomic arrangement within the molecule exhibits a sufficient degree of symmetry. Furthermore, it offers an approach to the study of molecular structure in cases in which the method of electron diffraction by gases fails owing to the complex nature of the pattern resulting from the lack of orientation of the molecules in the gaseous stream.

§1. INTRODUCTION

In a previous communication⁽¹⁾ it was shown that single-crystal electron-diffraction transmission patterns could be obtained from a variety of organic compounds, both aliphatic and aromatic. Later⁽²⁾ we drew attention to the fact that, in addition to the normal pseudo-cross-grating arrangement of spots, the patterns from crystals of certain aromatic compounds often contained diffuse bands or areas of blackening in an apparently orderly distribution which appeared to be related to the arrangement and separation of the carbon atoms in the molecules and thus seemed to be similar in origin to the well-known layer lines in reflection patterns obtained from monomolecular layers of normal straight-chain hydrocarbons⁽³⁾. The importance of the bearing of such a phenomenon upon the determination of the nature of molecular structure and its arrangement in the crystalline state need hardly be stressed; accordingly, we have undertaken a systematic study of the diffraction of electrons by organic compounds, selecting as a starting point anthracene, the structure of which has been determined by X rays.

§2. THE STRUCTURE OF ANTHRACENE

According to X-ray measurements(4), the anthracene unit cell is monoclinic, and its axial dimensions are as follows: $a=8{\cdot}58$ A., $b=6{\cdot}02$ A., $c=11{\cdot}18$ A., while $\beta=125°$. It contains two molecules and, since the ($h0l$) and (010) spacings are halved when h is odd, the space group is C_{2h}^5, and the general atomic positions are $\pm(xyz)$, $\pm(x+\frac{1}{2},\ \frac{1}{2}-y,\ z)$. Robertson(4) has determined the atomic co-ordinates by a Fourier analysis of the diffraction intensities obtained from spectrometer measurements, and the estimated values are set out in table 1, where *A*, *B*, *C*, ... represent the atoms as shown in figure 1. The co-ordinates expressed in fractions of the axial lengths are given in table 2, and it is convenient also for numerical work to express the atom co-ordinates in terms of orthogonal axes *a*, *b*, *c'*, as in table 3. The per-

Table 1. Carbon-atom co-ordinates in angstroms for anthracene, referred to the monoclinic axes *a*, *b*, *c* with the centre of symmetry of a molecule as origin

Atom	x	y	z	
			From the *a* projection	From the *b* projection
A	0·81	0·19	4·17	4·10
B	1·06	0·94	3·14	3·11
C	0·54	0·49	1·57	1·55
D	0·81	1·24	0·55	0·57
E	0·28	0·78	−1·0	−0·98
F	0·56	1·53	−2·02	−1·98
G	0·02	1·06	−3·60	−3·54
$P=D/2=$	$0{\cdot}40_5$	0·62	0·28	
$\frac{C+E'}{2}=Q=\frac{C-E}{2}=$	$0{\cdot}13_0$	$-0{\cdot}14_5$	$1{\cdot}27_5$	

Table 2. Carbon-atom co-ordinates for anthracene expressed as fractions of *a*, *b*, *c*

Atom	x	y	z
A	0·094	0·032	0·369
B	0·124	0·157	0·279
C	0·062	0·082	0·140
D	0·095	0·207	0·050
E	0·033	0·130	−0·089
F	0·065	0·254	−0·179
G	0·002	0·177	−0·319
$P=D/2=$	0·047	0·103	0·025
$\frac{C+E'}{2}=Q=\frac{C-E}{2}=$	0·015	−0·026	0·115

Table 3. Carbon-atom co-ordinates for anthracene expressed in angstroms and referred to the orthogonal axes *a*, *b*, *c'*

Atom	*x*	*y*	*z*
A	−1·55	0·19	3·37
B	−0·73	0·94	2·55
C	−0·35	0·49	1·28
D	0·49	1·24	0·46
E	0·85	0·78	−0·81
F	1·71	1·53	−1·64
G	2·07	1·06	−2·93

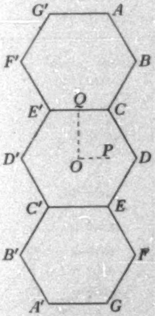
G'
A
F'
B
Q
E'
C
D'
P
O
D
C'
E
B'
F
A'
G

Figure 1 *a*. The anthracene molecule in plan.

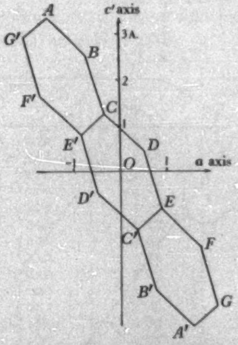
A
c' axis
3 A.
G'
B
2
F'
C
1
E'
D
-1
O
1
a axis
D'
E
C'
F
B'
G
A'

Figure 1 *b*. Projection of the anthracene molecule on the plane *ac'*.

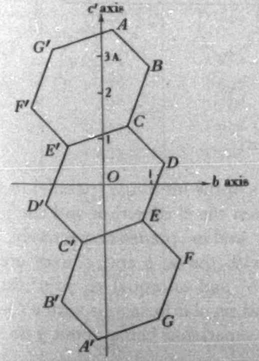
c' axis
A
G'
3 A.
B
2
F'
C
1
E'
D
O
1
b axis
D'
E
C'
F
B'
G
A'

Figure 1 *c*. Projection of the anthracene molecule on the plane *bc'*.

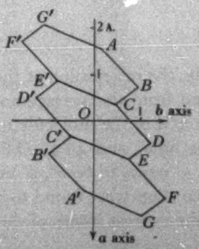
G'
2 A.
F'
A
1
E'
B
D'
C
O
1
b axis
C'
D
B'
E
A'
F
G
a axis

Figure 1 *d*. Projection of the anthracene molecule on the plane *ab*.

spective view, figure 2, has been drawn from the above data to show the arrangement of the molecules and the disposition of the axes.

Robertson gives the further details of the molecular setting as follows. The angles between the c' axis and the orthogonal projections of the long axis of the molecule upon the bc' and ac' planes are 8° and 30·1° respectively. Hence the long axis of the molecule encloses with the a, b and c' axes the angles χ equal to 119·7°, ψ equal to 96·9° and ω equal to 30·7° respectively. The long axis of the molecule lies at an angle of 8·5° to the crystallographic axis c.

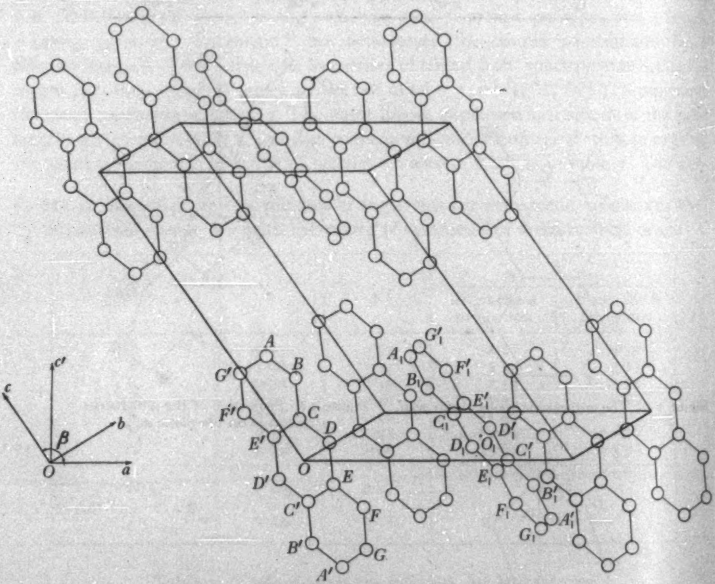

Figure 2.

Similarly, the orientation of the short axis of the molecule (parallel to CE', DD', etc.) is found from the average angles between the c' direction and the projections of the short axis of the molecule upon the bc' and ac' planes respectively, which are found to be 69·6° and 46·9°. The angles with the a, b and c' axes are thus, by calculation, χ' equal to 69·6°, ψ' equal to 28·6° and ω' equal to 70·9° respectively. The benzene rings were found to be plane and regular hexagons with a C–C spacing of 1·41 A., the nearest intermolecular atomic separation being about 3·80 A.

§ 3. ELECTRON-DIFFRACTION TRANSMISSION PATTERNS FROM POLYCRYSTALLINE ANTHRACENE FILMS

Polycrystalline films suitable for transmission were obtained by evaporation of a benzene or ether solution or by condensation of the vapour *in vacuo* on a collodion film supported on nickel gauze. Typical patterns, one taken with the film sufficiently inclined to the beam to show incipient arcing but the other much more inclined, are shown in figures 3 and 4 respectively. These and all other patterns discussed in what follows were taken with a camera-length L of approximately 47 cm. and an accelerating voltage between 50 and 70 kv. The analysis of figure 3 is set forth in table 4.

Table 4. Anthracene vaporized on to collodion: specimen film inclined by about 9° from setting normal to beam: 48 kv.

Intensity*	Ring radii R (cm.)	d/n (A.)	Indices, *hkl*	d/n by X rays (A.)	Angle between (*hkl*) and (001) planes
VF	0·457	6·027	010	6·02	90°
S	0·566	4·883	$11\bar{1}$	4·88	82° 16′
M	0·601	4·582	110 002	4·57 4·58	68° 7′ 0°
VS	0·660	4·174	$20\bar{1}$ $20\bar{2}$	4·17 4·17	76° 59′ 76° 42′
VVS	0·802	3·430	$21\bar{1}$ $21\bar{2}$	3·43 3·43	79° 18′ 79° 6′
M	0·906	3·040	210	3·03	60° 21′
M	0·914	3·014	020	3·01	90°
VF	0·969	2·848	021 $12\bar{1}$	2·86 2·83	71° 48′ 85° 31′
M	0·998	2·764	120 112	2·77 2·76	76° 58′ 34° 8′
VVF	1·071	2·571	$12\bar{2}$ 211	2·65 2·53	68° 46′ 46° 29′
MS	1·129	2·440	$22\bar{1}$ $22\bar{2}$ $33\bar{1}$	2·44 2·44 2·44	82° 25′ 82° 16′ 70° 43′
VF	1·324	2·082	$40\bar{2}$ $40\bar{4}$	2·09 2·08	76° 59′ 76° 42′
M	1·379	1·997	$32\bar{1}$	2·00	74° 19′
M	1·398	1·970	$40\bar{1}$	1·98	69° 49′
M	1·410	1·956	031 $13\bar{1}$	1·96 1·95	77° 38′ 86° 54′
M	1·431	1·925	130	1·93	80° 57′
MF	1·487	1·852	032 $12\underline{3}$ $20\bar{6}$ 203	1·84 1·85 1·84 1·84	66° 21′ 40° 45′ 25° 23′ 41° 14′
M	1·524	1·807	$23\bar{1}$ $23\bar{2}$	1·81 1·81	84° 24′ 83° 43′
F	1·692	1·628	$33\bar{3}$ 231	1·63 1·63	82° 16′ 63° 41′
VF	1·718	1·603	401	1·59	47° 27′
VF	1·860	1·481	041 140	1·49 1·47	80° 40′ 83° 6′
VF	1·909	1·443	$14\bar{2}$	1·45	78° 32′
F	1·946	1·417	$60\bar{4}$	1·42	87° 50′

* *V*, very; *F*, faint; *M*, medium; *S*, strong.

These results are in good agreement with those obtained by X rays and show further that the crystals orient preferably with the *ab* plane parallel to the substrate, i.e. in (001) orientation. Thus, in figure 4, the projection of the axis about which the film was inclined to the beam passes horizontally through the central spot, and the diffraction arcs fall into groups lying on elliptic loci corresponding to different pairs of *hk* indices and whose major axes pass vertically through the central spot(5). Since the orientation axis does not coincide with any important zone axis, a strongly marked development of layer lines is not to be expected. The 010 diffraction is not observed in X-ray patterns and is forbidden for the space-group C_{2h}^5; its occurrence here is probably due to secondary or "dynamic" scattering.

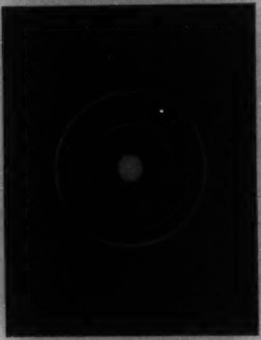

Figure 3.

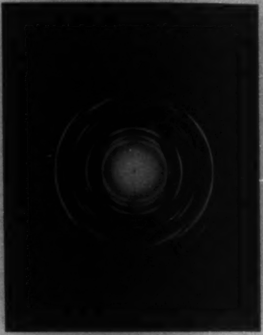

Figure 4.

§4. REFLECTION FROM POLYCRYSTALLINE ANTHRACENE SURFACES

Reflection specimens were readily prepared by evaporation of an ether solution on polished stainless steel. A typical pattern is shown in figure 5. The occurrence of $00l$ diffractions in the plane of incidence shows that the crystals are, as in the case of the previous transmission specimens, in (001) orientation with respect to the substrate surface. The remaining diffraction spots also fall on vertical row lines, each corresponding to one pair of *hk* indices. To complete the indexing of the pattern it is convenient to use the reciprocal lattice construction. Figure 6 shows the directions of the reciprocal axes a^*, b^*, c^* relative to the crystal axes a, b, c, where the *ab* plane is parallel to the substrate surface, indicated by shading in the diagram. a^*, b^*, etc. are given by

$$a^* = 1/a \sin\beta, \quad b^* = 1/b, \quad c^* = 1/c \sin\beta;$$

and

$$\alpha^* = \gamma^* = 90^\circ, \quad \beta^* = 180^\circ - \beta.$$

The pattern, figure 5, is equivalent to that which would be obtained by rotation of a single crystal about an axis normal to the (001) plane. Hence in the reciprocal lattice construction for the diffracted beams, this lattice must be rotated about the c^* axis to find where the reciprocal lattice points intersect the Ewald sphere, which in this case is approximately a plane normal to the beam and containing the c^* axis. Thus each reciprocal lattice point describes a circle about the c^* axis, whose intersections with the Ewald sphere (or, with sufficient accuracy, plane) have horizontal and vertical co-ordinates x and y in this plane, which are respectively normal and parallel to c^*, and are given by

Figure 5. Reflection from anthracene in (001) orientation.

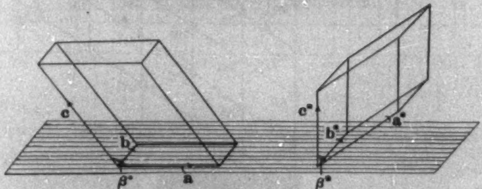

Figure 6. The anthracene unit cell and its reciprocal.

$$x = \pm\{(ha^* \sin \beta^*)^2 + k^2b^{*2}\}^{\frac{1}{2}} = \pm(h^2/a^2 + k^2/b^2)^{\frac{1}{2}},$$

$$y = ha^* \cos \beta^* + lc^*.$$

The horizontal and vertical co-ordinates of the corresponding diffractions in the pattern are accordingly λLx and λLy respectively. All vertical co-ordinates depend only on h and l; thus all points with the same h and l indices but different k index must lie on the same horizontal line in the pattern; and, similarly, diffractions with the same hk indices have the same horizontal co-ordinate and therefore lie on the same vertical row line. To construct the pattern from the intersection of the reciprocal lattice with the plane of reflection we have only to superpose the patterns of reciprocal lattice points lying in planes passing through the c^* axis, the diffractions corresponding to all the points in any one plane appearing in the pattern at or near the corresponding main azimuthal setting. For example, with the beam parallel to the *b* axis, the pattern is as shown in figure 7. The complete index diagram, figure 8, corresponding to the stronger diffractions in figure 5, was constructed in this manner, the size of each spot being made roughly proportional to its intensity in the diffraction pattern. The *hk* indices of each diffraction are given at the foot of each vertical row line and the *l* index beside the corresponding spot on the right-hand side of the row line in all cases except for the 11*l* and 13*l* rows, where the *l* indices are placed to the left of the row owing to space restrictions, while the 20*l*, 12*l* and $\bar{4}2l$ rows are indexed on the right-hand side of the diagram only for the same reason. Thus the most intense diffraction above the central spot is the 004, and the one immediately to its left is the 014. For the sake of clarity the indexing has been distributed over the whole pattern. The true rotation pattern would be symmetrical about the central vertical row line, and the fact that figure 5 is not completely symmetrical in this sense is to be ascribed to the presence in the path of the beam of a comparatively few and relatively large crystals, instead of many small ones with only one common axis of orientation.

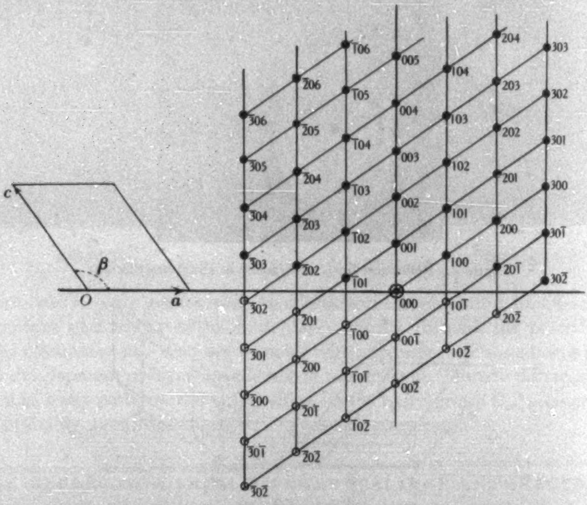
c
β
O
a
1̄06
005
104
204
303
2̄06
1̄05
004
103
203
302
3̄06
2̄05
1̄04
003
102
202
301
3̄05
2̄04
1̄03
002
101
201
300
3̄04
2̄03
1̄02
001
100
200
301̄
3̄03
2̄02
1̄01
000
101̄
201̄
302̄
3̄02
2̄01
1̄00
001̄
102̄
202̄
3̄01
2̄00
1̄01̄
002̄
3̄00
2̄01̄
1̄02̄
3̄01̄
2̄02̄
3̄02̄

Figure 7. Section through the reciprocal lattice normal to the b^* axis.

The relative intensities of the diffractions in figure 5 are approximately in agreement with those which would be expected according to the structure factors measured by x rays, when allowance is made for the radial decrease in intensity due to atom-form-factor variation with scattering angle and for the limited number of crystals contributing to the pattern. Table 5 shows the general agreement of the estimated intensities with the x-ray structure-amplitudes (Robertson's values) in the main zones of diffraction. Thus the diffractions which have a high structure

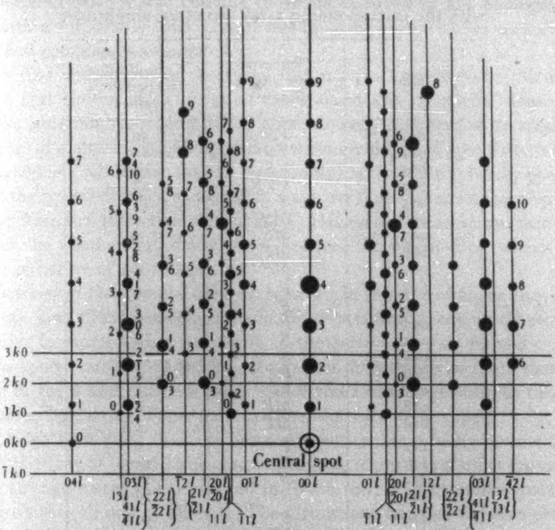
3k0
2k0
1k0
0k0
1̄k0
Central spot
04l
03l
13l
41l
4̄1l
22l
2̄2l
1̄2l
20l
21l
2̄0l
2̄1l
01l
11l
1̄1l
00l
01l
1̄1l
11l
20l
2̄0l
21l
2̄1l
12l
22l
2̄2l
03l
41l
4̄1l
13l
1̄3l
4̄2l

Figure 8. Index diagram for the stronger diffractions in figure 5.

Figure 9. Reflection from a rubbed anthracene surface in (001) orientation.

factor are the strongest in the electron-diffraction pattern. It may be pointed out that, as might be expected, the diffractions such as 001, 011, etc., occurring near the shadow edge in the pattern, appear abnormally weak, as a result of a partial screening by the appreciable roughness of the surface of the specimen.

A striking fact is that rubbing the surface of a reflection specimen in a given direction results in a pattern, figure 9, which is independent of the azimuthal direction of the beam, and in which the only clear diffractions recorded are those lying on the vertical central, i.e. *ool*, row. These are strong and show no appreciable broadening or arcing.

Table 5. Comparison of the intensities of diffractions in figure 5 with the corresponding x-ray structure-amplitudes

hkl	Observed intensity in figure 5	x-ray structure-amplitude (Robertson's values)
001	*VS*	30
002	*VS*	22
003	*VS*	14·5
004	*VVS*	22
005	*S*	16
006	*MS*	< 4
007	*MS*	< 4
008	*MF*	< 4
009	*MF*	3
011	*F*	9
012	*F*	3·5
013	*F*	4·5
014	*S*	12·5
015	*S*	14
016	*F*	< 4
017	*VF*	< 5
018	*MF*	6
019	*MF*	5·5
$\bar{1}12$	*F*	12
$\bar{1}13$	*F*	12·5
$\bar{1}14$	*S*	17·5
$\bar{1}15$	*S*	16·5
110	*S*	50·5
111	*M*	9·5
112	*F*	< 3
113	*F*	6
114	*M*	14
115	*VF*	?
200, $\bar{2}03$	*MS*	59, 14·5
201, $\bar{2}04$	*F*	5, 3
202, $\bar{2}05$	*F*	4·5, 5
203, $\bar{2}06$	*F*	4·5, 5
204, $\bar{2}07$	*MS*	22·5, <4
205, $\bar{2}08$	*F*	8, <4
210, $\bar{2}13$	*VS*	48·5, ?
220, $\bar{2}23$	*S*	13, <3
221, $\bar{2}24$	*S*	13, 23·5
222, $\bar{2}25$	*MS*	6, 19·5

§5. TRANSMISSION THROUGH ANTHRACENE SINGLE CRYSTALS

Single-crystal transmission specimens were prepared by condensation in air on nickel gauze or on collodion supported on gauze, or by picking up on gauze the film formed by the evaporation of a xylene solution on a cleaned water surface, either of these last two procedures being followed when a crystal oriented with the *ab* plane in the specimen film was required. The thin plate-like crystals often showed interference colours, and some with areas up to as much as 10 mm.^{2} were obtained. Owing to the appreciable volatility (sublimation) of anthracene *in vacuo*, the change in the pattern with decreasing thickness could be followed and recorded with one and the same crystal; it was possible to obtain as many as five photographs, by starting with a sufficiently thick crystal and breaking vacuum after each exposure, before it had completely evaporated.

As the first anthracene single-crystal transmission pattern to be discussed we reproduce that shown in figure 10*a*. Its unusual and composite nature is unmistakable, consisting as it does of an approximately symmetrical arrangement of diffuse areas of scattering superimposed on the normal type of spot pattern showing typical Laue-zone reinforcement. In electron diffraction we can hardly observe the setting of the crystal directly, as we can in X-ray work, and we must therefore deduce the setting from the diffraction pattern itself. Having done this we can then proceed to examine the relationship, if any exists, between the diffuse-area pattern and the molecular structure of anthracene.

The indexing of the normal Laue-spot pattern. In the case of figure 10*a*, L and V were 48 cm. and 58 kV. respectively, and the dimensions of the nearly rectangular pattern unit (measured near the centre of the pattern) are $0{\cdot}392_5$ and $0{\cdot}212_8$ cm. Hence the spots clearly lie at the intersections of the two sets of Laue zones corresponding to the b and c crystal axes. The k and l indices relating to these zones are marked in figure 10*a*. These pattern dimensions are in the ratio 1 : 1·85, whereas $b : c = 1 : 1{\cdot}857$ by X rays; thus the beam was not far from being normal to the *bc* plane. A third set of broad Laue zones exhibiting slight but distinct curvature lies near the strongly curved lines marked in figure 10*a*; they comprise spots whose l indices are either all odd or all even. The diffractions lying on the zero-order zone which passes through the central spot have even l indices, while those in consecutive zones have alternately l odd and l even. The angles between the beam and the b and c axes can be derived from the measurements of the spot pattern in figure 10*a*, as follows.

Consider the general case of a cross-grating whose axes $\mathbf{a}_1$ and $\mathbf{a}_2$ enclose an angle α_3 and are inclined to the reversed beam direction at the angles θ_1 and θ_2 respectively. Since the beam is normal to the screen, the projections, $\bar{\mathbf{a}}_1$ and $\bar{\mathbf{a}}_2$, of $\mathbf{a}_1$ and $\mathbf{a}_2$ on the screen enclose an angle $\bar{\alpha}_3$ such that

$$\cos \bar{\alpha}_3 = (\cos \alpha_3 - \cos \theta_1 \cos \theta_2)/\sin \theta_1 \sin \theta_2. \qquad \ldots\ldots(1)$$

The Laue zones, h_1 and h_2, relating to the axes a_1 and a_2 intersect $\bar{a}_1$ and $\bar{a}_2$ (produced) in points which, over the small range of angles of diffraction considered, are practically equidistant at intervals equal to $\lambda L/a_1 \sin \theta_1$ and $\lambda L/a_2 \sin \theta_2$ respectively when θ_1 and θ_2 lie between about 20° and 160°. The Laue zones will in general be curved to an extent depending upon θ_1 and θ_2; thus, from being practically straight lines when the corresponding θ lies within the range between about 80° and 100°, they become increasingly curved with further inclination of the lattice row outside this range, the concavity lying towards the point where the lattice row produced

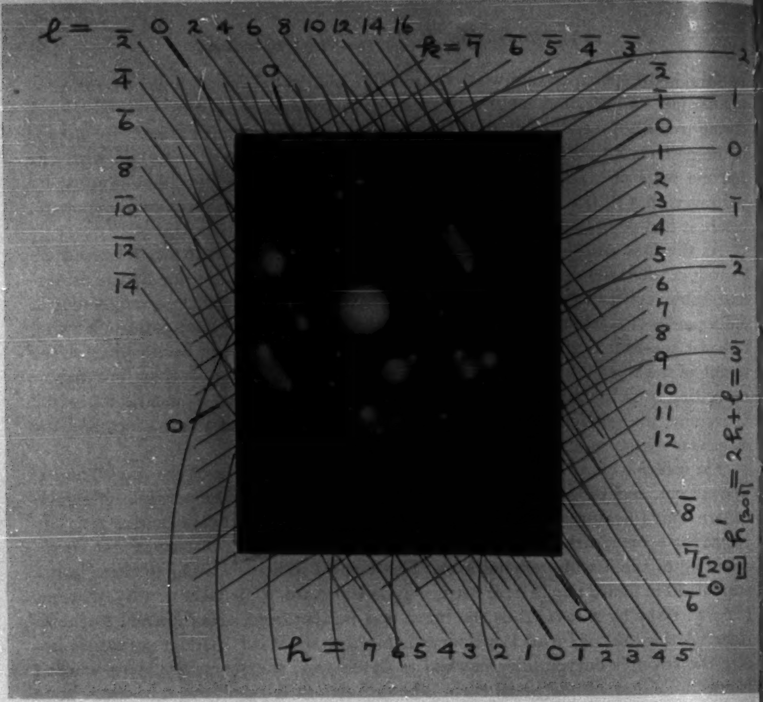
$\ell = \bar{2}$ 0 2 4 6 8 10 12 14 16
$\bar{4}$ $\bar{6}$ $\bar{8}$ $\bar{10}$ $\bar{12}$ $\bar{14}$
$k = \bar{7}$ $\bar{6}$ $\bar{5}$ $\bar{4}$ $\bar{3}$
$\bar{2}$ $\bar{1}$ 0 1 2 3 4 5 6 7 8 9 10 11 12
2 1 0 $\bar{1}$ $\bar{2}$ $\bar{3}$
$h'_{[20\bar{1}]} = 2h + \ell$
$\bar{8}$ $\bar{7}$ $\bar{6}$ $[20\bar{1}]$
0
$h = 7$ 6 5 4 3 2 1 0 $\bar{1}$ $\bar{2}$ $\bar{3}$ $\bar{4}$ $\bar{5}$

Figure 10*a*.

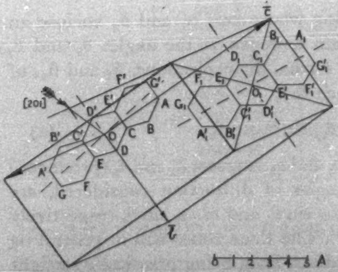
$\bar{c}$
B_1 A_1
D_1 C_1
G_1'
F′ G′
F_1 E_1
D_1' E_1' F_1'
[201]
D′ E′ A G_1
C_1' D_1'
B′ C′ O C B
A_1' B_1'
D
A′ E
$\bar{a}$
G F
ℓ
0 1 2 3 4 5 A

Figure 10*b*. $\theta_a = 44° 1'$, $\theta_b = 80° 45'$, $\theta_c = 81° 51'$. The negative direction of the [201] axis is towards the screen, as indicated by the feathered arrow.

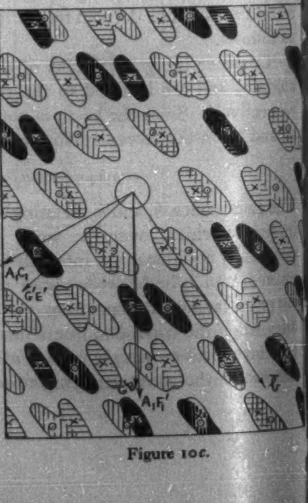
A_1C_1
$G'E'$
$G'E'$
A_1F_1'
ℓ

Figure 10*c*.

would meet the screen. The Laue zones intersect in diffraction spots whose positions can be specified in terms of their Laue indices h_1, h_2. $\bar{\alpha}_3$ can be calculated from the distances R from the central spot of three diffractions of known indices or equivalent translations in the pattern. For convenience we take, where possible, R_{10} and R_{01} together with any other suitable translations $R_{h_1 h_2}$, whence

$$\cos\bar{\alpha}_3 = (h_1^2 R_{10}^2 + h_2^2 R_{01}^2 - R^2_{h_1 h_2})/2h_1 h_2 R_{10} R_{01}. \qquad \text{......(2)}$$

From $\bar{\alpha}_3$, R_{10} and R_{01} we can derive θ_1 and θ_2 by the equations

$$\sin^2\theta_2 = [(1+m^2-2m\cos\alpha_3\cos\bar{\alpha}_3) \pm \sqrt{\{(1+m^2-2m\cos\alpha_3\cos\bar{\alpha}_3)^2 - 4m^2\sin^2\alpha_3\sin^2\bar{\alpha}_3\}}]/2m^2\sin^2\bar{\alpha}_3 \qquad \text{......(3)}$$

and
$$\sin\theta_1 = m\sin\theta_2; \qquad \text{......(4)}$$

where
$$m = (a_2/a_1)(R_{01}/R_{10}). \qquad \text{......(5)}$$

When $\alpha_3 = 90^\circ$ equation (3) reduces to

$$\sin^2\theta_2 = [(1+m^2) \pm \sqrt{\{(1+m^2)^2 - 4m^2\sin^2\bar{\alpha}_3\}}]/2m^2\sin^2\bar{\alpha}_3. \qquad \text{......(6)}$$

In the case of figure 10*a*, $\alpha_3 = \alpha = 90^\circ$ and b and c represent a_1 and a_2 respectively. Further $R_{10} = 0{\cdot}392_5$ cm., $R_{01} = 0{\cdot}212_8$ cm. and $R_{1\bar{2}} = 0{\cdot}575$ cm., these values being means obtained from the strongest and best defined diffractions in the vicinity of the central spot. Hence $\bar{\alpha} = 180^\circ - 88^\circ\ 23'$. We can also combine $R_{23} = 1{\cdot}027$ cm. with the values of R_{10} and R_{01} and obtain $\bar{\alpha} = 180^\circ - 88^\circ\ 42'$. Unlike $R_{1\bar{2}}$ and R_{23}, R_{12} is unsuitable for exact measurement as the corresponding row of diffraction spots lies in the direction of the third set of diffuse zones. The mean of five measurements of the corresponding angle taken directly from figure 10*a* gives $\bar{\alpha} = 180^\circ - 88^\circ\ 44'$. This directly measured angle is the most reliable in the present case since, owing to the thinness of the crystals, the Laue-zone relaxation allows spots to appear in positions markedly displaced from the points of intersection of maxima, i.e. medial lines, of the b and c zones.

From the above data we obtain, therefore, $m = 1{\cdot}007$, $\theta_b = 82^\circ\ 41'$ or $180^\circ - 82^\circ\ 41'$, and $\theta_c = 80^\circ\ 8'$ or $180^\circ - 80^\circ\ 8'$. The angles of tilt of b and c to the beam are thus so large that the curvatures of the corresponding zones are too slight to show whether the angles between these axes and the beam > or < 90°. Since $\bar{\alpha} > 90^\circ$, however, θ_b and θ_c must be both greater than or both less than 90°; and as the positive b and c directions are unknown in relation to the still undetermined direction of the a axis, this still leaves four possible crystal orientations. The set of Laue zones comprising diffractions all with l even or l odd, as judged from the spacing and the extent and direction of curvature, belongs to the [201] zone axis, if we assume b and c to be directed as in figure 10*b* and that θ_b and $\theta_c < 90^\circ$. The corresponding Laue index $h' = 2h + l$; hence h must be equal to $(h' - l)/2$, so that when h' is even l must also be even for h to be an integer and, similarly, when h' is odd l must also be odd; and the pattern agrees with these requirements. Furthermore, the a-axis Laue zones are easily identified in figure 10*a* and have approximately the required direction, curvature and spacing. None of the three alternative orientations agrees with the pattern.

Owing to the fact that the *bc* plane is in this case so nearly perpendicular to the beam and owing also to the Laue-zone relaxation, the measurements of spot-separation cannot yield more than a first approximation to the crystal setting, accurate to about 2°, but this is sufficient to furnish a complete indexing of the spot pattern upon which can be based a more accurate determination.

In calculating the direction and spacing of the Laue zones due to the *a* and [201] axes the first step was to determine the direction cosines $(l_1 m_1 n_1)$, $(l_2 m_2 n_2)$ and $(l_3 m_3 n_3)$ of the axial directions *a*, *b* and *c* respectively with reference to three orthogonal axes *OXYZ*, figure 11, *OZ* being parallel to the reversed direction of the beam while *OX* is taken in the plane containing *OZ* and *b*. We have directly

$$l_2=\sin\theta_b,\quad m_2=0,\quad n_2=\cos\theta_b;\quad n_3=\cos\theta_c; \qquad \text{......(7)}$$

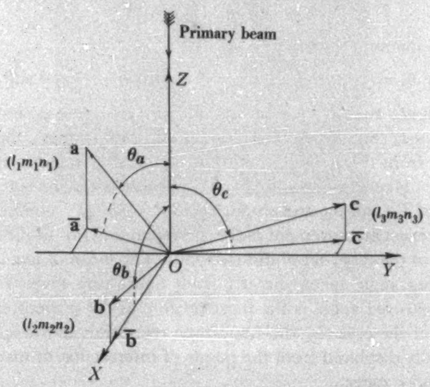

Figure 11.

and, since $\cos\alpha=l_2l_3+m_2m_3+n_2n_3=l_3\sin\theta_b+\cos\theta_b\cos\theta_c$,

$$l_3=(\cos\alpha-\cos\theta_b\cos\theta_c)/\sin\theta_b,\quad m_3=\pm(1-l_3^2-n_3^2)^{\frac{1}{2}},\quad n_3=\cos\theta_c. \qquad \text{......(8)}$$

Since θ_a is still undetermined, $(l_1 m_1 n_1)$ must be found from the relations expressing the fact that *a* is inclined at an angle β to *c* and at γ to *b*, namely

$$\left.\begin{aligned} &\cos\beta=l_1l_3+m_1m_3+n_1n_3,\\ \text{and}\qquad &\cos\gamma=l_1l_2+m_1m_2+n_1n_2,\end{aligned}\right\} \qquad \text{......(9)}$$

together with $$l_1^2+m_1^2+n_1^2=1. \qquad \text{......(10)}$$

Thus from equations (9) and (10) we obtain

$$\left.\begin{aligned} l_1&=\{n_1(n_2m_3-n_3m_2)+(m_2\cos\beta-m_3\cos\gamma)\}/(l_3m_2-l_2m_3),\\ m_1&=\{n_1(n_2l_3-n_3l_2)+(l_2\cos\beta-l_3\cos\gamma)\}/(l_2m_3-l_3m_2),\end{aligned}\right\} \qquad \text{......(11)}$$

in which can be substituted $(l_2m_2n_2)$, $(l_3m_3n_3)$, calculated from (7) and (8), so that the resulting expressions for l_1 and m_1 are in terms of n_1 only and can be substituted in (10) to give n_1 and thus l_1 and m_1. The angle $\bar{\gamma}$ between the projections $\bar{a}$, $\bar{b}$ of a and b respectively on the OXY plane normal to the beam (measured anti-clockwise from OX, i.e. the $\bar{b}$ direction) is $\tan^{-1}(m_1/l_1)$ and the inclination of the a axis to the beam is $\cos^{-1} n_1$, hence the construction of the a Laue zones follows in the usual way. The [201] axis projection on OXY makes an angle with $\bar{b}$ equal to

$$\tan^{-1}[\{(c/a)\,m_3+2m_1\}/\{(c/a)\,l_3+2l_1\}],$$

and its length is $\{(cm_3+2am_1)^2+(cl_3+2al_1)^2\}^{\frac{1}{2}}$; from which, together with the length of the [201] period T_{201}, equal to 14·12 A., the inclination of the [201] zone axis to the beam can be calculated and the Laue zones constructed.

Thus in the present case, the angle between the projections of the [201] zone axis and the b axis on the plane normal to the beam is calculated from the above data to be 180° + 33° 18′, and the angle between the projections of a and b is calculated to be 180° + 81° 25′, whereas the observed angles are about 180° + 20° and 180° + 80° 15′ respectively.

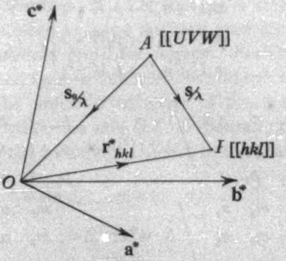

Figure 12.

Determination of the crystal orientation from the Laue-spot indices. When once the pattern has been indexed it becomes possible to determine the crystal-orientation more accurately. For this purpose we could use the measured angles between the projections of a, b and c, but the most accurate method makes use of the fact that the strongest spots in the pattern, which lie almost exactly on the medians of the Laue zones, must correspond very closely to Bragg reflections. In figure 10*a* there are several such spots which may be used for this purpose; thus the $03\bar{1}$ diffraction is much the strongest, the next most intense is $3\overline{44}$, and other slightly less strong diffractions are $24\bar{5}$, $\bar{1}54$ and $\bar{4}56$, in this order of intensity but all with nearly the same intensity. The condition for a diffraction hkl to be a Bragg reflection, i.e. to fulfil the three Laue conditions, is that the point [[hkl]] in the reciprocal lattice, figure 12, must lie on the Ewald sphere of reflection which passes through the origin O and whose centre A lies at a distance $1/\lambda$ along the reversed direction of the primary beam. Since four points define the sphere and O must be one of them, it is clear that if three other known points in the reciprocal lattice lie on the sphere the latter, and consequently the direction of the primary beam, is defined.

Let A be the point $[[UVW]]$ in the reciprocal lattice. Then

$$AO^2 = \Sigma U^2 a^{*2} + 2\Sigma UVa^* b^* \cos\gamma^* = 1/\lambda^2, \qquad \ldots\ldots(12)$$

and
$$AP^2 = \Sigma\,(U-h)^2\,a^{*2} + 2\Sigma\,(U-h)\,(V-k)\,a^* b^* \cos\gamma^* = 1/\lambda^2. \qquad \ldots\ldots(13)$$

Subtracting equation (13) from equation (12), we have

$$\Sigma\,(ha^{*2}\,U) + \Sigma\,(Uk+Vh)\,a^* b^* \cos\gamma^* = |\,\mathbf{r}^*_{hkl}\,|^2/2 = 1/2d^2_{hkl},$$

whence

$$\begin{aligned} &U\,(ha^{*2} + ka^* b^* \cos\gamma^* + la^* c^* \cos\beta^*) \\ &\quad + V\,(ha^* b^* \cos\gamma^* + kb^{*2} + lb^* c^* \cos\alpha^*) \\ &\quad + W\,(ha^* c^* \cos\beta^* + kb^* c^* \cos\alpha^* + lc^{*2}) \\ &\qquad = |\mathbf{r}^*_{hkl}\,|^2/2 = (\Sigma h^2 a^{*2} + 2\Sigma hka^* b^* \cos\gamma^*)/2. \end{aligned} \qquad \ldots\ldots(14)$$

If the indices of three Bragg reflections are known, three equations such as (14) can be obtained from which U, V and W can be calculated. Thus if the three equations are

$$\left.\begin{aligned} m_1U + n_1V + p_1W &= 1 \\ m_2U + n_2V + p_2W &= 1 \\ m_3U + n_3V + p_3W &= 1 \end{aligned}\right\} \qquad \ldots\ldots(15)$$

it follows that

$$\left.\begin{aligned} &U = \left|\begin{matrix} n_1 & p_1 & 1 \\ n_2 & p_2 & 1 \\ n_3 & p_3 & 1 \end{matrix}\right| \Bigg/ \Delta, \quad V = -\left|\begin{matrix} p_1 & 1 & m_1 \\ p_2 & 1 & m_2 \\ p_3 & 1 & m_3 \end{matrix}\right| \Bigg/ \Delta, \\ \text{and} \quad &W = \left|\begin{matrix} 1 & m_1 & n_1 \\ 1 & m_2 & n_2 \\ 1 & m_3 & n_3 \end{matrix}\right| \Bigg/ \Delta, \text{ where } \Delta = \left|\begin{matrix} m_1 & n_1 & p_1 \\ m_2 & n_2 & p_2 \\ m_3 & n_3 & p_3 \end{matrix}\right|. \end{aligned}\right\} \qquad \ldots\ldots(16)$$

We require to specify the direction of the beam by the angles θ_a, θ_b, θ_c which its reversed direction makes with **a**, **b** and **c** respectively. It suffices to calculate $U\Delta$, $V\Delta$, $W\Delta$, since the beam lies along the line $[UD, VD, WD]$ where D is any constant, i.e. along

$$\mathbf{r}^*_{UD,VD,WD} = UD\,\mathbf{a}^* + VD\,\mathbf{b}^* + WD\,\mathbf{c}^*,$$

so that
$$\left.\begin{aligned} \cos\theta_a &= \mathbf{r}^*.\mathbf{a}/|\,\mathbf{r}^*\,|\,a = (UD)/|\,\mathbf{r}^*_{UD,VD,WD}\,|\,a, \\ \cos\theta_b &= \mathbf{r}^*.\mathbf{b}/|\,\mathbf{r}^*\,|\,b = (VD)/|\,\mathbf{r}^*_{UD,VD,WD}\,|\,b, \\ \cos\theta_c &= \mathbf{r}^*.\mathbf{c}/|\,\mathbf{r}^*\,|\,c = (WD)/|\,\mathbf{r}^*_{UD,VD,WD}\,|\,c. \end{aligned}\right\} \qquad \ldots\ldots(17)$$

In the present case

$$a^* = 1/a \sin\beta = 0{\cdot}1422\ \text{A.}^{-1}, \quad b^* = 1/b = 0{\cdot}1622\ \text{A.}^{-1}, \quad c^* = 1/c \sin\beta = 0{\cdot}1091\ \text{A.}^{-1};$$

and $\alpha^* = \gamma^* = 90°$, $\beta^* = (180° - \beta) = 55°$. Hence the equation (14) for a Bragg reflection hkl becomes

$$\begin{aligned} &U\,(0{\cdot}02024h + 0{\cdot}00891_0 l) + V\,(0{\cdot}02759k) + W\,(0{\cdot}00891_0 h + 0{\cdot}01192l) \\ &\qquad = (0{\cdot}02024h^2 + 0{\cdot}02759k^2 + 0{\cdot}01192l^2 + 0{\cdot}00891_0 \times 2hl)/2. \end{aligned} \qquad \ldots\ldots(18)$$

The three equations corresponding to the diffractions $03\bar{1}$, $3\bar{4}\bar{4}$, and $24\bar{5}$ are respectively

$$\left.\begin{aligned} U(-0{\cdot}06850)+V(0{\cdot}6363)+W(-0{\cdot}09162)&=1,\\ U(0{\cdot}08354)+V(-0{\cdot}3676)+W(-0{\cdot}06979)&=1,\\ U(-0{\cdot}01268)+V(0{\cdot}3438)+W(-0{\cdot}1301)\ &=1.\end{aligned}\right\}\qquad\ldots\ldots(19)$$

Whence by (16)

$$U\Delta=0{\cdot}04503,\quad V\Delta=0{\cdot}00706,\quad W\Delta=0{\cdot}01157.$$

If we take $UD=4{\cdot}503$, $VD=0{\cdot}706$, $WD=1{\cdot}157$, then $|\,\mathbf{r}^*_{UD,VD,WD}\,|=0{\cdot}7300$; whence by (12), we obtain

$$\theta_a=44^\circ\ 1',\quad \theta_b=80^\circ\ 45',\quad \theta_c=81^\circ\ 51'.\qquad\ldots\ldots(20)$$

In order to gain some idea of the accuracy and validity of the method as applied to this and similar patterns we repeated the calculation using the three diffractions $03\bar{1}$, $3\bar{4}\bar{4}$ and $\bar{1}\bar{5}4$, which gave $\theta_a=43^\circ\ 52'$, $\theta_b=80^\circ\ 43'$, $\theta_c=82^\circ\ 2'$, in agreement with the above values to within 0° 11′. The first set of values corresponding to the three strongest spots was taken as being the most accurate obtainable.

Construction of the molecular projection diagram. For the purpose of comparing the observed and calculated Laue-zone directions and spacings, and also as one step in the construction of the projection diagram of figure 10*b*, we again refer the crystal axes *abc* to three orthogonal axes *OXYZ* (figure 11), such that *OZ* lies along the reversed direction of the beam and *OX* lies in the plane of *OZ* and the *b* axis. Then

$$l_2=\sin\theta_b,\quad m_2=0,\quad n_2=\cos\theta_b;\qquad\ldots\ldots(21)$$

and

$$\begin{aligned} n_1&=\cos\theta_a,\\ n_3&=\cos\theta_c,\\ \cos\alpha&=l_2l_3+m_2m_3+n_2n_3,\\ \cos\gamma&=l_1l_2+m_1m_2+n_1n_2;\end{aligned}$$

so that

$$l_1=(\cos\gamma-\cos\theta_a\cos\theta_b)/\sin\theta_b,\quad n_1=\cos\theta_a,\quad m_1=\pm\sqrt{(1-l_1^2-n_1^2)},\ \ldots\ldots(22)$$

and

$$l_3=(\cos\alpha-\cos\theta_b\cos\theta_c)/\sin\theta_b,\quad n_3=\cos\theta_c,\quad m_3=\pm\sqrt{(1-l_3^2-n_3^2)}.\ \ldots\ldots(23)$$

The values of (20) inserted in (21), (22), (23) give

$$\left.\begin{aligned} l_1&=-0{\cdot}1171, & m_1&=-0{\cdot}6850, & n_1&=0{\cdot}7190,\\ l_2&=\ \ 0{\cdot}9870, & m_2&=\ \ 0, & n_2&=0{\cdot}1606,\\ l_3&=-0{\cdot}02310, & m_3&=\ \ 0{\cdot}9896, & n_3&=0{\cdot}1418.\end{aligned}\right\}\qquad\ldots\ldots(24)$$

The *XY* co-ordinates of the end-points of the projections $\bar{a}$, $\bar{b}$, $\bar{c}$ of *a*, *b*, and *c* on the *OXY* plane normal to the beam are therefore (al_1, am_1), (bl_2, bm_2), (cl_3, cm_3), i.e. $(-1{\cdot}00_5, -5{\cdot}87_8)$, $(5{\cdot}94_1, 0)$ and $(-0{\cdot}25_8, 11{\cdot}0_8)$ A., and the lengths $\bar{a}$, $\bar{b}$, $\bar{c}$ are $5{\cdot}96_3$, $5{\cdot}94_1$ and $11{\cdot}0_8$ A.

The angles between the Laue-zone normals in the pattern are then given by

$$\bar{\alpha}=\tan^{-1}(m_3/l_3)=180^\circ-88^\circ\ 40',$$

$$\bar{\gamma}=\tan^{-1}(m_1/l_1)=180^\circ+80^\circ\ 18',$$

and agree well with the measured angles 180° − 88° 44′ and 180° + 80° 15′ respectively. The true value of λL calculated from the b Laue-zone spacing is

$$R_{10}\, b \sin\theta_b \sin\bar{\alpha}=2\cdot332 \text{ A. cm.},$$

hence the calculated a, b and c Laue-zone spacings are $\lambda L/\bar{a}=0\cdot391$ cm., $\lambda L/\bar{b}=0\cdot392_5$ cm., and $\lambda L/\bar{c}=0\cdot211$ cm., in very fair agreement with the observed values 0·390, $0\cdot392_5$, $0\cdot212_8$ cm. respectively. Further, the angle between the projection of [201] and $\bar{b}$ should be

$$\tan^{-1}[\{(c/a)\, m_3+2m_1\}/\{(c/a)\, l_3+2l_1\}]=180^\circ+17^\circ\ 2',$$

and the length of the projection on OXY of the [201] period ($T_{201}=14\cdot12$ A.) is $\{(cm_3+2am_1)^2+(cl_3+2al_1)^2\}^{\frac{1}{2}}=2\cdot371$ A., so that the [201] zone axis produced should intersect the screen at a distance $R_0=2\cdot371\,.\,47\cdot0/\{14\cdot12^2-2\cdot371^2\}^{\frac{1}{2}}=8\cdot00$ cm. from the central spot. The [201] Laue zones should therefore be practically circular and, indeed, it will be seen that in figure 10*a* circles can be drawn around the calculated intersection of [201] with the screen so as to pass through or near the strongest spots in the pattern, the measured radii of the 2nd, 1st, 0, −1st, −2nd and −3rd order zones being 9·75, 8·9, 8·0, 6·9, 5·75 and 4·2 cm. respectively. The radii, calculated from the relation $R_{h'}^{2}=R_0^{2}+h'(2\lambda L^2/T_{201})=64\cdot06+15\cdot52h'$, are 9·75, 8·92, 8·00, 6·97, 5·75 and 4·18 cm. respectively, i.e. in close agreement with the measured radii. The calculated crystal setting is thus in agreement with all the features of the spot pattern of figure 10*a*.

To complete the projection diagram we require the projections of the two molecules associated with the unit cell, whose atom co-ordinates x, y, z, expressed as fractions of a, b, c, are given in table 2.* The projection of any point xyz in the crystal can be conveniently constructed by marking off $x\bar{a}$, parallel to $\bar{a}$, followed by $y\bar{b}$ parallel to $\bar{b}$ and $z\bar{c}$ parallel to $\bar{c}$. Since the carbon hexagons are plane and regular, it suffices to find in this manner the projected positions of two points such as A and D for each molecule, whereupon the projection can be readily completed. With this crystal orientation, which we now know to an accuracy of within 15′, the co-ordinates of A and D along the $\bar{a}$, $\bar{b}$, $\bar{c}$ directions in the projection are ($0\cdot56_0$, $0\cdot19_0$, $4\cdot08_1$) and ($0\cdot56_6$, $1\cdot23_0$, $0\cdot55_3$) A., while those of A_1 and D_1 differ only in the $\bar{b}$ co-ordinate being negative, and the long axes of the two sets of molecules are very nearly normal to the beam, their projections enclosing an angle of 13½°.

The construction of the diffraction pattern from the anthracene molecules regarded as independent scatterers. In discussing the origin of the diffuse-zone pattern in figure 10*a*, we start from the assumption that this is due to scattering by molecules which, though oriented with respect to the beam in accordance with the crystal-orientation, have for some reason no specific phase relationship between each other.

---

* We can neglect the hydrogen atoms, because of their weak scattering-power relative to that of the carbon atoms.

This is equivalent to a stream of molecules in the gaseous state in which, however, the molecules fall into two groups which are oriented with respect to the beam as they would be in the crystal. As a preliminary to deriving the pattern given by an anthracene molecule in some definite orientation with respect to the beam which is, as usual, normal to the screen, we may note that in the general case of a spatial group of scattering centres such as is constituted by any molecule, if the molecule can be resolved into a series of similar line gratings which are parallel but not necessarily otherwise in ordered array with respect to each other, then the regions of reinforcement from all atoms of the molecule must lie on those of the atom rows. The Laue-zone positions and widths corresponding to these atom rows can be constructed from the spacings and inclination of the rows to the beam and the number of atoms in a row. If the atomic arrangement in the molecule is such that two or more sets of Laue zones can be constructed, then the regions of maximum diffracted intensity will be limited to the intersections of these zones.

The projection on the screen, i.e. on a plane normal to the incident beam, of the anthracene unit cell with its two molecules in the orientation corresponding to the spot pattern of figure 10*a* is shown in figure 10*b*. To construct the molecular, i.e. diffuse-area, pattern we construct the Laue zones for two mutually inclined atom rows from which the plane anthracene molecule can be regarded as built up, such as for example, the atom-row translations $G'E'$ and $G'B$. Then the regions of reinforcement from the molecule must lie at the intersections of the zones. In the projection diagram figure 10*b* (drawn to a suitable scale, e.g. 1 cm. for 1 A.) it was found by measurement that $G'E' = 2{\cdot}39$ A., $G'B = 2{\cdot}21$ A., $A_1C_1 = 2{\cdot}37$ A., and $A_1F_1' = 2{\cdot}28$ A., the angles made with $\bar{b}$ being respectively $-81^\circ\ 15'$, $-33^\circ\ 15'$, $-94^\circ\ 45'$ and $-32^\circ\ 45'$; thus since all of these atom rows are steeply inclined to the beam, the maxima of the Laue zones are with sufficient accuracy equidistant lines normal to the atom-row projections $G'E'$ etc., with spacings $\lambda L/G'E'$ etc., where $\lambda L = 2{\cdot}332$ A. cm., i.e. with spacings $0{\cdot}97_6$, $1{\cdot}05_5$, $0{\cdot}98_4$ and $1{\cdot}02_3$ cm. respectively. The atom rows parallel to $G'E'$ and A_1C_1 contain either three or four atoms, hence their Laue zones may be taken to extend on each side of the line of maximum intensity to nearly a third of the space between consecutive zone maxima before the intensity factor becomes negligible; and since rows parallel to $G'B$ and A_1F_1' contain only two atoms, their Laue zones practically coalesce. From the intersections of the two sets of Laue zones the position, shape and extent of the main maxima due to each molecule can be deduced. A diagrammatic representation of the pattern constructed in this manner from the two molecules by superposition of their individual contributions is shown in figure 10*c*, in which are noted also the directions of the projection of the *b* axis and $G'E'$ etc. In the representation of the regions of maxima in figure 10*c* and in later similar figures the points where maxima are due to the molecule based on O (i.e. [[000]]) are marked by a small circle, and the regions of appreciable scattering round these are shaded with vertical lines, while the maxima due to the molecule centred at O_1 (i.e. [[$\frac{1}{2}\frac{1}{2}$0]]) are marked by small crosses and the regions round them are shaded horizontally. The lines of maxima of the Laue zones are only shown in later cases where band-formation occurs, where they help to indicate the intensity-distribution more clearly by showing where the Laue zones overlap. In this representation the effect of the radial decrease in the carbon atom-form factor has not been included, and this must be allowed for in comparing the diagrams with the recorded diffraction pattern. The relative magnitudes of the maxima, apart from differences due to atom-form factor, can be roughly inferred from the structure factor corresponding to the co-ordinates (0, 0) and $(\frac{2}{3}, \frac{2}{3})$ of the two atoms in the unit cell of the cross-grating formed from $G'E'$ and $G'B$ (and similarly A_1C_1, A_1F_1') as axes, according to which the maxima which have Laue indices H and K, associated with $G'E'$ and $G'B$ respectively, such that $(H+K)$ is a multiple of three, are much stronger than the rest. These maxima are shaded darker in figure 10*c*. Owing to the very limited extent of the molecular cross-grating in anthracene, such a treatment is only qualitative. Comparison with figure 10*a* reveals, however, that this constructed molecular pattern adequately represents the positions of the regions of diffuse scattering in the diffraction pattern, figure 10*a*, and that the roughly estimated relative intensities are also in agreement.

The estimated and recorded intensity-distribution may be compared in greater detail by the following method, which can also be used conveniently for any plane molecule even when, through absence of marked molecular symmetry, the approximate Laue-zone method is inapplicable. Since the anthracene molecule consists of adjoining coplanar hexagon rings, the phase difference δ_n between the wavelet scattered in a given direction by the *n*th carbon atom in the molecule and that which would be scattered in the same direction by a point O at the centre of the molecule, figure 1, can be expressed as the sum of multiples of the phase differences ξ and η of the wavelets which would be scattered from the points P and Q respectively; e.g. the phase difference for the wavelet scattered by the atom A will be $\delta_A = \xi + 3\eta$. The total amplitude of scattering from a single molecule at a distance R in the direction considered can therefore be represented by $\sum_n (\Psi/R)\cos(\omega t + \delta_n)$, where Ψ is the scattering power of a carbon atom. The intensity of scattering from the molecule is thus

$$I_M = \Psi^2 S_M^2/R^2, \qquad \text{......(25)}$$

in which S_M^2 is analogous to the structure factor occurring in the standard expressions for the intensity of scattering from a space lattice, i.e.

$$S_M^2 = A_M^2 + B_M^2, \qquad \text{......(26)}$$

where

$$\left.\begin{aligned} A_M &= \sum_n \cos\delta_n, \\ B_M &= \sum_n \sin\delta_n. \end{aligned}\right\} \qquad \text{......(27)}$$

For the anthracene molecule

$$\left.\begin{aligned} A_M &= 2\,[\cos(\xi+3\eta) + \cos(-\xi+3\eta) + \cos(2\xi+2\eta) + \cos(-2\xi+2\eta) \\ &\qquad + \cos(\xi+\eta) + \cos(-\xi+\eta) + \cos 2\xi] \\ &= 2\cos 2\xi + 4\cos\xi\cos\eta + 4\cos 2\xi\cos 2\eta + 4\cos\xi\cos 3\eta, \\ \text{and} \qquad B_M &= 0. \end{aligned}\right\} \qquad \text{......(28)}$$

Table 6. Values of S_M throughout the representative range $0 \leqslant \xi \leqslant 180^\circ$, $0 \leqslant \eta \leqslant 180^\circ$

ξ^0 η^0	0	10	20	30	40	50	60	70	80	90	100	110	120	130	140	150	160	170	180
0	14	13·5	12·1	9·9	7·2	4·1	1	−1·8	−4·2	−6	−7	−7·3	−7·0	−6·2	−5·1	−3·9	−2·9	−2·2	−2·0
10	13·2	12·7	11·2	9·3	6·7	3·8	0·8	−1·9	−4·1	−5·8	−6·7	−7·0	−6·6	−5·8	−4·7	−3·5	−2·5	−1·9	−1·6
20	10·8	10·4	9·3	7·5	5·3	2·8	0·4	−1·9	−3·8	−5·1	−5·8	−5·9	−5·4	−4·6	−3·5	−2·5	−1·5	−0·9	−0·7
30	7·5	7·2	6·3	5·0	3·4	1·5	−0·3	−1·9	−3·1	−4	−4·4	−4·2	−3·7	−2·9	−2·0	−1·0	−0·2	0·4	0·5
40	3·8	3·6	3·1	2·3	1·2	0·2	−0·8	−1·7	−2·4	−2·7	−2·7	−2·4	−1·9	−1·1	−0·4	0·4	1·1	1·5	1·6
50	0·4	0·4	0·2	−0·1	−0·5	−0·8	−1·1	−1·3	−1·4	−1·3	−1·1	−0·7	−0·2	0·4	0·9	1·4	1·8	2·1	2·2
60	−2·0	−2·0	−1·9	−1·7	−1·5	−1·3	−1·0	−0·7	−0·4	0	0·4	0·7	1·0	1·3	1·5	1·7	1·9	2·0	2·0
70	−3·2	−3·1	−2·8	−2·4	−1·8	−1·2	−0·5	0·1	0·6	1·1	1·4	1·5	1·6	1·5	1·4	1·3	1·2	1·1	1·0
80	−3·1	−2·9	−2·6	−2·0	−1·3	−0·5	0·2	0·9	1·4	1·8	1·9	1·8	1·5	1·1	0·7	0·3	−0·1	−0·4	−0·5
90	−2·0	−1·9	−1·5	−1·0	−0·4	0·4	1·0	1·5	1·9	2·0	1·9	1·5	1·0	0·4	−0·4	−1·0	−1·5	−1·9	−2·0
100	−0·5	−0·4	−0·1	0·3	0·7	1·1	1·5	1·8	1·9	1·8	1·4	0·9	0·2	−0·5	−1·3	−2·0	−2·6	−2·9	−3·1
110	1·0	1·1	1·2	1·3	1·4	1·5	1·6	1·5	1·4	1·1	0·6	0·1	−0·5	−1·2	−1·8	−2·4	−2·8	−3·1	−3·2
120	2·0	2·0	1·9	1·7	1·5	1·3	1·0	0·7	0·4	0	−0·4	−0·7	−1·0	−1·3	−1·5	−1·7	−1·9	−2·0	−2·0
130	2·2	2·1	1·8	1·4	0·9	0·4	−0·2	−0·7	−1·1	−1·3	−1·4	−1·3	−1·1	−0·8	−0·5	0·1	0·2	0·4	0·4
140	1·6	1·5	1·1	0·4	−0·4	−1·1	−1·9	−2·4	−2·7	−2·7	−2·4	−1·7	−0·8	0·2	1·2	2·3	3·1	3·6	3·8
150	0·5	0·4	−0·2	−1·0	−2·0	−2·9	−3·7	−4·2	−4·4	−4·0	−3·1	−1·9	−0·3	1·5	3·4	5·0	6·3	7·2	7·5
160	−0·7	−0·9	−1·5	−2·5	−3·5	−4·6	−5·4	−5·9	−5·8	−5·1	−3·8	−1·9	0·4	2·8	5·3	7·5	9·3	10·4	10·8
170	−1·6	−1·9	−2·5	−3·5	−4·7	−5·8	−6·6	−7·0	−6·7	−5·8	−4·1	−1·9	0·8	3·8	6·7	9·3	11·2	12·7	13·2
180	−2·0	−2·2	−2·9	−3·9	−5·1	−6·2	−7·0	−7·4	−7·0	−6·0	−4·2	−1·8	1·0	4·1	7·2	9·9	12·1	13·5	14·0

The value of S_M, i.e. A_M, is given in table 6 for the characteristic range $0 \leqslant \xi \leqslant 180°$, $0 \leqslant \eta \leqslant 180°$, and figure 13, derived from figures obtained by graphical interpolation from the data in table 6, shows the contours for $S_M{}^2 = 0$, 20, 40, 60, 80, 100, 120, 140, 160 and 180. The values ξ and η appropriate to a given direction of scattering depend, of course, on the orientation of the molecule relative to the primary beam. The correlation of figure 13 with the theoretical distribution on the screen at a given molecular orientation may be carried out most simply by using the fact that the points of intersection of the Laue zones drawn, for example, for $G'E'$ and $G'B$, correspond to the (ξ, η) values $(n_1 . 60°, n_2 . 180°)$ where n_1 is even or odd when n_2 is even or odd respectively; hence if the contour diagram figure 13 is elongated, so that these points fall on the corresponding Laue-zone intersections constructed for any given molecular orientation, the detail of the intensity-distribution throughout the whole region is obtained. For example, the form of the pattern due to a molecule normal to the beam can be obtained simply by extending the diagram of figure 13 parallel to the ξ direction in the ratio $\sqrt{3} : 1$; but when one or both of the basic atom rows of the molecule are inclined at a relatively small or even zero angle to the beam their Laue zones become appreciably or even strongly curved and figure 13 must be more or less strongly distorted in order to represent the form of the pattern. In all cases, even where the plane of the molecule is parallel to the primary beam and

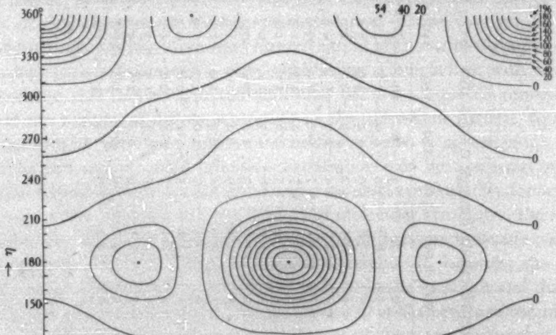

Figure 13.

inclined so that the two sets of Laue zones are practically straight and parallel, the medial lines of the zones due to OP and OQ can be drawn, and since the nth zone from the central spot corresponds to ξ or η respectively equal to $n.2\pi$, the whole field of the diffraction pattern can be mapped out in ξ and η values and the related S_M^2 values of figure 13 assigned to each point in the required field. In the present case of figure 10*c*, the molecular Laue zones have been constructed with sufficient accuracy from measurements made in the projection diagram of figure 10*b*, without the necessity of using a more exact calculation of the Laue zone positions. It will be seen that the more prominent details of the intensity-distribution expected in the present case are of the form already indicated in figure 10*c*, which was deduced by the approximate method of marking the regions where the Laue zones overlap. The superposed patterns due to the two molecules agree with the recorded pattern, figure 10*a*, (i) in the positions of the diffuse zones relative to each other, (ii) in the positions of the diffuse zones relative to the spot pattern, (iii) in the shape and extent of the maxima, and (iv) in their order of intensity relative to each other and to their intermediate regions.

That this agreement is in no sense fortuitous can best be proved by a study of further diffraction patterns from anthracene crystals in a series of different orientations. In putting the matter to the test, we first determine the crystal-orientation from the spot pattern and then construct a molecular-scattering pattern such as would be given by the two sets of molecules in the orientations corresponding to the crystal-orientation, assuming that there is no specific phase relationship between any of the molecules. If this deduced intensity distribution of the molecular pattern is in agreement with that recorded in the diffraction pattern, both as regards intensities and as regards orientation, then this supports the view that the background scattering is due to the scattering by molecules which, although they are in, or very nearly in, their proper orientations in the lattice, are nevertheless in some way so disturbed that there is no constant phase relationship between the scattering from individual molecules. A study of the diffraction patterns shown in figures 14–21 will suffice to test the views set forth in the preceding paragraph.

The effect of orientation on the diffuse-area pattern and the experimental proof of its molecular origin. Figure 14. Measurements along the main rows of spots in figure 14*a* gave the following values for the sides of the nearly rectangular unit of the pattern: $R_{10}=0{\cdot}282$ cm., $R_{01}=0{\cdot}379$ cm.; thus the spot pattern is evidently due to the *ab* cross-grating inclined to the beam at a steep angle. The mean value of $R_{2\bar{1}}$, namely 0·652 cm., together with R_{10} and R_{01} gives by equation (1) $\bar{\gamma}=180°-85°\ 5'$, and since $m=(b/a)(R_{01}/R_{10})=0{\cdot}9430$, it follows from equation (3) that $\theta_b=78°\ 6'$ or $180°-78°\ 6'$, and $\theta_a=67°\ 18'$ or $180°-67°\ 18'$. Since $\bar{\gamma}>90°$, θ_a and θ_b must both be greater than or both be less than 90°; thus, since the *a* zones are concave to the left in figure 14*a*, the *a* and *b* axes, if directed as in figure 14*b*, must make angles θ_a, equal to 67° 18′, and θ_b, equal to 78° 6′, with the reversed beam direction. The settings of the *a* and *b* axes are thus fixed, and the *c* axis must be in one of two possible positions, according to which are the positive directions of *a* and *b*. With the positive directions of *a* and *b* as shown in figure 14*b*, the corresponding *c* Laue zones can be

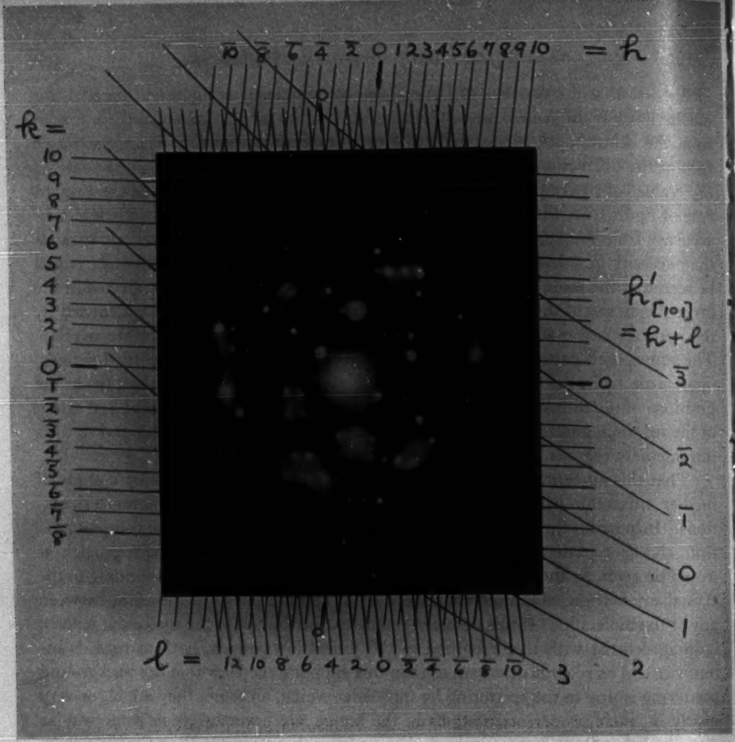
10 8 6 4 2 0 1 2 3 4 5 6 7 8 9 10 = h
k =
10 9 8 7 6 5 4 3 2 1 0 1 2 3 4 5 6 7 8
h'[101] = h + l
3 2 1 0 1 2 3
l = 12 10 8 6 4 2 0 2 4 6 8 10

Figure 14a.

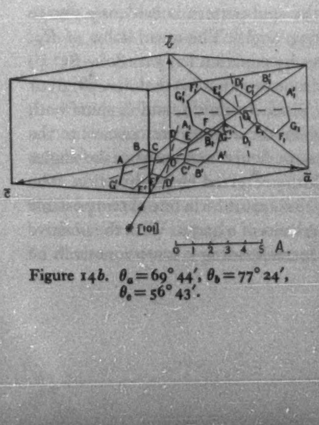
b
c
a
[101]
A B C D E F G
A' B' C' D' E' F' G'
A1 B1 C1 D1 E1 F1 G1
A1' B1' C1' D1' E1' F1' G1'
0 1 2 3 4 5 A.

Figure 14b. $\theta_a=69° 44'$, $\theta_b=77° 24'$, $\theta_c=56° 43'$.

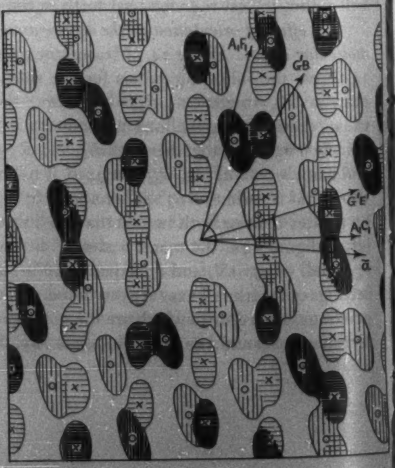
A1F1'
G'B
G'E'
A1C1
a

Figure 14c.

identified and the broad curved Laue zones marked on figure 14*a* are satisfactorily indexed as due to the [101] zone axis. The crystal orientation is thus uniquely determined to be as it is represented by the projection drawing, figure 14*b*. The positions of the expected Laue zones due to the *c* axis and to the [101] lattice rows were calculated, as in the corresponding stage of the analysis of figure 10*a*, in terms of the direction cosines of *a*, *b* and *c* with respect to an orthogonal system of axes, but these calculations based on the above approximate values for θ_a and θ_b will not be described further. The three strongest diffractions in the pattern shown in figure 14*a* are thus found to have the indices $03\bar{1}$, $\bar{8}\bar{1}.10$, $1\bar{3}0$, whence from equations (18), (16) and (17) the crystal setting is given by $\theta_a = 69^\circ\ 44'$, $\theta_b = 77^\circ\ 24'$, $\theta_c = 56^\circ\ 43'$. The direction cosines of *a*, *b* and *c* with respect to three orthogonal axes *OXYZ*, such that *OZ* lies along the reversed beam direction and *OX*, *OZ* and *a* are coplanar, were calculated by equations derived from (21), (22) and (23) by the appropriate change of suffixes and were found to be

$$
\begin{aligned}
l_1 &= 0{\cdot}9381, & m_1 &= 0, & n_1 &= 0{\cdot}3464,\\
l_2 &= -0{\cdot}08050, & m_2 &= 0{\cdot}9726, & n_2 &= 0{\cdot}2180,\\
l_3 &= -0{\cdot}8141, & m_3 &= -0{\cdot}1897, & n_3 &= 0{\cdot}5488.
\end{aligned}
$$

The *XY* co-ordinates of the end points of $\bar{a}$, $\bar{b}$, $\bar{c}$ were thus calculated to be $(8{\cdot}04_8, 0)$, $(-0{\cdot}48_5, 5{\cdot}85_6)$ and $(-9{\cdot}10_1, -2{\cdot}12_0)$ A. respectively, whence $\bar{a} = 8{\cdot}04_8$ A., $\bar{b} = 5{\cdot}87_6$ A. and $\bar{c} = 9{\cdot}34_5$ A.; and the $\bar{a}$, $\bar{b}$, $\bar{c}$ co-ordinates of *A* and *D* in the projection are $(0{\cdot}75_6, 0{\cdot}18_8, 3{\cdot}44_7)$ and $(0{\cdot}76_4, 1{\cdot}21_6, 0{\cdot}46_7)$ A. respectively. Measurement of the projection drawing yielded $G'E' = 1{\cdot}97$ A., $G'B = 2{\cdot}39$ A., $A_1C_1 = 1{\cdot}88$ A. and $A_1F_1' = 2{\cdot}10$ A., their directions making with $\bar{a}$ the angles 22° 30′, 63° 15′, 6° 30′ and 80° 40′ respectively. The mean value of λL calculated from R_{10} and R_{01} is $2{\cdot}24_0$ A.-cm.; hence the Laue-zone spacings corresponding to these atom rows are $1{\cdot}13_7$, $0{\cdot}93_7$, $1{\cdot}19_1$ and $1{\cdot}06_7$ cm. Finally, from these data the intensity-distribution which would be given by independent molecular scattering was deduced and is shown in figure 14*c*. It will be seen that this intensity-distribution is in satisfactory agreement with the diffuse area pattern shown in figure 14*a*.

Figure 15. It can be seen directly that figure 15*a* is somewhat similar to figure 14*a*, the crystal-orientation being therefore not far distant from that found for figure 14*a*. Measurement of the spot-separations yielded $R_{10} = 0{\cdot}271$ cm. and $R_{01} = 0{\cdot}381$ cm., and by direct measurement $\bar{\gamma} = 180^\circ - 87^\circ\ 40'$, whence $m = (b/a).(R_{01}/R_{10}) = 0{\cdot}9863$ and, by equation (3), $\theta_b = 81^\circ\ 1'$ or $180^\circ - 81^\circ\ 1'$, $\theta_a = 76^\circ\ 57'$ or $180^\circ - 76^\circ\ 57'$. Since $\bar{\gamma}$ is $> 90^\circ$, and in view of the directions of curvature of the *a* and *b* Laue zones, $\theta_a = 76^\circ\ 57'$ and $\theta_b = 81^\circ\ 1'$ with the positive *a* and *b* directions shown in figure 15*b*, so that two crystal-orientations are possible according to whether or not these are the true positive directions of *a* and *b*. From these approximate values of θ_a and θ_b a calculation of the type previously outlined enabled the orientation to be determined uniquely by identification of the Laue zones due to the *c* and [101] axes. The three strongest spots therefore have the indices $51\bar{5}$, $\bar{2}41$ and $\bar{6}06$, from which were calculated the more accurate values $\theta_a = 78^\circ\ 23'$,

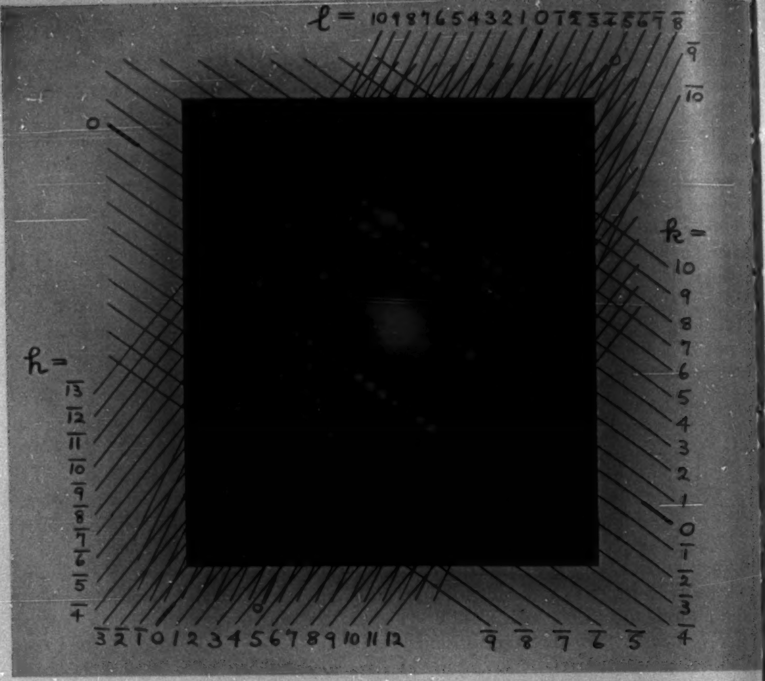
l = 10 9 8 7 6 5 4 3 2 1 0 1̄ 2̄ 3̄ 4̄ 5̄ 6̄ 7̄ 8̄
9̄
1̄0̄
0
k =
10 9 8 7 6 5 4 3 2 1 0 1̄ 2̄ 3̄ 4̄
h =
1̄3̄ 1̄2̄ 1̄1̄ 1̄0̄ 9̄ 8̄ 7̄ 6̄ 5̄ 4̄
3̄ 2̄ 1̄ 0 1 2 3 4 5 6 7 8 9 10 11 12
9̄ 8̄ 7̄ 6̄ 5̄

Figure 15*a*.

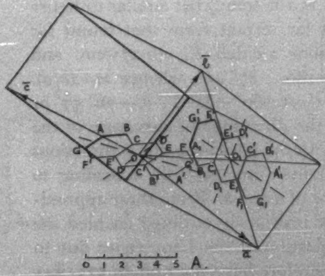
c̄
b̄
ā
A B C D E F G
A' B' C' D' E' F' G'
A₁ C₁ D₁ E₁ F₁ G₁
A₁' C₁' D₁' E₁' F₁' G₁'
0 1 2 3 4 5 A.

Figure 15*b*. $\theta_a = 78° 23'$, $\theta_b = 79° 52'$, $\theta_c = 47° 38'$.

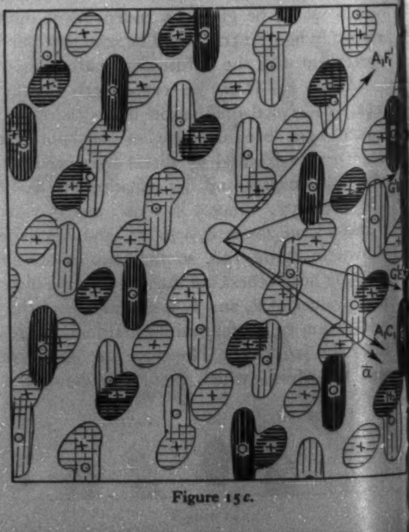
A₁F₁'
G₁
GE
A₁C₁
ā

Figure 15*c*.

$\theta_b=79^\circ\ 52'$, $\theta_c=47^\circ\ 38'$. Taking three orthogonal axes with OZ in the reversed beam direction and a in the OXZ plane, we find that the direction cosines of a, b and c are

$$\begin{array}{lll} l_1=\ 0{\cdot}9795, & m_1=\ 0, & n_1=0{\cdot}2014, \\ l_2=-0{\cdot}03617, & m_2=\ 0{\cdot}9838, & n_2=0{\cdot}1760, \\ l_3=-0{\cdot}7241, & m_3=-0{\cdot}1473, & n_3=0{\cdot}6738; \end{array}$$

hence the XY co-ordinates of the end points of $\bar{a}$, $\bar{b}$, $\bar{c}$ are $(8{\cdot}40_5, 0)$, $(-0{\cdot}21_8, 5{\cdot}92_4)$ and $(-8{\cdot}09_5, -1{\cdot}64_6)$ A. respectively, and $\bar{a}=8{\cdot}40_5$ A., $\bar{b}=5{\cdot}92_7$ A., $\bar{c}=8{\cdot}26_0$ A. The $\bar{a}$, $\bar{b}$, $\bar{c}$ co-ordinates of A and D in the projection diagram, figure 15*b*, are therefore $(0{\cdot}79_0, 0{\cdot}19_0, 3{\cdot}04_6)$ and $(0{\cdot}79_9, 1{\cdot}22_7, 0{\cdot}41_3)$ A. respectively. From the projection drawing $G'E'=1{\cdot}73$ A., $G'B=2{\cdot}44$ A., $A_1C_1=1{\cdot}62$ A. and $A_1F_1'=2{\cdot}01$ A. at angles with $\bar{a}$ equal to 22° 15′, 56° 40′, 3° 30′ and 85° 15′ respectively, and since λL was calculated from R_{10} and R_{01} to be $2{\cdot}26_3$ A. cm. the corresponding Laue-zone spacings are $1{\cdot}30_8$, $0{\cdot}92_7$, $1{\cdot}39_7$ and $1{\cdot}12_6$ cm. Figure 15*c* shows the intensity-distribution of the molecular diffraction deduced from these data.

Figure 16. The practically perpendicular unit translations of the spot pattern are $R_{10}=0{\cdot}305$ cm. and $R_{01}=0{\cdot}390_5$ cm., corresponding to the *ab* cross-grating pattern with a crystal-orientation such that $\theta_b\simeq90^\circ$, $\theta_a\simeq63^\circ\ 50'$ or $180^\circ-63^\circ\ 50'$. Owing to the limitation of the spot pattern to a set of broad curved Laue zones, the direction of curvature of the *a* zones cannot be clearly distinguished, but a consideration of the crystal-orientations permitted by the above data leads (by a calculation in terms of direction cosines) to satisfactory identification of the prominent broad curved zones as due to [101] if $\theta_a\simeq64^\circ$, $\theta_b\simeq89^\circ$, $\theta_c\simeq61^\circ$. Three of the strongest spots in figure 16*a* are thus indexed as $42\bar{5}$, 020 and $\bar{3}44$, from which are calculated the more accurate values $\theta_a=64^\circ\ 4'$, $\theta_b=89^\circ\ 32'$, $\theta_c=60^\circ\ 55'$. Referred to orthogonal axes $OXYZ$ such that OZ lies along the reversed direction of the beam and a lies in the plane OXZ, the direction cosines of a, b, c are

$$\begin{array}{lll} l_1=\ 0{\cdot}8994, & m_1=0, & n_1=0{\cdot}4373, \\ l_2=-0{\cdot}00389, & m_2=0{\cdot}99999, & n_2=0{\cdot}0080, \\ l_3=-0{\cdot}8740, & m_3\simeq0, & n_3=0{\cdot}4860. \end{array}$$

The XY co-ordinates of the end points of $\bar{a}$, $\bar{b}$, $\bar{c}$ are thus $(7{\cdot}71_8, 0)$, $(-0{\cdot}02_3, 6{\cdot}02_6)$ and $(-9{\cdot}77_0, 0{\cdot}00_5)$ A. respectively, and $\bar{a}=7{\cdot}71_8$ A., $\bar{b}=6{\cdot}02_0$ A., $\bar{c}=9{\cdot}77_0$ A. The $\bar{a}$, $\bar{b}$, $\bar{c}$ co-ordinates of A and D in the OXY projection are therefore $(0{\cdot}70_9, 0{\cdot}19_3, 3{\cdot}60_4)$ and $(0{\cdot}71_6, 1{\cdot}24_7, 0{\cdot}48_8)$ A. respectively. From the projection drawing $G'E'=2{\cdot}03$ A. and $G'B=2{\cdot}41$ A., making 8° 0′ and 56° 20′ respectively with $\bar{a}$, and the projection of the other molecule is practically the mirror image of the projection of the first molecule with respect to the line $\bar{a}$. Since $\lambda L=2{\cdot}35_1$ A. cm., as calculated from R_{10} and R_{01}, the Laue-zone spacings corresponding to $G'E'$ and $G'B$ are $1{\cdot}15_8$ and $0{\cdot}97_6$ cm., whence the intensity-distribution of the molecular scattering shown in figure 16*c* has been deduced.

Figure 17. The nearly perpendicular unit translations of the spot pattern are as follows: $R_{10}=0{\cdot}292$ cm. and $R_{01}=0{\cdot}506$ cm. They therefore correspond to the *ab*

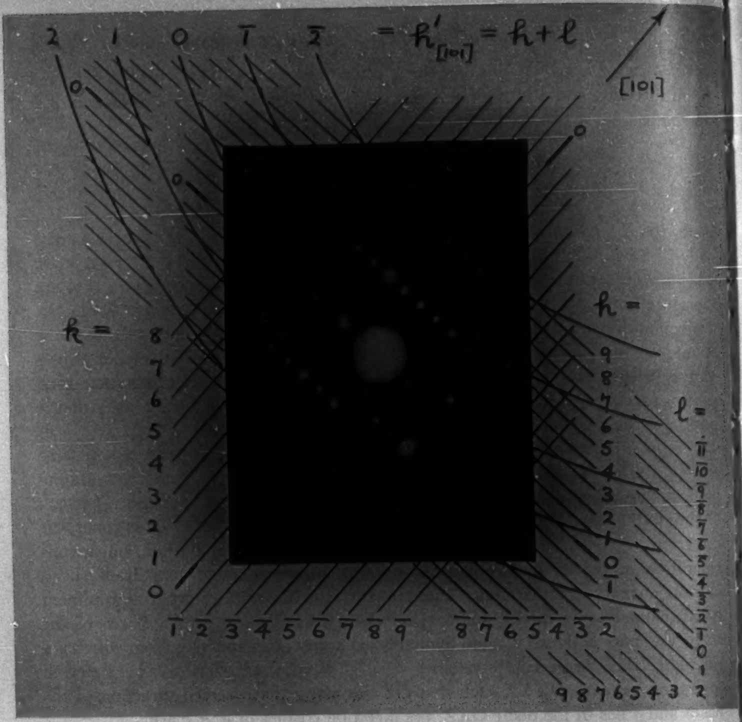
2 1 0 1̄ 2̄ = h′[101] = h+l
[101]
0
0
0
0
k =
8 7 6 5 4 3 2 1 0
h =
9 8 7 6 5 4 3 2 1 0 1̄
l =
1̄1̄ 1̄0̄ 9̄ 8̄ 7̄ 6̄ 5̄ 4̄ 3̄ 2̄ 1̄ 0 1 2
1̄ 2̄ 3̄ 4̄ 5̄ 6̄ 7̄ 8̄ 9̄
8̄ 7̄ 6̄ 5̄ 4̄ 3̄ 2̄
9 8 7 6 5 4 3 2

Figure 16*a*.

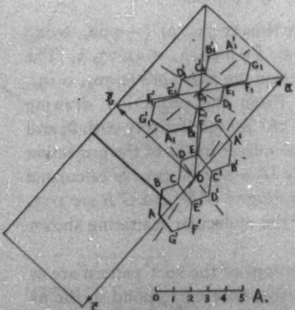
b
a
c
A′1 B′1 C′1 D′1 E′1 F′1 G1
A1 B1 C1 D1 E1 F1 G′1
A B C D E F′ G′
A′ B′ C′ D′ E′ G
0 1 2 3 4 5 A.

Figure 16*b*. $\theta_a = 64° \, 4'$, $\theta_b = 89° \, 32'$, $\theta_c = 60° \, 55'$.

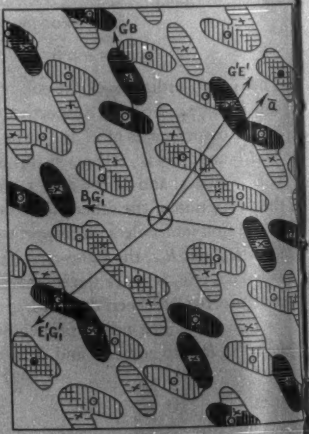
G′B
G′E′
a
B1G′1
E′1G′1

Figure 16*c*.

cross-grating pattern. Since $R_{11}=0{\cdot}603$ cm., equation (1) yields $\bar{\gamma}=180^\circ-85^\circ\,39'$ and, since $m=(b/a)(R_{m}/R_{10})=1{\cdot}216$, we have by equation (3), $\theta_b=54^\circ\,48'$ or $180^\circ-54^\circ\,48'$, $\theta_a=83^\circ\,30'$ or $180^\circ-83^\circ\,30'$. From the fact that $\bar{\gamma}>90^\circ$, and from the direction of curvature of the *a* and *b* zones, θ_a and θ_b must both be less than 90°; i.e. $\theta_a=83^\circ\,30'$, $\theta_b=54^\circ\,48'$ with *a* and *b* directed as in figure 17*b*. Calculation of the position of the *c* axis and its Laue zones corresponding to these *a* and *b* directions by the method previously described leads to the identification of the *c* zones in figure 17*a*; thus the positive *a* and *b* directions were indeed as in figure 17*b*. The broad circular Laue zones to which the spot pattern is limited are then found to be due to the [111] zone axis. A complete indexing of the spot pattern has thus been obtained, and the indices of the three strongest diffractions are found to be $\bar{2}\bar{2}4$, $60\bar{5}$ and $14\bar{5}$, whence the more accurate calculation gives the crystal setting as $\theta_a=84^\circ\,59'$, $\theta_b=54^\circ\,26'$ and $\theta_c=52^\circ\,14'$. In order to show this setting by means of a projection diagram, the direction cosines of *a*, *b* and *c* were calculated with reference to orthogonal axes *OXYZ* with *OZ* along the reversed direction of the beam and *a* in the plane *OXZ*, and were found to be

$$\begin{aligned} l_1&=0{\cdot}9962, & m_1&=0, & n_1&=0{\cdot}08738,\\ l_2&=-0{\cdot}05112, & m_2&=0{\cdot}8119, & n_2&=0{\cdot}5816,\\ l_3&=-0{\cdot}6295, & m_3&=-0{\cdot}4783, & n_3&=0{\cdot}6124. \end{aligned}$$

The *XY* co-ordinates of the end points of $\bar{a}$, $\bar{b}$, $\bar{c}$ are thus $(8{\cdot}54_9, 0)$, $(-0{\cdot}30_8, 4{\cdot}88_2)$ and $(-7{\cdot}03_7, -5{\cdot}34_7)$ A. respectively; hence $\bar{a}=8{\cdot}54_9$ A., $b=4{\cdot}89_7$ A., $c=8{\cdot}83_7$ A. The $\bar{a}$, $\bar{b}$, $\bar{c}$ co-ordinates of *A* and *D* are $(0{\cdot}80_4, 0{\cdot}15_7, 3{\cdot}26_0)$ A. and $(0{\cdot}81_2, 1{\cdot}01_4, 0{\cdot}44_2)$ A. Figure 17*b* shows the completed projection drawing. Measurements made in the projection drawing (scale 1 cm. for 1 A.) gave $G'E'=1{\cdot}96$ A., $G'B=2{\cdot}22$ A., $A_1C_1=1{\cdot}68$ A., $A_1F_1'=2{\cdot}40$ A., the angles between $G'E'$ etc. and $\bar{a}$ being 47° 45′, 56° 0′, 37° 0′ and 92° 30′.

Since the accuracy of the measurements, and particularly that of the angles, was doubtful for the molecule at *O* owing to its small inclination to the beam, their calculation from the *A* and *D* co-ordinates and $(l_1m_1n_1)$ etc. was carried out as a check. Thus the *a*, *b*, *c* components of the vector $G'E'$ are twice those of $-OQ$, i.e. are $(-0{\cdot}26, 0{\cdot}29, -2{\cdot}55)$ A.; while the *a*, *b*, *c* components of $G'B$ are the sum of those of *D* and *E* in table 1, i.e. $(1{\cdot}09, 2{\cdot}02, -0{\cdot}43)$ A. The *X*, *Y*, *Z* components of the radius vector from the origin to the point whose co-ordinates are (x, y, z) A. parallel to *a*, *b*, *c*, are given by

$$\left.\begin{aligned} X&=l_1x+l_2y+l_3z,\\ Y&=m_1x+m_2y+m_3z,\\ Z&=n_1x+n_2y+n_3z. \end{aligned}\right\} \qquad \text{......(29)}$$

We thus obtain for the *X*, *Y*, *Z* components of $G'E'$ and $G'B$ $(1{\cdot}33_1, 1{\cdot}45_5, -1{\cdot}36_2)$ A. and $(1{\cdot}25_4, 1{\cdot}84_6, 1{\cdot}01_2)$ A.; whence the projection of $G'E'$ on the plane *OXY* normal to the beam is of length $(X^2+Y^2)^{\frac{1}{2}}$ or $1{\cdot}97_0$ A. and makes an angle $\tan^{-1}(Y/X)$ equal to 47° 33′ with $\bar{a}$; and similarly the projection of $G'B$ on *OXY* is of length $2{\cdot}23_1$ A. and makes an angle of 55° 49′ with $\bar{a}$. The values obtained from the

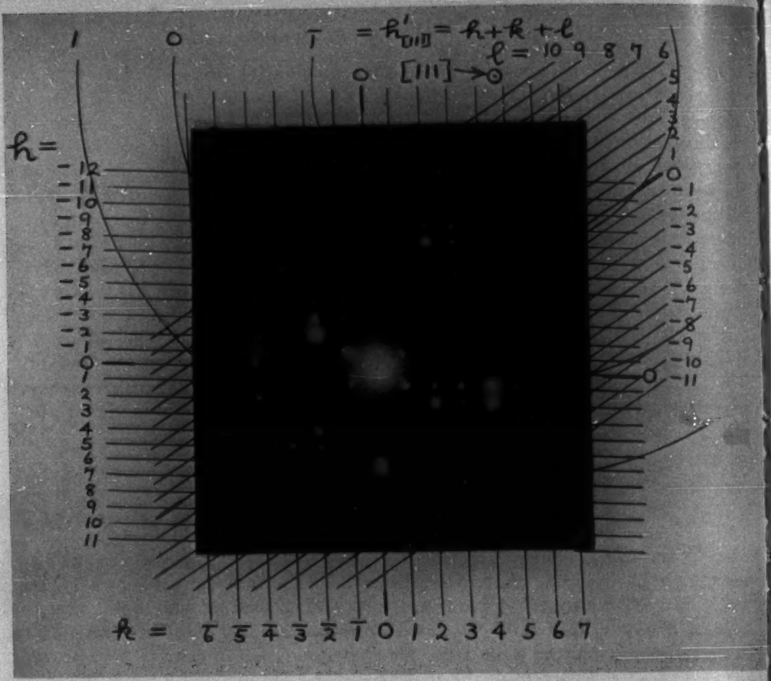

1 0 $\bar{1}$ = $h'_{[111]}$ = h + k + l
l = 10 9 8 7 6
0 [111]
h =
-12 -11 -10 -9 -8 -7 -6 -5 -4 -3 -2 -1 0 1 2 3 4 5 6 7 8 9 10 11
5 4 3 2 1 0 -1 -2 -3 -4 -5 -6 -7 -8 -9 -10 -11
k = $\bar{6}$ $\bar{5}$ $\bar{4}$ $\bar{3}$ $\bar{2}$ $\bar{1}$ 0 1 2 3 4 5 6 7

Figure 17*a*.

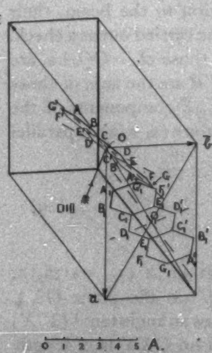

c
b
a
[111]
A B C D E F G O
0 1 2 3 4 5 A.

Figure 17*b*. $\theta_a = 84° 59'$, $\theta_b = 54° 26'$, $\theta_c = 52° 14'$.

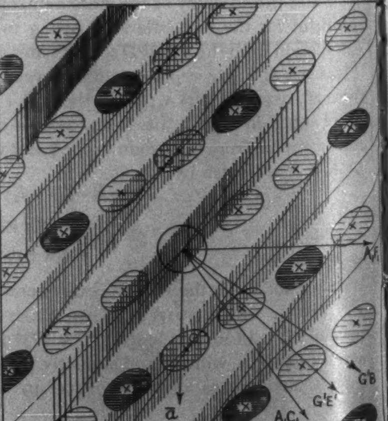

a
A_1F_1
G'B
G'E'
A_1C_1

Figure 17*c*.

projection drawing by measurement are therefore, even for such a case as this, still of sufficient accuracy.

A value $2\cdot48_2$ A. cm. of λL was calculated from R_{10} and R_{01}; hence the spacings of the Laue zones due to $G'E'$ etc. are $1\cdot26_7$, $1\cdot11_8$, $1\cdot47_8$ and $1\cdot03_5$ cm. and the pattern of molecular scattering, figure 17*c*, was thus constructed. It may be noted that, since the Laue zones due to $G'E'$ and $G'B$ are nearly parallel, the inclination of the bands is intermediate between the directions of the two sets of zones; and, further, that when allowance is made for radial decrease in the atom-form factor the maxima along each band will occur nearer to the foot of the perpendicular from the central spot to the band than the zone intersections marked in figure 17*c*, as is actually seen in figure 17*a*.

Figure 18. The spot pattern of figure 18*a* corresponds to that of the *ab* cross grating, since $R_{10}=0\cdot283$ cm., $R_{01}=0\cdot401$ cm. and $R_{11}=0\cdot513$ cm., so that

$$\bar{\gamma}=180^\circ-84^\circ\,35', \quad m=(b/a)\,(R_{01}/R_{10})=0\cdot9940,$$

and $$\theta_b=72^\circ\,30' \text{ or } 180^\circ-72^\circ\,30', \quad \theta_a=71^\circ\,26' \text{ or } 180^\circ-71^\circ\,26'.$$

From the fact that $\bar{\gamma}>90^\circ$ and from the direction of curvature of the *a* and *b* zones, $\theta_a=180^\circ-71^\circ\,26'$ and $\theta_b=180^\circ-72^\circ\,30'$ if *a* and *b* are directed as indicated in figure 18*b*; and the *c* axis is then in one of two possible directions, according to whether the positive *a* and *b* directions are as shown in figure 18*b* or are reversed. A calculation of the corresponding *c* direction ($\theta_c=20^\circ\,54'$ and $\beta=180^\circ-33^\circ\,15'$) and Laue-zone positions leads to the identification of the latter for the case shown by figure 18*b* although, owing to their relaxation through the thinness of the crystal and also owing to the presence of extraneous spots evidently provided by small bent edges of the crystal, these zones are not very well marked. From this first approximation to the crystal-orientation it was possible to index decisively at least those spots not too remote from the central spot, and the orientation was calculated more accurately from the indices, 021, $\overline{4}\overline{1}1$ and 320, of three outstandingly strong spots yielding $\theta_a=180^\circ-70^\circ\,25'$, $\theta_b=180^\circ-73^\circ\,26'$, $\theta_c=21^\circ\,52'$. The direction cosines of *a*, *b* and *c* with respect to three orthogonal axes *OXYZ*, such that *OZ* lay along the reversed direction of the beam and *OX*, *OZ* and *a* were coplanar, were calculated from these angles to be as follows:

$$\begin{aligned} l_1&=0\cdot9422, & m_1&=0, & n_1&=-0\cdot3353,\\ l_2&=-0\cdot1014, & m_2&=0\cdot9531, & n_2&=-0\cdot2851,\\ l_3&=-0\cdot2786, & m_3&=0\cdot1860, & n_3&=0\cdot9281; \end{aligned}$$

whence the *XY* co-ordinates of $\bar{a}$, $\bar{b}$, $\bar{c}$ in *OXY* are $(8\cdot08_5,\ 0)$, $(-0\cdot61_1,\ 5\cdot73_7)$, $(-3\cdot11_4,\ 2\cdot07_9)$ A. Thus $\bar{a}=8\cdot08_5$ A., $\bar{b}=5\cdot80_4$ A., $\bar{c}=3\cdot74_8$ A. and

$$\bar{\gamma}=\tan^{-1}(m_2/l_2)=180^\circ-83^\circ\,56', \quad \beta=\tan^{-1}(m_3/l_3)=180^\circ-33^\circ\,44'.$$

The *c* axis thus meets the plate at 16·5 cm. from the central spot, and the *c* Laue zones will be approximately circular about this point and roughly equidistant, with a spacing $\lambda L/\bar{c}$ equal to 0·61 cm., since λL was calculated from R_{10}, R_{01} and $\bar{\gamma}$ to be $2\cdot28_8$ A. cm. These zones are marked in figure 18*a*, and the calculated positions of the

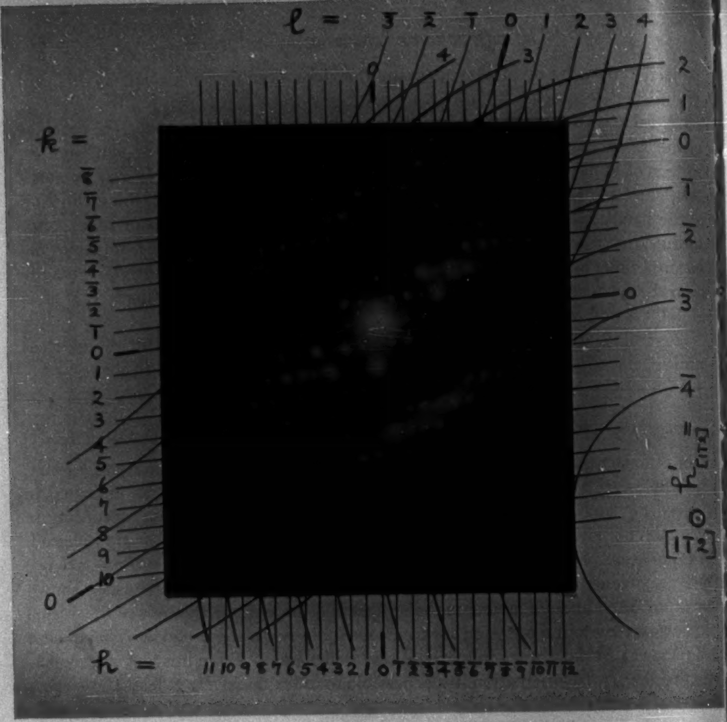
l = 3̄ 2̄ 1̄ 0 1 2 3 4
4
3
0
k =
8̄ 7̄ 6̄ 5̄ 4̄ 3̄ 2̄ 1̄ 0 1 2 3 4 5 6 7 8 9 10
0
h = 11 10 9 8 7 6 5 4 3 2 1 0 1̄ 2̄ 3̄ 4̄ 5̄ 6̄ 7̄ 8̄ 9̄ 10̄ 11̄ 12̄
2 1 0 1̄ 2̄ 3̄ 4̄
0
h'[11̄2] =
0
[11̄2]

Figure 18*a*.

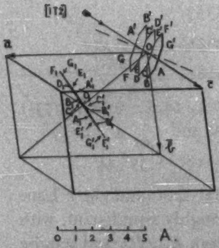
[11̄2]
a
c
b
A′ B′ C′ D′ E′ F′ G′
A B C D E F G
0 1 2 3 4 5 A.

Figure 18*b*. $\theta_a = 180° - 70° 25'$, $\theta_b = 180° - 73° 26'$, $\theta_c = 21° 52'$.

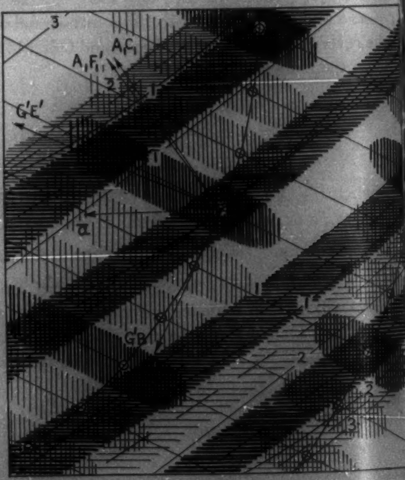
3
A₁C₁
A₁F₁′
G′E′
1
2
a
G′B
1
2
3̄
3

Figure 18*c*.

$[1\bar{1}2]$ axis and Laue zones are also shown, although the latter also are ill-defined. The $\bar{a}$, $\bar{b}$, $\bar{c}$ co-ordinates of A and D in figure 18*a* were calculated to be $(0{\cdot}76_0, 0{\cdot}18_8, 1{\cdot}38_2)$ and $(0{\cdot}76_8, 1{\cdot}20_1, 0{\cdot}18_7)$ A. respectively. Finally, measurement of the projection drawing, corresponding to figure 18*b*, gave $G'E'=0{\cdot}51$ A., $G'B=2{\cdot}08$ A., $A_1C_1=0{\cdot}92$ A. and $A_1F_1'=1{\cdot}50$ A., these lines being inclined to $\bar{a}$ at angles $-24°\ 0'$, $62°\ 15'$, $-57°\ 45'$ and $180°-54°\ 45'$ respectively, whence the Laue zones due to $G'B$ and A_1F_1' are practically straight and equidistant lines normal to the projection of $G'B$ and A_1F_1' respectively on the screen, over the small angles of deviation concerned, with spacings of 1·10 and 1·52 cm. respectively. Since $G'E'$ is inclined to the beam at the fairly small angle θ_0 equal to $\sin^{-1}(0{\cdot}51/1{\cdot}41\sqrt{3})$ or $12°\ 3'$, the corresponding Laue zones will be considerably curved and will not be equidistant, and their positions may be found from the Laue relation expressing the semi-apical angles θ of the Laue cones round the atom row of spacing d, i.e.

$$\cos\theta=\cos\theta_0+n\lambda/d.$$

In the present case $\cos\theta=0{\cdot}9779-n.(0{\cdot}0190_1)$, whence the Laue zones, which may be taken to be practically circles about the point of intersection of the atom row with the screen, cut the projection of $G'E'$ on the screen (distant 10·0 cm. from the central spot) at distances R equal to $L\tan(\theta_0-\theta)$ or $46{\cdot}5\tan(\theta_0-\theta)$ cm. from the central spot. The distance R from the central spot to the zones of order 1, 0, $\bar{1}$, $\bar{2}$ and $\bar{3}$ are therefore 6·16, 0, −3·60, −6·47 and −8·96 cm. In a similar manner it was calculated that A_1C_1 was inclined to the beam at $22°\ 8'$, and this line produced would meet the screen at 18·9 cm. from the central spot; and that the Laue zones of order 3, 2, 1, 0, $\bar{1}$, $\bar{2}$ and $\bar{3}$ cut the projection of A_1C_1 on the screen at distances 9·57, 5·52, 2·52, 0, −2·22, −4·23 and −6·12 cm. from the central spot. Figure 18*c* represents the intensity-distribution deduced for the two molecules, the curves of Laue zone maxima being shown for clearness, and the broken lines indicating the regions of maximum intensity along the main bands.

Figure 19. The unit translations of the cross-grating spot pattern are as follows: $R_{10}=0{\cdot}303$ cm. and $R_{01}=0{\cdot}377$ cm., inclined at an angle $180°-86°\ 15'$. This corresponds to the *ab* cross-grating with $\bar{\gamma}=86°\ 15'$, $m=(b/a)(R_{01}/R_{10})=0{\cdot}8730$, $\theta_b=86°\ 6'$ or $180°-86°\ 6'$, and $\theta_a=60°\ 34'$ or $180°-60°\ 34'$. From the curvature of the *a* and *b* zones and since $\bar{\gamma}<90°$, it follows that for *a* and *b* directed as in figure 19*b*, $\theta_a=180°-60°\ 34'$, $\theta_b=86°\ 6'$, and the broad circular zones to which the spots are limited are due to the *c* axis which is inclined at a small angle to the beam. Three of the strongest spots are thus indexed as $2\bar{1}0$, $\bar{6}\bar{1}1$ and $34\bar{1}$, whence were calculated the more accurate values $\theta_a=180°-59°\ 22'$, $\theta_b=83°\ 36'$, $\theta_c=7°\ 24'$. Referred to orthogonal axes $OXYZ$ such that OZ is along the reversed beam direction and *a* lies in the plane OXZ, the direction cosines of *a*, *b*, and *c* are therefore

$$\begin{aligned} l_1&=0{\cdot}8605, & m_1&=0, & n_1&=-0{\cdot}5095,\\ l_2&=0{\cdot}06595, & m_2&=0{\cdot}9916, & n_2&=0{\cdot}1114,\\ l_3&=-0{\cdot}07925, & m_3&=-0{\cdot}1010, & n_3&=0{\cdot}9917. \end{aligned}$$

The XY co-ordinates of $\bar{a}$, $\bar{b}$, $\bar{c}$ are $(7{\cdot}38_4, 0)$, $(0{\cdot}39_7, 5{\cdot}97_0)$ and $(-0{\cdot}88_6, -1{\cdot}12_9)$ A., and $\bar{a}=7{\cdot}38_4$ A., $\bar{b}=5{\cdot}98_3$ A., $\bar{c}=1{\cdot}43_5$ A., whence the $\bar{a}$, $\bar{b}$, $\bar{c}$ co-ordinates of A and D are $(0{\cdot}69_4, 0{\cdot}19_1, 0{\cdot}52_9)$ and $(0{\cdot}70_1, 1{\cdot}23_9, 0{\cdot}07_2)$ A. respectively. Measurement of the projection drawing, figure 19*b*, gave $G'E'=0{\cdot}53$ A., $G'B=2{\cdot}30$ A., $A_1C_1=0{\cdot}07$ A., $A_1F_1'=2{\cdot}09$ A., and their angles with $\bar{a}$ were 90° 10′, 61° 0′, 22° and 115° respectively. Finally the value of λL calculated from R_{10} and R_{01} was $2{\cdot}24_0$ A. cm., hence the spacings of the nearly straight and equidistant Laue zones corresponding to $G'B$ and A_1F_1' were $0{\cdot}97_4$ and $1{\cdot}07_2$ cm. respectively. By calculations similar to those described in connexion with figure 18 it was found that $G'E'$ was inclined to the beam at 12° 32′ and when produced would meet the screen at a point 10·2 cm. from the central spot; and that the Laue zones of order 1, 0, $\bar{1}$ and $\bar{2}$ would cut the projection of $G'E'$ in points distant 5·67, 0, $-3{\cdot}42$ and $-6{\cdot}21$ cm. respectively from the central spot. Since A_1C_1 is so nearly parallel to the beam, its broad zero-order Laue zone will cover the whole region of the recorded pattern.

The theoretical molecular scattering pattern constructed from these data is shown in figure 19*c*, and may be seen to correspond well with that recorded in figure 19*a* when allowance is made for the radial decrease in intensity due to the atom-form factor and for the fact that, owing to the thickness of the crystal, the pattern contains a considerable secondary scattering contribution. Moreover, the apparent slope of the bands is affected by the presence of the circular Laue-zone system of spots, although the slope does actually correspond well with that in figure 19*c*. For the sake of clarity the more prominent Kikuchi line-pairs are marked and have been indexed.

Figure 19*a* also shows clearly the occurrence, already referred to, of a noticeable displacement of spots from the intersections of the Laue-zone medians due to the cross-grating defined by two of the crystal axes, here the *a* and *b* axes. In this case the systematic nature of the deviations can be clearly observed; the inclination of the spot rows across each of the broad circular *c* Laue zones is slightly different from the mean direction of the *a* zones taken across the various *c* zone regions. The positions of the spots appear to be in accordance with the supposition that the crystal had the shape of a thin sheet normal to the *c* axis or nearly so, rather than of a thin sheet bounded by the *ab* plane. The spot positions agree well with the intersections of the *b* and [301] Laue zones; thus the crystal may have been a thin sheet bounded by the cross-grating plane containing these axes.

Figures 20 *and* 21. The crystal-orientation in the case of figure 20 approximates closely to that of figure 14*a*, but the crystal was thicker so that the third Laue condition has acquired such a degree of comparative rigidity that the cross-grating spots are nearly limited to true Bragg positions. The effect of increased crystal-thickness in bringing about a decrease in intensity of the diffuse-area pattern relative to the Bragg spots is very pronounced.

Figure 21 was also obtained from a relatively thick crystal oriented so that the beam was only a few degrees inclined to the [101] zone axis, to the zero-order Laue zone of which nearly all the *ab* cross-grating spots in the pattern are limited. Here also may be clearly observed the relative weakness of the diffuse-area pattern and its occurrence in regions distinct from the spot pattern.

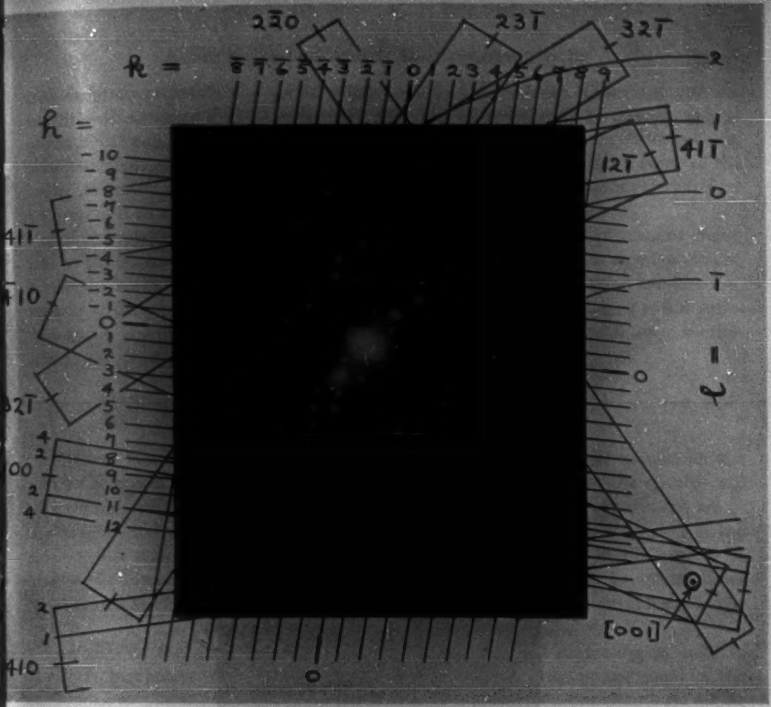
$2\bar{2}0$
$23\bar{1}$
$32\bar{1}$
k =
$\bar{8}\ \bar{7}\ \bar{6}\ \bar{5}\ \bar{4}\ \bar{3}\ \bar{2}\ \bar{1}\ 0\ 1\ 2\ 3\ 4\ 5\ 6\ 7\ 8\ 9$
h =
-10 -9 -8 -7 -6 -5 -4 -3 -2 -1 0 1 2 3 4 5 6 7 8 9 10 11 12
$41\bar{1}$
$\bar{4}10$
$32\bar{1}$
4 2 100 2 4
2 1 410
$12\bar{1}$
$41\bar{1}$
2 1 0 $\bar{1}$
0
l =
[001]
0

Figure 19*a*.

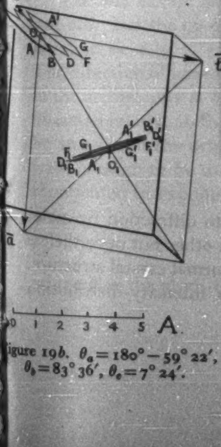
$\bar{c}$
A'
O
G
A
B
D
F
$\bar{b}$
A_1'
B_1'
D_1'
F_1
G_1
G_1'
F_1'
D_1 B_1
A_1
O_1
$\bar{a}$
0 1 2 3 4 5 A

igure 19*b*. $\theta_a = 180° - 59° 22'$, $\theta_b = 83° 36'$, $\theta_c = 7° 24'$.

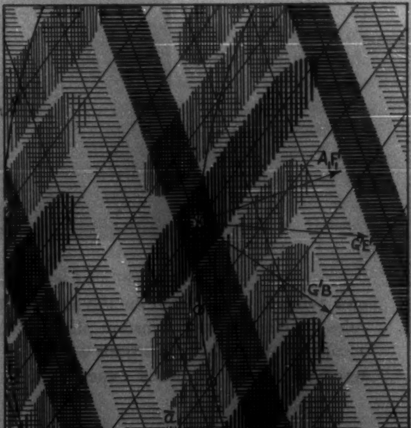
$A_1'F_1'$
$G'E'$
$G'B$
O
$\bar{a}$
O

Figure 19*c*.

We have thus considered a representative series of diffraction patterns from single crystals of anthracene in different orientations. In every case the diffuse-area pattern, constructed on the assumption that it is due to diffraction by molecules which exhibit no constant phase relationship with each other but nevertheless occupy the same mean positions within the lattice as in the normal crystal structure, agrees with that recorded experimentally both as regards intensity-distribution

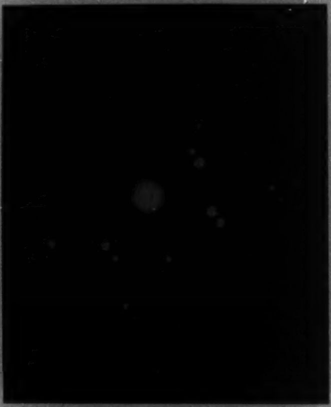

Figure 20.

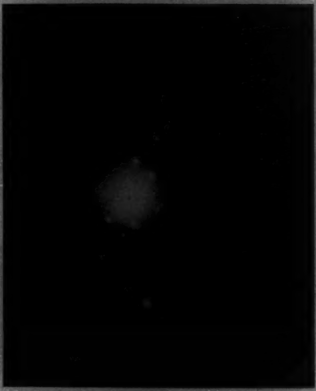

Figure 21.

and orientation relative to the spot pattern. It is clear that the diffuse-area pattern must be due to reinforced diffraction arising from the regular distribution of atoms in the molecules. Thus, since the normal spot and diffuse-area patterns occur simultaneously, the phase differences between wavelets scattered from some of the molecules must vary from molecule to molecule. These molecules must therefore be displaced in some way from their proper positions in the lattice.

Whilst several possibilities of accounting for the molecular displacement giving rise to the molecular diffraction effect suggested themselves, such as edge effects, distortion, superficial melting or incipient transition to the molten state, evaporation, mosaic structure and crystal imperfections generally, none of these proved satisfactory on inspection. Another cause, however, namely molecular heat motion within the crystal, seems able to explain the phenomenon.

§6. A THEORY OF THE EFFECT OF THERMAL MOTION ON DIFFRACTION BY A MOLECULAR LATTICE

Debye, Waller and James(6) have discussed the effect of heat motion on the x-ray diffraction from a crystal, but confined their discussions to the special case of a simple cubic lattice with a single type of atom. Theory and experiment are in agreement in showing that, apart from the displacement due to expansion of the lattice with rising temperature, the only effect of heat motion in this case is to reduce the intensity of, but not to broaden, the diffraction spots. In what follows we discuss the effect of heat motion on the diffraction phenomena from a molecular lattice.

In view of the nature of the interatomic bindings, and neglecting as hitherto the hydrogen atoms, we disregard the intramolecular heat motion and consider the molecules as vibrating as a whole about their normal lattice positions. As a first approximation, suppose that the molecules vibrate without rotation in a simple harmonic manner, so that the restoring force is proportional to the displacement from the mean position, and suppose also that the molecules vibrate independently, their motions being in accordance with the Maxwell-Boltzmann law. To begin with, we consider the case of a crystal of which the unit cell contains only one molecule.

Thermal motion and diffraction by a lattice of the type having a monomolecular unit-cell. Let the co-ordinates of any atom in the crystal referred to a lattice point as origin be x, y, z, expressed as fractions of the axial lengths a, b, c respectively. The direction of any diffracted ray is specified by the Laue numbers h, k, l referring to the crystal axes a, b, c. The phase of the wavelet scattered from the atom in this direction relative to that of a wavelet which would be scattered in the same direction by an atom at the origin is $2\pi(hx+ky+lz)$. Thus if the amplitude of the incident wave is taken to be unity, the wavelet scattered by any atom in the crystal may be represented in exponential notation by the real part of the expression

$$Fe^{i\{\omega t+2\pi(hx+ky+lz)\}},$$

i.e.

$$Fe^{i\omega t}\,e^{2\pi i\Sigma hx}, \qquad \ldots\ldots(30)$$

where F is the atom-form factor.

Let x_0, y_0, z_0 be the co-ordinates defining the mean position of the atom with respect to the lattice point with which it is associated as origin, the co-ordinates of the latter being the three integers n_1, n_2, n_3. Then if x, y and z vary harmonically about their mean values n_1+x_0, n_2+y_0, n_3+z_0, we have

$$\left.\begin{aligned} x&=n_1+x_0+x_1\sin(\omega_x t+\alpha_x),\\ y&=n_2+y_0+y_1\sin(\omega_y t+\alpha_y),\\ z&=n_3+z_0+z_1\sin(\omega_z t+\alpha_z),\end{aligned}\right\} \quad\text{......(31)}$$

where the α's denote the arbitrary phase angles between the oscillations of adjacent molecules. As each molecule is assumed to vibrate as a whole, $x_1\sin(\omega_x t+\alpha_x)$, etc. have the same values $x_{n_1n_2n_3}$, etc. at any instant for all atoms of the same molecule; hence, if we consider only the molecule associated with n_1, n_2, n_3,

$$\left.\begin{aligned} x&=n_1+x_0+x_{n_1n_2n_3},\\ y&=n_2+y_0+y_{n_1n_2n_3},\\ z&=n_3+z_0+z_{n_1n_2n_3}.\end{aligned}\right\} \quad\text{......(32)}$$

Then from equation (30) the total displacement scattered by the atoms of the molecule associated with the lattice point n_1, n_2, n_3 is

$$\Psi_{n_1n_2n_3}=\sum_{x_0}\sum_{y_0}\sum_{z_0} F\exp(i\omega t)\exp(2\pi i\Sigma hn_1)\exp(2\pi i\Sigma hx_0)\exp(2\pi i\Sigma hx_{n_1n_2n_3}), \quad\text{......(33)}$$

where the summation is taken over all the atoms in the molecule.

We may write the molecular structure amplitude,

$$\sum_{x_0}\sum_{y_0}\sum_{z_0} F\exp(2\pi i\Sigma hx_0),$$

in the usual form $A+iB$, where

$$\left.\begin{aligned} A&=\Sigma F\cos 2\pi(hx_0+ky_0+lz_0),\\ \text{and}\qquad B&=\Sigma F\sin 2\pi(hx_0+ky_0+lz_0),\end{aligned}\right\} \quad\text{......(34)}$$

both summations being taken over all atoms of the molecule.

Thus $\Psi_{n_1n_2n_3}=\exp(i\omega t)\exp(2\pi i\Sigma hn_1)(A+iB)\exp(2\pi i\Sigma hx_{n_1n_2n_3})$. ......(35)

The total diffracted intensity in the *hkl* direction, relative to that of the primary beam, due to the whole crystal is

$$I=\left(\sum_{n_1=0}^{M_1-1}\sum_{n_2=0}^{M_2-1}\sum_{n_3=0}^{M_3-1}\Psi_{n_1n_2n_3}\right)\left(\sum_{n_1=0}^{M_1-1}\sum_{n_2=0}^{M_2-1}\sum_{n_3=0}^{M_3-1}\Psi_{n_1n_2n_3}\right)^*, \quad\text{......(36)}$$

where the *M*'s are the number of lattice points along the corresponding axial directions *a*, *b* and *c* in the crystal, which is supposed to be a parallelepiped, and the asterisked expression represents the conjugate of the first expression. This is equivalent to

$$I=\left(\sum_{n_1=0}^{M_1-1}\sum_{n_2=0}^{M_2-1}\sum_{n_3=0}^{M_3-1}\Psi_{n_1n_2n_3}\right)\left(\sum_{n_1=0}^{M_1-1}\sum_{n_2=0}^{M_2-1}\sum_{n_3=0}^{M_3-1}\Psi^*_{n_1n_2n_3}\right), \quad\text{......(37)}$$

and therefore contains terms of the types $\Psi_{n_1n_2n_3}\Psi^*_{n_1n_2n_3}$ and $\Psi_{n_1n_2n_3}\Psi^*_{n_1'n_2'n_3'}$. Thus from equation (35)

$$\sum_{n_1=0}^{M_1-1}\sum_{n_2=0}^{M_2-1}\sum_{n_3=0}^{M_3-1}\Psi_{n_1n_2n_3}\Psi^*_{n_1n_2n_3}=M_1M_2M_3(A^2+B^2)$$
$$=N(A^2+B^2), \qquad\qquad \ldots\ldots(38)$$

where N is the number of molecules in the crystal.

The remaining part of equation (37) is equal to

$$\sum_{n_1=0}^{M_1-1}\sum_{n_2=0}^{M_2-1}\sum_{n_3=0}^{M_3-1}\sum_{n_1'=0}^{M_1-1}\sum_{n_2'=0}^{M_2-1}\sum_{n_3'=0}^{M_3-1}(A^2+B^2)$$
$$\times\exp\{2\pi i\Sigma h(n_1-n_1')\}\exp\{2\pi i\Sigma h(x_{n_1n_2n_3}-x_{n_1'n_2'n_3'})\}, \qquad \ldots\ldots(39)$$

the cases where n_1, n_2, n_3 and n_1', n_2', n_3' are the same sets of integers simultaneously being excluded. It is assumed that the thermal displacement of any molecule from its mean position is equally probable in all directions and that the probability of a given displacement in any direction is in accordance with the Maxwell-Boltzmann law. For the purpose of the calculation the displacement will be split up into its three components parallel to the axes of co-ordinates and, in order to fit in with the first assumption, we must specify the co-ordinates of the displacement in terms of three orthogonal axes, if the crystal axes are not already orthogonal, so that the values of the separate linear components are independent, i.e. the Maxwell-Boltzmann distribution of probabilities can be applied to each component separately. Thus let the orthogonal co-ordinate axes for the displacement be chosen as $\mathbf{a}', \mathbf{b}', \mathbf{c}'$, not necessarily equal, and defined by

$$\left.\begin{aligned}\mathbf{a}'&=\alpha_1\mathbf{a}+\beta_1\mathbf{b}+\gamma_1\mathbf{c},\\ \mathbf{b}'&=\alpha_2\mathbf{a}+\beta_2\mathbf{b}+\gamma_2\mathbf{c},\\ \mathbf{c}'&=\alpha_3\mathbf{a}+\beta_3\mathbf{b}+\gamma_3\mathbf{c},\end{aligned}\right\} \qquad \ldots\ldots(40)$$

i.e. $\mathbf{a}', \mathbf{b}', \mathbf{c}'$ are the lattice rows $[\alpha_1\beta_1\gamma_1]$, $[\alpha_2\beta_2\gamma_2]$, $[\alpha_3\beta_3\gamma_3]$ in the lattice $\mathbf{a}, \mathbf{b}, \mathbf{c}$. Let the displacement of the molecule based on the crystal lattice point n_1, n_2, n_3 be $\mathbf{r}$, where

$$\mathbf{r}=x_{n_1n_2n_3}\mathbf{a}+y_{n_1n_2n_3}\mathbf{b}+z_{n_1n_2n_3}\mathbf{c}, \qquad \ldots\ldots(41)$$

and

$$\mathbf{r}=X_{n_1n_2n_3}\mathbf{a}'+Y_{n_1n_2n_3}\mathbf{b}'+Z_{n_1n_2n_3}\mathbf{c}', \qquad \ldots\ldots(42)$$

whence by substitution of (40) in (42) and comparing the coefficients of $\mathbf{a}$, $\mathbf{b}$ and $\mathbf{c}$ with those in (41)

$$\left.\begin{aligned}x_n&=X_n\alpha_1+Y_n\alpha_2+Z_n\alpha_3,\\ y_n&=X_n\beta_1+Y_n\beta_2+Z_n\beta_3,\\ z_n&=X_n\gamma_1+Y_n\gamma_2+Z_n\gamma_3,\end{aligned}\right\} \qquad \ldots\ldots(43)$$

where for brevity the suffix n is written instead of $n_1n_2n_3$. The expression (39) now becomes

$$\sum_{n_1}\sum_{n_2}\sum_{n_3}\sum_{n_1'}\sum_{n_2'}\sum_{n_3'}(A^2+B^2)\exp\{2\pi i\Sigma h(n_1-n_1')\}\exp\{2\pi i\Sigma(h\alpha_1+k\beta_1+l\gamma_1)(X_n-X_{n'})\},$$

which may be written

$$\Sigma\,\Sigma\,\Sigma\,\Sigma\,\Sigma\,\Sigma\,(A^2+B^2)\exp\{2\pi i\Sigma h\,(n_1-n_1')\}\exp\{2\pi i\Sigma H\,(X_n-X_{n'})\}, \quad \ldots\ldots(44)$$

where

$$\left.\begin{aligned} H&=h\alpha_1+k\beta_1+l\gamma_1,\\ K&=h\alpha_2+k\beta_2+l\gamma_2,\\ L&=h\alpha_3+k\beta_3+l\gamma_3.\end{aligned}\right\} \quad \ldots\ldots(45)$$

Suppose now that the different molecules vibrate independently and that the energy associated with a displacement r along the $\mathbf{a}'$ direction is

$$W=\tfrac{1}{2}fr^2=\tfrac{1}{2}fa'^2X_n^2, \quad \ldots\ldots(46)$$

with similar expressions relating to the other component displacements Y_n and Z_n, involving the same force f per unit displacement, since the restoring force acting on the molecule is supposed to be the same in all directions. According to the Maxwell-Boltzmann law, the probability $p\,dX_n$ of the molecule lying between X_n and X_n+dX_n is given by

$$p\,dX_n=C\exp\left(-\frac{W}{kT}\right)dX_n=C\exp\left(-\frac{fa'^2X_n^2}{2kT}\right)dX_n, \quad \ldots\ldots(47)$$

with the normalizing condition that the constant C must satisfy

$$1=\int_{-\infty}^{+\infty}p\,dX_n=\int_{-\infty}^{+\infty}C\exp\left(-\frac{fa'^2X_n^2}{2kT}\right)dX_n=C\left(\frac{2\pi kT}{fa'^2}\right)^{\frac{1}{2}}. \quad \ldots\ldots(48)$$

In order to find the mean value of the expression (44) we multiply it by the corresponding probability factors of type (47) characteristic of the vibration state considered and integrate for all possible values of X_n, treating X_n, Y_n and Z_n as independent. Thus the mean value of the expression (44) is

$$\sum_{n_1}\sum_{n_2}\sum_{n_3}\sum_{n_1'}\sum_{n_2'}\sum_{n_3'}(A^2+B^2)\exp\{2\pi i\Sigma h\,(n_1-n_1')\}$$

$$\times\prod_6\left\{\int_{-\infty}^{+\infty}\exp(2\pi iHX_n)\,C\exp\left(-\frac{fa'^2X_n^2}{2kT}\right)dX_n\right\}, \quad \ldots\ldots(49)$$

in which $\prod_6$ denotes the product of six independent integrals of the type shown in the bracket, with variables respectively X_n, Y_n, Z_n, $X_{n'}$, $Y_{n'}$, $Z_{n'}$, the three latter having the negative sign in the power of e. Since

$$-\frac{fa'^2X_n^2}{2kT}+2\pi iHX_n=-\frac{fa'^2}{2kT}\left(X_n+\frac{\pi iH\,2kT}{fa'^2}\right)^2-\frac{\pi^2H^2}{fa'^2}\,2kT,$$

the integral in expression (49) becomes

$$\int_{-\infty}^{+\infty}\exp\left\{-\frac{fa'^2}{2kT}\left(X_n+\pi iH\frac{2kT}{fa'^2}\right)^2\right\}C\exp\left(-\frac{\pi^2H^2\,2kT}{fa'^2}\right)d\left(X_n+\frac{\pi iH\,2kT}{fa'^2}\right)$$

$$=\exp\left(-\frac{\pi^2H^2\,2kT}{fa'^2}\right)C\int_{-\infty}^{+\infty}\exp\left(-\frac{fa'^2\,X_n'^2}{2kT}\right)dX_n'$$

$$=\exp\left(-\frac{\pi^2H^2\,2kT}{fa'^2}\right),$$

since the integral has the value

$$\sqrt{\frac{2\pi kT}{fa'^2}},$$

and C is given by equation (48). The remaining integrals in the product $\prod_6$ in (49) have similar values and this therefore reduces to

$$\Sigma\Sigma\Sigma\Sigma\Sigma\Sigma\,(A^2+B^2)\exp\{2\pi i\Sigma h(n_1-n_1')\}\exp\left(-\frac{\pi^2\,2kT}{f}\,2\Sigma\frac{H^2}{a'^2}\right). \qquad \text{......(50)}$$

The indices H, K and L are defined by equations (45) and are thus the Laue indices of the diffracted beam referred to the lattice rows $\mathbf{a}'$, $\mathbf{b}'$, $\mathbf{c}'$ as axes; hence we have

$$\Sigma\frac{H^2}{a'^2}=\frac{H^2}{a'^2}+\frac{K^2}{b'^2}+\frac{L^2}{c'^2}=\frac{1}{d^2_{HKL}}=\frac{1}{d^2_{hkl}}, \qquad \text{......(51)}$$

where d_{HKL} is the spacing of the net planes whose indices are H, K, L referred to a', b', c' as axes and d_{hkl} is the spacing of the same plane group referred to the axes a, b, c. By Bragg's law,

$$2d_{HKL}\sin\theta=\lambda, \qquad \text{......(52)}$$

where 2θ is the angle between the primary and diffracted beams; whence equation (51) becomes

$$\Sigma\frac{H^2}{a'^2}=\frac{4\sin^2\theta}{\lambda^2}, \qquad \text{......(53)}$$

and the expression (50) reduces to

$$(A^2+B^2)\exp\left(-\frac{8\pi^2\sin^2\theta}{\lambda^2}\,\frac{2kT}{f}\right)\Sigma\Sigma\Sigma\Sigma\Sigma\Sigma\exp\{2\pi i\Sigma h(n_1-n_1')\}. \qquad \text{......(54)}$$

The summation of the expression (54) must now be made by summing all the terms including those in which n_1, n_2, n_3 and n_1', n_2', n_3' are the same set of integers, then summing the latter group and subtracting this result from the first, whence we obtain

$$\begin{aligned}&(A^2+B^2)\exp\left(-\frac{8\pi^2\sin^2\theta}{\lambda^2}\,\frac{2kT}{f}\right)\sum_{n_1=0}^{M_1-1}\exp(2\pi ihn_1)\sum_{n_2=0}^{M_2-1}\exp(2\pi ikn_2)\\ &\times\sum_{n_3=0}^{M_3-1}\exp(2\pi iln_3)\sum_{n_1'=0}^{M_1-1}\exp(-2\pi ihn_1')\sum_{n_2'=0}^{M_2-1}\exp(-2\pi ikn_2')\sum_{n_3'=0}^{M_3-1}\exp(-2\pi iln_3')\\ &\qquad\qquad -N(A^2+B^2)\exp\left(-\frac{8\pi^2\sin^2\theta}{\lambda^2}\,\frac{2kT}{f}\right). \qquad \text{......(55)}\end{aligned}$$

As a typical factor in the first part of the expression (55) we have

$$\sum_{n_1=0}^{M_1-1}e^{2\pi ihn_1}=\frac{e^{2\pi ihM_1}-1}{e^{2\pi ih}-1},$$

and the value of the other factor involving M_1 is $(e^{-2\pi i h M_1}-1)/(e^{-2\pi i h}-1)$. The product of the two factors is therefore

$$\frac{2-(e^{2\pi i h M_1}-e^{-2\pi i h M_1})}{2-(e^{2\pi i h}-e^{-2\pi i h})}=\frac{2-2\cos 2\pi h M_1}{2-2\cos 2\pi h}=\frac{\sin^2 M_1 h\pi}{\sin^2 h\pi}. \qquad \ldots\ldots(56)$$

The product of the six Σ terms in (55) is thus

$$\frac{\sin^2 M_1 h\pi}{\sin^2 h\pi}\,\frac{\sin^2 M_2 k\pi}{\sin^2 k\pi}\,\frac{\sin^2 M_3 l\pi}{\sin^2 l\pi}.$$

Finally, the total intensity of scattering I in the direction defined by the Laue numbers h, k, l referred to **a**, **b** and **c** is obtained by adding expressions (38) and (55), whence after simplication we have

$$I=(A^2+B^2)\frac{\sin^2 M_1 h\pi}{\sin^2 h\pi}\,\frac{\sin^2 M_2 k\pi}{\sin^2 k\pi}\,\frac{\sin^2 M_3 l\pi}{\sin^2 l\pi}\exp\left(-\frac{16\pi^2\sin^2\theta}{\lambda^2}\frac{kT}{f}\right)$$
$$+N(A^2+B^2)\left\{1-\exp\left(-\frac{16\pi^2\sin^2\theta}{\lambda^2}\frac{kT}{f}\right)\right\}, \qquad \ldots\ldots(57)$$

which holds for the case of the unit cell containing a single molecule.

Extension of the theory to a polymolecular unit-cell lattice. An expression analogous to (57), but valid for the case where the crystal structure is such that there are q molecules per unit cell instead of only one, can be derived as follows. Again suppose that all the molecules in the crystal oscillate independently. Then the co-ordinates (x, y, z) of any atom in the crystal can be expressed by three equations similar to (31), of type $x=n_1+x_0+{}_px_1\sin(\omega_x t+{}_p\alpha_x)$ which may be written

$$x=n_1+x_0+{}_px_{n_1n_2n_3}. \qquad \ldots\ldots(58)$$

The total displacement ${}_p\Psi_{n_1n_2n_3}$ scattered in a direction hkl from the atoms in the pth molecule in the unit cell associated with the lattice point (n_1, n_2, n_3) is

$${}_p\Psi_{n_1n_2n_3}=\exp(i\omega t)\exp(2\pi i\Sigma hn_1)\exp(2\pi i\Sigma h\,{}_px_{n_1n_2n_3})\,{}_p\Sigma F\exp(2\pi i\Sigma hx_0), \qquad \ldots\ldots(59)$$

where the p in the summation sign indicates that the summation is carried out over the pth molecule only. We may put

$$\sum_{x_0y_0z_0}{}_p\, Fe^{2\pi i\Sigma hx_0}=A_p+iB_p, \qquad \ldots\ldots(60)$$

representing the structure amplitude of the pth molecule, and we may also put

$$\sum_{p=1}^{p=q}(A_p+iB_p)=A+iB \qquad \ldots\ldots(61)$$

for the normal structure amplitude S corresponding to the whole unit cell, so that

$$\begin{aligned}S^2&=A^2+B^2\\&=\sum_p(A_p+iB_p)\sum_{p'}(A_{p'}-iB_{p'})\\&=\left(\sum_p A_p+i\sum_p B_p\right)\left(\sum_{p'}A_{p'}-i\sum_{p'}B_{p'}\right)\\&=\left(\sum_p A_p\right)^2+\left(\sum_p B_p\right)^2.\end{aligned} \qquad \ldots\ldots(62)$$

Thus

$$ {}_{p}\Psi_{n_1n_2n_3}=\exp(i\omega t)\exp(2\pi i\,\Sigma hn_1)\exp(2\pi i\,\Sigma h\,{}_{p}x_{n_1n_2n_3})(A_p+iB_p). \quad \ldots\ldots(63) $$

Hence the intensity of scattering in the direction *hkl* due to the whole crystal is

$$ I=\left(\sum_{p=1}^{p=q}\sum_{n_1=0}^{M_1-1}\sum_{n_2=0}^{M_2-1}\sum_{n_3=0}^{M_3-1}{}_{p}\Psi_{n_1n_2n_3}\right)\left(\sum_{p'=1}^{p'=q}\sum_{n_1'=0}^{M_1-1}\sum_{n_2'=0}^{M_2-1}\sum_{n_3'=0}^{M_3-1}{}_{p'}\Psi^{*}_{n_1'n_2'n_3'}\right) $$

$$ =\sum_{p=1}^{p=q}\sum_{n_1=0}^{M_1-1}\sum_{n_2=0}^{M_2-1}\sum_{n_3=0}^{M_3-1}\sum_{p'=1}^{p'=q}\sum_{n_1'=0}^{M_1-1}\sum_{n_2'=0}^{M_2-1}\sum_{n_3'=0}^{M_3-1}{}_{p}\Psi_{n_1n_2n_3}\,{}_{p'}\Psi^{*}_{n_1'n_2'n_3'}. \quad \ldots\ldots(64) $$

This sum consists of products of two kinds, ${}_{p}\Psi_{n_1n_2n_3}\,{}_{p}\Psi^{*}_{n_1n_2n_3}$ for the cases where $p=p'$, $n_1=n_1'$, $n_2=n_2'$, $n_3=n_3'$, and ${}_{p}\Psi_{n_1n_2n_3}\,{}_{p}\Psi^{*}_{n_1'n_2'n_3'}$ where at least one of the following conditions holds:

$$ p\neq p',\ n_1\neq n_1',\ n_2\neq n_2',\ n_3\neq n_3'. \quad \ldots\ldots(65) $$

Thus, from equation (63), the sum of all terms of the first type is

$$ \begin{aligned} I_1&=\sum_{p}\sum_{n_1}\sum_{n_2}\sum_{n_3}{}_{p}\Psi_{n_1n_2n_3}\,{}_{p}\Psi^{*}_{n_1n_2n_3}\\ &=\sum_{p}\sum_{n_1}\sum_{n_2}\sum_{n_3}(A_p+iB_p)(A_p-iB_p)\\ &=N\sum_{p}(A_p^2+B_p^2), \end{aligned} \quad \ldots\ldots(66) $$

where N is the number of unit cells in the crystal. The sum of the terms of the second type in equation (64) is

$$ I_2=\sum_{n_1}\sum_{n_2}\sum_{n_3}\sum_{n_1'}\sum_{n_2'}\sum_{n_3'}\sum_{p}\sum_{p'}\exp\{2\pi i\Sigma h(n_1-n_1')\}\exp\{2\pi i\Sigma h({}_{p}x_{n_1n_2n_3}-{}_{p'}x_{n_1'n_2'n_3'})\} $$
$$ \times(A_p+iB_p)(A_{p'}-iB_{p'}). $$

Thus

$$ I_2=\sum_{n_1}\sum_{n_2}\sum_{n_3}\sum_{n_1'}\sum_{n_2'}\sum_{n_3'}\exp\{2\pi i\Sigma h(n_1-n_1')\}\exp\{2\pi i\Sigma h({}_{p}x_{n_1n_2n_3}-{}_{p'}x_{n_1'n_2'n_3'})\} $$
$$ \times\left\{\sum_{p}(A_p+iB_p)\sum_{p'}(A_{p'}-iB_{p'})\right\}, \quad \ldots\ldots(67) $$

subject to the conditions (65).

To find the mean value of I_2 we proceed as before, whence

$$ I_2=\sum_{\substack{n_1n_2n_3\\ n\neq n'}}\ \sum_{n_1'n_2'n_3'}\left\{\sum_{p}(A_p+iB_p)\sum_{p'}(A_{p'}-iB_{p'})\right\}\exp\{2\pi i\Sigma h(n_1-n_1')\} $$
$$ \times\prod_{6}\left\{\int_{-\infty}^{+\infty}\exp 2\pi iH_p X_n\,C\exp\left(-\frac{fa'^2\,{}_{p}X_n^2}{2kT}\right)d({}_{p}X_n)\right\} $$
$$ =\sum_{p}(A_p+iB_p)\sum_{p'}(A_{p'}-iB_{p'})\exp\left(-\frac{16\pi^2\sin^2\theta}{\lambda^2}\frac{kT}{f}\right) $$
$$ \times\sum_{n_1=0}^{M_1-1}\sum_{n_2=0}^{M_2-1}\sum_{n_3=0}^{M_3-1}\sum_{n_1'=0}^{M_1-1}\sum_{n_2'=0}^{M_2-1}\sum_{n_3'=0}^{M_3-1}\exp\{2\pi i\Sigma h(n_1-n_1')\}. \quad \ldots\ldots(68) $$

The summation of (68) is effected by summing all the terms including those for which n_1, n_2, n_3 and p are identical with n_1', n_2', n_3', p', then summing the latter group separately and subtracting this sum from the first. We thus obtain

$$I_2 = \sum_{n_1=0}^{M_1-1} \sum_{n_2=0}^{M_2-1} \sum_{n_3=0}^{M_3-1} \sum_{n_1'=0}^{M_1-1} \sum_{n_2'=0}^{M_2-1} \sum_{n_3'=0}^{M_3-1} \exp\{2\pi i \Sigma h (n_1 - n_1')\} \sum_p (A_p + iB_p) \sum_{p'} (A_{p'} - iB_{p'})$$

$$\times \exp\left(-\frac{16\pi^2 \sin^2\theta}{\lambda^2} \frac{kT}{f}\right) - \sum_{n_1} \sum_{n_2} \sum_{n_3} \sum_p (A_p + iB_p)(A_p - iB_p) \exp\left(-\frac{16\pi^2 \sin^2\theta}{\lambda^2} \frac{kT}{f}\right)$$

$$= (A^2 + B^2) \frac{\sin^2 M_1 h\pi}{\sin^2 h\pi} \frac{\sin^2 M_2 k\pi}{\sin^2 k\pi} \frac{\sin^2 M_3 l\pi}{\sin^2 l\pi}$$

$$\times \exp\left(-\frac{16\pi^2 \sin^2\theta}{\lambda^2} \frac{kT}{f}\right) - N \sum_p (A_p^2 + B_p^2) \exp\left(-\frac{16\pi^2 \sin^2\theta}{\lambda^2} \frac{kT}{f}\right). \qquad \text{......(69)}$$

The total intensity I of scattering from the crystal in the direction h, k, l is therefore given by

$$I = I_1 + I_2$$

$$= (A^2 + B^2) \frac{\sin^2 M_1 h\pi}{\sin^2 h\pi} \frac{\sin^2 M_2 k\pi}{\sin^2 k\pi} \frac{\sin^2 M_3 l\pi}{\sin^2 l\pi} \exp\left(-\frac{16\pi^2 \sin^2\theta}{\lambda^2} \frac{kT}{f}\right)$$

$$+ N \cdot \sum_p (A_p^2 + B_p^2) \left\{1 - \exp\left(-\frac{16\pi^2 \sin^2\theta}{\lambda^2} \frac{kT}{f}\right)\right\}. \qquad \text{......(70)}$$

The intensity-distribution given by equation (70) is closely similar to that represented by equation (57), which holds for the case in which there is one molecule per unit cell, the only difference being that instead of the normal crystal-structure factor $(A^2 + B^2)$ in the second term of equation (57) we now have the sum of the separate molecular structure factors $\sum_p (A_p^2 + B_p^2)$.

It will be seen that the intensity-distribution given by equation (57) or equation (70) is the sum of two parts, the first part being the usual Laue interference function of the crystal space lattice multiplied by the normal crystal structure $(A^2 + B^2)$, multiplied by a temperature factor $\exp \{[-(16\pi^2 \sin^2\theta)/\lambda^2] (kT/f)\}$ which weakens the spots without broadening them and which may be regarded as part of the atom-form factor. The first term is thus represented in the diffraction pattern by the usual strong and more or less sharp Laue spots. The second parts of equations (57) and (70), however, represent scattering which is characteristic of the atomic arrangement in the molecule and of the orientation of the molecules with respect to the beam. The factor $\sum_p (A_p^2 + B_p^2)$ in equation (70) is the sum of the independent scattering powers of the molecules associated with the unit cell, relative to that of a single electron for the direction considered and is independent of the grouping of the molecules into a lattice. The second term of equations (57) and (70) is also proportional to the number N of molecules in the crystal, instead of being proportional to N^2 like the maxima of the first part of equations (57) and (70). Thus, since with increasing crystal-thickness the ratio N/N^2 decreases in value, the diffuse-zone pattern should become weaker in comparison with the true Bragg spots. It must be remembered, however, that most of the spots in the electron-diffraction single-crystal transmission pattern are not true Bragg spots.

The thermal factor in the expression for the intensities of the diffracted spots falls in an exponential manner from the value 1 at the central spot, whereas the corresponding factor in the expression for the background scattering rises asymptotically to a maximum value of 1. Thus, if curve 1 in figure 22 represents the atom-form factor for the atoms when thermal agitation is absent, curve 2 will be the corresponding curve when the thermal factor is appreciable, i.e. the effective atom-form factor in the expression representing the intensity of the spot pattern, while curve 3 is the effective atom-form-factor curve for the intensity of the diffuse area pattern.

Application of the theory to the case of anthracene. In deriving the equations (57) and (70) certain simplifying assumptions were made. That these are justified in the case under consideration, namely anthracene, can be shown as follows.

In the first place it was assumed that the molecule could be regarded as a rigid unit vibrating as a whole. If each carbon atom were to vibrate independently of its neighbours, it could be treated as an independent oscillating system which would give rise to diffuse scattering, the intensity expression for which will contain as thermal factor

$$1-\exp\{[-(16\pi^2\sin^2\theta)/\lambda^2]\,(\boldsymbol{k}T/f)\}.$$

f has been calculated from spectroscopic data(7), and has the value $7{\cdot}6\times10^5$ dyne/cm. for the carbon-carbon stretching force in the benzene ring. Since $\lambda \doteqdot 0{\cdot}05$ A., $\sin\theta \doteqdot 0{\cdot}01$ and $T \doteqdot 300°$ K., the above thermal factor has a value of the order of $1-\exp\{-(3{\cdot}4\times10^{-3})\}$, which is negligible. On the other hand, if we assume a wave-number 20 cm.$^{-1}$* for the oscillation of the molecule about its mean position, the force constant f, calculated for a simple harmonic oscillator, has the value 4×10^3 dyne/cm. Then, with the above values of λ, $\sin\theta$ and T, the thermal factor becomes $1-e^{-0{\cdot}646}$ or 0·48, and thus rises rapidly to an appreciable value near the central spot. Another way of regarding this effect is to consider the mean energy of oscillation in any direction of a carbon atom to be $\frac{1}{2}\boldsymbol{k}T$. Owing to the high wave number 992 cm.$^{-1}$, however, the amplitude of vibration must be minute.

Furthermore, the physical properties of anthracene (softness, low melting point and volatility) are such as to show that the cohesion between adjacent molecules must be weak. Hence we are justified in regarding the molecules as vibrating independently.

Quantum considerations do not seriously affect the above conclusions. The Maxwell probability distribution, $Ce^{-W/\boldsymbol{k}T}$, which is continuous, should then be replaced by the discontinuous factor $Ce^{-n\boldsymbol{h}\nu/\boldsymbol{k}T}$. For the above values of ν and T for molecular oscillation, however, $\boldsymbol{h}\nu/\boldsymbol{k}T \doteqdot 0{\cdot}1$ so that the permitted energy levels are so close together that they may, to a first approximation, be treated as continuous. For the separate carbon atoms $\boldsymbol{h}\nu/\boldsymbol{k}T$ is large (ν is high) and almost all the carbon atoms will be in the lowest possible energy levels.

---

* This approximate value was suggested to us by Dr M. Blackman.

It was also assumed that the force f is the same in all directions; but it is unlikely that this is the case with anthracene. However, as we have already pointed out, the thermal factor, $1-\exp\{[-(16\pi^2\sin^2\theta)/\lambda^2]\,(kT/f)\}$, rises rapidly towards the value 1 with increasing θ. Thus, provided θ be not too small, the value of the second term will be inappreciable and, even if f should depend on the direction considered, the effect on the diffuse-area scattering at a sufficient distance from the central spot will be negligible. In the case of the patterns reproduced above, this minimum distance is of the order of 1 cm.

§7. COMPARISON OF THE THEORETICAL AND EXPERIMENTAL RESULTS

It remains to draw attention to further points of agreement between the theory outlined in § 6 and the experimental results.

All the diffraction patterns, and especially figures 10, 14 and 17, in which a diffuse area maximum from the one group of molecules is superimposed on that from the other group show that the intensities are simply added and never weakened by such superposition; hence the waves diffracted from the different molecules into the diffuse area pattern have no specific phase relationship. Also in the patterns, such as figures 10, 17, 20 and 21, areas of diffuse scattering are often to be seen in regions where the Laue conditions forbid the occurrence of spots. Thus the diffracted waves arising from each molecule are independent in the same way as are the waves emitted from different light-sources, only the orientation and atomic structure of each molecule being of importance. The theory, in which the Maxwell-Boltzmann law was assumed, leads indeed, as we have pointed out in § 6, to this result. In fact, it is not even necessary to assume that this law governs the thermal motions of the molecules for, from equation (64), we have

$$\begin{aligned}I&=\Sigma\ldots\Sigma\exp(i\omega t)\exp(2\pi i\,\Sigma hn_1)\exp(2\pi i\,\Sigma h_p x_{n_1n_2n_3})(A_p+iB_p)\\&\qquad\times\exp(-i\omega t)\exp(-2\pi i\,\Sigma hn_1{}')\exp(-2\pi i\,\Sigma h_{p'}x_{n_1'n_2'n_3'})(A_{p'}-iB_{p'})\\&=\Sigma\ldots\Sigma\exp\{2\pi i\,\Sigma h(n_1-n_1{}')\}(A_p+iB_p)(A_{p'}-iB_{p'})\exp(2\pi i\,\Sigma h_p x_{n_1n_2n_3})\\&\qquad\times\exp(-2\pi i\,\Sigma h_p x_{n_1'n_2'n_3'}).\end{aligned}$$

Let $\quad 2\pi\Sigma h_p x_{n_1n_2n_3}=\phi \quad$ and $\quad 2\pi\Sigma h_{p'}x_{n_1'n_2'n_3'}=\phi'.$

We have then

$$\begin{aligned}I&=\Sigma\ldots\Sigma\exp\{2\pi i\Sigma h(n_1-n_1{}')\}(A_p+iB_p)(A_{p'}-iB_{p'})(\cos\phi+i\sin\phi)(\cos\phi'\quad i\sin\phi')\\&=\Sigma\ldots\Sigma\exp\{2\pi i\,\Sigma h(n_1-n_1{}')\}(A_p+iB_p)(A_{p'}-iB_{p'})\\&\qquad\times[\cos\phi\cos\phi'+\sin\phi\sin\phi'+i(\sin\phi\cos\phi'-\cos\phi\sin\phi')].\end{aligned}$$

In general ϕ and ϕ' are independent for different molecules and are equally probably negative or positive. Hence the mean values of $\sin\phi\sin\phi'$, $\sin\phi\cos\phi'$, $\cos\phi\sin\phi'$ are zero, except for the same molecule when $\sin^2\phi$ is always positive. Thus the mean value of the first term in this expression is the ordinary spot-pattern expression, modified by the temperature factor written in the form $\overline{\cos\phi\cos\phi'}$. The second term comprises only those cross products which involve the same molecule twice.

Thus

$$I=\Sigma\ldots\Sigma\exp\{2\pi i\Sigma h(n_1-n_1')\}\{(\Sigma A_p)^2+(\Sigma B_p)^2\}\overline{\cos\phi\cos\phi'}+\Sigma(A_p^2+B_p^2)\overline{\sin^2\phi}$$

$$=(A^2+B^2)\frac{\sin^2 M_1h\pi}{\sin^2 h\pi}\frac{\sin^2 M_2k\pi}{\sin^2 k\pi}\frac{\sin^2 M_3l\pi}{\sin^2 l\pi}(\overline{\cos\phi})^2+N\sum_p(A_p^2+B_p^2)\overline{\sin^2\phi}. \quad\ldots\ldots(71)$$

Hence each molecule adds its own intensity to the diffuse bands, the average of all terms relating to cross products of different molecules vanishing. This is precisely what happens when light is emitted by several independent sources.

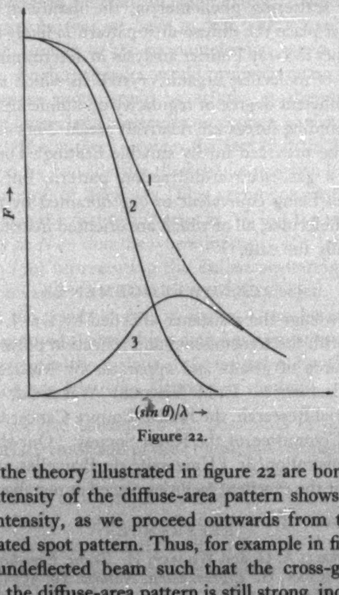

Figure 22.

Those results of the theory illustrated in figure 22 are borne out in practice by the facts that the intensity of the diffuse-area pattern shows a very much slower radial decrease in intensity, as we proceed outwards from the undeflected spot, than does the associated spot pattern. Thus, for example in figures 10 and 17, at a distance from the undeflected beam such that the cross-grating spots are too weak to be recorded, the diffuse-area pattern is still strong, indeed even remarkably so.

According to the theory, the ratio of the intensity of a diffuse pattern to that of a Bragg spot of the same (sin θ)/λ should decrease with increasing thickness of crystal; and comparison of figure 20 with figure 14*a* shows that this is the case. Monochromatic X-ray patterns from molecular single crystals such as anthracene could not be expected to give rise to a visible pattern of diffuse areas, since h, k and l must have integral values, owing to the relatively large size of the crystal required; thus the theory states that at a given (sin θ)/λ the ratio of the Bragg spot and diffuse-area intensities is proportional to $M_1^2M_2^2M_3^2/M_1M_2M_3$ and will therefore be very large. A mosaic crystal in which the individual crystals are very small might, however, give rise to the diffuse-area effect with X rays. On the other hand, the diminution of spot intensities due to thermal agitation is, as we know from X-ray work, quite notable.

In view of this agreement between the theory and experimental results, we may now conclude that the diffuse-area pattern is due to scattering by molecules which, owing to thermal agitation, scatter independently, although their mean positions are those of the crystal lattice.

§8. CONCLUSION

In conclusion we would specially draw attention to the significance of the electronic molecular scattering phenomenon, the nature of which we have now discussed. In the first place the diffuse-area pattern is likely to prove of assistance as an important adjunct to X-ray Fourier analysis in determining both the molecular and crystal structure of molecular organic crystals in which the molecules exhibit, as in anthracene, a sufficient degree of regularity of atomic arrangement, and where the inter-molecular binding forces are relatively weak. This second factor could no doubt in most cases be provided for by suitable heating. The diffuse-area pattern is, indeed, virtually a gas electron-diffraction pattern, but has the inestimable advantage over this of being equivalent to one obtained by the diffraction of the beam by a stream of molecules, all of which are oriented instead of being completely at random, as is usually the case.

§9. ACKNOWLEDGEMENTS

We wish to acknowledge the assistance afforded by Drs J. B. Warren and J. T. Tyson in connexion with the transmission and reflection polycrystalline specimens, and the generous awards of grants and apparatus by Messrs Ferranti, Ltd. and Imperial Chemical Industries, Ltd., Viscount Wakefield, the Department of Scientific and Industrial Research, the British Empire Cancer Campaign and by the Government Grant Committee of the Royal Society. Our thanks are also due to the Conseils d'Administration de l'Université de Bruxelles and of the Fondation Francqui, Brussels, for the excellent facilities placed at our disposal during 1937–8.

REFERENCES

(1) Finch, G. I., Quarrell, A. G. and Wilman, H. *Trans. Faraday Soc.* **31**, 1050 (1935).
(2) Finch, G. I. and Wilman, H. *Ergebn. exakt. Naturw.* **16**, 353 (1937).
(3) Thomson, G. P. and Murison, C. A. *Nature, Lond.*, **131**, 237 (1933).
Murison, C. A. *Phil. Mag.* **17**, 201 (1934).
(4) Bragg, W. H. *Proc. Phys. Soc.* **34**, 33 (1921); **35**, 167 (1923).
Robertson, J. M. *Proc. Roy. Soc.* A, **125**, 542 (1929).
Banerjee, K. *Nature, Lond.*, **125**, 456 (1930); *Indian J. Phys.* **4**, 557 (1930).
Robertson, J. M. *Proc. Roy. Soc.* A, **140**, 79 (1933).
(5) Finch, G. I. and Wilman, H. *Trans. Faraday Soc.* **33**, 1435 (1937).
(6) Debye, P. *Ber. dtsch. Phys. Ges.* **15**, 678, 738, 857 (1913); *Ann. Phys., Lpz.*, **43**, 49 (1914).
Waller, I. *Z. Phys.* **17**, 398 (1923); **51**, 213 (1928); *Ann. Phys., Lpz.*, **79**, 261 (1926); **83**, 154 (1927).
Waller, I. and James, R. W. *Proc. Roy. Soc.* A, **117**, 214 (1927).
See also Blake, F. C. *Rev. Mod. Phys.* **5**, 169 (1933) and Compton, A. H. and Allison, S. K. *X-Rays in Theory and Experiment.* (Macmillan, London, 1933.)
(7) Kellner, L. *Rep. Progr. Phys.* **4**, 323 (1937).

DISCUSSION

Professor G. P. Thomson. The phenomena described in this paper are an important addition to the subject of electron diffraction. There can, I think, be no doubt that the authors are right in ascribing the diffuse areas to electronic waves scattered by molecules which, though oriented as in the crystal lattice, are for some reason displaced relatively to one another so that the scattered waves are incoherent. The authors attribute this displacement to heat motion. While such an explanation is possible, and must indeed be valid to some extent, I should like to suggest an alternative view. It may be that we have to deal with a layer of molecules on the surface of the crystal, similar to the monomolecular layers on water studied by Langmuir and others. Such molecules would probably retain their relative orientations, but their distances apart would be erratic, as they were found to be by Murison in the case of long-chain molecules on copper, so that the waves from them would be incoherent. The authors explain the fact that thick films give relatively little diffuse diffraction by considering the relative magnitudes of the two terms in equation (70) as a function of thickness. This argument seems to be invalid. It is true that *at the maximum* the first term varies as N^2, but the width of the diffraction maximum is inversely as N so that the whole intensity of a spot varies as N, as does the term in equation (70) representing the diffuse scattering. If the latter is due to a surface effect, the variation with thickness is explained.

I think also that the result shown in figure 9 can be explained in the same general way, if it is supposed that rubbing detaches minute crystal fragments which, while they remain resting on the surface of the crystal and with the plane of cleavage parallel to that surface, are otherwise disposed at random.

Authors' reply. We had considered the possibility of the diffuse-area pattern being due to some surface condition of the crystal, but rejected it for several reasons. It cannot be supposed that thermal vibrations are absent, and this by itself suffices to negative the suggestion of a surface layer in which the molecules are stationary but imperfectly positioned. Again, the fact that anthracene sublimes *in vacuo* at room temperature leads independently to the view that the molecules, at least in the surface layers, are not stationary. Furthermore, it seems improbable that molecules more or less isolated from contact with their neighbours in the surface layer could remain standing in exactly the same orientations as the molecules in the lattice, whose orientations are governed by the packing together of molecules in the closest possible way. Thus, in addition to parallel displacements from the lattice positions, such more or less isolated molecules would certainly be expected to take up orientations differing considerably from those of the molecules which form part of the lattice; and we have pointed out that in the patterns there is no noticeable broadening of the outer diffuse areas, such as would correspond to appreciable deviations, either static or oscillatory, from the latter orientations. This fact also suffices to show that the diffuse-area pattern cannot be due to surface effects alone, since the molecules at the surface must have considerable angular as well as translational motion, unless it be assumed that the surface is always bounded by a complete and perfect layer of molecules even during sublimation, which is highly improbable.

With respect to the variation of intensity of the diffuse-area pattern with crystal thickness, $N : N^2$ refers to the intensity at a point in the diffuse-area pattern relative to that of a Bragg spot at the same value of $(\sin \theta)/\lambda$. The cross-grating spots, which occur at the intersections of the Laue zones due to two atom rows normal to the beam, are sharp, and their positions do not vary appreciably if the crystal-orientation is altered through a fairly wide range on either side of the setting considered. On the other hand, the Laue zones due to atom rows parallel, or nearly so, to the beam are always relatively much broader, and their positions are sensitive to changes in the crystal-setting; thus, when the setting is such that a cross-grating spot becomes a Bragg spot, the whole of the spot may be considered to lie at the maximum of one of these zones, so that the intensity of the Bragg spot is effectively independent of the breadth of these zones, but depends only on the maximum value of the corresponding intensity factor, and is thus proportional to N^2. We pointed out in the text, however, that most spots in a pattern are not true Bragg spots, i.e., have not the full maximum intensity, so that the intensity of the diffuse-area pattern relative to the mean spot-intensity will decrease less quickly than $N : N^2$ but more rapidly than $N : N$, with increasing crystal-thickness.

OBSERVATION AND THEORY IN COSMOLOGY

By G. C. McVITTIE, Ph.D., F.R.A.S.

Read at a discussion on the expanding universe held jointly with the Royal Astronomical Society, 27 January 1939

§ 1. HISTORICAL INTRODUCTION

The attempts hitherto made to solve the problem of the size and structure of the universe on the basis of general relativity have involved three stages. There is firstly the purely observational work. This consists, on one hand, of the measurement of the red-shift δ, equal to $d\lambda/\lambda$, in the wave-length λ of light emitted by a number of nebulae of known apparent photographic magnitude* m. On the other hand, counts of the numbers N_m of nebulae per square degree of the sky have been made down to a series of limiting magnitudes m lying chiefly between 18 and 21·03. Observations of red-shift are practically restricted to bright nebulae for which $m \leqslant 17$, and in this region the values of δ are so small that the red-shift has a negligible effect on the apparent magnitudes of the nebulae. The nebular counts are made for regions for which no observed values of δ exist. But assuming that the red-shifts continue to obey even roughly the law found when $m \leqslant 17$, it follows that when $18 \leqslant m \leqslant 21{\cdot}03$, the shifting of the spectrum must have a considerable effect on the apparent magnitudes.

The second step consists in summarizing the observations into so-called empirical equations. Hubble's solution$^{(1,2)}$ of this problem produces the three equations

$$\log_{10} \delta \;= 0{\cdot}2\,(m - \Delta') - 4{\cdot}707 \pm 0{\cdot}016, \qquad \ldots\ldots(1)$$

$$\log_{10} N_m = 0{\cdot}6\,(m - \Delta) - 9{\cdot}052 \pm 0{\cdot}013, \qquad \ldots\ldots(2)$$

$$\log_{10} \Delta \;= 0{\cdot}2\,(m - \Delta) - 4{\cdot}239 \pm 0{\cdot}024, \qquad \ldots\ldots(3)$$

where Δ, Δ' are the corrections applied to the apparent magnitudes in order to allow for the dimming effect of the red-shift. The form of these equations is arrived at by means of the following argument. It is known that, if the nebulae were moving slowly in flat Euclidean space, the theoretical relation between δ and m would be

$$\log_{10} \delta = 0{\cdot}2m + \textit{constant}.$$

Moreover, if the nebulae were uniformly distributed and at rest in flat space, the relation between N_m and m would be

$$\log_{10} N_m = 0{\cdot}6m + \textit{constant}.$$

Since the observed nebulae with apparent magnitudes down to about 18 do in fact follow rules of this kind, it is legitimate to suppose that the form of the relations would be retained for the greater depths of space provided m were replaced by some suitably corrected magnitude. In his attempt to carry out this extension, Hubble makes the four following assumptions:

---

* For the explanation of this and other astronomical terms see *Reports on Progress in Physics*, pp. 24–9 (1934).

(*a*) The value of the correction Δ' is 3δ. With the aid of the observed values of δ and m it is then possible to calculate numerical coefficients, and equation (1) is obtained(1).

(*b*) The equation (1) is valid down to $m=21{\cdot}03$.

(*c*) The correction Δ in the relation between N_m and m is proportional to the distance of the nebula. But Hubble does not enter into the thorny problem of distance.* He writes down(2) instead

$$\log_{10}\Delta=0{\cdot}2\,(m-\Delta)+\textit{constant}, \qquad \ldots\ldots(4)$$

as the definition of Δ in terms of m. The observed values of N_m and m are then sufficient to give all the numerical coefficients, and the equations (2) and (3) emerge(2).

(*d*) The corrections Δ' and Δ are equal. Subtracting equations (1) and (3), we then have

$$\Delta'=\Delta=2{\cdot}94\delta, \qquad \ldots\ldots(5)$$

which, in Hubble's work(2), is regarded as the fundamental observational equation.

The third and last step consists in comparing some or all of the equations (1) to (5) with the corresponding predicted equations of general relativity. Hitherto controversy has raged over this step, for it emerges that a further observational datum is needed before this union of empirical and theoretical equations will give the details of the structure of the universe. Hubble(2) finds the additional datum in the effective temperature of the nebular radiation, and arrives at an extremely small universe of finite size. The present author's(3) arbitrary datum is the average mass of a nebula, with which he arrives at a hyperbolic universe of infinite extent.

In the present paper we try to push the discussion back from the third to the second step. The question arises: Are the assumptions (*a*) to (*d*), on which equations (1) to (5) rest, valid in the expanding universes of general relativity in terms of which the observations are ultimately interpreted? Our answer is mainly in the negative, and we shall suggest an alternative method of interpretation which omits most of the second step and passes directly from the first to the third.

We deal first with the validity of the assumptions, the universe being supposed to have the metric

$$ds^2=dt^2-e^{g(t)}\left\{\frac{dr^2}{1-kr^2/R_0^2}+r^2d\theta^2+r^2\sin^2\theta\,d\phi^2\right\}. \qquad \ldots\ldots(6)$$

Here $k=-1, 0$ or 1 according as space is hyperbolic, flat or spherical. We suppose that an observer situated at $r=0$, $\theta=0$, $\phi=0$ is making the observations at time t_0. The function $g(t)$ is arbitrary, but we can always choose it so that $g(t_0)=0$. R_0 is then the value of the radius of curvature of space at $t=t_0$, provided, of course, that $k=1$ or -1. The coordinates r, t are supposed to be measured in parsecs.† In such a universe it can be shown⁽⁴⁾ that

---

* The meaning of the term "distance" in general relativity is fully discussed by G. Temple(16).

† 1 parsec $=3{\cdot}08\times10^{18}$ cm.

$$\log_{10}\delta = 0{\cdot}2\left\{m - \left[K + \frac{5}{E}(1 + g_0''/g_0'^2)\,\delta\right]\right\} + 1 - 0{\cdot}2M + \log_{10}\tfrac{1}{2}g_0', \quad \ldots\ldots(7)$$

where $E = \log_e 10 = 2{\cdot}303$. In this equation, a dash denotes differentiation with respect to t and the suffix zero indicates that the functions are evaluated at time t_0. M is the absolute photographic magnitude of an average nebula and K is the part of the red-shift correction which must be applied to m in respect of the shifting of the nebular spectrum over the sensitive region of the photographic plate. It is believed that K is proportional to δ, and K obviously depends on the distribution of energy in the spectrum, in other words, on the effective temperature of the nebular radiation. Now in equation (7) neither K nor $g_0''/g_0'^2$ is known a priori so that theory has no light to shed on assumptions (*a*) and (*b*). The latter however has been almost universally criticized⁽⁵⁾. One objection is that the correction $\Delta' = 3\delta$ cannot be considered as verified, since in the observable region of δ this correction is negligible. But it is by no means negligible when δ is being calculated for the extrapolated region between $m = 17$ and $m = 21{\cdot}03$.

With regard to (*c*), we note that the relation between N_m and m in the universe denoted by equation (6) is approximately⁽⁴⁾

$$\log_{10} N = 0{\cdot}6\left\{m - \left(K + \frac{5}{E}\,\delta\right)\right\} + \log_{10}\left(\frac{4\pi\alpha}{3R_0^3}\right) - 0{\cdot}6M + 3, \quad \ldots\ldots(8)$$

where, however, there appears N, the number of nebulae over the whole sky. This is related to N_m by

$$N = 4{\cdot}1 \times 10^4 N_m$$

and is the quantity we shall use henceforward. α is a number proportional to the number of material particles per unit volume in the universe denoted by equation (6). Now the Δ of equation (2) must be the $(K + 5\delta/E)$ of equation (8) and, if Δ is proportional to δ, then equation (7) would give

$$\log_{10}\Delta = 0{\cdot}2\left\{m - \left(\Delta + \frac{5}{E}\frac{g_0''}{g_0'^2}\right)\delta\right\} + \textit{constant}. \quad \ldots\ldots(9)$$

This is, in general, not identical with equation (4) which is Hubble's interpretation of assumption (*c*). Indeed it is clear that assumptions (*c*) and (*d*) are but two aspects of the same hypothesis, viz. that $g_0''/g_0'^2$ is negligible compared with unity. There is no justification for such an assumption, and acceptance of it would rule out a priori many interesting possibilities. Notably, the case of motion in approximately flat space with uniform velocity (in the sense of Milne) would be dismissed without investigation, since it implies⁽⁶⁾ that $g(t) = 2\log_e t$ and $g_0''/g_0'^2 = -\tfrac{1}{2}$.

The arbitrariness of the four assumptions from the theoretical point of view suggests that the conclusions as to the structure of the universe hitherto arrived at may be as much conditioned by these hypotheses as by the observations themselves. We now proceed to an alternative interpretation of the latter.

§ 2. THE RELATION BETWEEN N AND m

In principle, observation gives us two functional relations, one between δ and m the other between N and m. With regard to the former, we have Hubble's result (1) in which, however, the value of Δ' is speculative. It has been suggested by ten Bruggencate⁽⁷⁾ that the constant term, $-4{\cdot}707 \pm 0{\cdot}016$, should be replaced by $-4{\cdot}907$. Hubble and Humason⁽⁸⁾ in 1934 had obtained $-4{\cdot}967 \pm 0{\cdot}012$ from very much the same observational material. When comparing the theoretical equation (7) with the observational relation, we shall include all probable values of the constant term if we put

$$1 - 0{\cdot}2M + \log_{10}(g_0'/2) = -X, \qquad \text{......(10)}$$

where X is a number satisfying the condition

$$4{\cdot}707 \leqslant X \leqslant 4{\cdot}967. \qquad \text{......(11)}$$

This is the only use we shall make of the relation between δ and m. We have thus rejected assumptions (*a*) and (*b*) and replaced them by the consideration that, whatever form the observational relation between δ and m may take if and when red-shifts are measured down to $m = 21{\cdot}03$, this form must reduce to equation (1), within the limits given by equation (11), when $m \leqslant 17$.

The rejection of assumptions (*c*) and (*d*) makes the equations (2) and (3) unsuitable as empirical relations between N and m. Moreover equation (8) is now also useless as the corresponding theoretical equation, since it involves δ. We require N as a function of m alone. Now it is known⁽⁹⁾ that, in the universe denoted by equation (6), the number of nebulae within radius r is

$$N = \frac{4\pi\alpha}{3}\left(\frac{r}{R_0}\right)^3 \left\{1 + \frac{3}{10}\frac{kr^2}{R_0^2} + \dots\right\}, \qquad \text{......(12)}$$

on the assumption that powers of r/R_0 higher than the fifth are negligible. Again the theory of luminosity-distance⁽¹⁰⁾ gives us

$$\log_{10}\{r(1+\delta)\} = 0{\cdot}2(m-K) + 1 - 0{\cdot}2M. \qquad \text{......(13)}$$

We define a number a by means of the equation

$$\log_{10}(1 + a\delta) = 0{\cdot}2K \qquad \text{......(14)}$$

in accordance with the hypothesis that K is approximately a linear function of δ. Again we write

$$\log_{10}\mu = 0{\cdot}2(m - M) + 1 \qquad \text{......(15)}$$

and then equation (13) becomes

$$r\{1 + (1+a)\delta + a\delta^2\} = \mu. \qquad \text{......(16)}$$

It is also known⁽⁴⁾ that the relation between r and δ in the universe denoted by equation (6) is

$$\frac{g_0'}{2} r = \delta + \frac{g_0''}{g_0'^2}\delta^2 + \dots. \qquad \text{......(17)}$$

We solve this equation for δ and find

$$\delta = \frac{g_0'}{2} r - \frac{g_0''}{g_0'^2}\left(\frac{g_0'}{2} r\right)^2 \ldots. \qquad \ldots\ldots(18)$$

Hence by equation (16)

$$r\left[1 + (1+a)\left(\frac{g_0'}{2} r\right) - \left\{(1+a)\frac{g_0''}{g_0'^2} - a\right\}\left(\frac{g_0'}{2} r\right)^2\right] = \mu,$$

which gives

$$r = \mu\left[1 - (1+a)\left(\frac{g_0'}{2}\mu\right) + \left\{2(1+a)^2 + (1+a)\frac{g_0''}{g_0'^2} - a\right\}\left(\frac{g_0'}{2}\mu\right)^2\right]. \qquad \ldots\ldots(19)$$

Now write equation (12) in the approximate form

$$\log_e N = \log_e\left(\frac{4\pi\alpha}{3R_0^3}\right) + 3\log_e r + \frac{3}{10}\frac{kr^2}{R_0^2} \qquad \ldots\ldots(20)$$

and then substitute for r from equation (19), neglecting terms involving powers of $(g_0'\mu/2)$ higher than the second. There comes

$$\log_e N = \log_e(4\pi\alpha/3R_0^3) + 3\log_e\mu - 3(1+a)(g_0'\mu/2)$$
$$+3\left[\frac{3}{2}(1+a)^2 + (1+a)\frac{g_0''}{g_0'^2} - a + \frac{1}{10}\frac{k}{R_0^2}\left(\frac{2}{g_0'}\right)^2\right]\left(\frac{g_0'}{2}\mu\right)^2. \qquad \ldots\ldots(21)$$

This is the theoretical relation between N and m, which, however, involves the absolute nebular magnitude M, through μ. We replace M by X, using equations (10) and (15), so that

$$\log_{10}(g_0'\mu/2) = 0{\cdot}2m - X.$$

Hence equation (20) becomes

$$\log_{10} N = \log_{10}\left\{\frac{4\pi\alpha}{3R_0^3}\left(\frac{2}{g_0'}\right)^3\right\} - 3X + 0{\cdot}6m - \frac{3}{E}(1+a)\,10^{0\cdot 2m-X}$$
$$+\frac{3}{E}\left[\frac{3}{2}(1+a)^2 - a + (1+a)\frac{g_0''}{g_0'^2} + \frac{1}{10}\frac{k}{R_0^2}\left(\frac{2}{g_0'}\right)^2\right]10^{2(0\cdot 2m-X)}, \qquad \ldots\ldots(22)$$

which we shall regard as the theoretical relation between N and m. It is correct to the second order of small quantities, these being represented by the terms in $10^{0\cdot 2m-X}$. The relation may be expected to hold when $m \leqslant 21{\cdot}03$, since in this range of m the powers of $10^{0\cdot 2m-X}$ decrease fairly rapidly.

To find the values of the various coefficients in equation (22) from observation we write

$$\left.\begin{aligned} y &= 0{\cdot}6m - \log_{10} N, \\ x &= 10^{0\cdot 2m-X}, \end{aligned}\right\} \qquad \ldots\ldots(23)$$

$$\left.\begin{aligned} a_0 &= 3X - \log_{10}\left\{\frac{4\pi\alpha}{3R_0^3}\left(\frac{2}{g_0'}\right)^3\right\}, \\ a_1 &= 3(1+a)/E, \\ a_2 &= -\frac{3}{E}\left\{\frac{3}{2}(1+a)^2 - a + (1+a)\frac{g_0''}{g_0'^2} + \frac{1}{10}\frac{k}{R_0^2}\left(\frac{2}{g_0'}\right)^2\right\}, \end{aligned}\right\} \qquad \ldots\ldots(24)$$

so that equation (22) becomes

$$y=a_0+a_1x+a_2x^2. \qquad \text{......(25)}$$

We shall see below, in § 4, that a_0, a_1, a_2 can be determined from the nebular counts by a least-squares solution.

§ 3. THE FIELD-EQUATIONS

The equations (10) and (24) show that the information we can hope to secure from observation is not as extensive as recent researches on the structure of the universe might lead us to suppose. An estimate of the absolute nebular magnitude M will give us, through equation (10), the value of the parameter g_0'. A knowledge of a_1 gives us, by one of equations (24), the constant a and hence K. In addition we may learn something of the density of matter in space, since a_0 yields the ratio α/R_0^3, but even here we shall require a preliminary estimate of the mass of an average particle of matter in the universe. The last of equations (24) shows that, since g_0'' is unknown, we cannot determine k and R_0 independently. Hence the amount of the curvature as well as its nature remains undetermined.

To advance further we must again appeal to theory. Einstein's field equations(11), relating the density and pressure of matter in the universe to g_0', g_0'', k and R_0, provide two additional equations which combine with equations (24). We have, if ρ, p denote the density and pressure respectively at the instant t_0,

$$\kappa\rho=\frac{3k}{R_0^2}+3\left(\frac{g_0'}{2}\right)^2-\Lambda, \qquad \text{......(26)}$$

$$\kappa p=-\frac{k}{R_0^2}-g_0''-3\left(\frac{g_0'}{2}\right)^2+\Lambda. \qquad \text{......(27)}$$

Here κ is a constant involving the gravitational constant G, given in equation (33) below, and Λ is the cosmical constant. These equations imply(11) that

$$[d\,(R_0^3e^{\frac{3}{2}g}\rho)]_{t=t_0}+[p\,d\,(R_0^3e^{\frac{3}{2}g})]_{t=t_0}=0. \qquad \text{......(28)}$$

It is usual to assume that $p=0$ in the actual universe, on the ground that p would be a measure of the proper motions of the nebulae, of the pressure of radiation, and so on, and that all these effects are small. This hypothesis leads, by equation (28), to

$$\rho=\alpha M_0/R_0^3, \qquad \text{......(29)}$$

where the constant of integration αM_0 is interpreted as the product of α, the number of nebulae per unit volume, and of M_0, the mass of an average nebula. Thus we identify the material particles of the theoretical universe denoted by equation (6) with the nebulae of the actual universe. When $p=0$, equations (26), (27) and (29) give

$$g_0''=\frac{2k}{R_0^2}-\frac{\kappa\alpha}{R_0^3}M_0. \qquad \text{......(30)}$$

Returning to equation (24) we have

$$\rho=\frac{\alpha M_0}{R_0^3}=\frac{3}{4\pi}\left(\frac{g_0'}{2}\right)^3\frac{10^{3X-a_0-54}}{(3{\cdot}08)^3}M_0\ \text{g./cm.}^3, \qquad \text{......(31)}$$

whilst the last of the three equations (24), together with (30) and (31), becomes

$$\frac{k}{R_0^2}=-\frac{10E}{5Ea_1+3}\left\{a_2+\tfrac{1}{2}Ea_1^2+\frac{3}{E}-a_1-\frac{3\kappa}{16\pi}10^{2X-a_0}\frac{g_0'}{2}M_0\right\}\left(\frac{g_0'}{2}\right)^2. \quad \text{......(32)}$$

This equation will give both k and R_0. We suppose that M_0 is measured in grammes and $g_0'/2$ in reciprocals of the parsec. Hence if G, the gravitational constant, and c the velocity of light, are both measured in c.g.s. units, the appropriate value of κ in equation (32) is

$$\kappa=\frac{8\pi G}{3{\cdot}08\times10^{18}\times c^2}=6{\cdot}039\times10^{-46}\ \text{parsec-g.-sec. unit.} \quad \text{......(33)}$$

The second of equations (24), together with (14), gives approximately

$$K=\left(\frac{10}{6}a_1-\frac{5}{E}\right)\delta, \quad \text{......(34)}$$

which determines the value of the correction factor depending on the effective temperature of the nebular radiation.

§4. NUMERICAL ESTIMATES

We shall now find the constants a_0, a_1, a_2 in equation (25) from the observed values of N and m. We shall compute them for the two limiting values of X in equation (11). In table 1 the first two lines give the results of the nebular counts; the first five columns contain the Mount Wilson material⁽²⁾ and the other two that from the Harvard Observatory⁽¹²⁾. The third line gives the value of y, and the fourth and fifth give the values of x for the two cases $X=4{\cdot}707$ and $X=4{\cdot}967$ respectively.

Table 1

m	21·03	20	19·4	18·47	18·2	12·78
$\log_{10} N$	7·777	7·301	6·955	6·502	6·328	3·233
y	4·841	4·699	4·685	4·580	4·592	4·435
x	0·3155	0·1963	0·1489	0·0971	0·0857	0·0071
	0·1734	0·1079	0·0818	0·0533	0·0471	0·0039

The results obtained by a least-squares solution are as follows:

In the case in which $X=4{\cdot}707$:

$$a_0=5{\cdot}124,\qquad a_1=1{\cdot}816,\qquad a_2=-1{\cdot}718. \quad \text{......(35)}$$

Using equation (34) we then have

$$K=0{\cdot}86\delta, \quad \text{......(36)}$$

whilst equations (32), (33) yield

$$k/R_0^2=-0{\cdot}963\,\{1{\cdot}564-3{\cdot}579\times10^{-38}\,(\tfrac{1}{2}g_0'M_0)\}\,(\tfrac{1}{2}g_0')^2. \quad \text{......(37)}$$

To find $\frac{1}{2}g_0'$ we use equation (10) and adopt for M the value $-15{\cdot}15$ associated by Hubble⁽¹³⁾ with the form (1) of the relation between δ and m. We have

$$\tfrac{1}{2}g_0'=1{\cdot}83\times10^{-9}\ \text{parsec}^{-1}. \quad \text{......(38)}$$

We still require a value for M_0. The estimates of the masses⁽¹⁴⁾ of the visible nebulae range from 4×10^{42} g. to 4×10^{44} g., but it is speculated that there is probably a good deal of dark invisible matter scattered throughout the universe. Let us therefore take the upper value of the mass of a visible nebula for our average and put

$$M_0 = 4 \times 10^{44} \text{ g.} \qquad \ldots\ldots(39)$$

Introducing equations (39) and (38) into equation (37) we find that

$$k/R_0^2 = -0\cdot963\,\{1\cdot564 - 2\cdot624 \times 10^{-2}\}\,(\tfrac{1}{2}g_0')^2. \qquad \ldots\ldots(40)$$

Hence $k = -1$, so that space is hyperbolic and infinite in extent. This conclusion persists even if we increase the value of M_0 given in equation (39) by a factor of about 50. This is equivalent to supposing that, for every luminous nebula counted, there were nearly 50 invisible nebulae present as well. Equations (40) and (38) give

$$R_0 = 4\cdot515 \times 10^8 \text{ parsecs} \qquad \ldots\ldots(41)$$

and equation (31) yields $\quad \rho = 2 \times 10^{-29}$ g./cm³. $\qquad$ ......(42)

In the case in which $X = 4\cdot967$:

$$a_0 = 4, \quad a_1 = 3\cdot125, \quad a_2 = -5.$$

Equation (34) yields $\quad K = 3\cdot04\delta, \qquad$ ......(43)

whilst equation (32) becomes

$$k/R_0^2 = -0\cdot591\,\{4\cdot420 - 2\cdot870 \times 10^{-36}\,(\tfrac{1}{2}g_0'M_0)\}\,(\tfrac{1}{2}g_0')^2. \qquad \ldots\ldots(44)$$

To find $\frac{1}{2}g_0'$ we use equation (10) with M equal to $-14\cdot2$, a value which Hubble and Humason⁽⁸⁾ associated in 1934 with the constant term $-4\cdot967$ in the relation between δ and m. We find

$$\tfrac{1}{2}g_0' = 1\cdot56 \times 10^{-9} \text{ parsec}^{-1}. \qquad \ldots\ldots(45)$$

Again, assuming equation (39), we have

$$k/R_0^2 = -0\cdot591\,\{4\cdot420 - 1\cdot789\}\,(\tfrac{1}{2}g_0')^2. \qquad \ldots\ldots(46)$$

It would appear that space is again hyperbolic provided, at least, that the invisible nebulae do not exist to any appreciable extent. But the fact that the two numbers in the bracket are now of the same order of magnitude must lead us to treat this conclusion with some reserve. Equations (45), (46) and (31) give

$$R_0 = 5\cdot14 \times 10^8 \text{ parsecs}, \qquad \ldots\ldots(47)$$

$$\rho = 9\cdot87 \times 10^{-28} \text{ g./cm}^3 \qquad \ldots\ldots(48)$$

Equations (30), (31) and (27) with p equal to 0 will give the value of the cosmical constant Λ for each of the two values of X. It turns out that Λ is negative for both. But this conclusion depends on a delicate balance between numbers of the same order of magnitude, as in the case of equation (46) above. We can therefore feel little confidence in the values of Λ so derived.

It seems clear from the foregoing discussion that we can escape from the conclusion that space is hyperbolic only by postulating considerable quantities of unobservable matter in the universe. Indeed, even the results (41), (42) and (47), (48) must be regarded as lower limits for R_0 and upper ones for ρ, since the assumption $M_0 = 4 \times 10^{44}$ g., on which they depend, is probably too high.

It is worthy of note that the cases determined by the two values of X include between them the probable values of K as calculated by Hubble's direct method(15). He assumes that nebular spectra are similar, on the average, to that of the sun and that the solar spectrum can be represented as a black-body spectrum. The results are given in table 2, T_0 being the effective temperature of the black-body radiation. Hubble(2) regards 6000° as the correct temperature(17) and the equation $K = 1{\cdot}83\delta$ as strictly true. If we adopt this view, it would seem that the value 4·707 for the constant X in the relation between δ and m is too small, but that the value 4·967 is rather large.

Table 2

T_0 (° C.)	7500	7000	6500	6000	5500	5000
K/δ	0·83	1·23	1·48	1·83	2·43	3·28

For the sake of comparison we give here the results calculated on the basis of the relations (1) to (5). Hubble(2) finds, assuming that $K = 1{\cdot}83\delta$, that

$$k = 1, \quad R_0 = 1{\cdot}45 \times 10^8 \text{ parsecs}, \quad \rho = 6 \times 10^{-27} \text{ g./cm}^3$$

McVittie(3, 9), assuming that the average mass of a nebula is $4 \times 10^{43 \pm 1}$ g. and that there are no invisible nebulae, obtains

$$k = -1, \quad R_0 = 1{\cdot}5 \times 10^9 \text{ parsecs}, \quad \rho = 8{\cdot}29 \times 10^{-30 \pm 1} \text{ g./cm}^3, \quad K = (1{\cdot}08 \pm 0{\cdot}10)\,\delta.$$

Our analysis of the observations leads to much more cautious conclusions than these. That space is hyperbolic seems nearly certain. The radius of space lies probably between 10^8 and 10^9 parsecs, being nearer to the latter if the universe contains many dark nebulae in addition to the visible ones. The average density is certainly not greater than 10^{-27} g./cm³ and is more probably of the order of 10^{-29} g./cm³ The effective temperature of the nebular radiation consonant with these results lies between 5000° and 7500°. Beyond such tentative conclusions it seems impossible to advance without introducing arbitrary and unjustified hypotheses.

REFERENCES

(1) Hubble, E. *Astrophys. J.* **84**, 270 (1936).
(2) Hubble, E. *Astrophys. J.* **84**, 517 (1936).
(3) McVittie, G. C. *Z. Astrophys.* **14**, 274 (1937).
(4) McVittie, G. C. *Observatory*, **61**, 209 (1938).
(5) See e.g. *Nature, Lond.*, **140**, 1105 (25 Dec. 1937); and Fricke, W. *Z. Astrophys.* **16**, 11, § 1 (1938).
(6) Kermack, W. O. and McCrea, W. H. *Mon. Not. R. Astr. Soc.* **93**, 519 (1933).
(7) Bruggencate, P. ten. *Naturwiss.* **35**, 561 (1937).
(8) Hubble, E. and Humason, M. L. *Astrophys. J.* **74**, 43 (1931) and *Proc. Nat. Acad. Sci.* **20**, 264 (1934).
(9) McVittie, G. C. *Mon. Not. R. Astr. Soc.* **98**, 384, § 3 (ii) (1938).

(10) Hubble, E. and Tolman, R. C. *Astrophys. J.* **82**, 303 (1935).
McVittie, G. C. *Z. Astrophys.* **14**, 312 (1937).
(11) *Reports on Progress in Physics*, 1934, pp. 24–9.
McVittie, G. C. *Cosmological Theory*, eqn. 4.6 (Methuen, 1937).
(12) Shapley, H. and Ames, A. *Ann. Harv. Coll. Obs.* **88**, No. 2 (1932).
Shapley, H. *Proc. Nat. Acad. Sci.* **24**, 148 (1938).
(13) Hubble, E. *Proc. Nat. Acad. Sci.* **22**, 621, Note 8 (1936).
(14) Hubble, E. *The Realm of the Nebulae*, p. 29 (Oxford Press, 1936).
(15) Hubble, E. *Astrophys. J.* **84**, 538, Tab. VI (1936).
(16) Temple, G. *Proc. Roy. Soc.* Ser. A, **168**, 122 (1938).
(17) Greenstein, G. L. {*Astrophys. J.* **88**, 605 (1938)} gives 5250°.

MUTUAL AND SELF INDUCTORS COMPENSATED FOR CHANGE OF FREQUENCY

By ALBERT CAMPBELL, M.A.

Received 26 *October* 1938. *Read and demonstrated, in the absence of the author, by Dr L. Hartshorn* 10 *February* 1939

ABSTRACT. The effects of self and mutual capacitance on the electrical constants of mutual and self inductors can be compensated by various devices. For mutual inductors the usual system is a closed tertiary circuit coupled to both primary and secondary coils; the complete case of this is discussed mathematically and it is also shown that a similar arrangement (of closed secondary circuit) is effective for self inductors. A simpler system for these consists of a non-inductive shunt across the terminals, but the closed secondary is usually preferable. Several experimental examples are given.

---

§1. INTRODUCTION

The electrical constants of mutual and self inductors usually are to some extent dependent on the frequency of the a.-c. circuit in which they are used. With mutual inductors, mutual and self capacitances of the two circuits or eddy currents (due to the skin effect or the proximity of other closed circuits or both) cause impurity and variation of M with frequency; while similar causes give change of effective L and R in self inductors. The variations are often proportional to the square of the frequency. They can be much reduced or even entirely nullified by the addition of compensating devices such as those which I proceed to discuss. When the effects are relatively small they can be considered as merely superposed; thus to correct $L(1-xw^2)$, the compensator must introduce a term $+Lxw^2$.

§2. MUTUAL INDUCTORS

It is well known that a mutual inductor can be compensated by the addition of a tertiary closed circuit coupled to both the primary and the secondary circuits. The formulas have hitherto been deduced for the simple case of an open-circuit secondary⁽¹⁾. The more complete case is shown in figure 1.

Let the resistances and self inductances of the secondary and the tertiary circuits be r, l and ρ, λ respectively, while i_1, i_2 and i_3 are the instantaneous values of the currents as in the figure, and $\omega = 2\pi n$, where n is the frequency. Also let M, m and μ be the three mutual inductances as shown. Without the tertiary coil we should have

$$(r+lj\omega)\,i_2 = Mj\omega i, \qquad \ldots\ldots(1)$$

but with the tertiary circuit closed we have

$$\left[r+\frac{\mu^2\omega^2\rho}{\rho^2+\lambda^2\omega^2}+\left(l-\frac{\mu^2\omega^2\lambda}{\rho^2+\lambda^2\omega^2}\right)j\omega\right] i_2 = \left[-\frac{m\mu\omega^2\rho}{\rho^2+\lambda^2\omega^2}+\left(M+\frac{m\mu\omega^2\lambda}{\rho^2+\lambda^2\omega^2}\right)j\omega\right] i. \qquad \ldots(2)$$

Thus r, l and M are altered to r', l', M', where

$$r' = r + \frac{\mu^2\omega^2\rho}{\rho^2+\lambda^2\omega^2}, \qquad \text{......(3)}$$

$$l' = l - \frac{\mu^2\omega^2\lambda}{\rho^2+\lambda^2\omega^2}, \qquad \text{......(4)}$$

$$M' = M + \frac{m\mu\omega^2\lambda}{\rho^2+\lambda^2\omega^2}, \qquad \text{......(5)}$$

while impurity σ' is introduced, where

$$\sigma' = -\frac{m\mu\omega^2\rho}{\rho^2+\lambda^2\omega^2}. \qquad \text{......(6)}$$

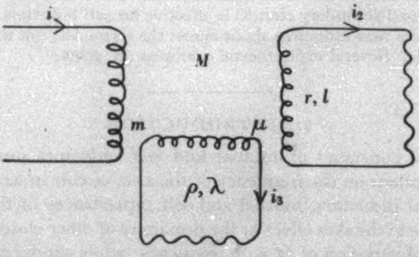

Figure 1.

It will be noticed that r is always increased and l always diminished; also since both m and μ can be either positive or negative, $(M'-M)$ and σ' can have either sign, but when one is positive the other must be negative, unless λ can be made negative.

It is best to choose ρ and λ so that $\rho \gg \lambda\omega$, for then

$$M' \doteq M + \frac{m\mu\omega^2\lambda}{\rho^2}, \qquad \text{......(7)}$$

and

$$\sigma' \doteq -\frac{m\mu\omega^2}{\rho}. \qquad \text{......(8)}$$

Thus if the inductor has impurity and variation with frequency, either but not both of these can be corrected by the tertiary circuit with properly chosen values of ρ, λ, m and μ. Two recent examples of its use may be mentioned. In the new standard M inductometer designed by Astbury and Ford (2) at the National Physical Laboratory, elaborate screening is used, which much increases the impurity, but this is practically annulled by the addition of a tertiary closed circuit. They state clearly the necessary conditions and also mention that it is sometimes helpful to reduce λ by means of a condenser put in parallel with part of ρ, which makes the correction more nearly proportional to ω^2.

In M inductometers which I have recently designed for use at radio frequencies(3) I have successfully used the tertiary loop system to annul the errors due to variation of frequency.

It should be remarked that in most of the ordinary measuring systems the altered values of r' and l' do not cause any error.

§3. SELF INDUCTORS

The compensation of self inductors is not so important as that of mutual inductors. I have investigated two different systems, namely (A) simple shunt, and (B) secondary closed circuit. By either of these the variation of L due to frequency may be largely reduced and often practically eliminated. If the self capacitance of an inductive coil (R, L) is equivalent to capacitance c across its terminals, then, if the effect is relatively small,

$$R' \doteqdot R\,(1+2Lc\omega^2), \qquad \text{......(9)}$$

and

$$L' \doteqdot L\,(1+Lc\omega^2). \qquad \text{......(10)}$$

§4. SYSTEM A. SIMPLE SHUNT

The system (shown in figure 2) of an induction coil (R, L) with self capacitance C shunted by a non-inductive resistance S was investigated by Mr T. L. Eckersley and myself many years ago(4). We found that the effective L' of the coil was reduced by the presence of the shunt, but we did not notice that the shunt could be used to correct the variation of L with frequency, shown in equation (10).

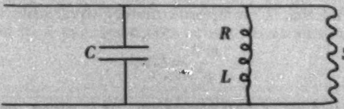

Figure 2.

The addition of a shunt may either raise or lower the effective resistance of the coil, but it *always* lowers the effective self inductance, and hence can be used to compensate the increase ($L^2C\omega^2$) due to frequency.

If (R, L) is shunted by S, where $S \gg R$, we have

$$R' \doteqdot R+(R^2+L^2\omega^2)/S, \qquad \text{......(11)}$$

and

$$L' \doteqdot L\left[1-\frac{2R}{S}-\frac{R^2}{S^2}-\left(\frac{L\omega}{S}\right)^2\right]. \qquad \text{......(12)}$$

When also capacitance C is across the coil, L' will not vary with ω when

$$S=L/C^2, \qquad \text{......(13)}$$

which is the condition for L compensation. The resulting L', however, becomes $L\,(1-2R/S-R^2/S^2)$, and this is a weak point in the method.

§5. SYSTEM B. SELF INDUCTOR WITH CLOSED LOOP COMPENSATOR

As shown in figure 3, let the self inductor (R, L) with self capacitance c have a closed secondary circuit (ρ, λ) coupled to it by mutual inductance m. Then

$$R' \fallingdotseq R\,(1+2Lc\omega^2)+\frac{m^2\rho\omega^2}{\rho^2+\lambda^2\omega^2},$$

and

$$L' \fallingdotseq L\,(1+Lc\omega^2)-R^2c-\frac{m^2\lambda\omega^2}{\rho^2+\lambda^2\omega^2}.$$

When $\rho \gg \lambda\omega$, we have

$$R' \fallingdotseq R+\left(2RLc+\frac{m^2}{\rho}\right)\omega^2 \qquad \text{......(14)}$$

and

$$L' \fallingdotseq L-R^2c+\left(L^2c-\frac{m^2\lambda}{\rho^2}\right)\omega^2. \qquad \text{......(15)}$$

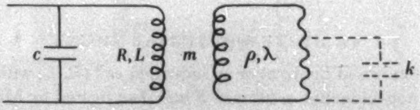

Figure 3.

From equation (14), since m^2/ρ is always positive, it is clear that R' cannot thus be compensated; it is always increased by the presence of the loop circuit.

Equation (15) shows that L' is approximately invariable with frequency where

$$\frac{m^2\lambda}{\rho^2}=L^2c, \qquad \text{......(16)}$$

and this gives a good system of compensation. It is often desirable to reduce λ by a condenser (k) across a part of ρ, as shown in dotted lines in figure 3.

When $m^2\lambda/\rho^2=L^2c$,

$$R' \fallingdotseq 2RLc\omega^2\,(1+L\rho/\lambda). \qquad \text{......(17)}$$

Since ρ/λ is usually much greater than 1, the factor $(1+L\rho/\lambda)$ may cause considerable increase in R'.

§6. EXPERIMENTAL EXAMPLES

The compensating systems (A) and (B) were applied successfully to various L coils. It will be sufficient to give the following three examples.

System A. Coil C 798 ($R \fallingdotseq 7{\cdot}6\ \Omega$. and $L=10{\cdot}00$ mH.) had capacitance 0·4 μF., put across its terminals, which caused L' to increase by about 20 per cent at 1000 c./sec. By trial it was found that a simple shunt (S) of 185 Ω. made L' almost invariable, as table 1 shows.

Table 1

n (c./sec.)	S (Ω.)	R' (Ω.)	L' (mH.)
500	∞	8·0	10·39
700	∞	9·0	10·84
1000	∞	11·0	12·06
500	185	12·8	9·29
700	185	18·9	9·32
1000	185	35·4	9·28

System B. (i) The same coil (C 798), still with 0·4 μF. in parallel, was coupled (by mutual inductance of approximately 5 mH.) to a secondary coil with λ approximately equal to 11mH. By trial, closing this secondary through 65 Ω. with 1 μF. in parallel gave compensation as shown in table 2.

Table 2

n (c./sec.)	R' (Ω.)	L' (μH.)
500	11·8	10·10
700	16·4	10·14
1000	27·2	10·08

The increase in R' is considerable.

System B. (ii) A small coil (C 743) having L approximately equal to 10·40 μH. from $n=0$ up to 800 kc./sec. was rendered incorrect by a capacitance of 100 picofarads across its terminals, as is seen in the first three lines of table 3. A secondary of 1 turn with ρ equal to 3·5 Ω. gave compensation as shown.

Table 3

n (kc./sec.)	ρ (Ω.)	L' (μH.)
200	∞	10·44
400	∞	10·48
800	∞	10·79
200	3·5	10·40
400	3·5	10·36
800	3·5	10·39

These examples show that quite extreme variations can be well compensated. In practice the variations due to self capacitance are usually much smaller, and it is clear that in nearly all such cases very exact compensation can be obtained.

APPENDIX

Negative self inductance

As has already been mentioned, the self inductance of the tertiary circuit can be reduced by putting a condenser in parallel with part of its resistance. Capacitance c across resistance r gives

$$r' = r/(1 + r^2c^2\omega^2), \qquad \text{......(18)}$$

and

$$l' = -r^2c/(1 + r^2c^2\omega^2), \qquad \text{......(19)}$$

and this forms a convenient device for introducing negative self inductance into any circuit.

At very low frequencies, where $rc\omega \ll 1$,

$$r' \doteqdot r \quad \text{and} \quad l' \doteqdot -r^2c,$$

and the system usually works well; but the effect of the divisor $(1 + r^2c^2\omega^2)$ gradually limits the possible range of $-l'$ as ω is increased, and brings it to zero in the extreme case. Two cases may be noticed.

(i) When r and ω are constant and c is varied, l' is a maximum and equal to $r/2\omega$ when $c = 1/r\omega$.

For example, at 800 kc./sec. with r equal to $100\,\Omega$., the maximum possible $-l'$ is only about $10\,\mu$H.

(ii) When c and ω are constant and r is varied, l' increases to a maximum of $1/c\omega^2$ as r increases to ∞.

In all cases the negative l' is nearly independent of frequency only as long as $r^2c^2\omega^2$ is $\ll 1$.

REFERENCES

(1) Campbell and Childs. *Measurement of Inductance, Capacitance and Frequency*, pp. 190, 207, 364 (1935).

(2) Astbury, N. F. and Ford, L. H. *Phil. Mag.* (7) **25**, 1009 (1938).

(3) Campbell, A. *Proc. Phys. Soc.* **50**, 335 (1938).

(4) Campbell and Eckersley, *Electrician*, 10 Dec. 1909.

DISCUSSION

Mr N. F. Astbury. It may be of interest to note two applications of the principles outlined by the author which have occurred in recent work at the National Physical Laboratory. The capacitance-measuring bridge recently described in these *Proceedings*$^{(1)}$ provides an example of the complete case of a mutual inductometer with a tertiary winding, while in the work on the absolute measurement of resistance by Mr Campbell's a.-c. method$^{(2)}$ use was made of a tertiary circuit coupled resistively to the secondary circuit.

Author's reply. I thank Mr Astbury for kindly giving references to two further examples of the use of a compensating tertiary circuit. In both cases very high accuracy was aimed at, and the compensating loop proved distinctly helpful towards the attainment of this.

REFERENCES

(1) Astbury, N. F. and Ford, L. H. *Proc. Phys. Soc.* **51**, 37 (1939).

(2) Hartshorn, L. and Astbury, N. F. *Philos. Trans.* A, **236**, 442 (1937).

SIMPLE DEMONSTRATION OF THE PELTIER EFFECT WITH APPROXIMATE MEASUREMENT

By ALBERT CAMPBELL, M.A.

Received 18 *October* 1938. *Read* 10 *February* 1939

ABSTRACT. Three strips of two metals A and B are soldered together to give junctions P and Q. A current I sent through the combination cools P and heats Q; when I is reversed, P is heated and Q cooled, these effects being shown by means of a galvanometer connected to an iron-constantan thermopile whose opposite junctions are close up to P and Q respectively. To obtain an approximate measurement, a current I_2 is sent through a short wire of resistance R close to the cooled junction. When the effects are small and I_2 is adjusted so as to make the galvanometer deflection zero, the Peltier coefficient Π is equal to

$$RI_2^2/2I.$$

Many years ago the author made direct measurements of the Peltier effect for various pairs of metals$^{(1)}$, but the results were only relative, and no absolute values were obtained. By a small addition to the original apparatus it is easy to get absolute values which are approximately correct.

Strips of the two metals A and B to be tested are hard-soldered or soft-soldered in the order ABA, giving two junctions P and Q. By bending the strip B the junctions are made to face one another with about 5 mm. between them as shown in the figure.

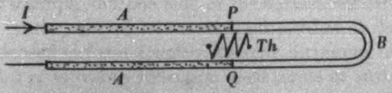

The opposite ends of a small multiple-junction iron-constantan thermopile *Th* are placed against P and Q with thin insulation between.

When a current I is sent in the proper direction, the junction P is cooled and the junction Q warmed, and the galvanometer is deflected. Where I is reversed, a deflection in the opposite direction occurs. This gives a qualitative demonstration of the Peltier effect.

To obtain a measurement of the actual heating and cooling, a short length (say 1 cm.) of thin wire of resistance $R\,\Omega$., with suitable leads, is arranged round the junction P cooled by current I. By sending an appropriate current I_2 through this heater wire the cooling at P and heating at Q can be exactly balanced, as is shown by the galvanometer deflection being reduced to zero. Thus the Peltier effect at the two junctions is equal to the Joule effect in the heater wire. I and I_2 are measured on separate ammeters and the changes of temperature are kept small.

Then, if Π is the Peltier coefficient,

$$2\Pi I \risingdotseq RI_2^2,$$

and hence

$$\Pi \risingdotseq RI_2^2/2I \text{ v.}$$

In the apparatus shown A and B are iron and constantan. The resistance R is about 4 Ω., and I is of the order of 0·2 amp. If T is the absolute temperature, Π/T comes out about 50 μv./° C., in fair agreement with the thermo-electric power determined in the ordinary way by voltage and temperature measurements.

REFERENCE

(1) Campbell, A. *Proc. Roy. Soc. Edinb.* p. 807 (1882) and p. 387 (1887).

THE ORIGIN OF RADIO-WAVE REFLECTIONS IN THE TROPOSPHERE

By J. H. PIDDINGTON, M.Sc., B.E., Ph.D., Walter and Eliza Hall Fellow of the University of Sydney, Cavendish Laboratory, Cambridge

Paper and discussion published on pp. 129–37 *of this volume*

AUTHOR'S REPLY TO THE DISCUSSION

Dr Whipple has pointed out that because ordinary clouds are efficient reflectors of light waves, it is not very surprising that they should reflect wireless waves. It is, of course, true that a discontinuity in dielectric constant encountered by any electromagnetic wave will result in energy being reflected. In the case of light waves reflected from water droplets, however, we are dealing with scattering from particles of dimensions considerably greater than the wave-length of the incident energy, while for wireless waves the dimensions of the particles are much smaller than the wave-length. It would be unsafe to draw any conclusion regarding the efficiency of reflection of wireless waves from clouds from a comparison with the reflection of light waves.

Dr Smith-Rose infers from the paper that the suggested process of reflection of wireless waves takes place at a surface of discontinuity between air and a cloud containing water in the liquid or solid form. I have apparently failed to make myself sufficiently clear in describing the suggested process. It is shown that if the total mass of water per cm.^{3} in the atmosphere remains unchanged, its contribution to the dielectric constant will increase by a factor of about 7 as the state changes from vapour to liquid, and will decrease by a factor of about 27 as the state changes from liquid to solid. It is, therefore, possible to have a surface of discontinuity of dielectric constant while having the same concentration of water on each side of the boundary. For example, on one side of the surface the air may contain water vapour only, while on the other side a certain proportion of this vapour, say one-half, may have condensed to form droplets, thereby increasing $(K-1)$ by a factor 4.

The table on p. 134 indicates reflection coefficients of surfaces on one side of which the air is dry and on the other side of which all the water corresponding to saturation vapour pressure has condensed into the form of droplets. In the sentence above this table it is stated that no such complete discontinuity is suggested—it is much more probable that water vapour would be found on either side of the boundary with partial condensation on one side. Such conditions will result in the reflection coefficient being lower than those given in the table but still of the right order.

Dr Smith-Rose asks what justification I find for assuming that the relations giving the dielectric constant of gaseous mixtures may be applied to non-molecular mixtures of air and water in the solid or liquid form. If the particles are small compared to the wave-length of the vibration for which we are measuring the dielectric constant, and if they have no regular distribution and no permanent electric movement, it is to be expected that the laws governing gaseous mixtures will apply to mixtures containing these particles, and that their contribution to the dielectric constant of the medium will be independent of their size or shape, within limits, and proportional to the concentration.

Measurements of the refractive indices of colloidal suspensions[*] support this view, the contribution of the suspended matter to the dielectric constant obeying the same laws as those applying to molecular mixtures, provided that the dimensions of the suspended particles are small compared to the wave-length of the light for which the index of refraction is measured.

If the equations $(K-1)=80q$ e.s.u. for water, and $(K-1)=3q$ e.s.u. for ice are to hold, there is a lower limit, as well as an upper limit, to the size of the particles. They must contain a large number of molecules so that mutual effect between the molecules, which is so effective in increasing the dielectric constant, may play its full part.

As has been pointed out by Dr Smith-Rose, the value of $(K-1)$ given in line 7 on p. 133 is not correct for saturated water vapour at 0° C., and should have been described as $(K-1)$ for a distribution of water droplets with mean density equal to the saturation vapour density of water at 0° C. The heading of column 4 of the table on p. 134 has been shortened from "Contribution to the total dielectric constant", and as has been pointed out by Dr Smith-Rose does not mean that these values give the total dielectric constant of the atmosphere.

I do not think it likely that the frequency variations observed by Dr Rayner when making standard frequency comparisons are due to reflections or refractions in the troposphere. Multiple-path transmission within the troposphere of ultra-short waves has been observed,[†] but the observed path-difference was only 240 metres and the effect should be observable during the day as well as at night. Lateral deviation effects in the ionosphere could perhaps account for the observed fluctuations, and phase instability in line and frequency multiplier might possibly have a diurnal variation, which would account for the observed phenomena.

Mr Naismith has suggested that *B*-region echoes might be due to reflections at geographical discontinuities, and says that this would explain the semi-permanent nature of the reflecting strata. If observations did suggest that reflections came from semi-permanent strata, this explanation would appear more probable, but in fact they do not. The low echoes arrive at random, their intensity fluctuating continuously and its mean value decreasing steadily as their time delay increases, as indicated in §2.

The possibility of reflections at ground irregularities has not been discarded, however, and it is hoped that further tests may show if this effect plays an important part, compared to the type of reflection described in the paper. If so, then it is probable that water in the atmosphere plays an important part in bending the waves, as has been suggested by numerous workers, and the irregular variation in the strength and delay times of *B*-region echoes is due to fluctuations in the efficiency of transmission of the different echoes, due to changes in the degree of refraction of the wave in the atmosphere.

---

[*] W. Ostwald, *Licht und Farbe in Kolloiden-Steinkopff* (Dresden, 1924).

[†] C. R. Englund, A. B. Crawford and W. W. Mumford, *Nature, Lond.*, **137**, 743 (1936).

ACOUSTIC SPECTRA OBTAINED BY THE DIFFRACTION OF LIGHT FROM SOUND FILMS

By D. BROWN, PH.D., Auckland University College, New Zealand

Paper published on pp. 244–55 *of this volume*

DISCUSSION

DR A. G. GAYDON. For the variable-density type of sound film the diffraction pattern observed will presumably depend upon the type of photographic emulsion used and its conditions of development; an emulsion giving strong contrast will obviously produce spectra of the second and higher orders in addition to the strong first-order spectrum. For the purpose of detecting harmonics of the original sound-frequency it would be necessary to ensure that these spectra of higher order should be absent. I should be interested to know whether it is possible to eliminate them in practice by the choice of a suitable emulsion, and if so whether the necessary conditions are very stringent.

Mr E. C. ATKINSON. It would be interesting to consider the transients, which cannot be represented by a finite Fourier's series. Does the author think that the spectra can throw light on the nature of speech transients?

AUTHOR'S REPLY. In reply to Dr GAYDON: The conditions of exposure and development demanded by variable-density film are certainly somewhat critical. Commercial practice requires in effect that the film be developed to a gamma not sensibly different from unity, and only the straight portion of the characteristic curve may be used. The recording is commonly made on positive film rather than on negative film, speed being sacrificed for the advantage of the finer grain. Although careful control is necessary, I think the film industry has shown that sound-recording of high quality can be made a routine matter. In the case of films intended for the production of acoustic spectra, the same limits of density and development must be observed; if these limits are overstepped in any way that would produce amplitude-distortion in the commercial product, then false harmonics and combination frequencies will automatically appear to some extent in the diffraction spectra.

In reply to Mr ATKINSON: In the sense that a transient wave-form may be analysed by means of Fourier's integral theorem, which may possibly give an infinite number of terms in any finite frequency range, the diffraction method seems well adapted to the problem. It performs this analysis automatically, and presents the frequency-distribution as a continuous spectrum in such a case. To the extent to which a knowledge of the frequency-distribution and intensity-distribution in a transient is of value, I think the method should prove a useful one.

DEMONSTRATIONS

Demonstrated 10 *March* 1938

A SIMPLE DEMONSTRATION OF THE VOLTA CONTACT E.M.F. By J. NICOL, B.A., B.Sc.

THE apparatus consists of a single gold leaf suspended from an insulated brass rod so that its lower end hangs midway between the upturned ends of two L-shaped metal strips, one of copper and the other of zinc, fixed to the wooden base board. The height of the leaf is adjusted so that it just swings clear of the ends of the two strips, which are connected externally by a wire.

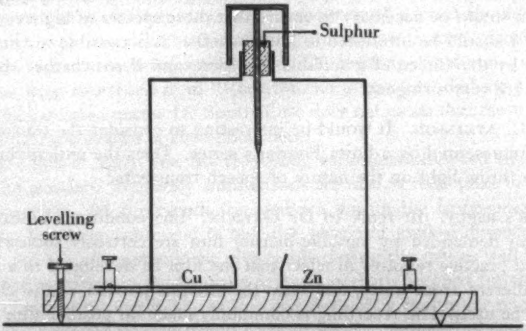

When a charged rod is brought near the top of the insulated rod from which the leaf hangs, the leaf is observed to move towards the zinc strip if an ebonite rod rubbed with fur is used, and towards the copper strip if a glass rod rubbed with silk is used. The leaf must be midway between the upturned ends of the strips, otherwise it moves towards the nearer strip, whatever the nature of the charge used. The midway adjustment is secured by tilting the base board by means of a levelling-screw. In the apparatus shown, the distance between the copper and zinc strips is about 2 cm., the length of the gold leaf 4 cm., the length of the base 20 cm., and the pitch of the levelling-screw 1 mm. For the experiment to succeed, this screw has to be adjusted to within a quarter-turn on either side of the best position.

A HEAVY CURRENT HYDROGEN DISCHARGE-TUBE. *Demonstration given before the Society* 25 *November* 1938, *by* W. R. S. GARTON, B.Sc., A.R.C.S., Imperial College of Science and Technology.

THE discharge tube shown in the accompanying diagram provides a convenient and reasonably intense source of the ultra-violet continuum of hydrogen. The design of the tube is based on a modification of a principle introduced by Pearse and Gaydon(1) into the technique of producing intense positive-column spectra, by the constriction of the appropriate portion of the discharge within a silica tube of small diameter supported by annular metal rings inside an outer envelope.

The electrode assembly is contained in an envelope 1 of glazed translucent silica, 2 in. in internal diameter and 2 ft. in length, attached with sealing wax to a brass boring 2, to which is sealed the quartz window 18; a side tube 3 passes through the boring 2, providing a gas inlet. A silica tube 5, of 5 mm. internal diameter and about 4 in. long, serves to constrict the positive column of the discharge between the electrodes 6 and 8, which may be of aluminium or, preferably, of nickel. The electrode 6 forms part of the support for the tube 5, and other metal rings 7 are spaced along the length of the latter; the connexion to the electrode 6 is made by means of a piece of 6 B.A. steel 10 sheathed in a silica sleeve 11, which passes through holes in the rings 7 and emerges at the rear end of the tube, as does the similarly shielded lead 12 from the other electrode 8. If only one ring such as 7 is employed, the discharge will pass along the tube 5 provided the pressure is low enough; as the latter is raised a point is reached where the potential-drop along the length of the positive column within the tube 5 becomes of the order of the cathode fall, and the discharge strikes between the parts 6, 7 and 8. The pressure at which this occurs can be raised by using a number of the rings 7, and as the production of the hydrogen continuum is favoured by relatively high pressures, it is desirable to use several of the rings; if the length of the constricting tube is increased, then a larger number should be introduced. To keep the rings apart, short lengths 9 of close-fitting Pyrex tube are slipped over the tube 5. The rear end of the tube has been made demountable, so that the electrode arrangement may be easily altered, by means of the ground brass flanges 14 and 15, of which the former is waxed to 1; the joint between the flanges is sealed with Apiezon *Q* compound. Through holes in the brass end piece 15 the silica sleeves covering the

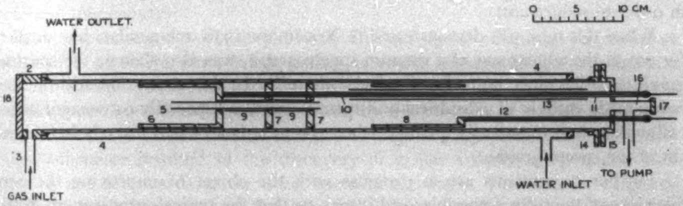

electrode leads are sealed with wax, and a glass T piece 16 provides a pump connexion and a second window 17. It is advisable to cover the sleeve 11 with a second sleeve 13, as it otherwise has a tendency to puncture where it passes within the electrode 8. The envelope 1 and the seal between it and the boring 2 are cooled by the circulation of water within the brass jacket 4, which screws on to the boring 2.

In operation a current of about 1 amp. is passed through the tube, from a source of a few thousand volts, and hydrogen flows through continuously, being introduced through a needle valve at such a pressure that the discharge appears whitish; if the colour of the discharge is markedly red, either the pressure is too low or the gas is damp; in such cases the Balmer series is enhanced and the continuum is poorly developed. If an a.-c. source is used, both electrodes should have as large an area as possible; if a d.-c. source is used, then only the cathode need be large. Whether much gain results from the use of a longer tube to constrict the discharge, and the precise effect of varying the number of the rings 7, are matters still being examined.

The tube is robust, thermally and mechanically, since the outer envelope is of silica under very little strain; it is of very simple construction, as the only glass working lies in the T joint 16. Where extreme safety is not essential, it is probable that the envelope 1 may without disadvantage be made of Pyrex instead of silica in order to reduce cost.

When this tube was demonstrated in November 1938 one similar, but smaller, for use in the adjustment of a vacuum spectrograph, was also shown; the spectrograph itself has since been described elsewhere⁽²⁾. In this connexion such a tube, being made entirely of cylindrical and turned parts, is especially convenient, since collimation is automatically attained when the tube is attached directly before the slit of the spectrograph.

Further experiments are in progress with the object of improving the performance of the tube if possible, and it may be that the typical arrangement of the electrodes shown is not the best that can be devised.

REFERENCES

(1) Pearse, R. W. B. and Gaydon, A. G. *Proc. Phys. Soc.* **50**, 201 (1938).
(2) Garton, W. R. S. *J. Sci. Instrum.* (1939).

OBITUARY NOTICES

SIR ROBERT MOND, F.R.S.

Sir Robert Mond, a Fellow of the Physical Society since 1891, died in Paris on 22 October 1938. He was the elder son of Dr Ludwig Mond and brother of Alfred Mond, the first Lord Melchett.

Robert Ludwig Mond was born on 9 September 1867, at Farnworth in Lancashire. He was educated at Cheltenham College and Peterhouse, Cambridge, and afterwards at Zurich and the Universities of Edinburgh and Glasgow. His early scientific activities were largely determined by those of his father—and indeed it may be said that, in his scientific interests, his artistic tastes and his enlightened and discriminating patronage of research he followed closely, all through his life, the example of his distinguished parent. In the year 1867, the year of Robert's birth, Ludwig Mond settled finally in England, and a few years later he established at Winnington near Northwich, in co-operation with Sir John Brunner, the firm of Brunner, Mond and Co., for the purpose of working the Solvay ammonia-soda process in this country.

In the experimental work carried on by Dr Ludwig Mond and his collaborators Robert took an active part. While acting as works manager of an experimental plant for obtaining chlorine and ammonia from ammonium chloride he noticed a black deposit on the nickel valves, caused by the presence of a small percentage of monoxide in the carbon dioxide used at one stage of the process. An examination of this substance resulted in the discovery of a new volatile compound, nickel carbonyl, and afterwards of the other metallic carbonyls. This was the origin of one of the most important of the Mond developments, for the nickel-carbonyl reaction was used as the basis of a new method of extraction of nickel from its ores; and a plant for the production of pure nickel, working in connexion with mines at Sudbury, Ontario, was set up in South Wales.

On the business side Robert Mond also took his part. He was a director of Brunner, Mond and Co., and also of the Mond Nickel Company, of which he succeeded his father as managing director. He continued experimental work on the carbonyls, and an interesting history of their discovery and applications, from his pen, will be found in the *Journal of the Society of Chemical Industry* for the year 1930.

Mond will be remembered among men of science for the generous encouragement he gave to the work of others. His interests were wide, and a number of different institutions became the channels of his activity. Thus for a long period of years he was Honorary Treasurer of the Faraday Society, until he became its President in 1930. That peculiarly valuable feature of the Society's work, the general discussions on physico-chemical subjects, owed much to him during his years of office; for the hospitality which enabled many distinguished foreign guests to attend, and gave to the meetings their special character, was largely his. Another example is his interest in the Norman Lockyer Observatory at Sidmouth. Of this he was Chairman of the Corporation for twenty-one years, and a generous benefactor.

With the Royal Institution he had special ties. In 1896 his father founded and presented to the Institution, with an endowment, the Davy Faraday Research Laboratory at 20 Albemarle Street. In the deed of trust Robert was appointed Honorary Secretary, and this office he held to the end of his life. In the early years he was principally responsible for the furnishing and equipping of the Laboratory. In the Institution itself he held office as Visitor and Manager for several periods. He gave generously to it, notably £5000 to the reconstruction fund in 1929; and in 1937, having heard that it might be necessary, owing to lack of funds, to restrict the researches in the Davy Faraday Laboratory, he sent a cheque for £2000, as a Coronation Year gift.

A visit to Egypt to recuperate after an illness aroused his interest in Egyptology, and the study became an absorbing passion with him. After assisting Howard Carter and P. E. Newberry in excavations of the tombs at Thebes, he took over the latter's concessions and early in 1903 began work himself. His own exertions, and the financial support he gave to other workers, resulted in the preservation of a large number of tombs and the publication of reports upon them. The production of the *Topographical Catalogue of the Theban Tombs* in 1913 was made possible by his liberality.

The work in Egypt was interrupted by the War, and when in 1924 Mond returned to Thebes, it was in association with the Institute of Archaeology of the University of Liverpool, to clear and restore the famous tomb of Ramose. In 1926 work was begun on a new site at Armant, identified as the burial place of the sacred bulls of Hermonthis. Later the concession was transferred to the Egypt Exploration Society, of which Mond became President in 1928. The excavations at Armant, financed entirely by him, he described jointly with O. H. Myers and other writers in *The Bucheum* (3 vols. 1934) and *The Cemeteries of Armant* (2 vols. 1937). He was particularly happy in his association with the work of the Egypt Exploration Society and with its members. Prof. S. R. K. Glanville describes him as "a colleague who shared completely their enthusiasm for their science, and a leader who inspired confidence in his counsels and, above all, great affection for himself".

Mond's first wife, the mother of his two daughters, died in Egypt in 1905. In 1922 he married Marie Louise le Manach, who survives him. In later years he lived much in France, and became as well known in Paris as in London, extending his interest and encouragement to French institutions with which he was in sympathy. In the founding of the Maison de la Chimie he took a leading part; his French colleagues elected him President of the Société de Chimie Industrielle. He was Membre de l'Institut and Commandeur de la Légion d'Honneur. The University of Liverpool made him LL.D. in 1930; he was knighted in 1932; and in 1937 received the honour he valued highest, the Fellowship of the Royal Society.

T. M.

GEORGE ELLERY HALE

G. E. HALE died on 22 February 1938. His memory is to be cherished as that of a most noteworthy leader in the recent advances of our knowledge of the phenomena presented by the surface of the sun. By his invention of the spectroheliograph in the early years of his youthful studies, he opened up a new method of recording photographically the contribution made by any selected monochromatic solar radiation (and hence of any chosen chemical element) to the pictures of the features of the sun's surface as scrutinized in ordinary telescopic vision.

After four years spent in the Massachusetts Institute of Technology, where he graduated in 1890, he brought his spectroheliograph to completion with thousands of solar observations at Kenwood Observatory with a 12-in. telescope mounted to his own design and provided by his father. In 1895 he undertook the initiation and direction of the Yerkes Observatory of the University of Chicago, and he carried the work forward for ten years with marked success. His genial temperament, enthusiastic outlook, and infectious inspiration of confidence gained for him and his beloved science the splendid support not only of his contemporary associates and of devoted staffs, but also of the trustees of great endowments. Before he had reached the age of 27 years he had gained recognition as a leader, without a trace of self-assertion. Failure of health and the desire for better physical conditions for astronomical observations led him to California, whither he was attracted by the prospect of the foundation, by the Carnegie Institute of Washington, of a mountain observatory for intensive study of the sun. There on the summit of Mount Wilson he gradually established a solar observatory with a novel equipment of powerful instruments. With these he discovered definite indications of vortical motions in and about sunspots, and was led thereby to look for signs of the Zeeman effect in the broadened lines of the spectra of sunspots. His observations proved that a sunspot is the seat of magnetic fields, having intensities of many kilogauss, and that in a vast number of cases of obviously related pairs of sunspots, the polarities of the two components are of opposite signs. The success of his design of the 60-ft. tower telescope, with a 30-ft. spectrograph sunk in a vertical shaft beneath the tower, led him to design the 150-ft. tower telescope with a spectrograph of 75 ft. in a shaft 80 ft. deep. With this equipment specially designed for the purpose he proceeded to detect and measure the intensity of the general magnetic field of the sun, analogous to the earth's magnetic field. It is not to be wondered at that his health gave way in 1909 and 1913 under the stress of this activity. He resigned the directorship of the Mount Wilson Observatory in 1921, but continued his own observational work in an observatory in Pasadena, in which he completed the design and construction of the spectrohelioscope intended for special studies of restricted regions of the sun's surface by visual observations in cases of unusual local eruptive outbursts. Nor can we overlook his activity in the provision of increasingly large reflecting telescopes. The 60-in. disk of the Snow telescope had been given to Hale by his father before he went to the Yerkes Observatory, and it was completed and set up at Mount Wilson with such success that a 100-in. reflector was constructed, thanks to the munificence of Mr J. D. Hooker. The remarkable success attained by the use of it in studies of the remoter nebulae encouraged Hale to take a prominent part in the colossal enterprise of the 200-in. reflector, which is being constructed and is to be erected at Palomar in the joint control of the California Institute of Technology and the Mount Wilson Observatory. To our deep regret it has not been given to Hale to see its completion. Hale became one of the Honorary Fellows of the Physical Society in 1910 and was awarded the Copley Medal of the Royal Society in 1932.

DR J. E. R. CONSTABLE

THE early and sudden death of Dr J. E. R. Constable on 3 February 1939 was a severe blow to all who had known him. He was a Londoner, having been born in the capital on 31 March 1906. After a brilliant school career he went up to Cambridge in 1924 and was awarded an exhibition and later a senior scholarship at Trinity College. After taking a first class in both parts of the Natural Sciences Tripos and obtaining a first-class London B.Sc., he joined Rutherford's band of investigators in nuclear physics, and in collaboration with Chadwick and Pollard published two experimental papers on the energy levels of light atomic nuclei; this work gained him a Cambridge Ph.D.

In 1931 he joined the staff of the National Physical Laboratory, where he was assigned to the relatively new Acoustics Division, and speedily made himself popular by his cheerful, breezy manner and his ready willingness to undertake leisure-time activities. He soon selected for himself a branch of enquiry in building acoustics, viz. the transmission of sound through the component parts of buildings, a subject on which he rapidly became a leading authority, and in a series of papers he demonstrated the sound insulation given by double windows, and the contribution of flanking walls and water pipes to the transmission of sound between neighbouring rooms in a building. Several of his papers on these and allied subjects were read before this Society, and few will quickly forget the witty, attractive and yet strictly logical and convincing manner in which he presented them. His personality had obviously made a mark with the Society, and when a Constable paper was to be read one could sense a feeling of keen and joyous expectation among his audience as he rose to speak.

The various demonstration models which he designed to illustrate the methods employed for reducing noise in buildings were admirably adapted to their purpose and were much appreciated at the many exhibitions at which they were shown.

Constable's interests were by no means confined to his work. He took a leading part in many of the social activities of the Laboratory; he had a considerable knowledge of music and had made a special study of organs. He was one of the gayest of companions and his vital personality will be sorely missed by his many friends. The sympathy of all must go out to his widow, herself a Cambridge physicist, who helped and encouraged him in his work, and to his four-year-old son.

REVIEWS OF BOOKS

Raman Jubilee Volume of the Proceedings of the Indian Academy of Sciences, vol. 8, pp. 243–565, November 1938.

This is a special volume of thirty-eight papers presented by authors in many countries in commemoration of the fiftieth birthday of Sir C. Venkata Raman, 7 November 1938. As the tenth anniversary of the discovery of the Raman effect also fell in that year, it is fitting that most of the papers should deal with that subject. Twenty-two of the papers are in English (a few by authors in this country and in the U.S.A., but most by Indian authors), thirteen are in German (seven of them from the Technische Hochschule, Graz—the 89th to the 95th from that institution on the Raman effect alone!), two are in French and one is in Italian. In ten years nearly 1700 papers have appeared on the Raman effect, and in one of the papers in this volume J. H. Hibben presents a statistical analysis of trends of research in the subject as a function of time and geographical distribution.

W. J.

The Principles of Statistical Mechanics, by RICHARD C. TOLMAN. Pp. xx + 662. (Oxford: Clarendon Press, 1938.) Price 40*s*.

The methods of statistical mechanics for treating the behaviour of systems about whose condition less than the maximal possible knowledge is available are essential for linking together theoretically postulated atomic properties with experimentally observed molar properties. The importance of the part played in this way by statistical mechanics in physico-chemical investigations is widely appreciated, but the basic principles and the powerful general methods are not, perhaps, so widely understood. This is partly because statistical mechanics has developed almost as an esoteric cult in that expositions of the subject, if not addressed exclusively to the fully initiated, often seem expressly designed as ordeals for the aspiring neophyte. In this monumental work Tolman has performed a most valuable service, for he has succeeded no less in being comprehensible than in being comprehensive.

In the first part of the book, roughly a quarter of the whole, classical statistical mechanics is developed. A brief treatment of classical mechanics, dealing in particular with the Hamiltonian formulation, is followed by a discussion of statistical ensembles. After an account of Liouville's theorem, the principle of equal *a priori* probabilities for equal phase extensions can be introduced as a reasonable postulate on which to base the development. The classical statistical methods are then applied in the derivation of the Maxwell-Boltzmann distribution law, and a consideration of collisions, as a mechanism of change in time, leads up to a full discussion of Boltzmann's H theorem.

Part II (pp. 180–523), on quantum statistical mechanics, opens with a presentation of the elements of quantum mechanics. An appropriate postulatory basis is stated and developed, and a number of simple applications are made. These sections form, in effect, an admirable treatise (144 pages) on quantum mechanics, independently of the statistical applications to be made. Ensembles are then discussed, and after a derivation of the analogue of Liouville's theorem, the hypothesis of equal *a priori* probabilities and random *a priori* phases for quantum-mechanical states is introduced as an appropriate basic postulate for the statistical treatment. After a derivation of the various quantum distribution laws, as dependent on the particular symmetry conditions, changes in time are discussed, and the development of a quantum-mechanical H theorem leads to a full treatment of equilibrium conditions.

The statistical-mechanical explanation of the laws of thermodynamics is taken up in the third part, and a number of applications are considered as illustrative of the general methods of treatment in connexion with physical questions. The author, very wisely, does not attempt to deal in detail with actual physico-chemical systems, for, as he says, the needs for a full account of specific applications are already met by Fowler's *Statistical Mechanics*.

The outstanding contribution in this book is the thorough fundamental exposition of statistical mechanics on the basis of quantum mechanics. In respect of the more purely statistical technique, the accounts of the micro-canonical, canonical and grand-canonical ensembles, and the discussions of their physical relevance, also form an invaluable contribution to the general subject. As the book is so long, it is perhaps worth while to mention that particular later chapters can be read with understanding without any necessity for more than occasional reference back to earlier sections. The whole work is a masterpiece of clear exposition, consistently maintained, of a difficult subject of wide scientific importance.

E. C. S.

Molekülspektren und Molekülstruktur, I. Zweiatomige Moleküle, by G. HERZBERG. Pp. xvi + 404. (Dresden and Leipzig: Theodor Steinkopff, 1939.) RM. 28, bound RM. 30.

In recent years Prof. Herzberg has undertaken the writing of three volumes of a good-sized work on spectra which will eventually appear not only in the original German, but also in English translations by Dr J. W. T. Spinks, one of his colleagues in the University of Saskatchewan. The first of these volumes, *Atomspektren und Atomstruktur*, was published in 1936, and its English edition was reviewed in these *Proceedings*.* The second is now before us, and the third, which is to bear the subtitle *II. Mehratomige Moleküle*, has yet to appear. Since much headway has been made during the last two or three years in the practical investigation and the theoretical interpretation of outstanding problems in band spectra, the present volume appears at an opportune time.

An attempt to survey the contents in the course of this brief notice would probably not serve any useful purpose, for it might apply almost as well to the diatomic sections of previous German works on the subject, such as Weizel's and Sponer's, whereas Herzberg's treatment of the subject departs very much from that of either of those authors. It blends the observational and the modern theoretical sides of the subject in an altogether admirable way. The text contains 169 figures, including energy-level diagrams, potential curves, Fortrat diagrams, vector-model diagrams, remarkably good and well-chosen spectrograms, etc. In the text are also 37 tables of observational data for typical vibrational and rotational analyses, theoretical material, and molecular constants. The table of constants derived from all the known diatomic spectra differs from the corresponding tables in the Physical Society's *Report* (1932) and Sponer's volume 1 (1935) in that it is limited to ground states. The tabulation of the numerical data for all the known excited states, which even in 1935 occupied about a half of Sponer's volume, has now become a very formidable undertaking. The bibliography, author index, and subject index are all adequate, and the book is well produced. Although, perhaps, not the most detailed, it is certainly one of the best, if not the best, of the presentations of the subject that have yet appeared.

W. J.

---

* *Proc. Phys. Soc.* 49, 712 (1937).

Grimsehl's Lehrbuch der Physik, revised by R. TOMASCHEK. Vol. 1, Mechanics, Heat and Sound. Pp. iv+681. (Leipzig: B. G. Teubner.) RM. 19.80.

The appearance of a tenth edition of vol. 1 of Grimsehl's text-book concludes the 1938 revision of the complete work. Compared with the ninth edition, the changes in this volume are mostly of a minor character. Some additions to the chapters on sound and ballistics, and a revised treatment of surface tension stressing the molecular aspect, may be mentioned. A feature of the whole work is the easy way in which the reader is led from a physical principle treated as part of experimental science to the application of the principle in technology. For example, in the present volume the discussion of fluid motion merges into a simple account of the dynamics of flight, with illuminating notes on such technicalities as the slotted wing and propellor efficiency.

An exceptional standard of accuracy and clarity distinguishes this text-book which may be warmly recommended to the student whether his later interests will lie in applied or pure science.

An authorized translation of the 7th German edition, by L. A. Woodward, has been published by Messrs Blackie and Sons.

W. S. S.

Tables of $\tan^{-1} x$ *and* $\log(1+x^2)$, by L. J. COMRIE. (Tracts for Computers, edited by E. S. Pearson, No. 23.) Pp. 18. (Cambridge: University Press.) Price 3*s*. 9*d*.

The tables in this volume, as in other volumes of the series of *Tracts for Computers*, are designed primarily for the assistance of statisticians, in this case for the calculations of a curve of Pearson's type IV. Nevertheless, some of them, such as those of $\log \Gamma(x)$ and of $\log x$ to 20 figures, are found useful by other mathematicians. The present table is of this class. It gives $\tan^{-1} x$ and $\log(1+x^2)$ from 0 to 5 at intervals of 0·01 and from 5 to 15 at intervals of 0·1, followed by $\tan^{-1} x$ up to 20 at intervals of 0·1 and up to 164 at unit intervals, in every case to seven decimal places.

The table of $\tan^{-1} x$ has been obtained by inverse interpolation, and that of $\log(1+x^2)$ direct from log tables, whilst accurate interpolation is made convenient by the printing of second differences.

J. H. A.

The Nomogram, by H. J. ALCOCK and J. R. JONES. Pp. viii+224. (London: Pitman and Co.) Second edition. 10*s*. 6*d*.

The second edition of this well-known book follows very much the same lines as the first. It treats of the construction of nomograms to represent formulae of different types (has anything been written on the construction of nomograms to represent observations given in the form of tables or curves rather than of formulae?), giving full weight to practical points of the drawing work involved. The underlying theory is that of co-ordinate geometry, with the theorem that the intersection of two or more curves is the solution to the simultaneous equations representing them, so that the condition for concurrence is the condition for the equations to have a common solution. The curves concerned, of course, are those shown in the nomogram, together with the straight-edge used in reading off from it.

One curious blemish survives, and that is the use of the symbol $f(v)$ to mean merely "a function of v", irrespective of how many functions may be under consideration. Thus we are told that in practice a formula involving two variables only can be written in the form $f(u)=f(v)$, and as an illustration, we are told that a formula $f(u)f(v)=k$ can be written $f(u)=k/f(v)=kf_1(v)$, and that this is of the form first mentioned, i.e. $f(u)=f(v)$. This usage is continued throughout the book, so that when for example $f(u)$ and $f(v)$ both appear in the same determinant, the reader must remember that $f(\ )$ may be a different function in the two cases. For this reason the book is less valuable as a work of reference than it would otherwise be, since the investigation must be traced through on each occasion to find whether $f(\ )$ is one or more than one function.

Nevertheless, as a text-book it is excellent. Most of those troublesome points that readers are often left to puzzle over have obviously been sought out and mentioned, so that in every respect the matter shall always be clear. To those who have a nomogram to draw, or to those who merely wish to satisfy their curiosity on these diagrams, the book is one to be recommended.

J. H. A.

Background to Modern Science, edited by J. NEEDHAM and W. PAGEL. Pp. xii + 243. (Cambridge: University Press.) 7*s.* 6*d.*

Among the paths which scientists have followed when attempting to explain to the layman what it is that they are doing, and how and why they do it, the historical approach has been least common. The present work, the second volume in the Cambridge Library of Modern Science, represents a thoroughgoing attempt to follow the historical method. It consists of the substance of ten lectures by different specialists, organized by the History of Science Committee, and delivered at Cambridge during 1936.

The first lecture, by the Laurence Professor of Ancient Philosophy, is the least satisfactory from the point of view of the scientist. The man in the street can be trusted to judge for himself whether it is logical or right to say that "There is also the class war, to decide whether the money and the goods shall go to the rich or to the poor", but he cannot guess that the philosophy of science put forward is one which many scientists would repudiate. The difference between our science and that of the Greeks is well brought out, but it is implied that this difference is so fundamental that no similarities could be found. Indeed, the author seems to deny that the aim of Greek science was "a pure and dispassionate love of truth for its own sake", though probably he only meant to deny that it aimed at the control of Nature.

The second lecture, by Sir William Dampier, forms a bridge between ancient and modern physics, the latter being represented by two lectures of Lord Rutherford (the last which he gave, and particularly recapturing his personality, since they were prepared for publication from shorthand notes and not from a manuscript written beforehand), one on crystal physics by the present Cavendish professor, and one by Dr Aston on atomic theory. The series on the physical sciences is brought to a close by an address from Sir Arthur Eddington on "Forty years of astronomy".

The last four articles deal with the biological sciences in the last forty years. Prof. Ryle writes on physiology, the late Prof. Nuttall on parasitology and tropical medicine (a delightfully written essay, often in a more personally reminiscent vein than most of the others), Dr Punnett on evolution theory and Prof. Haldane on genetics. The present reviewer has no knowledge by which to judge their merits, but can testify to their interesting nature, though he hopes that physics does not appear to the non-specialist to bristle with unfamiliar words to the same extent as do these sciences.

Altogether, the book is highly to be recommended for reading in leisure hours.

J. H. A.